ESSENTIAL GRADUATE PHYSICS - CLASSICAL MECHANICS

Konstantin K. Likharev
Stony Brook University

Stony Brook University

Essential Graduate Physics - Classical Mechanics

Konstantin K. Likharev

The LibreTexts libraries are Powered by NICE CXOne and are supported by the Department of Education Open Textbook Pilot Project, the UC Davis Office of the Provost, the UC Davis Library, the California State University Affordable Learning Solutions Program, and Merlot. This material is based upon work supported by the National Science Foundation under Grant No. 1246120, 1525057, and 1413739.

Any opinions, findings, and conclusions or recommendations expressed in this material are those of the author(s) and do not necessarily reflect the views of the National Science Foundation nor the US Department of Education.

TABLE OF CONTENTS

6: From Oscillations to Waves

7: Deformations and Elasticity

8: Fluid Mechanics

9: Deterministic Chaos

10: A Bit More of Analytical Mechanics

Detailed Licensing

Licensing

*A detailed breakdown of this resource's licensing can be found in **Back Matter/Detailed Licensing**.*

CHAPTER OVERVIEW

1: Review of Fundamentals

After elaborating a bit on the title and contents of the course, this short introductory chapter reviews the basic notions and facts of the non-relativistic classical mechanics, that are supposed to be known to the readers from undergraduate studies. [1] Due to this reason, the discussion is very brief.

1.1: Terminology- Mechanics and dynamics

A more fair title of this course would be Classical Mechanics and Dynamics, because the notions of mechanics and dynamics, though much intertwined, are still somewhat different. The term mechanics, in its narrow sense, means deriving the equations of motion of point-like particles and their systems (including solids and fluids), solution of these equations, and interpretation of the results. Dynamics is a more ambiguous term; it may mean, in particular:

(i) the part of physics that deals with motion (in contrast to statics);

(ii) the part of physics that deals with reasons for motion (in contrast to kinematics);

(iii) the part of mechanics that focuses on its two last tasks, i.e. the solution of the equations of motion and discussion of the results. [2]

Because of this ambiguity, after some hesitation, I have opted to use the traditional name Classical Mechanics, implying its broader meaning that includes (similarly to Quantum Mechanics and Statistical Mechanics) studies of dynamics of some non-mechanical systems as well.

---

[1] The reader is advised to perform (perhaps after reading this chapter as a reminder) a self-check by solving a few problems of the dozen listed in Sec. 1.6. If the results are not satisfactory, it may make sense to start from some remedial reading. For that, I could recommend, for example (in the alphabetical order):

- G. Fowles and G. Cassiday, Analytical Mechanics, 7^{th} ed., Brooks Cole, 2004;
- J. Marion and S. Thornton, Classical Dynamics of Particles and Systems, 5^{th} ed., Saunders, 2003;
- K. Symon, Mechanics, 3^{rd} ed., Addison-Wesley, 1971.

[2] The reader may have noticed that the last definition of dynamics is suspiciously close to the part of mathematics devoted to the differential equation analysis; what is the difference? An important bit of philosophy: physics may be defined as an art (and a bit of science :-) of describing Mother Nature by mathematical means; hence in many cases the approaches of a mathematician and a physicist to a problem are very similar. The main difference between them is that physicists try to express the results of their analyses in terms of properties of the systems under study, rather than the functions describing them, and as a result develop a sort of intuition ("gut feeling") about how other similar systems may behave, even if their exact equations of motion are somewhat different - or not known at all. The intuition so developed has an enormous heuristic power, and most discoveries in physics have been made through gut-feeling-based insights rather than by just plugging one formula into another one

---

1.2: Kinematics- Basic Notions

The basic notions of kinematics may be defined in various ways, and some mathematicians pay much attention to analyzing such systems of axioms, and relations between them. In physics, we typically stick to less rigorous ways (in order to proceed faster to particular problems) and end debating any definition as soon as "everybody in the room" agrees that we are all speaking about the same thing - at least in the context they are discussed. Let me hope that the following notions used in classical mechanics do satisfy this criterion in our "room":

(i) All the Euclidean geometry notions, including the point, the straight line, the plane, etc.

(ii) Reference frames: platforms for observation and mathematical description of physical phenomena. A reference frame includes a coordinate system used for measuring the point's position (namely, its radius vector $\mathbf{r}$ that connects the coordinate origin to the point - see Figure 1) and a clock that measures time t. A coordinate system may be understood as a certain method of expressing the radius vector $\mathbf{r}$ of a point as a set of its scalar coordinates. The most important of such systems (but by no means the only one) are the Cartesian (orthogonal, linear) coordinates ${}^3r_j$ of a point, in which its radius vector may be represented as the following sum:

$$\mathbf{r} = \sum_{j=1}^{3} \mathbf{n}_j r_j, \tag{1.2.1}$$

where $\mathbf{n}_1, \mathbf{n}_2$, and $\mathbf{n}_3$ are unit vectors directed along the coordinate axis - see Figure 1. [4]

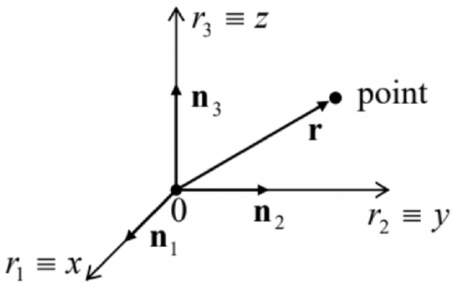

Figure 1.1. Cartesian coordinates of a point

(iii) The absolute ("Newtonian") space/time, [5] which does not depend on the matter distribution. The space is assumed to have the Euclidean metric, which may be expressed as the following relation between the length r of any radius vector $\mathbf{r}$ and its Cartesian coordinates:

$$r \equiv |\mathbf{r}| = \left(\sum_{j=1}^{3} r_j^2 \right)^{1/2} \tag{1.2.2}$$

while time t is assumed to runs similarly in all reference frames.

(iv) The (instant) velocity of the point,

Velocity

$$\mathbf{v}(t) \equiv \frac{d\mathbf{r}}{dt} \equiv \dot{\mathbf{r}}, \tag{1.2.3}$$

and its acceleration:

Acceleration

$$\begin{aligned} \mathbf{v}(t) &\equiv \tfrac{d\mathbf{r}}{dt} \equiv \dot{\mathbf{r}} \\ \mathbf{a}(t) &\equiv \tfrac{d\mathbf{v}}{dt} \equiv \dot{\mathbf{v}} = \ddot{\mathbf{r}} \end{aligned} \tag{1.2.4}$$

(v) Transfer between reference frames. The above definitions of vectors $\mathbf{r}, \mathbf{v}$, and a depend on the chosen reference frame (are "reference-frame-specific"), and we frequently need to relate those vectors as observed in different frames. Within the Euclidean

geometry, the relation between the radius vectors in two frames with the corresponding axes parallel in the moment of interest (Figure 2), is very simple:

Radius transformation

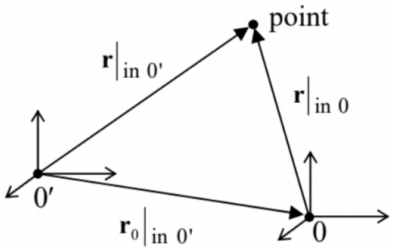

Figure 1.2. Transfer between two reference frames.

If the frames move versus each other by translation only (no mutual rotation!), similar relations are valid for the velocity and the acceleration as well:

$$\mathbf{v}|_{\text{in } 0'} = \mathbf{v}|_{\text{in } 0} + \mathbf{v}_0|_{\text{in } 0'}$$
$$\mathbf{a}|_{\text{in } 0'} = \mathbf{a}|_{\text{in } 0} + \mathbf{a}_0|_{\text{in } 0'}$$

Note that in the case of mutual rotation of the reference frames, the transfer laws for velocities and accelerations are more complex than those given by Eqs. (6) and (7). Indeed, in this case the notions like $\mathbf{v}_0|_{\text{in } 0'}$ are not well defined: different points of an imaginary rigid body connected to frame 0 may have different velocities when observed in frame 0 '. It will be more natural for me to discuss these more general relations in the end of Chapter 4 , devoted to rigid body motion.

(vi) A particle (or "point particle"): a localized physical object whose size is negligible, and the shape is irrelevant for the given problem. Note that the last qualification is extremely important. For example, the size and shape of a spaceship are not too important for the discussion of its orbital motion but are paramount when its landing procedures are being developed. Since classical mechanics neglects the quantum mechanical uncertainties, [6] in it the position of a particle, at any particular instant t, may be identified with a single geometrical point, i.e. with a single radius vector $\mathbf{r}(t)$. The formal final goal of classical mechanics is finding the laws of motion $\mathbf{r}(t)$ of all particles participating in the given problem.

---

[3] In this series, the Cartesian coordinates (introduced in 1637 by René Descartes, a.k.a. Cartesius) are denoted either as either $\{r_1, r_2, r_3\}$ or $\{x, y, z\}$, depending on convenience in each particular case. Note that axis numbering is important for operations like the vector ("cross") product; the "correct" (meaning generally accepted) numbering order is such that the rotation $\mathbf{n}_1 \to \mathbf{n}_2 \to \mathbf{n}_3 \to \mathbf{n}_1 \ldots$ looks counterclockwise if watched from a point with all $r_j > 0$ - like that shown in Figure 1 .

[4] Note that the representation (1) is also possible for locally-orthogonal but curvilinear (for example, cylindrical/polar and spherical) coordinates, which will be extensively used in this series. However, such coordinates are not Cartesian, and for them some of the relations given below are invalid - see, e.g., MA Sec. 10 .

[5] These notions were formally introduced by Sir Isaac Newton in his main work, the three-volume Philosophiae Naturalis Principia Mathematica published in 1686-1687, but are rooted in earlier ideas by Galileo Galilei, published in 1632.

[6] This approximation is legitimate when the product of the coordinate and momentum scales of the particle motion is much larger than Planck's constant $\hbar \sim 10^{-34}$ J·s . More detailed conditions of the classical mechanics' applicability depend on a particular system - see, e.g., the QM part of this series.

1.3: Dynamics- Newton Laws

Generally, the classical dynamics is fully described (in addition to the kinematic relations discussed above) by three Newton laws. In contrast to the impression some textbooks on theoretical physics try to create, these laws are experimental in nature, and cannot be derived from purely theoretical arguments.

I am confident that the reader of these notes is already familiar with the Newton laws, [7] in one or another formulation. Let me note only that in some formulations, the 1^{st} Newton law looks just as a particular case of the 2^{nd} law - when the net force acting on a particle equals zero. To avoid this duplication, the 1^{st} law may be formulated as the following postulate:

There exists at least one reference frame, called inertial, in which any free particle (i.e. a particle fully isolated from the rest of the Universe) moves with $\mathbf{v} = \text{const}$, i.e. with $\mathbf{a} = 0$.

Note that according to Eq. (7), this postulate immediately means that there is also an infinite number of inertial frames because all frames 0 ' moving without rotation or acceleration relative to the postulated inertial frame 0 (i.e. having $\mathbf{a}_0|$ in 0 , $= 0$) are also inertial.

On the other hand, the 2^{nd} and 3^{rd} Newton laws may be postulated together in the following elegant way. Each particle, say number k, may be characterized by a scalar constant (called mass m_k), such that at any interaction of N particles (isolated from the rest of the Universe), in any inertial system,

$$\mathbf{P} \equiv \sum_{k=1}^{N} \mathbf{p}_k \equiv \sum_{k=1}^{N} m_k \mathbf{v}_k = \text{ const.} \tag{1.3.1}$$

(Each component of this sum,

$$\mathbf{p}_k \equiv m_k \mathbf{v}_k, \tag{1.3.2}$$

is called the mechanical momentum [8] of the corresponding particle, while the sum $\mathbf{P}$, the total momentum of the system.)

Let us apply this postulate to just two interacting particles. Differentiating Eq. (8), written for this case, over time, we get

$$\dot{\mathbf{p}}_1 = -\dot{\mathbf{p}}_2. \tag{1.3.3}$$

Let us give the derivative $\dot{\mathbf{p}}_1$ (which is a vector) the name of force $\mathbf{F}$ exerted on particle 1 . In our current case, when the only possible source of the force is particle 2 , it may be denoted as $\mathbf{F}_{12}$: $\dot{\mathbf{p}}_1 \equiv \mathbf{F}_{12}$. Similarly, $\mathbf{F}_{21} \equiv \dot{\mathbf{p}}_2$, so that Eq. (10) becomes the 3^{rd} Newton law

$$\mathbf{F}_{12} = -\mathbf{F}_{21}. \tag{1.3.4}$$

Plugging Eq. (1.9) into these force definitions, and differentiating the products $m_k \mathbf{v}_k$, taking into account that particle masses are constants, [9] we get that for k and k ' taking any of values 1,2 ,

$$m_k \dot{\mathbf{v}}_k \equiv m_k \mathbf{a}_k = \mathbf{F}_{kk'}, \quad \text{where } k' \neq k.. \tag{1.3.5}$$

Now, returning to the general case of several interacting particles, and making an additional (but very natural) assumption that all partial forces $\mathbf{F}_{kk'}$ acting on particle k add up as vectors, we may generalize Eq. (12) into the 2^{nd} Newton law

$$m_k \mathbf{a}_k \equiv \dot{\mathbf{p}}_k = \sum_{k' \neq k} \mathbf{F}_{kk'} \equiv \mathbf{F}_k, \tag{1.3.6}$$

that allows a clear interpretation of the mass as a measure of particle's inertia.

As a matter of principle, if the dependence of all pair forces $\mathbf{F}_{kk'}$ of particle positions (and generally of time as well) is known, Eq. (13), augmented with the kinematic relations (2) and (3), allows calculation of the laws of motion $\mathbf{r}_k(t)$ of all particles of the system. For example, for one particle the 2^{nd} law (13) gives an ordinary differential equation of the second order,

$$m\ddot{\mathbf{r}} = \mathbf{F}(\mathbf{r}, t), \tag{1.3.7}$$

which may be integrated - either analytically or numerically.In certain cases, this is very simple. As an elementary example, Newton's gravity force [10]

$$\mathbf{F} = -G\frac{mm'}{R^3}\mathbf{R} \tag{1.3.8}$$

(where $\mathbf{R} \equiv \mathbf{r} - \mathbf{r}'$ is the distance between particles of masses m and m')[11], is virtually uniform and may be approximated as be approximated as

$$\mathbf{F} = m\mathbf{g} \tag{1.3.9}$$

with the vector $\mathbf{g} \equiv \left(Gm'/r'^3\right)\mathbf{r}'$ being constant, for local motions with $r << r'$.[12] As a result, m in Eq. (13) cancels, it is reduced to just $\ddot{\mathbf{r}} = \mathbf{g} =$ const, and may be easily integrated twice:

$$\dot{\mathbf{r}}(t) \equiv \mathbf{v}(t) = \int_0^t \mathbf{g}dt' + \mathbf{v}(0) = \mathbf{g}t + \mathbf{v}(0), \quad \mathbf{r}(t) = \int_0^t \mathbf{v}\,(t')\,dt' + \mathbf{r}(0) = \mathbf{g}\frac{t^2}{2} + \mathbf{v}(0)t + \mathbf{r}(0), \tag{1.3.10}$$

thus giving the generic solution of all those undergraduate problems on the projectile motion, which should be so familiar to the reader.

All this looks (and indeed is) very simple, but in most other cases, Eq. (13) leads to more complex calculations. As an example, let us think about would we use it to solve another simple problem: a bead of mass m sliding, without friction, along a round ring of radius R in a gravity field obeying Eq. (16) - see Figure 3. (This system is equivalent to the usual point pendulum, i.e. a point mass suspended from point 0 on a light rod or string, and constrained to move in one vertical plane.)

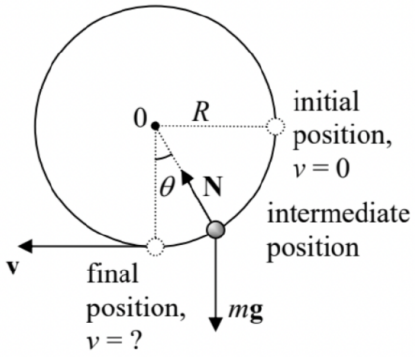

Figure 1.3. A bead sliding along a vertical ring.

Suppose we are only interested in the bead's velocity v at the lowest point, after it has been dropped from the rest at the rightmost position. If we want to solve this problem using only the Newton laws, we have to make the following steps:

(i) consider the bead in an arbitrary intermediate position on a ring, described, for example by the angle θ shown in Figure 3;

(ii) draw all the forces acting on the particle - in our current case, the gravity force mg and the reaction force $\mathbf{N}$ exerted by the ring - see Figure 3 above

(iii) write the Cartesian components of the 2nd Newton law (14) for the bead acceleration: $ma_x = N_x, ma_y = N_y - mg$,

(iv) recognize that in the absence of friction, the force $\mathbf{N}$ should be normal to the ring, so that we can use two additional equations, $N_x = -N\sin\theta$ and $N_y = N\cos\theta$;

(v) eliminate unknown variables N, N_x, and N_y from the resulting system of four equations, thus getting a single second-order differential equation for one variable, for example θ,

$$mR\ddot{\theta} = -mg\sin\theta; \tag{1.3.11}$$

(vi) use the mathematical identity $\ddot{\theta} = (d\dot{\theta}/d\theta)\dot{\theta}$ to integrate this equation over θ once to get an expression relating the velocity $\dot{\theta}$ and the angle θ; and, finally,

(vii) using our specific initial condition ($\dot{\theta} = 0$ at $\theta = \pi/2$), find the final velocity as $v = R\dot{\theta}$ at $\theta = 0$.

All this is very much doable, but please agree that the procedure it too cumbersome for such a simple problem. Moreover, in many other cases even writing equations of motion along relevant coordinates is very complex, and any help the general theory may provide is highly valuable. In many cases, such help is given by conservation laws; let us review the most general of them.

[7] Due to the genius of Sir Isaac, these laws were formulated in the same Principia (1687), well ahead of the physics of his time.

[8] The more extended term linear momentum is typically used only in cases when there is a chance of its confusion with the angular momentum of the same particle/system - see below. The present-day definition of the linear momentum and the term itself belong to John Wallis (1670), but the concept may be traced back to more vague notions of several previous scientists - all the way back to at least a 570 AD work by John Philoponus.

[9] Note that this may not be true for composite bodies of varying total mass M (e.g., rockets emitting jets, see Problem 11), in these cases the momentum's derivative may differ from $M\mathbf{a}$.

[10] Introduced in the same famous Principia!

[11] The fact that the masses participating in Eqs. (14) and (16) are equal, the so-called weak equivalence principle, is actually highly nontrivial, but has been repeatedly verified experimentally with gradually improved relative accuracy, currently reaching $\sim 10^{-14}$ - see P. Touboul et al., Phys. Rev. Lett. 119, 231101 (2017).

[12] Of course, the most important particular case of Eq. (16) is the motion of objects near the Earth's surface. In this case, using the fact that Eq. (15) remains valid for the gravity field created by a heavy sphere, we get $g = GM_{\rm E}/{R_{\rm E}}^2$, where $M_{\rm E}$ and $R_{\rm E}$ are the Earth's mass and radius. Plugging in their values, $M_{\rm E} \approx 5.97 \times 10^{24}$ kg and $R_{\rm E} \approx 6.37 \times 10^{6}$ m, we get $g \approx 9.82\ \mathrm{m/s^2}$. The experimental value of g varies from 9.78 to $9.83\ \mathrm{m/s^2}$ at various locations on Earth's surface (due to the deviations of Earth's shape from a sphere, and the location-dependent effect of the centrifugal "inertial force" - see Sec. 4.5 below), with an average value of $g \approx 9.807\ \mathrm{m/s^2}$.

1.4: Conservation Laws

(i) Energy conservation is arguably the most general law of physics, but in mechanics, it takes a more humble form of mechanical energy conservation, which has limited applicability. To derive it, we first have to define the kinetic energy of a particle as [13]

$$T \equiv \frac{m}{2} v^2 \tag{1.4.1}$$

and then recast its differential as [14]

$$dT \equiv d\left(\frac{m}{2} v^2\right) \equiv d\left(\frac{m}{2} \mathbf{v} \cdot \mathbf{v}\right) = m\mathbf{v} \cdot d\mathbf{v} = m\frac{d\mathbf{r} \cdot d\mathbf{v}}{dt} = d\mathbf{r} \cdot \frac{d\mathbf{p}}{dt}. \tag{1.4.2}$$

Now plugging in the momentum's derivative from the 2nd Newton law, $d\mathbf{p}/dt = \mathbf{F}$, where $\mathbf{F}$ is the full force acting on the particle, we get $dT = \mathbf{F} \cdot d\mathbf{r}$. The integration of this equality along the particle's trajectory connecting some points A and B gives the formula that is sometimes called the work-energy principle:

$$\Delta T \equiv T(\mathbf{r}_{\mathrm{B}}) - T(\mathbf{r}_{\mathrm{A}}) = \int_{\mathrm{A}}^{\mathrm{B}} \mathbf{F} \cdot d\mathbf{r}, \tag{1.4.3}$$

where the integral on the right-hand side is called the work of the force $\mathbf{F}$ on the path from A to B.

The following step may be made only for a potential (also called "conservative") force that may be represented as the (minus) gradient of some scalar function $U(\mathbf{r})$, called the potential energy. [15] The vector operator ∇ (called either del or nabla) of spatial differentiation [16] allows a very compact expression of this fact:

$$\mathbf{F} = -\nabla U. \tag{1.4.4}$$

For example, for the uniform gravity field (16),

$$U = mgh + \text{ const}, \tag{1.4.5}$$

where h is the vertical coordinate directed "up" - opposite to the direction of the vector $\mathbf{g}$.Integrating the tangential component F_τ of the vector $\mathbf{F}$ given by Eq. (22), along an arbitrary path connecting the points A and $\boldsymbol{B}$, we get

$$\int_{\mathrm{A}}^{\mathrm{B}} F_\tau dr \equiv \int_{\mathrm{A}}^{\mathrm{B}} \mathbf{F} \cdot d\mathbf{r} = U(\mathbf{r}_{\mathrm{A}}) - U(\mathbf{r}_{\mathrm{B}}), \tag{1.4.6}$$

i.e. work of potential forces may be represented as the difference of values of the function $U(\mathbf{r})$ in the initial and final points of the path. (Note that according to Eq. (24), the work of a potential force on any closed path, with $\mathbf{r}_{\mathrm{A}} = \mathbf{r}_{\mathrm{B}}$, is zero.)

Now returning to Eq. (21) and comparing it with Eq. (24), we see that

$$T(\mathbf{r}_{\mathrm{B}}) - T(\mathbf{r}_{\mathrm{A}}) = U(\mathbf{r}_{\mathrm{A}}) - U(\mathbf{r}_{\mathrm{B}}), \text{ i.e. } T(\mathbf{r}_{\mathrm{A}}) + U(\mathbf{r}_{\mathrm{A}}) = T(\mathbf{r}_{\mathrm{A}}) + U(\mathbf{r}_{\mathrm{A}}), \tag{1.4.7}$$

so that the total mechanical energy E, defined as

is indeed conserved:

$$E \equiv T + U,$$
$$E(\mathbf{r}_{\mathrm{A}}) \equiv E(\mathbf{r}_{\mathrm{B}}),$$

but for conservative forces only. (Non-conservative forces may change E by either transferring energy from its mechanical form to another form, e.g., to heat in the case of friction, or by pumping the energy into the system under consideration from another, "external" system.)

The mechanical energy conservation allows us to return for a second to the problem shown in Figure 3 and solve it in one shot by writing Eq. (27) for the initial and final points: [17]

$$0 + mgR = \frac{m}{2} v^2 + 0. \tag{1.4.8}$$

The (elementary) solution of Eq. (28) for v immediately gives us the desired answer. Let me hope that the reader agrees that this way of problem's solution is much simpler, and I have earned their attention to discuss other conservation laws - which may be equally effective.

(ii) Linear momentum. The conservation of the full linear momentum of any system of particles isolated from the rest of the world was already discussed in the previous section, and may serve as the basic postulate of classical dynamics - see Eq. (8). In the case of one free particle, the law is reduced to the trivial result $\mathbf{p} = \text{const}$, i.e. $\mathbf{v} = \text{const}$. If a system of N particles is affected by external forces $\mathbf{F}^{(\text{ext})}$, we may write

$$\mathbf{F}_k = \mathbf{F}_k^{(\text{ext})} + \sum_{k=1}^{N} \mathbf{F}_{kk'}. \tag{1.4.9}$$

If we sum up the resulting Eqs. (13) for all particles of the system then, due to the 3^{rd} Newton law (11), valid for any indices $k \neq k'$, the contributions of all internal forces $\mathbf{F}_{kk}$ ' to the resulting double sum on the right-hand side cancel, and we get the following equation:

$$\dot{\mathbf{P}} = \mathbf{F}^{(\text{ext})}, \qquad \text{where } \mathbf{F}^{(\text{ext})} \equiv \sum_{k=1}^{N} \mathbf{F}_k^{(\text{ext})} \tag{1.4.10}$$

It tells us that the translational motion of the system as the whole is similar to that of a single particle, under the effect of the net external force $\mathbf{F}^{(\text{ext})}$. As a simple sanity check, if the external forces have a zero sum, we return to the postulate (8). Just one reminder: Eq. (30), as its precursor Eq. (13), is only valid in an inertial reference frame.

I hope that the reader knows numerous examples of application of the linear momentum's conservation law, including all these undergraduate problems on car collisions, where the large collision forces are typically not known so that the direct application of Eq. (13) to each car is impracticable.

(iii) The angular momentum of a particle [18] is defined as the following vector: [19]

$$\mathbf{L} \equiv \mathbf{r} \times \mathbf{p} \tag{1.4.11}$$

where $\mathbf{a} \times \mathbf{b}$ means the vector (or "cross-") product of the vector operands. [20] Differentiating Eq. (31) over time, we get

$$\dot{\mathbf{L}} = \dot{\mathbf{r}} \times \mathbf{p} + \mathbf{r} \times \dot{\mathbf{p}} \tag{1.4.12}$$

In the first product, $\dot{\mathbf{r}}$ is just the velocity vector $\mathbf{v}$, parallel to the particle momentum $\mathbf{p} = m\mathbf{v}$, so that this term vanishes since the vector product of any two parallel vectors equals zero. In the second product, $\dot{\mathbf{p}}$ is equal to the full force $\mathbf{F}$ acting on the particle, so that Eq. (32) is reduced to

where the vector

$$\underline{\dot{\mathbf{L}} = \boldsymbol{\tau}, \quad \boldsymbol{\tau} \equiv \mathbf{r} \times \mathbf{F},}$$

is called the torque exerted by force $\mathbf{F}$. [21] (Note that the torque is reference-frame specific - and again, the frame has to be inertial for Eq. (33) to be valid, because we have used Eq. (13) for its derivation.) For an important particular case of a central force $\mathbf{F}$ that is directed along the radius vector $\mathbf{r}$ of a particle, the torque vanishes, so that (in that particular reference frame only!) the angular momentum is conserved:

$$\mathbf{L} = \text{ const}. \tag{1.4.13}$$

For a system of N particles, the total angular momentum is naturally defined as

$$\mathbf{L} \equiv \sum_{k=1}^{N} \mathbf{L}_k \tag{1.4.14}$$

Differentiating this equation over time, using Eq. (33) for each $\dot{\mathbf{L}}_k$, and again partitioning each force per Eq. (29), we get

$$\dot{\mathbf{L}} = \sum_{\substack{k,k'=1 \\ k' \neq k}}^{N} \mathbf{r}_k \times \mathbf{F}_{kk'} + \boldsymbol{\tau}^{(\text{ext})}, \qquad \text{where } \boldsymbol{\tau}^{(\text{ext})} \equiv \sum_{k=1}^{N} \mathbf{r}_k \times \mathbf{F}_k^{(\text{ext})} \tag{1.4.15}$$

The first (double) sum may be always divided into pairs of the type $(\mathbf{r}_k \times \mathbf{F}_{kk'} + \mathbf{r}_{k'} \times \mathbf{F}_{k'k})$. With a natural assumption of the central forces, $\mathbf{F}_{kk'} \parallel (\mathbf{r}_k - \mathbf{r}_{k'})$, each of these pairs equals zero. Indeed, in this case, each component of the pair is a vector

perpendicular to the plane containing the positions of both particles and the reference frame origin, i.e. to the plane of the drawing of Figure 4.

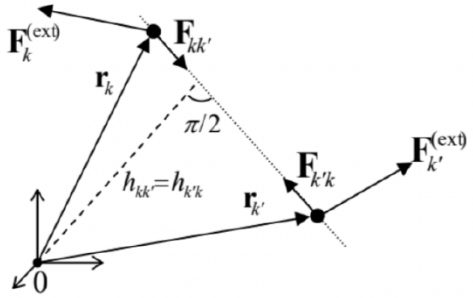

Figure 1.4. Internal and external forces, and the internal torque cancellation in a system of two particles.

Also, due to the 3^{rd} Newton law (11), these two forces are equal and opposite, and the magnitude of each term in the sum may be represented as $|F_{kk}|\, h_{kk}$, with equal to the "lever arms" $h_{kk} = h_{k'k}$. As a result, each sum $(\mathbf{r}_k \times \mathbf{F}_{kk'} + \mathbf{r}_k \times \mathbf{F}_{k'k})$, and hence the whole double sum in Eq. (37) vanish, and it is reduced to a very simple result,

$$\dot{\mathbf{L}} = \boldsymbol{\tau}^{(\mathrm{ext})} \tag{1.4.16}$$

which is similar to Eq. (33) for a single particle, and is the angular analog of Eq. (30).

In particular, Eq. (38) shows that if the full external torque $\tau^{(\mathrm{ext})}$ vanishes by some reason (e.g., if the system of particles is isolated from the rest of the Universe), the conservation law (35) is valid for the full angular momentum $\mathbf{L}$, even if its individual components $\mathbf{L}_k$ are not conserved due to interparticle interactions.

Note again that since the conservation laws may be derived from the Newton laws (as was done above), they do not introduce anything absolutely new to the dynamics of any system. Indeed, from the mathematical point of view, the conservation laws discussed above are just the first integrals of the second-order differential equations of motion following from the Newton laws, which may liberate us from the necessity to integrate the equations twice.

---

[13] In such quantitative form, the kinetic energy was introduced (under the name "living force") by Gottfried Leibniz and Johann Bernoulli (circa 1700), though its main properties (21) and (27) had not been clearly revealed until an 1829 work by Gaspard-Gustave de Coriolis. The modern term "kinetic energy" was coined only in $1849-1851$ by Lord Kelvin (born William Thomson).

[14] In these notes, $\mathbf{a}\cdot\mathbf{b}$ denotes the scalar (or "dot-") product of vectors $\mathbf{a}$ and $\mathbf{b}$ - see, e.g., MA Eq. (7.1).

[15] Note that because of its definition via the gradient, the potential energy is only defined to an arbitrary additive constant. This notion had essentially been used already by G. Leibniz, though the term we are using for it now was introduced much later (in the mid- 19^{th} century) by William Rankine.

[16] Its basic properties are listed in MA Sec. 8.

[17] Here the arbitrary constant in Eq. (23) is chosen so that the potential energy is zero in the final point.

[18] Here we imply that the internal motions of the particle, including its rotation about its axis, are negligible. (Otherwise, it could not be represented by a point, as was postulated in Sec. 1.)

[19] Such explicit definition of the angular momentum (in different mathematical forms, and under the name of "moment of rotational motion") has appeared in scientific publications only in the 1740s, though the fact of its conservation (35) in the field of central forces, in the form of the 2^{nd} Kepler law (see Figure 3.4 below), was proved by I. Newton in his Principia.

[20] See, e.g., MA Eq. (7.3).

[21] Alternatively, especially in mechanical engineering, torque is called the force moment. This notion may be traced all the way back to Archimedes' theory of levers developed in the 3^{rd} century BC.

1.5: Potential Energy and Equilibrium

Another important role of the potential energy U, especially for dissipative systems whose total mechanical energy E is not conserved because it may be drained to the environment, is finding the positions of equilibrium (sometimes called the fixed points of the system under analysis) and analyzing their stability with respect to small perturbations. For a single particle, this is very simple: the force (22) vanishes at each extremum (either minimum or maximum) of the potential energy. [22] Of those fixed points, only the minimums of $U(\mathbf{r})$ are stable - see Sec. 3.2 below for a discussion of this point.

A slightly more subtle case is a particle with potential energy $U(\mathbf{r})$, subjected to an additional external force $\mathbf{F}^{(\mathrm{ext})}(\mathbf{r})$. In this case, the stable equilibrium is reached at the minimum of not the function $U(\mathbf{r})$, but of what is sometimes called the Gibbs potential energy

$$U_{\mathrm{G}}(\mathbf{r}) \equiv U(\mathbf{r}) - \int^{\mathbf{r}} \mathbf{F}^{(\mathrm{ext})}(\mathbf{r}') \cdot d\mathbf{r}', \tag{1.5.1}$$

$$(1.39) \tag{1.5.2}$$

which is defined, just as $U(\mathbf{r})$ is, to an arbitrary additive constant. [23] The proof of Eq. (39) is very simple: in an extremum of this function, the total force acting on the particle,

$$\mathbf{F}^{(\mathrm{tot})} = \mathbf{F} + \mathbf{F}^{(\mathrm{ext})} \equiv -\nabla U + \nabla \int^{\mathbf{r}} \mathbf{F}^{(\mathrm{ext})}(\mathbf{r}') \cdot d\mathbf{r}' \equiv -\nabla U_{\mathrm{G}}, \tag{1.5.3}$$

vanishes, as it should.

Physically, the difference $U_{\mathrm{G}} - U$ specified by Eq. (39) is the $\mathbf{r}$-dependent part of the potential energy $U^{(\mathrm{ext})}$ of the external system responsible for the force $\mathbf{F}^{(\mathrm{ext})}$, so that U_{G} is just the total potential energy $U + U^{(\mathrm{ext})}$, excluding its part that does not depend on $\mathbf{r}$ and hence is irrelevant for the analysis. According to the 3rd Newton law, the force exerted by the particle on the external system equals $\left(-\mathbf{F}^{(\mathrm{ext})}\right)$, so that its work (and hence the change of $U^{(\mathrm{ext})}$ due to the change of $\mathbf{r}$) is given by the second term on the right-hand side of Eq. (39). Thus the condition of equilibrium, $-\nabla U_{\mathrm{G}} = 0$, is just the condition of an extremum of the total potential energy, $U + U^{(\mathrm{ext})} +$ const, of the two interacting systems.

For the simplest (and very frequent) case when the applied force is independent of the particle's position, the Gibbs potential energy (39) is just [24]

$$U_{\mathrm{G}}(\mathbf{r}) \equiv U(\mathbf{r}) - \mathbf{F}^{(\mathrm{ext})} \cdot \mathbf{r} + \text{ const} \tag{1.5.4}$$

As the simplest example, consider a 1D deformation of the usual elastic spring providing the returning force $(-\kappa x)$, where x is the deviation from its equilibrium. As follows from Eq. (22), its potential energy is $U = \kappa x^2/2 +$ const, so that its minimum corresponds to $x = 0$. Now let us apply an additional external force F, say independent of x. Then the equilibrium deformation of the spring, $x_0 = F/\kappa$, corresponds to the minimum of not U, but rather of the Gibbs potential energy (41), in our particular case taking the form

$$U_{\mathrm{G}} \equiv U - Fx = \frac{\kappa x^2}{2} - Fx \tag{1.5.5}$$

[22] Assuming that the additional, non-conservative forces (such as viscosity) responsible for the mechanical energy drain, vanish at equilibrium - as they typically do. (The static friction is one counter-example.)

[23] Unfortunately, in most textbooks, the association of the (unavoidably used) notion of U_{G} with the glorious name of Josiah Willard Gibbs is postponed until a course of statistical mechanics and/or thermodynamics, where U_{G} is a part of the Gibbs free energy, in contrast to U, which is a part of the Helmholtz free energy - see, e.g., SM Sec. 1.4. I use this notion throughout my series, because the difference between U_{G} and U, and hence that between the Gibbs and Helmholtz free energies, has nothing to do with statistics or thermal motion, and belongs to the whole physics, including not only mechanics but also electrodynamics and quantum mechanics.

[24] Note that Eq. (41) is a particular case of what mathematicians call the Legendre transformations.

1.6: OK, Can We Go Home Now?

Sorry, not yet. In many cases, the conservation laws discussed above provide little help, even in systems without dissipation. Consider for example a generalization of the bead-on-the-ring problem shown in Figure 3, in which the ring is rotated by external forces, with a constant angular velocity ω, about its vertical diameter. [25] In this problem (to which I will repeatedly return below, using it as an analytical mechanics "testbed"), none of the three conservation laws listed in the last section, holds. In particular, bead's energy,

$$E = \frac{m}{2}v^2 + mgh, \tag{1.6.1}$$

is not constant, because the external forces rotating the ring may change it. Of course, we still can solve the problem using the Newton laws, but this is even more complex than for the above case of the ring at rest, in particular because the force $\mathbf{N}$ exerted on the bead by the ring now may have three rather than two Cartesian components, which are not simply related. On the other hand, it is clear that the bead still has just one degree of freedom (angle θ), so that its dynamics should not be too complicated.

This fact gives the clue how situations like this one could be simplified: if we only could exclude the so-called reaction forces such as $\mathbf{N}$, that take into account the external constraints imposed on the particle motion, in advance, that should help a lot. Such a constraint exclusion may be provided by analytical mechanics, in particular its Lagrangian formulation, to which we will now proceed.

Of course, the value of the Lagrangian approach goes far beyond simple systems such as the bead on a rotating ring. Indeed, this system has just two externally imposed constrains: the fixed distance of the bead from the center of the ring, and the instant angle of rotation of the ring about its vertical diameter. Now let us consider the motion of a rigid body. It is essentially a system of a very large number, $N \gg 1$, of particles (10^{23} of them if we think about atoms in a 1-cm-scale body). If the only way to analyze its motion would be to write the Newton laws for each of the particles, the situation would be completely hopeless. Fortunately, the number of constraints imposed on its motion is almost similarly huge. (At negligible deformations of the body, the distances between each pair of its particles should be constant.) As a result, the number of actual degrees of freedom of such a body is small (at negligible deformations, just six - see Sec. 6.1), so that with the kind help from analytical mechanics, the motion of the body may be, in many important cases, analyzed even without numerical calculations.

One more important motivation for analytical mechanics is given by dynamics of "nonmechanical" systems, for example, of the electromagnetic field - possibly interacting with charged particles, conducting bodies, etc. In many such systems, the easiest (and sometimes the only practicable) way to find the equations of motion is to derive them from either the Lagrangian or Hamiltonian function of the system. Moreover, the Hamiltonian formulation of the analytical mechanics (to be discussed in Chapter 10) offers a direct pathway to deriving quantum-mechanical Hamiltonian operators of various systems, which are necessary for the analysis of their quantum properties.

---

[25] This is essentially a simplified model of the mechanical control device called the centrifugal (or "flyball", or "centrifugal flyball") governor - see, e.g., http://en.wikipedia.org/wiki/Centrifugal governor. (Sometimes the device is called the "Watt's governor", after the famous James Watts who used it in 1788 in one of his first steam engines, but it had been used in European windmills at least since the early 1600s.) Just as a curiosity: the nowubiquitous term cybernetics was coined by Norbert Wiener in 1948 from the word "governor" (or rather from its ancient-Greek original κυβ\varepsilon\rhovν\tauης) exactly in this meaning because it had been the first well-studied control device.

1.7: Self-test Problems

1.1. A bicycle, ridden with velocity v on a wet pavement, has no mudguards on its wheels. How far behind should the following biker ride to avoid being splashed over? Neglect the air resistance effects.

1.2. Two round disks of radius R are firmly connected with a coaxial cylinder of a smaller radius r, and a thread is wound on the resulting spool. The spool is placed on a horizontal surface, and the thread's end is being pooled out at angle φ - see the figure on the right. Assuming that the spool does not slip on the surface, what direction would it roll?

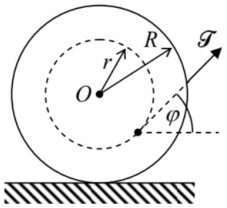

1.3.* Calculate the equilibrium shape of a flexible, heavy rope of length l, with a constant mass μ per unit length, if it is hung in a uniform gravity field between two points separated by a horizontal distance d - see the figure on the right.

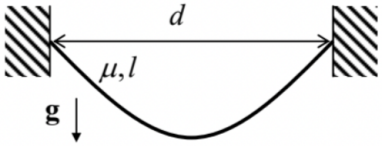

1.4. A uniform, long, thin bar is placed horizontally on two similar round cylinders rotating toward each other with the same angular velocity ω and displaced by distance $d-$ see the figure on the right. Calculate the laws of relatively slow horizontal motion of the bar within the plane of the drawing, for both possible directions of cylinder rotation, assuming that the friction force between the slipping surfaces of the bar and each cylinder obeys the simple Coulomb approximation [26] $|F| = \mu N$, where N is the normal pressure force between them, and μ is a constant (velocity-independent) coefficient. Formulate the condition of validity of your result.

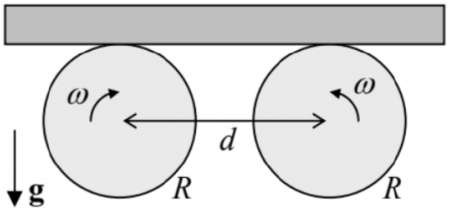

1.5. A small block slides, without friction, down a smooth slide that ends with a round loop of radius R - see the figure on the right. What smallest initial height h allows the block to make its way around the loop without dropping from the slide if it is launched with negligible initial velocity?

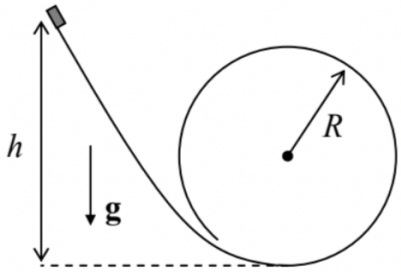

1.6. A satellite of mass m is being launched from height H over the surface of a spherical planet with radius R and mass $M \gg m-$ see the figure on the right. Find the range of initial velocities $\mathbf{v}_0$ (normal to the radius) providing closed orbits above the planet's surface.

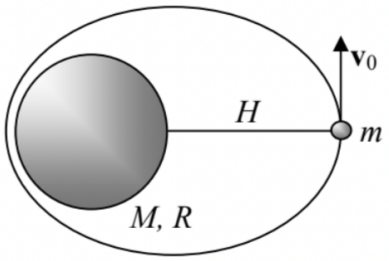

1.7. Prove that the thin-uniform-disk model of a galaxy describes small harmonic oscillations of stars inside it along the direction normal to the disk, and calculate the frequency of these oscillations in terms of Newton's gravitational constant G and density ρ of the disk's matter.

1.8. Derive differential equations of motion for small oscillations of two similar pendula coupled with a spring (see the figure on the right), within their common vertical plane. Assume that at the vertical position of both pendula, the spring is not stretched $(\Delta L = 0)$.

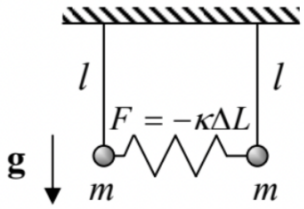

1.9. One of the popular futuristic concepts of travel is digging a straight railway tunnel through the Earth and letting a train go through it, without initial velocity - driven only by gravity. Calculate the train's travel time through such a tunnel, assuming that the Earth's density ρ is constant, and neglecting the friction and planet-rotation effects.

1.10. A small bead of mass m may slide, without friction, along a light string, stretched with a force $\mathcal{T} \gg mg$, between two points separated by a horizontal distance $2d-$ see the figure on the right. Calculate the frequency of horizontal oscillations of the bead about its equilibrium position.

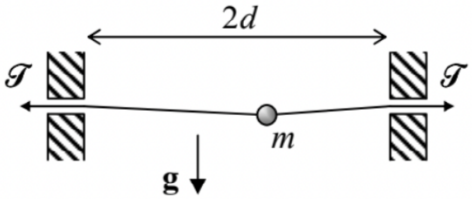

1.11. For a rocket accelerating due to its working jet motor (and hence spending the jet fuel), calculate the relation between its velocity and the remaining mass.

Hint: For the sake of simplicity, consider the 1D motion.

1.12. Prove the following virial theorem: [27] for a set of N particles performing a periodic motion,

$$\bar{T} = -\frac{1}{2}\sum_{k=1}^{N} \overline{\mathbf{F}_k \cdot \mathbf{r}_k}, \tag{1.7.1}$$

where the top bar means averaging over time - in this case over the motion period. What does the virial theorem say about:

(i) a 1D motion of a particle in the confining potential28 $U(x) = ax^{2s}$, with $a > 0$ and $s > 0$, and

(ii) an orbital motion of a particle in the central potential $U(r) = -C/r$?

Hint: Explore the time derivative of the following scalar function of time: $G(t) \equiv \sum_{k=1}^{N} \mathbf{p}_k \cdot \mathbf{r}_k$.

[26] It was suggested in 1785 by the same Charles-Augustin de Coulomb who has discovered the famous Coulomb law of electrostatics, and hence pioneered the whole quantitative science of electricity - see EM Ch. 1.

[27] It was first stated by Rudolf Clausius in 1870 .

[28] Here and below I am following the (regretful) custom of using the single word "potential" for the potential energy of the particle - just for brevity. This custom is also common in quantum mechanics, but in electrodynamics these two notions should be clearly distinguished - as they are in the EM part of this series.

CHAPTER OVERVIEW

2: Lagrangian Analytical Mechanics

The goal of this chapter is to describe the Lagrangian formalism of analytical mechanics, which is extremely useful for obtaining the differential equations of motion (and sometimes their first integrals) not only for mechanical systems with holonomic constraints but also some other dynamic systems.

2.1: Lagrange Equation

In many cases, the constraints imposed on the 3D motion of a system of N particles may be described by N vector (i.e. $3N$ scalar) algebraic equations

$$\mathbf{r}_k = \mathbf{r}_k\left(q_1, q_2, \ldots, q_j, \ldots, q_J, t\right), \quad \text{with } 1 \le k \le N, \tag{2.1.1}$$

where q_j are certain generalized coordinates that (together with constraints) completely define the system position. Their number $J \le 3N$ is called the number of the actual degrees of freedom of the system. The constraints that allow such description are called holonomic. [1]

For example, for the problem discussed briefly in Section 1.5, namely the bead sliding along a rotating ring (Figure 1), $J = 1$, because with the constraints imposed by the ring, the bead's position is uniquely determined by just one generalized coordinate - for example, its polar angle θ.

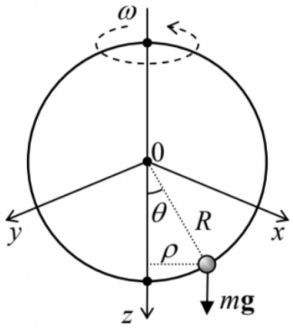

Figure 2.1. A bead on a rotating ring as an example of a system with just one degree of freedom $(J = 1)$.

Indeed, selecting the reference frame as shown in Figure 1 and using the well-known formulas for the spherical coordinates, [2] we see that in this case, Eq. (1) has the form

$$\mathbf{r} \equiv \{x, y, z\} = \{R\sin\theta\cos\varphi, R\sin\theta\sin\varphi, R\cos\theta\}, \quad \text{where } \varphi = \omega t + \text{ const}, \tag{2.1.2}$$

with the last constant depending on the exact selection of the axes x and y and the time origin. Since the angle φ, in this case, is a fixed function of time, and R is a fixed constant, the particle's position in space at any instant t is completely determined by the value of its only generalized coordinate θ. (Note that its dimensionality is different from that of Cartesian coordinates!)

Now returning to the general case of J degrees of freedom, let us consider a set of small variations (alternatively called "virtual displacements") δq_j allowed by the constraints. Virtual displacements differ from the actual small displacements (described by differentials dq_j proportional to time variation dt) in that δq_j describes not the system's motion as such, but rather its possible variation see Figure 1 .

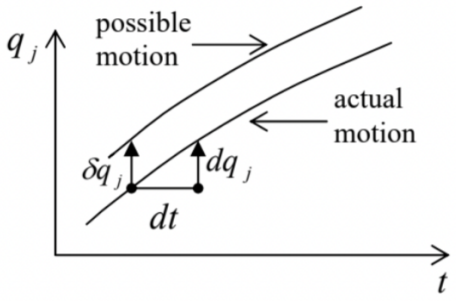

Figure 2.2. Actual displacement dq_j vs. the virtual one (i.e. variation) δq_j.

Generally, operations with variations are the subject of a special field of mathematics, the calculus of variations. [3] However, the only math background necessary for our current purposes is the understanding that operations with variations are similar to those with the usual differentials, though we need to watch carefully what each variable is a function of. For example, if we consider the variation of the radius vectors (1), at a fixed time t, as a function of independent variations δq_j, we may use the usual formula for the differentiation of a function of several arguments: [4]

$$\delta \mathbf{r}_k = \sum_j \frac{\partial \mathbf{r}_k}{\partial q_j} \delta q_j. \tag{2.1.3}$$

Now let us break the force acting upon the k^{th} particle into two parts: the frictionless, constraining part $\mathbf{N}_k$ of the reaction force and the remaining part $\mathbf{F}_k$ - including the forces from other sources and possibly the friction part of the reaction force. Then the 2^{nd} Newton law for the k^{th} particle of the system may be rewritten as

$$m_k \dot{\mathbf{v}}_k - \mathbf{F}_k = \mathbf{N}_k. \tag{2.1.4}$$

Since any variation of the motion has to be allowed by the constraints, its $3N$-dimensional vector with N 3D-vector components $\delta \mathbf{r}_k$ has to be perpendicular to the $3N$-dimensional vector of the constraining forces, also with N 3D-vector components $\mathbf{N}_k$. (For example, for the problem shown in Figure 2.1, the virtual displacement vector $\delta \mathbf{r}_k$ may be directed only along the ring, while the constraining force $\mathbf{N}$, exerted by the ring, has to be perpendicular to that direction.) This condition may be expressed as

$$\sum_k \mathbf{N}_k \cdot \delta \mathbf{r}_k = 0 \tag{2.1.5}$$

where the scalar product of $3N$-dimensional vectors is defined exactly like that of 3D vectors, i.e. as the sum of the products of the corresponding components of the operands. The substitution of Eq. (4) into Eq. (5) results in the so-called D 'Alembert principle: [5]

$$\sum_k (m_k \dot{\mathbf{v}}_k - \mathbf{F}_k) \cdot \delta \mathbf{r}_k = 0 \tag{2.1.6}$$

Now we may plug Eq. (3) into Eq. (6) to get

$$\sum_j \left\{ \sum_k m_k \dot{\mathbf{v}}_k \cdot \frac{\partial \mathbf{r}_k}{\partial q_j} - \mathscr{F}_j \right\} \delta q_j = 0, \tag{2.1.7}$$

where the scalars $\mathscr{J}_j$, called the generalized forces, are defined as follows: [6]

Generalized force

$$\mathscr{F}_j \equiv \sum_k \mathbf{F}_k \cdot \frac{\partial \mathbf{r}_k}{\partial q_j}. \tag{2.1.8}$$

Now we may use the standard argument of the calculus of variations: for the left-hand side of Eq. (7) to be zero for an arbitrary selection of independent variations δq_j, the expressions in the curly brackets, for every j, should equal zero. This gives us the desired set of $J \leq 3N$ equations

$$\sum_k m_k \dot{\mathbf{v}}_k \cdot \frac{\partial \mathbf{r}_k}{\partial q_j} - \mathscr{F}_j = 0; \tag{2.1.9}$$

what remains is just to recast them in a more convenient form.

First, using the differentiation by parts to calculate the following time derivative:

$$\frac{d}{dt}\left(\mathbf{v}_k \cdot \frac{\partial \mathbf{r}_k}{\partial q_j} \right) = \dot{\mathbf{v}}_k \cdot \frac{\partial \mathbf{r}_k}{\partial q_j} + \mathbf{v}_k \cdot \frac{d}{dt}\left(\frac{\partial \mathbf{r}_k}{\partial q_j} \right), \tag{2.1.10}$$

we may notice that the first term on the right-hand side is exactly the scalar product in the first term of Eq. (9).

Second, let us use another key fact of the calculus of variations (which is, essentially, evident from Figure 3): the differentiation of a variable over time and over the generalized coordinate variation (at a fixed time) are interchangeable operations. As a result, in the second term on the right-hand side of Eq. (10) we may write

$$\frac{d}{dt}\left(\frac{\partial \mathbf{r}_k}{\partial q_j} \right) = \frac{\partial}{\partial q_j}\left(\frac{d\mathbf{r}_k}{dt} \right) \equiv \frac{\partial \mathbf{v}_k}{\partial q_j} \tag{2.1.11}$$

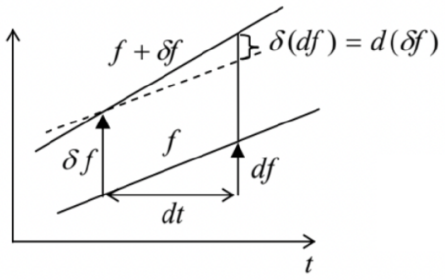

Figure 2.3. The variation of the differential (of any smooth function f) is equal to the differential of its variation.

Finally, let us differentiate Eq. (1) over time:

$$\mathbf{v}_k \equiv \frac{d\mathbf{r}_k}{dt} = \sum_j \frac{\partial \mathbf{r}_k}{\partial q_j}\dot{q}_j + \frac{\partial \mathbf{r}_k}{\partial t}. \tag{2.1.12}$$

This equation shows that particle velocities $\mathbf{v}_k$ may be considered to be linear functions of the generalized velocities $\dot{q}_j$ considered as independent variables, with proportionality coefficients

$$\frac{\partial \mathbf{v}_k}{\partial \dot{q}_j} = \frac{\partial \mathbf{r}_k}{\partial q_j}. \tag{2.1.13}$$

With the account of Eqs. (10), (11), and (13), Eq. (9) turns into

$$\frac{d}{dt}\sum_k m_k \mathbf{v}_k \cdot \frac{\partial \mathbf{v}_k}{\partial \dot{q}_j} - \sum_k m_k \mathbf{v}_k \cdot \frac{\partial \mathbf{v}_k}{\partial q_j} - \mathscr{F}_j = 0 \tag{2.1.14}$$

This result may be further simplified by making, for the total kinetic energy of the system,

$$T \equiv \sum_k \frac{m_k}{2} v_k^2 = \frac{1}{2}\sum_k m_k \mathbf{v}_k \cdot \mathbf{v}_k, \tag{2.1.15}$$

the same commitment as for $\mathbf{v}_k$, i.e. considering T a function of not only the generalized coordinates q_j and time t but also of the generalized velocities $\dot{q}_i$ – as variables independent of q_j and t. Then we may calculate the partial derivatives of T as

$$\frac{\partial T}{\partial q_j} = \sum_k m_k \mathbf{v}_k \cdot \frac{\partial \mathbf{v}_k}{\partial q_j}, \quad \frac{\partial T}{\partial \dot{q}_j} = \sum_k m_k \mathbf{v}_k \cdot \frac{\partial \mathbf{v}_k}{\partial \dot{q}_j} \tag{2.1.16}$$

and notice that they are exactly the two sums participating in Eq. (14). As a result, we get a system of J Lagrange equations, [7]

$$\frac{d}{dt}\frac{\partial T}{\partial \dot{q}_j} - \frac{\partial T}{\partial q_j} - \mathscr{F}_j = 0, \quad \text{for } j = 1, 2, \ldots, J \tag{2.1.17}$$

Their big advantage over the initial Newton law equations (4) is that the Lagrange equations do not include the constraining forces $\mathbf{N}_k$, and thus there are only J of them - typically much fewer than $3N$.

This is as far as we can go for arbitrary forces. However, if all the forces may be expressed in the form similar to, but somewhat more general than Eq. (1.22), $\mathbf{F}_k = -\nabla_k U(\mathbf{r}_1, \mathbf{r}_2, \ldots, \mathbf{r}_N, t)$, where U is the effective potential energy of the system, [8] and ∇_k denotes the spatial differentiation over coordinates of the k^{th} particle, we may recast Eq. (8) into a simpler form:

$$\mathscr{T}_j \equiv \sum_k \mathbf{F}_k \cdot \frac{\partial \mathbf{r}_k}{\partial q_j} = -\sum_k \left(\frac{\partial U}{\partial x_k}\frac{\partial x_k}{\partial q_j} + \frac{\partial U}{\partial y_k}\frac{\partial y_k}{\partial q_j} + \frac{\partial U}{\partial z_i}\frac{\partial z_i}{\partial q_j} \right) \equiv -\frac{\partial U}{\partial q_j}. \tag{2.1.18}$$

Since we assume that U depends only on particle coordinates (and possibly time), but not velocities: $\partial U/\partial \dot{q}_j = 0$, with the substitution of Eq. (18), the Lagrange equation (17) may be represented in the socalled canonical form:

$$\frac{d}{dt}\frac{\partial L}{\partial \dot{q}_j} - \frac{\partial L}{\partial q_j} = 0, \tag{2.1.19}$$

where L is the Lagrangian function (sometimes called just the "Lagrangian"), defined as

$$L \equiv T - U. \tag{2.1.20}$$

(It is crucial to distinguish this function from the mechanical energy (1.26), $E = T + U$.)

Note also that according to Eq. (2.18), for a system under the effect of an additional generalized external force $\mathscr{T}_j(t)$ we have to use, in all these relations, not the internal potential energy $U^{(\mathrm{int})}$ of the system, but its Gibbs potential energy $U \equiv U^{(\mathrm{int})} - \mathscr{J}_j q_j -$ see the discussion in Sec. 1.4.

Using the Lagrangian approach in practice, the reader should always remember that, first, each system has only one Lagrange function (19b), but is described by $J \geq 1$ Lagrange equations (19a), with j taking values $1, 2, \ldots, J$, and second, that differentiating the function L, we have to consider the generalized velocities as its independent arguments, ignoring the fact they are actually the time derivatives of the generalized coordinates.

---

[1] Possibly, the simplest counter-example of a non-holonomic constraint is a set of inequalities describing the hard walls confining the motion of particles in a closed volume. Non-holonomic constraints are better dealt with other methods, e.g., by imposing proper boundary conditions on the (otherwise unconstrained) motion.

[2] See, e.g., MA Eq. (10.7).

[3] For a concise introduction to the field see, e.g., either I. Gelfand and S. Fomin, Calculus of Variations, Dover, 2000 , or L. Elsgolc, Calculus of Variations, Dover, 2007. An even shorter review may be found in Chapter 17 of Arfken and Weber - see MA Sec. 16. For a more detailed discussion, using many examples from physics, see R. Weinstock, Calculus of Variations, Dover, 2007.

[4] See, e.g., MA Eq. (4.2). In all formulas of this section, all summations over j are from 1 to J, while those over the particle number k are from 1 to N, so that for the sake of brevity, these limits are not explicitly specified.

[5] It was spelled out in a 1743 work by Jean le Rond d'Alembert, though the core of this result has been traced to an earlier work by Jacob (Jean) Bernoulli (1667 - 1748) - not to be confused with his son Daniel Bernoulli (17001782) who is credited, in particular, for the Bernoulli equation for ideal fluids, to be discussed in Sec. 8.4 below.

[6] Note that since the dimensionality of generalized coordinates may be arbitrary, that of generalized forces may also differ from the newton.

[7] They were derived in 1788 by Joseph-Louis Lagrange, who pioneered the whole field of analytical mechanics not to mention his key contributions to the number theory and celestial mechanics.

[8] Note that due to the possible time dependence of U, Eq. (17) does not mean that the forces $\mathbf{F}_k$ have to be conservative - see the next section for more discussion. With this understanding, I will still use for function U the convenient name of "potential energy".

2.2: Three Simple Examples

As the first, simplest example, consider a particle constrained to move along one axis (say, x):

$$T = \frac{m}{2}\dot{x}^2, \quad U = U(x,t). \tag{2.2.1}$$

In this case, it is natural to consider x as the (only) generalized coordinate, and $\dot{x}$ as the generalized velocity, so that

$$L \equiv T - U = \frac{m}{2}\dot{x}^2 - U(x,t). \tag{2.2.2}$$

Considering $\dot{x}$ as an independent variable, we get $\partial L/\partial \dot{x} = m\dot{x}$, and $\partial L/\partial x = -\partial U/\partial x$, so that Eq. (19) (the only Lagrange equation in this case of the single degree of freedom!) yields

$$\frac{d}{dt}(m\dot{x}) - \left(-\frac{\partial U}{\partial x}\right) = 0 \tag{2.2.3}$$

evidently the same result as the x-component of the 2^{nd} Newton law with $F_x = -\partial U/\partial x$. This example is a good sanity check, but it also shows that the Lagrange formalism does not provide too much advantage in this particular case.

Such an advantage is, however, evident for our testbed problem - see Figure 1. Indeed, taking the polar angle θ for the (only) generalized coordinate, we see that in this case, the kinetic energy depends not only on the generalized velocity but also on the generalized coordinate: 9

$$T = \frac{m}{2}R^2\left(\dot{\theta}^2 + \omega^2 \sin^2\theta\right), \quad U = -mgz + \text{ const } \equiv -mgR\cos\theta + \text{ const },$$
$$L \equiv T - U = \frac{m}{2}R^2\left(\dot{\theta}^2 + \omega^2 \sin^2\theta\right) + mgR\cos\theta + \text{ const}.$$

Here it is especially important to remember that at substantiating the Lagrange equation, θ and $\dot{\theta}$ have to be treated as independent arguments of L, so that

$$\frac{\partial L}{\partial \dot{\theta}} = mR^2\dot{\theta}, \quad \frac{\partial L}{\partial \theta} = mR^2\omega^2 \sin\theta\cos\theta - mgR\sin\theta, \tag{2.2.4}$$

giving us the following equation of motion:

$$\frac{d}{dt}\left(mR^2\dot{\theta}\right) - \left(mR^2\omega^2 \sin\theta\cos\theta - mgR\sin\theta\right) = 0. \tag{2.2.5}$$

As a sanity check, at $\omega = 0$, Eq. (25) is reduced to the equation (1.18) of the usual pendulum:

$$\ddot{\theta} + \Omega^2 \sin\theta = 0, \quad \text{where } \Omega \equiv \left(\frac{g}{R}\right)^{1/2}. \tag{2.2.6}$$

We will explore the full dynamic equation (25) in more detail later, but please note how simple its derivation was - in comparison with writing the 3D Newton law and then excluding the reaction force.

Next, though the Lagrangian formalism was derived from the Newton law for mechanical systems, the resulting equations (19) are applicable to other dynamic systems, especially those for which the kinetic and potential energies may be readily expressed via some generalized coordinates. As the simplest example, consider the well-known connection (Figure 4) of a capacitor with capacitance C to an inductive coil with self-inductance $\mathscr{L}^0$ (Electrical engineers frequently call it the LC tank circuit.)

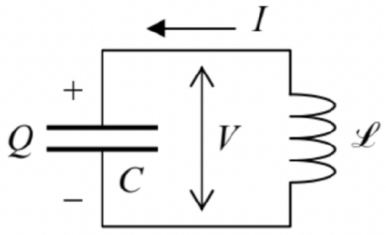

Figure 2.4. LC tank circuit.

As the reader (hopefully :-) knows, at relatively low frequencies we may use the so-called lumped-circuit approximation, in which the total energy of the system is the sum of two components, the electric energy $E_{\rm e}$ localized inside the capacitor, and the magnetic energy $E_{\rm m}$ localized inside the inductance coil:

$$E_{\rm e} = \frac{Q^2}{2C}, \quad E_{\rm m} = \frac{\mathscr{L} I^2}{2}. \tag{2.2.7}$$

Since the electric current I through the coil and the electric charge Q on the capacitor are connected by the charge continuity equation $dQ/dt = I$ (evident from Figure 4), it is natural to declare the charge the generalized coordinate of the system, and the current, its generalized velocity. With this choice, the electrostatic energy $E_{\rm e}(Q)$ may be treated as the potential energy U of the system, and the magnetic energy $E_{\rm m}(I)$, as its kinetic energy T. With this attribution, we get

$$\frac{\partial T}{\partial \dot{q}} \equiv \frac{\partial E_{\rm m}}{\partial I} = \mathscr{L} I \equiv \mathscr{L} \dot{Q}, \quad \frac{\partial T}{\partial q} \equiv \frac{\partial E_{\rm m}}{\partial Q} = 0, \quad \frac{\partial U}{\partial q} \equiv \frac{\partial E_{\rm e}}{\partial Q} = \frac{Q}{C}, \tag{2.2.8}$$

so that the Lagrange equation (19) becomes

$$\frac{d}{dt}(\mathscr{L}\dot{Q}) - \left(-\frac{Q}{C}\right) = 0. \tag{2.2.9}$$

Note, however, that the above choice of the generalized coordinate and velocity is not unique. Instead, one can use, as the generalized coordinate, the magnetic flux Φ through the inductive coil, related to the common voltage V across the circuit (Figure 4) by Faraday's induction law $V = -d\Phi/dt$. With this choice, $(-V)$ becomes the generalized velocity, $E_{\rm m} = \Phi^2/2\mathscr{L}$ should be understood as the potential energy, and $E_{\rm e} = CV^2/2$ treated as the kinetic energy. For this choice, the resulting Lagrange equation of motion is equivalent to Eq. (29). If both parameters of the circuit, $\mathscr{L}$ and C, are constant in time, Eq. (29) is just the harmonic oscillator equation and describes sinusoidal oscillations with the frequency

$$\omega_0 = \frac{1}{(\mathscr{L}C)^{1/2}}. \tag{2.2.10}$$

This is of course a well-known result, which may be derived in a more standard way - by equating the voltage drops across the capacitor $(V = Q/C)$ and the inductor $\left(V = -\mathscr{L} dI/dt \equiv -\mathrm{l} d^2Q/dt^2\right)$. However, the Lagrangian approach is much more convenient for more complex systems - for example, for the general description of the electromagnetic field and its interaction with charged particles. [11]

---

[9] The above expression for $T \equiv (m/2)\left(\dot{x}^2 + \dot{y}^2 + \dot{z}^2\right)$ may be readily obtained either by the formal differentiation of Eq. (2) over time, or just by noticing that the velocity vector has two perpendicular components: one (of magnitude $R\dot{\theta}$) along the ring, and another one (of magnitude $\omega\rho = \omega R \sin\theta$) normal to the ring's plane.

[10] A fancy font is used here to avoid any chance of confusion between the inductance and the Lagrange function.

[11] See, e.g., EM Secs. 9.7 and 9.8.

2.3: Hamiltonian Function and Energy

The canonical form (19) of the Lagrange equation has been derived using Eq. (18), which is formally similar to Eq. (1.22) for a potential force. Does this mean that the system described by Eq. (19) always conserves energy? Not necessarily, because the "potential energy" U that participates in Eq. (18), may depend not only on the generalized coordinates but on time as well. Let us start the analysis of this issue with the introduction of two new (and very important!) notions: the generalized momentum corresponding to each generalized coordinate q_j,

$$p_j \equiv \frac{\partial L}{\partial \dot{q}_j}, \tag{2.3.1}$$

and the Hamiltonian function 12

$$H \equiv \sum_j \frac{\partial L}{\partial \dot{q}_j}\dot{q}_j - L \equiv \sum_j p_j \dot{q}_j - L. \tag{2.3.2}$$

To see whether the Hamiltonian function is conserved during the motion, let us differentiate both sides of its definition (32) over time:

$$\frac{dH}{dt} = \sum_j \left[\frac{d}{dt}\left(\frac{\partial L}{\partial \dot{q}_j}\right)\dot{q}_j + \frac{\partial L}{\partial \dot{q}_j}\ddot{q}_j\right] - \frac{dL}{dt}. \tag{2.3.3}$$

If we want to make use of the Lagrange equation (19), the last derivative has to be calculated considering L as a function of independent arguments q_j, $\dot{q}_j$, and t, so that

$$\frac{dL}{dt} = \sum_j \left(\frac{\partial L}{\partial q_j}\dot{q}_j + \frac{\partial L}{\partial \dot{q}_j}\ddot{q}_j\right) + \frac{\partial L}{\partial t}, \tag{2.3.4}$$

where the last term is the derivative of L as an explicit function of time. We see that the last term in the square brackets of Eq. (33) immediately cancels with the last term in the parentheses of Eq. (34). Moreover, using the Lagrange equation (19a) for the first term in the square brackets of Eq. (33), we see that it cancels with the first term in the parentheses of Eq. (34). As a result, we arrive at a very simple and important result:

$$\frac{dH}{dt} = -\frac{\partial L}{\partial t}. \tag{2.3.5}$$

The most important corollary of this formula is that if the Lagrangian function does not depend on time explicitly $(\partial L/\partial t = 0)$, the Hamiltonian function is an integral of motion:

$$H = \text{ const}. \tag{2.3.6}$$

Let us see how this works, using the first two examples discussed in the previous section. For a 1D particle, the definition (31) of the generalized momentum yields

$$p_x \equiv \frac{\partial L}{\partial v} = mv, \tag{2.3.7}$$

so that it coincides with the usual linear momentum - or rather with its x-component. According to Eq. (32), the Hamiltonian function for this case (with just one degree of freedom) is

$$H \equiv p_x v - L = p_x \frac{p_x}{m} - \left(\frac{m}{2}\dot{x}^2 - U\right) = \frac{p_x^2}{2m} + U, \tag{2.3.8}$$

i.e. coincides with particle's mechanical energy $E = T + U$. Since the Lagrangian does not depend on time explicitly, both H and E are conserved.

However, it is not always that simple! Indeed, let us return again to our testbed problem (Figure 1). In this case, the generalized momentum corresponding to the generalized coordinate θ is

$$p_\theta \equiv \frac{\partial L}{\partial \dot{\theta}} = mR^2\dot{\theta}, \tag{2.3.9}$$

and Eq. (32) yields:

$$H \equiv p_\theta \dot{\theta} - L = mR^2\dot{\theta}^2 - \left[\frac{m}{2}R^2\left(\dot{\theta}^2 + \omega^2 \sin^2\theta\right) + mgR\cos\theta\right] + \text{const}$$
$$\equiv \frac{m}{2}R^2\left(\dot{\theta}^2 - \omega^2\sin^2\theta\right) - mgR\cos\theta + \text{const}.$$

This means that (as soon as $\omega \neq 0$), the Hamiltonian function differs from the mechanical energy

$$E \equiv T + U = \frac{m}{2}R^2\left(\dot{\theta}^2 + \omega^2\sin^2\theta\right) - mgR\cos\theta + \text{const} \tag{2.3.10}$$

The difference, $E - H = mR^2\omega^2\sin^2\theta$ (besides an inconsequential constant), may change at bead's motion along the ring, so that although H is an integral of motion (since $\partial L/\partial t = 0$), the energy is not conserved.In this context, let us find out when these two functions, E and H, do coincide. In mathematics, there is a notion of a homogeneous function $f(x_1, x_2, \ldots)$ of degree λ, defined in the following way: for an arbitrary constant a,

$$f(ax_1, ax_2, \ldots) = a^\lambda f(x_1, x_2, \ldots). \tag{2.3.11}$$

Such functions obey the following Euler theorem: 13

$$\sum_j \frac{\partial f}{\partial x_j}x_j = \lambda f, \tag{2.3.12}$$

which may be readily proved by differentiating both parts of Eq. (42) over a and then setting this parameter to the particular value $a = 1$. Now, consider the case when the kinetic energy is a quadratic form of all generalized velocities $\dot{q}_j$:

$$T = \sum_{j,j'} t_{jj'}(q_1, q_2, \ldots, t)\,\dot{q}_j\dot{q}_{j'} \tag{2.3.13}$$

with no other terms. It is evident that such T satisfies the definition of a homogeneous function of the velocities with $\lambda = 2$, [14] so that the Euler theorem (43) gives

$$\sum_j \frac{\partial T}{\partial \dot{q}_j}\dot{q}_j = 2T. \tag{2.3.14}$$

But since U is independent of the generalized velocities, $\partial L/\partial\dot{q}_j = \partial T/\partial\dot{q}_j$, and the left-hand side of Eq. (45) is exactly the first term in the definition (32) of the Hamiltonian function, so that in this case

$$H = 2T - L = 2T - (T - U) = T + U = E. \tag{2.3.15}$$

So, for a system with a kinetic energy of the type (44), for example, a free particle with T considered as a function of its Cartesian velocities,

$$T = \frac{m}{2}\left(v_x^2 + v_y^2 + v_z^2\right), \tag{2.3.16}$$

the notions of the Hamiltonian function and the mechanical energy are identical. Indeed, some textbooks, very regrettably, do not distinguish these notions at all! However, as we have seen from our bead-on-the-rotating-ring example, these variables do not always coincide. For that problem, the kinetic energy, in addition to the term proportional to $\dot{\theta}^2$, has another, velocity-independent term – see the first of Eqs. (23) - and hence is not a quadratic-homogeneous function of the angular velocity, giving $E \neq H$.

Thus, Eq. (36) expresses a new conservation law, generally different from that of mechanical energy conservation.

---

[12] It is named after Sir William Rowan Hamilton, who developed his approach to analytical mechanics in 1833, on the basis of the Lagrangian mechanics. This function is sometimes called just the "Hamiltonian", but it is advisable to use the full term "Hamiltonian function" in classical mechanics, to distinguish it from the Hamiltonian operator used in quantum mechanics. (Their relation will be discussed in Sec. 10.1 below.)

[13] This is just one of many theorems bearing the name of their author - the genius mathematician Leonhard Euler (1707-1783).

[14] Such functions are called quadratic-homogeneous.

[15] Such coordinates are frequently called cyclic, because in some cases (like in the second example considered below) they represent periodic coordinates such as angles. However, this terminology is misleading, because some "cyclic" coordinates (e.g., x in our first example) have nothing to do with rotation.

2.4: Other Conservation Laws

Looking at the Lagrange equation (19), we immediately see that if $L \equiv T - U$ is independent of some generalized coordinate q_j, $\partial L/\partial q_j = 0$, [15] then the corresponding generalized momentum is an integral of motion: 16

$$p_j \equiv \frac{\partial L}{\partial \dot{q}_j} = \text{const}. \tag{2.4.1}$$

For example, for a 1D particle with the Lagrangian (21), the momentum p_x is conserved if the potential energy is constant (and hence the x-component of force is zero) - of course. As a less obvious example, let us consider a 2D motion of a particle in the field of central forces. If we use polar coordinates r and φ in the role of generalized coordinates, the Lagrangian function, [17]

$$L \equiv T - U = \frac{m}{2}\left(\dot{r}^2 + r^2\dot{\varphi}^2\right) - U(r), \tag{2.4.2}$$

is independent of φ and hence the corresponding generalized momentum,

$$p_\varphi \equiv \frac{\partial L}{\partial \dot{\varphi}} = mr^2\dot{\varphi}, \tag{2.4.3}$$

is conserved. This is just a particular (2D) case of the angular momentum conservation - see Eq. (1.24). Indeed, for the 2 D motion within the $[x, y]$ plane, the angular momentum vector,

$$\mathbf{L} \equiv \mathbf{r} \times \mathbf{p} = \begin{vmatrix} \mathbf{n}_x & \mathbf{n}_y & \mathbf{n}_z \\ x & y & z \\ m\dot{x} & m\dot{y} & m\dot{z} \end{vmatrix}, \tag{2.4.4}$$

has only one component different from zero, namely the component normal to the motion plane:

$$L_z = x(m\dot{y}) - y(m\dot{x}). \tag{2.4.5}$$

Differentiating the well-known relations between the polar and Cartesian coordinates,

$$x = r\cos\varphi, \quad y = r\sin\varphi, \tag{2.4.6}$$

over time, and plugging the result into Eq. (52), we see that

$$L_z = mr^2\dot{\varphi} \equiv p_\varphi. \tag{2.4.7}$$

Thus the Lagrangian formalism provides a powerful way of searching for non-evident integrals of motion. On the other hand, if such a conserved quantity is evident or known a priori, it is helpful for the selection of the most appropriate generalized coordinates, giving the simplest Lagrange equations. For example, in the last problem, if we knew in advance that p_φ had to be conserved, this could provide a motivation for using the angle φ as one of generalized coordinates.

---

[16] This fact may be considered a particular case of a more general mathematical statement called the Noether theorem - named after its author, Emmy Nöther, sometimes called the "greatest woman mathematician ever lived". Unfortunately, because of time/space restrictions, for its discussion I have to refer the interested reader elsewhere - for example to Sec. 13.7 in H. Goldstein et al., Classical Mechanics, 3rd ed. Addison Wesley, 2002

[17] Note that here $\dot{r}^2$ is the square of the scalar derivative $\dot{r}$, rather than the square of the vector $\dot{\mathbf{r}} = \mathbf{v}$.

2.5: Exercise Problems

In each of Problems 2.1-2.11, for the given system:

(i) introduce a set of convenient generalized coordinate(s) q_j,

(ii) write down the Lagrangian L as a function of q_j, $\dot{q}_j$, and (if appropriate) time,

(iii) write down the Lagrange equation(s) of motion,

(iv) calculate the Hamiltonian function H; find out whether it is conserved,

(v) calculate energy E; is $E = H$?; is the energy conserved?

(vi) any other evident integrals of motion?

2.1. A double pendulum - see the figure on the right. Consider only the motion in the vertical plane containing the suspension point.

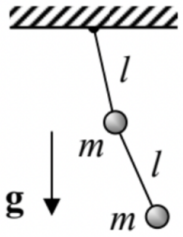

2.2. A stretchable pendulum (i.e. a massive particle hung on an elastic cord that exerts force $F = -\kappa\,(l - l_0)$, where κ and l_0 are positive constants), also confined to the vertical plane:

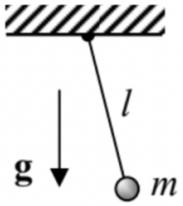

2.3. A fixed-length pendulum hanging from a horizontal support whose motion law $x_0(t)$ is fixed. (No vertical plane constraint here.)

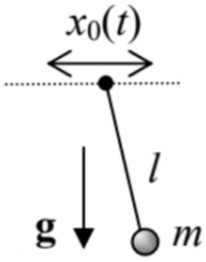

2.4. A pendulum of mass m, hung on another point mass m ', which may slide, without friction, along a straight horizontal rail - see the figure on the right. The motion is confined to the vertical plane that contains the rail.

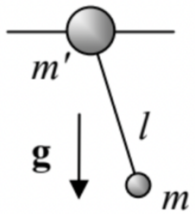

2.5. A point-mass pendulum of length l, attached to the rim of a disk of radius R, which is rotated in a vertical plane with a constant angular velocity ω - see the figure on the right. (Consider only the motion within the disk's plane.)

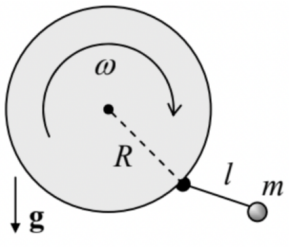

2.6. A bead of mass m, sliding without friction along a light string stretched by a fixed force $\mathscr{T}$ between two horizontally displaced points – see the figure on the right. Here, in contrast to the similar Problem 1.10, the string tension $\mathscr{T}$ may be comparable with the bead's weight mg, and the motion is not restricted to the vertical plane.

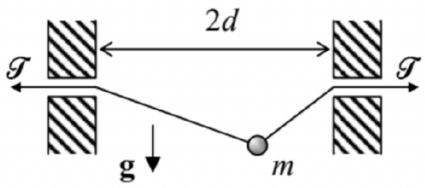

2.7. A bead of mass m, sliding without friction along a light string of a fixed length $2l$, which is hung between two points, horizontally displaced by distance $2d < 2l$ – see the figure on the right. As in the previous problem, the motion is not restricted to the vertical plane.

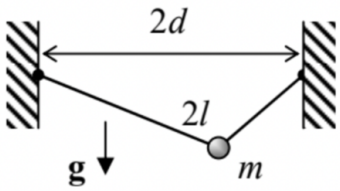

2.8. A block of mass m that can slide, without friction, along the inclined plane surface of a heavy wedge with mass m '. The wedge is free to move, also without friction, along a horizontal surface - see the figure on the right. (Both motions are within the vertical plane containing the steepest slope line.)

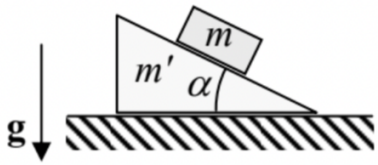

2.9. The two-pendula system that was the subject of Problem 1.8 – see the figure on the right.

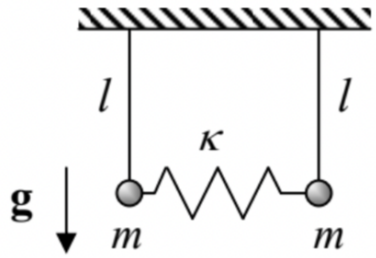

2.10. A system of two similar, inductively-coupled LC circuits – see the figure on the right.

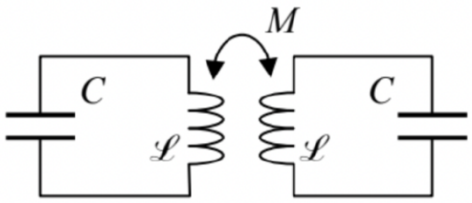

2.11.* A small Josephson junction - the system consisting of two superconductors (S) weakly coupled by Cooper-pair tunneling through a thin insulating layer (I) that separates them - see the figure on the right.

Hints:

(i) At not very high frequencies (whose quantum $\hbar\omega$ is lower than the binding energy 2Δ of the Cooper pairs), the Josephson effect in a sufficiently small junction may be described by the following coupling energy:

$$U(\varphi) = -E_J \cos\varphi + \text{const} \tag{2.5.1}$$

where the constant E_J describes the coupling strength, while the variable φ (called the Josephson phase difference) is connected to the voltage V across the junction by the famous frequency-to-voltage relation

$$\frac{d\varphi}{dt} = \frac{2e}{\hbar}V, \tag{2.5.2}$$

where $e \approx 1.602 \times 10^{-19}\text{C}$ is the fundamental electric charge and $\hbar \approx 1.054 \times 10^{-34}\ \text{J}\cdot\text{s}$ is the Planck constant. [18]

(ii) The junction (as any system of two close conductors) has a substantial electric capacitance C.

[18] More discussion of the Josephson effect and the physical sense of the variable φ may be found, for example, in EM Sec. 6.5 and QM Secs. 1.6 and 2.8 of this lecture note series, but the given problem may be solved without that additional information.

CHAPTER OVERVIEW

3: A Few Simple Problems

The objective of this chapter is to solve a few simple but very important particle dynamics problems that may be reduced to $1D$ motion. They notably include the famous "planetary" problem of two particles interacting via a spherically-symmetric potential, and the classical particle scattering problem. In the process of solution, several methods that will be very essential for the analysis of more complex systems are also discussed.

3.1: One-dimensional and 1D-reducible Systems

If a particle is confined to motion along a straight line (say, axis x), its position is completely determined by this coordinate. In this case, as we already know, particle's Lagrangian is given by Eq. (2.21):

$$L = T(\dot{x}) - U(x,t), \quad T(\dot{x}) = \frac{m}{2}\dot{x}^2, \tag{3.1.1}$$

so that the Lagrange equation of motion, given by Eq. (2.22),

$$m\ddot{x} = -\frac{\partial U(x,t)}{\partial x} \tag{3.1.2}$$

is just the x-component of the 2^{nd} Newton law.

It is convenient to discuss the dynamics of such really-1D systems as a part of a more general class of effectively-1D systems, whose position, due to holonomic constraints and/or conservation laws, is also fully determined by one generalized coordinate q, and whose Lagrangian may be represented in a form similar to Eq. (1):

$$L = T_{\text{ef}}(\dot{q}) - U_{\text{ef}}(q,t), \quad T_{\text{ef}} = \frac{m_{\text{ef}}}{2}\dot{q}^2, \tag{3.1.3}$$

where m_{ef} is some constant which may be considered as the effective mass of the system, and the function U_{ef} its effective potential energy. In this case, the Lagrange equation (2.19), describing the system's dynamics, has a form similar to Eq. (2):

$$m_{\text{ef}}\ddot{q} = -\frac{\partial U_{\text{ef}}(q,t)}{\partial q}. \tag{3.1.4}$$

As an example, let us return again to our testbed system shown in Figure 2.1. We have already seen that for this system, having one degree of freedom, the genuine kinetic energy T, expressed by the first of Eqs. (2.23), is not a quadratically-homogeneous function of the generalized velocity. However, the system's Lagrangian function (2.23) still may be represented in the form (3),

$$L = \frac{m}{2}R^2\dot{\theta}^2 + \frac{m}{2}R^2\omega^2\sin^2\theta + mgR\cos\theta + \text{const} = T_{\text{ef}} - U_{\text{ef}}, \tag{3.1.5}$$

if we take

$$T_{\text{ef}} \equiv \frac{m}{2}R^2\dot{\theta}^2, \quad U_{\text{ef}} \equiv -\frac{m}{2}R^2\omega^2\sin^2\theta - mgR\cos\theta + \text{const} \tag{3.1.6}$$

In this new partitioning of the function L, which is legitimate because U_{ef} depends only on the generalized coordinate θ, but not on the corresponding generalized velocity, T_{ef} includes only a part of the full kinetic energy T of the bead, while U_{ef} includes not only its real potential energy U in the gravity field but also an additional term related to ring rotation. (As we will see in Sec. 4.6, this term may be interpreted as the effective potential energy due to the inertial centrifugal "force" arising at the problem's solution in the non-inertial reference frame rotating with the ring.)

Returning to the general case of effectively-1D systems with Lagrangians of the type (3), let us calculate their Hamiltonian function, using its definition (2.32):

$$H = \frac{\partial L}{\partial \dot{q}}\dot{q} - L = m_{\text{ef}}\dot{q}^2 - (T_{\text{ef}} - U_{\text{ef}}) = T_{\text{ef}} + U_{\text{ef}}. \tag{3.1.7}$$

So, H is expressed via T_{ef} and U_{ef} exactly as the energy E is expressed via genuine T and U.

3.2: Equilibrium and Stability

Autonomous systems are defined as dynamic systems whose equations of motion do not depend on time explicitly. For the effectively-1D (and in particular the really-1D) systems obeying Eq. (4), this means that their function U_{ef}, and hence the Lagrangian function (3) should not depend on time explicitly. According to Eqs. (2.35), in such systems, the Hamiltonian function (7), i.e. the sum $T_{\text{ef}} + U_{\text{ef},}$ is an integral of motion. However, be careful! Generally, this conclusion is not valid for the mechanical energy E of such a system; for example, as we already know from Sec. 2.2, for our testbed problem, with the generalized coordinate $q = \theta$ (Figure 2.1), E is not conserved.

According to Eq. (4), an autonomous system, at appropriate initial conditions, may stay in equilibrium at one or several stationary (alternatively called fixed) points q_n, corresponding to either the minimum or a maximum of the effective potential energy (see Figure 1):

$$\frac{dU_{\text{ef}}}{dq}(q_n) = 0 \tag{3.2.1}$$

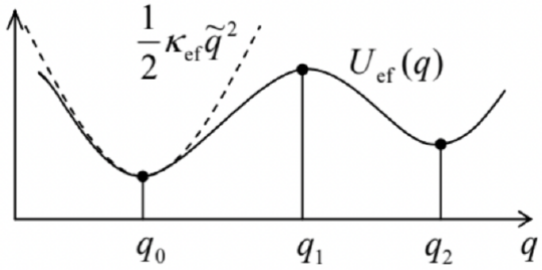

Figure 3.1. The effective potential energy profile near stable (q_0, q_2) and unstable (q_1) fixed points, and its quadratic approximation (10) near point q_0 - schematically.

In order to explore the stability of such fixed points, let us analyze the dynamics of small deviations

$$\tilde{q}(t) \equiv q(t) - q_n \tag{3.2.2}$$

from the equilibrium. For that, let us expand the function $U_{\text{ef}}(\text{q})$ in the Taylor series at a fixed point:

$$U_{\text{ef}}(q) = U_{\text{ef}}(q_n) + \frac{dU_{\text{ef}}}{dq}(q_n)\,\tilde{q} + \frac{1}{2}\frac{d^2U_{\text{ef}}}{dq^2}(q_n)\,\tilde{q}^2 + \ldots \tag{3.2.3}$$

The first term on the right-hand side, $U_{\text{ef}}(q_n)$, is arbitrary and does not affect motion. The next term, linear in deviation $\tilde{q}$, equals zero - see the fixed point's definition (8). Hence the fixed point stability is determined by the next term, quadratic in $\tilde{q}$, more exactly by its coefficient,

$$\kappa_{\text{ef}} \equiv \frac{d^2U_{\text{ef}}}{dq^2}(q_n), \tag{3.2.4}$$

which plays the role of the effective spring constant. Indeed, neglecting the higher terms of the Taylor expansion (10),[1] we see that Eq. (4) takes the familiar form:

$$m_{\text{ef}}\ddot{\tilde{q}} + \kappa_{\text{ef}}\tilde{q} = 0. \tag{3.2.5}$$

I am confident that the reader of these notes knows everything about this equation, but since we will soon run into similar but more complex equations, let us review the formal procedure of its solution. From the mathematical standpoint, Eq. (12) is an ordinary, linear differential equation of the second order, with constant coefficients. The theory of such equations tells us that its general solution (for any initial conditions) may be represented as

$$\tilde{q}(t) = c_+ e^{\lambda_+ t} + c_- e^{\lambda_- t}, \tag{3.2.6}$$

where the constants $c_\pm$are determined by initial conditions, while the so-called characteristic exponents $\lambda_\pm$are completely defined by the equation itself. To calculate these exponents, it is sufficient to plug just one partial solution, $e^{\lambda t}$, into the equation. In our simple case (12), this yields the following characteristic equation:

$$m_{\text{ef}}\lambda^2 + \kappa_{\text{ef}} = 0. \tag{3.2.7}$$

If the ratio $k_{\rm ef}/m_{\rm ef}$ is positive, i.e. the fixed point corresponds to the minimum of potential energy (e.g., see points q_0 or q_2 in Figure 1), the characteristic equation yields

$$\lambda_{\pm} = \pm i\omega_0, \quad \text{with } \omega_0 \equiv \left(\frac{\kappa_{\rm ef}}{m_{\rm ef}}\right)^{1/2}, \tag{3.2.8}$$

(where i is the imaginary unit, $i^2 = -1$), so that Eq. (13) describes sinusoidal oscillations of the system, [2]

$$\tilde{q}(t) = c_+ e^{+i\omega_0 t} + c_- e^{-i\omega_0 t} \equiv c_c \cos\omega_0 t + c_s \sin\omega_0 t, \tag{3.2.9}$$

with the frequency ω_0, about the fixed point - which is thereby stable. [3] On the other hand, at the potential energy maximum ($k_{\rm ef} < 0$, e.g., at point q_1 in Figure 1), we get

$$\lambda_{\pm} = \pm\lambda, \quad \lambda \equiv \left(\frac{|\kappa_{\rm ef}|}{m_{\rm ef}}\right)^{1/2}, \quad \tilde{q}(t) = c_+ e^{+\lambda t} + c_- e^{-\lambda t} \tag{3.2.10}$$

Since the solution has an exponentially growing part, [4] the fixed point is unstable.

Note that the quadratic expansion of function $U_{\rm ef}(q)$, given by the truncation of Eq. (10) to the three displayed terms, is equivalent to a linear Taylor expansion of the effective force:

$$F_{\rm ef} \equiv -\frac{dU_{\rm ef}}{dq} \approx -\kappa_{\rm ef}\,\tilde{q}, \tag{3.2.11}$$

immediately resulting in the linear equation (12). Hence, to analyze the stability of a fixed point q_n, it is sufficient to linearize the equation of motion with respect to small deviations from the point, and study possible solutions of the resulting linear equation. This linearization procedure is typically simpler to carry out than the quadratic expansion (10).

As an example, let us return to our testbed problem (Figure 2.1) whose function $U_{\rm ef}$ we already know - see the second of Eqs. (6). With it, the equation of motion (4) becomes

$$mR^2\ddot{\theta} = -\frac{dU_{\rm ef}}{d\theta} = mR^2\left(\omega^2\cos\theta - \Omega^2\right)\sin\theta, \quad \text{i.e. } \ddot{\theta} = \left(\omega^2\cos\theta - \Omega^2\right)\sin\theta, \tag{3.2.12}$$

where $\Omega \equiv (g/R)^{1/2}$ is the frequency of small oscillations of the system at $\omega = 0$ - see Eq. (2.26) .[5] From requirement (8), we see that on any 2π-long segment of the angle θ, [6] the system may have four fixed points; for example, on the half-open segment $(-\pi, +\pi]$ these points are

$$\theta_0 = 0, \quad \theta_1 = \pi, \quad \theta_{2,3} = \pm\cos^{-1}\frac{\Omega^2}{\omega^2}. \tag{3.2.13}$$

The last two fixed points, corresponding to the bead shifted to either side of the rotating ring, exist only if the angular velocity ω of the rotation exceeds Ω. (In the limit of very fast rotation, $\omega >> \Omega$, Eq. (20) yields $\theta_{2,3} \to \pm\pi/2$, i.e. the stationary positions approach the horizontal diameter of the ring - in accordance with our physical intuition.)To analyze the fixed point stability, we may again use Eq. (9), in the form $\theta = \theta_n + \tilde{\theta}$, plug it into Eq. (19), and Taylor-expand the trigonometric functions of θ up to the first term in $\tilde{\theta}$:

$$\ddot{\tilde{\theta}} = \left[\omega^2\left(\cos\theta_n - \sin\theta_n\tilde{\theta}\right) - \Omega^2\right]\left(\sin\theta_n + \cos\theta_n\tilde{\theta}\right). \tag{3.2.14}$$

Generally, this equation may be linearized further by purging its right-hand side of the term proportional to $\tilde{\theta}^2$; however in this simple case, Eq. (21) is already convenient for analysis. In particular, for the fixed point $\theta_0 = 0$ (corresponding to the bead's position at the bottom of the ring), we have $\cos\theta_0 = 1$ and $\sin\theta_0 = 0$, so that Eq. (21) is reduced to a linear differential equation

$$\ddot{\tilde{\theta}} = \left(\omega^2 - \Omega^2\right)\tilde{\theta}, \tag{3.2.15}$$

whose characteristic equation is similar to Eq. (14) and yields

$$\lambda^2 = \omega^2 - \Omega^2, \text{ for } \theta \approx \theta_0. \tag{3.2.16}$$

This result shows that if $\omega < \Omega$, when both roots λ are imaginary, this fixed point is orbitally stable. However, if the rotation speed is increased so that $\omega > \Omega$, the roots become real, $\lambda_{\pm} = \left(\omega^2 - \Omega^2\right)^{1/2}$, with one of them positive, so that the fixed point becomes

unstable beyond this threshold, i.e. as soon as fixed points $\theta_{2,3}$ exist. Absolutely similar calculations for other fixed points yield

$$\lambda^2 = \begin{cases} \Omega^2 + \omega^2 > 0, & \text{for } \theta \approx \theta_1, \\ \Omega^2 - \omega^2, & \text{for } \theta \approx \theta_{2,3}. \end{cases} \tag{3.2.17}$$

These results show that the fixed point θ_1 (bead on the top of the ring) is always unstable - just as we could foresee, while the side fixed points $\theta_{2,3}$ are orbitally stable as soon as they exist (at $\omega > \Omega$).

Thus, our fixed-point analysis may be summarized very simply: an increase of the ring rotation speed ω beyond a certain threshold value, equal to Ω given by Eq. (2.26), causes the bead to move to one of the ring sides, oscillating about one of the fixed points $\theta_{2,3}$. Together with the rotation about the vertical axis, this motion yields quite a complex (generally, open) spatial trajectory as observed from a lab frame, so it is fascinating that we could analyze it quantitatively in such a simple way.

Later in this course, we will repeatedly use the linearization of the equations of motion for the analysis of stability of more complex systems, including those with energy dissipation.

---

[1] Those terms may be important only in very special cases then κ_{ef} is exactly zero, i.e. when a fixed point is an inflection point of the function $U_{\text{er}}(q)$.

[2] The reader should not be scared of the first form of (16), i.e. of the representation of a real variable (the deviation from equilibrium) via a sum of two complex functions. Indeed, any real initial conditions give $c_-^* = c_+$, so that the sum is real for any t. An even simpler way to deal with such complex representations of real functions will be discussed in the beginning of the next chapter, and then used throughout the series.

[3] This particular type of stability, when the deviation from the equilibrium oscillates with a constant amplitude, neither growing nor decreasing in time, is called either the orbital, or "neutral", or "indifferent" stability.

[4] Mathematically, the growing part vanishes at some special (exact) initial conditions which give $c_+ = 0$. However, the futility of this argument for real physical systems should be obvious for anybody who had ever tried to balance a pencil on its sharp point.

[5] Note that Eq. (19) coincides with Eq. (2.25). This is a good sanity check illustrating that the procedure (5)-(6) of moving of a term from the potential to the kinetic energy within the Lagrangian function is indeed legitimate.

[6] For this particular problem, the values of θ that differ by a multiple of 2π, are physically equivalent.

3.3: Hamiltonian 1D Systems

Autonomous systems that are described by time-independent Lagrangians are frequently called Hamiltonian ones because their Hamiltonian function H (again, not necessarily equal to the genuine mechanical energy E!) is conserved. In our current 1D case, described by Eq. (3),

$$H = \frac{m_{\text{ef}}}{2}\dot{q}^2 + U_{\text{ef}}(q) = \text{ const}\,. \tag{3.3.1}$$

From the mathematical standpoint, this conservation law is just the first integral of motion. Solving Eq. (24) for $\dot{q}$, we get the first-order differential equation,

$$\frac{dq}{dt} = \pm\left\{\frac{2}{m_{\text{ef}}}[H - U_{\text{ef}}(q)]\right\}^{1/2}, \quad \text{i.e. } \pm\left(\frac{m_{\text{ef}}}{2}\right)^{1/2}\frac{dq}{[H - U_{\text{ef}}(q)]^{1/2}} = dt, \tag{3.3.2}$$

which may be readily integrated:

$$\pm\left(\frac{m_{\text{ef}}}{2}\right)^{1/2}\int_{q(t_0)}^{q(t)}\frac{dq'}{[H - U_{\text{ef}}(q')]^{1/2}} = t - t_0. \tag{3.3.3}$$

Since the constant H (as well as the proper sign before the integral - see below) is fixed by initial conditions, Eq. (26) gives the reciprocal form, $t = t(q)$, of the desired law of system motion, $q(t)$. Of course, for any particular problem the integral in Eq. (26) still has to be worked out, either analytically or numerically, but even the latter procedure is typically much easier than the numerical integration of the initial, second-order differential equation of motion, because at the addition of many values (to which any numerical integration is reduced [7]) the rounding errors are effectively averaged out.

Moreover, Eq. (25) also allows a general classification of 1D system motion. Indeed:

(i) If $H > U_{\text{ef}}(q)$ in the whole range of interest, the effective kinetic energy T_{ef} (3) is always positive. Hence the derivative dq/dt cannot change its sign, so that the effective velocity retains the sign it had initially. This is an unbound motion in one direction (Figure 2a).

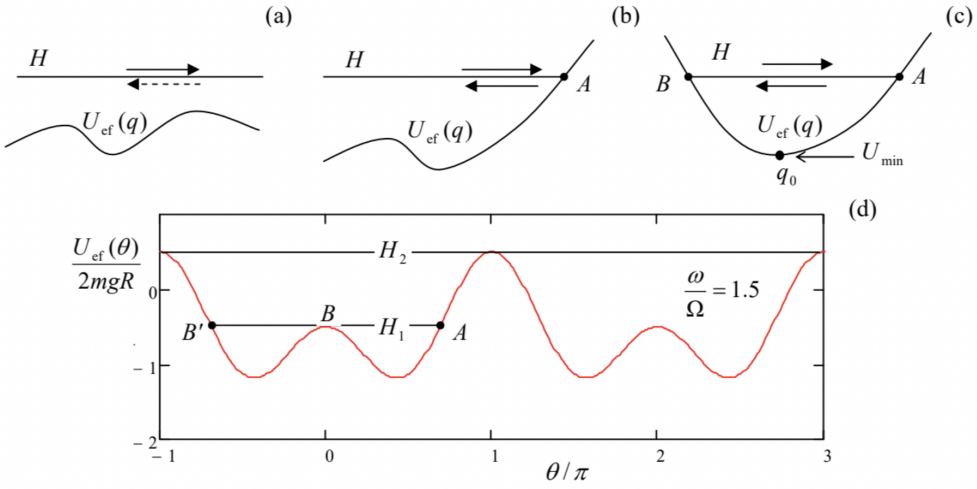

Figure 3.2. Graphical representations of Eq. (25) for three different cases: (a) an unbound motion, with the velocity sign conserved, (b) a reflection from a "classical turning point", accompanied by the velocity sign change, and (c) bound, periodic motion between two turning points - schematically. (d) The effective potential energy (6) of the bead on the rotating ring (Figure 2.1) for a particular case with $\omega > \Omega$.

(ii) Now let the particle approach a classical turning point A where $H = U_{\text{ef}}(q)$ – see Fig .2 b. [8] According to Eq. (25), at that point the particle velocity vanishes, while its acceleration, according to Eq. (4), is still finite. This corresponds to the particle reflection from this potential wall, with the change of the velocity sign.

(iii) If, after the reflection from point A, the particle runs into another classical turning point B (Figure 2c), the reflection process is repeated again and again, so that the particle is bound to a periodic motion between two turning points.

The last case of periodic oscillations presents a large conceptual and practical interest, and the whole next chapter will be devoted to a detailed analysis of this phenomenon and numerous associated effects. Here I will only note that for an autonomous Hamiltonian system described by Eq. (4), Eq. (26) immediately enables the calculation of the oscillation period:

$$\tau = 2\left(\frac{m_{\text{ef}}}{2}\right)^{1/2} \int_B^A \frac{dq}{[H - U_{\text{ef}}(q)]^{1/2}} \tag{3.3.4}$$

where the additional front factor 2 accounts for two time intervals: of the motion from B to A and back see Figure 2c. Indeed, according to Eq. (25), in each classically allowed point q, the velocity magnitude is the same so that these time intervals are equal to each other.

(Note that the dependence of points A and B on H is not necessarily continuous. For example, for our testbed problem, whose effective potential energy is plotted in Figure 2 d for a particular value of $\omega > \Omega$, a gradual increase of H leads to a sudden jump, at $H = H_1$, of the point B to a new position B ', corresponding to a sudden switch from oscillations about one fixed point $\theta_{2,3}$ to oscillations about two adjacent fixed points - before the beginning of a persistent rotation around the ring at $H > H_2$.)

Now let us consider a particular, but very important limit of Eq. (27). As Figure 2c shows, if H is reduced to approach $U_{\min}$, the periodic oscillations take place at the very bottom of "potential well", about a stable fixed point q_0. Hence, if the potential energy profile is smooth enough, we may limit the Taylor expansion (10) to the displayed quadratic term. Plugging it into Eq. (27), and using the mirror symmetry of this particular problem about the fixed point q_0, we get

$$\tau = 4\left(\frac{m_{\text{ef}}}{2}\right)^{1/2} \int_0^A \frac{d\tilde{q}}{\left[H - \left(U_{\min} + \kappa_{\text{ef}}\tilde{q}^2/2\right)\right]^{1/2}} = \frac{4}{\omega_0} I, \quad \text{with } I \equiv \int_0^1 \frac{d\xi}{\left(1-\xi^2\right)^{1/2}} \tag{3.3.5}$$

where $\xi \equiv \tilde{q}/A$, with $A \equiv (2/\kappa_{\text{ef}})^{1/2}(H - U_{\min})^{1/2}$ being the classical turning point, i.e. the oscillation amplitude, and ω_0 the frequency given by Eq. (15). Taking into account that the elementary integral I in that equation equals $\pi/2$, [9] we finally get

$$\tau = \frac{2\pi}{\omega_0}, \tag{3.3.6}$$

as it should be for the harmonic oscillations (16). Note that the oscillation period does not depend on the oscillation amplitude A, i.e. on the difference $(H - U_{\min}) -$ while it is sufficiently small.

---

[7] See, e.g., MA Eqs. (5.2) and (5.3).

[8] This terminology comes from quantum mechanics, which shows that a particle (or rather its wavefunction) actually can, to a certain extent, penetrate into the "classically forbidden range" where $H < U_{\text{ef}}(q)$.

[9] Indeed, introducing a new variable ζ as $\xi \equiv \sin\zeta$, we get $d\xi = \cos\zeta d\zeta = \left(1-\xi^2\right)^{1/2} d\zeta$, so that the function under the integral is just $d\zeta$, and its limits are $\zeta = 0$ and $\zeta = \pi/2$.

3.4: Planetary Problems

Leaving a more detailed study of oscillations for Chapter 5, let us now discuss the so-called planetary systems [10] whose description, somewhat surprisingly, may be also reduced to an effectively 1D problem. Consider two particles that interact via a conservative, central force $\mathbf{F}_{21} = -\mathbf{F}_{12} = \mathbf{n}_r F(r)$, where r and $\mathbf{n}_r$ are, respectively, the magnitude and direction of the distance vector $\mathbf{r} \equiv \mathbf{r}_1 - \mathbf{r}_2$ connecting the two particles (Figure 3).

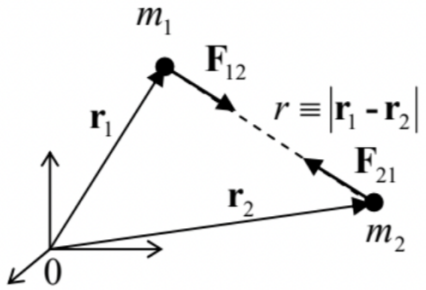

Figure 3.3. Vectors in the "planetary" problem.

Generally, two particles moving without constraints in 3D space, have $3+3=6$ degrees of freedom, which may be described, e.g., by their Cartesian coordinates $\{x_1, y_1, z_1, x_2, y_2, z_2\}$ However, for this particular form of interaction, the following series of tricks allows the number of essential degrees of freedom to be reduced to just one.

First, the central, conservative force of particle interaction may be described by a timeindependent potential energy $U(r)$, such that $F(r) = -\partial U(r)/\partial r$. [11] Hence the Lagrangian of the system is

$$L \equiv T - U(r) = \frac{m_1}{2}\dot{\mathbf{r}}_1^2 + \frac{m_2}{2}\dot{\mathbf{r}}_2^2 - U(r). \tag{3.4.1}$$

Let us perform the transfer from the initial six scalar coordinates of the particles to the following six generalized coordinates: three Cartesian components of the distance vector

$$\mathbf{r} \equiv \mathbf{r}_1 - \mathbf{r}_2, \tag{3.4.2}$$

and three scalar components of the following vector:

$$\mathbf{R} \equiv \frac{m_1\mathbf{r}_1 + m_2\mathbf{r}_2}{M}, \quad \text{with } M \equiv m_1 + m_2, \tag{3.4.3}$$

which defines the position of the center of mass of the system, with the total mass M. Solving the system of two linear equations (31) and (32) for $\mathbf{r}_1$ and $\mathbf{r}_2$, we get

$$\mathbf{r}_1 = \mathbf{R} + \frac{m_2}{M}\mathbf{r}, \quad \mathbf{r}_2 = \mathbf{R} - \frac{m_1}{M}\mathbf{r}. \tag{3.4.4}$$

Plugging these relations into Eq. (30), we see that it is reduced it to

$$L = \frac{M}{2}\dot{\mathbf{R}}^2 + \frac{m}{2}\dot{\mathbf{r}}^2 - U(r), \tag{3.4.5}$$

where m is the so-called reduced mass:

$$m \equiv \frac{m_1 m_2}{M}, \text{ so that } \frac{1}{m} \equiv \frac{1}{m_1} + \frac{1}{m_2}. \tag{3.4.6}$$

Note that according to Eq. (35), the reduced mass is lower than that of the lightest component of the two-body system. If one of $m_{1,2}$ is much less than its counterpart (like it is in most star-planet or planetsatellite systems), then with a good precision $m \approx \min[m_1, m_2]$.

Since the Lagrangian function (34) depends only on $\mathbf{R}$ rather than $\mathbf{R}$ itself, according to our discussion in Sec. 2.4, all Cartesian components of R are cyclic coordinates, and the corresponding generalized momenta are conserved:

$$P_j \equiv \frac{\partial L}{\partial \dot{R}_j} \equiv M\dot{R}_j = \text{const}, \quad j = 1, 2, 3. \tag{3.4.7}$$

Physically, this is just the conservation law for the full momentum $\mathbf{P} \equiv M\mathbf{R}$ of our system, due to the absence of external forces. Actually, in the axiomatics used in Sec. 1.3 this law is postulated - see Eq. (1.10) - but now we may attribute the momentum $\mathbf{P}$ to a certain geometric point, with the center-of-mass radius vector $\mathbf{R}$. In particular, since according to Eq. (36) the center moves with a constant velocity in the inertial reference frame used to write Eq. (30), we may consider a new inertial frame with the origin at point $\mathbf{R}$. In this new frame, $\mathbf{R} \equiv 0$, so that the vector $\mathbf{r}$ (and hence the scalar r) remain the same as in the old frame (because the frame transfer vector adds equally to $\mathbf{r}_1$ and $\mathbf{r}_2$, and cancels in $\mathbf{r} = \mathbf{r}_1 - \mathbf{r}_2$), and the Lagrangian (34) is now reduced to

$$L = \frac{m}{2}\dot{\mathbf{r}}^2 - U(r) \tag{3.4.8}$$

Thus our initial problem has been reduced to just three degrees of freedom - three scalar components of the vector $\mathbf{r}$. Moreover, Eq. (37) shows that dynamics of the vector $\mathbf{r}$ of our initial, twoparticle system is identical to that of the radius vector of a single particle with the effective mass m, moving in the central potential field $U(r)$.

Two more degrees of freedom may be excluded from the planetary problem by noticing that according to Eq. (1.35), the angular momentum $\mathbf{L} = \mathbf{r} \times \mathbf{p}$ of our effective single particle of mass m is also conserved, both in magnitude and direction. Since the direction of $\mathbf{L}$ is, by its definition, perpendicular to both of $\mathbf{r}$ and $\mathbf{v} = \mathbf{p}/m$, this means that the particle's motion is confined to the plane whose orientation is determined by the initial directions of the vectors $\mathbf{r}$ and $\mathbf{v}$. Hence we can completely describe particle's position by just two coordinates in that plane, for example by the distance r to the origin, and the polar angle φ. In these coordinates, Eq. (37) takes the form identical to Eq. (2.49):

$$L = \frac{m}{2}\left(\dot{r}^2 + r^2\dot{\varphi}^2\right) - U(r). \tag{3.4.9}$$

Moreover, the latter coordinate, polar angle φ, may be also eliminated by using the conservation of angular momentum's magnitude, in the form of Eq. (2.50) : [12]

$$L_z = mr^2\dot{\varphi} = \text{ const.} \tag{3.4.10}$$

A direct corollary of this conservation is the so-called 2nd Kepler law: [13] the radius vector $\mathbf{r}$ sweeps equal areas A in equal times. Indeed, in the linear approximation in $dA << A$, the area differential dA is equal to the area of a narrow right triangle with the base being the arc differential $rd\varphi$, and the height equal to r-see Figure 4. As a result, according to Eq. (39), the time derivative of the area,

$$\frac{dA}{dt} = \frac{r(rd\varphi)/2}{dt} \equiv \frac{1}{2}r^2\dot{\varphi} = \frac{L_z}{2m}, \tag{3.4.11}$$

remains constant. Since the factor $L_z/2m$ is constant, integration of this equation over an arbitrary (not necessarily small!) time interval Δt proves the 2nd Kepler law: $A \propto \Delta t$.

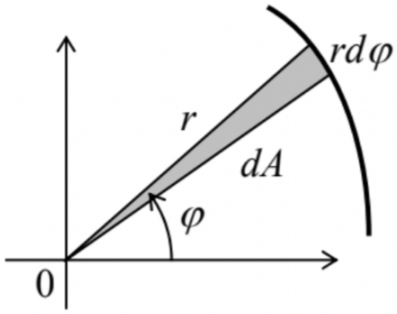

Figure 3.4. The area differential dA in the polar coordinates.

Now note that since $\partial L/\partial t = 0$, the Hamiltonian function H is also conserved, and since, according to Eq. (38), the kinetic energy of the system is a quadratic-homogeneous function of the generalized velocities $\dot{r}$ and $\dot{\varphi}$, we have $H = E$, so that the system's energy E,

$$E = \frac{m}{2}\dot{r}^2 + \frac{m}{2}r^2\dot{\varphi}^2 + U(r), \tag{3.4.12}$$

is also a first integral of motion. [14] But according to Eq. (39), the second term on the right-hand side of Eq. (41) may be represented as

$$\frac{m}{2}r^2\dot{\varphi}^2 = \frac{L_z^2}{2mr^2}, \tag{3.4.13}$$

so that the energy (41) may be expressed as that of a 1D particle moving along axis r,

$$E = \frac{m}{2}\dot{r}^2 + U_{\text{ef}}(r), \tag{3.4.14}$$

in the following effective potential:

$$U_{\text{ef}}(r) \equiv U(r) + \frac{L_z^2}{2mr^2} \tag{3.4.15}$$

(The physical sense of the second term is similar to that of the first term in the U_{ef} spelled out in Eq. (6), and will be discussed again in Sec. 4.6 below.) So the planetary motion problem has been reduced to the dynamics of an effectively-1D system. [15]

Now we may proceed just like we did in Sec. 3, with due respect to the very specific effective potential (44) which, in particular, diverges at $r \to 0$ - besides the very special case of an exactly radial motion, $L_z = 0$. In particular, we may solve Eq. (43) for dr/dt to get

$$dt = \left(\frac{m}{2}\right)^{1/2} \frac{dr}{[E - U_{\text{ef}}(r)]^{1/2}} \tag{3.4.16}$$

This equation allows us not only to get a direct relationship between time t and distance r, similar to Eq. (26),

$$t = \pm\left(\frac{m}{2}\right)^{1/2} \int \frac{dr}{[E - U_{\text{ef}}(r)]^{1/2}} = \pm\left(\frac{m}{2}\right)^{1/2} \int \frac{dr}{\left[E - U(r) - L_z^2/2mr^2\right]^{1/2}}, \tag{3.4.17}$$

but also do a similar calculation of the angle φ. Indeed, integrating Eq. (39),

$$\varphi \equiv \int \dot{\varphi} dt = \frac{L_z}{m} \int \frac{dt}{r^2}, \tag{3.4.18}$$

and plugging dt from Eq. (45), we get an explicit expression for the particle trajectory $\varphi(r)$:

$$\varphi = \pm\frac{L_z}{(2m)^{1/2}} \int \frac{dr}{r^2[E - U_{\text{ef}}(r)]^{1/2}} = \pm\frac{L_z}{(2m)^{1/2}} \int \frac{dr}{r^2\left[E - U(r) - L_z^2/2mr^2\right]^{1/2}}. \tag{3.4.19}$$

Note that according to Eq. (39), the derivative $d\varphi/dt$ does not change sign at the reflection from any classical turning point $r \neq 0$, so that, in contrast to Eq. (46), the sign on the right-hand side of Eq. (48) is uniquely determined by the initial conditions and cannot change during the motion.

Let us use these results, valid for any interaction law $U(r)$, for the planetary motion's classification. (Following a good tradition, in what follows I will select the arbitrary constant in the potential energy in the way to provide $U \to 0$, and hence $U_{\text{ef}} \to 0$ at $r \to \infty$.) The following cases should be distinguished.

If $U(r) < 0$, i.e. the particle interaction is attractive (as it always is in the case of gravity), and the divergence of the attractive potential at $r \to 0$ is faster than $1/r^2$, then $U_{\text{ef}}(r) \to -\infty$ at $r \to 0$, so that at appropriate initial conditions the particle may drop on the center even if $L_z \neq 0$ - the event called the capture. On the other hand, with $U(r)$ either converging or diverging slower than $1/r^2$, at $r \to 0$, the effective energy profile $U_{\text{ef}}(r)$ has the shape shown schematically in Figure 5. This is true, in particular, for the very important case

$$U(r) = -\frac{\alpha}{r}, \quad \text{with } \alpha > 0 \tag{3.4.20}$$

which describes, in particular, the Coulomb (electrostatic) interaction of two particles with electric charges of opposite signs, and the Newton gravity law (1.15). This particular case will be analyzed below, but now let us return to the analysis of an arbitrary attractive potential $U(r) < 0$ leading to the effective potential shown in Figure 5 , when the angular-momentum term in Eq. (44) dominates at small distances r.

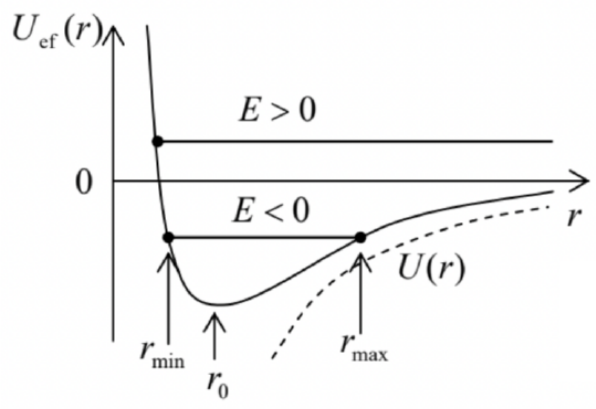

Figure 3.5. Effective potential profile of an attractive central field, and two types of motion in it.

According to the analysis in Sec. 3, such potential profile, with a minimum at some distance r_0, may sustain two types of motion, depending on the energy E (which is determined by initial conditions):

(i) If $E > 0$, there is only one classical turning point where $E = U_{ef}$, so that the distance r either grows with time from the very beginning or (if the initial value of $\dot{r}$ was negative) first decreases and then, after the reflection from the increasing potential U_{ef}, starts to grow indefinitely. The latter case, of course, describes the scattering of the effective particle by the attractive center. [16]

(ii) On the opposite, if the energy is within the range

$$U_{ef}(r_0) \le E < 0, \tag{3.4.21}$$

the system moves periodically between two classical turning points r_{min} and r_{max} – see Figure 5. These oscillations of the distance r correspond to the bound orbital motion of our effective particle about the attracting center.

Let us start with the discussion of the bound motion, with the energy within the range (50). If the energy has its minimal possible value,

$$E = U_{ef}(r_0) \equiv \min\left[U_{ef}(r)\right], \tag{3.4.22}$$

the distance cannot change, $r = r_0 =$ const, so that the orbit is circular, with the radius r_0 satisfying the condition $dU_{ef}/dr = 0$. Using Eq. (44), we see that the condition for r_0 may be written as

$$\frac{L_z^2}{mr_0^3} = \left.\frac{dU}{dr}\right|_{r=r_0}. \tag{3.4.23}$$

Since at circular motion, the velocity $\mathbf{v}$ is perpendicular to the radius vector $\mathbf{r}$, L_z is just mr_0v, the lefthand side of Eq. (52) equals mv^2/r_0, while its right-hand side is just the magnitude of the attractive force, so that this equality expresses the well-known 2^{nd} Newton law for the circular motion. Plugging this result into Eq. (47), we get a linear law of angle change, $\varphi = \omega t +$ const, with the angular velocity

$$\omega = \frac{L_z}{mr_0^2} = \frac{v}{r_0}, \tag{3.4.24}$$

and hence the rotation period $\tau_\varphi \equiv 2\pi/\omega$ obeys the elementary relation

$$\tau_\varphi = \frac{2\pi r_0}{v}. \tag{3.4.25}$$

Now let the energy be above its minimum value (but still negative). Using Eq. (46) just as in Sec. 3, we see that the distance r now oscillates with the period

$$\tau_r = (2m)^{1/2} \int_{r_{min}}^{r_{max}} \frac{dr}{\left[E - U(r) - L_z^2/2mr^2\right]^{1/2}}. \tag{3.4.26}$$

This period is not necessarily equal to another period, T_φ, that corresponds to the 2π-change of the angle. Indeed, according to Eq. (48), the change of the angle φ between two sequential points of the nearest approach,

$$|\Delta\varphi| = 2\frac{L_z}{(2m)^{1/2}}\int_{r_{\min}}^{r_{\max}} \frac{dr}{r^2\left[E - U(r) - L_z^2/2mr^2\right]^{1/2}} \tag{3.4.27}$$

is generally different from 2π. Hence, the general trajectory of the bound motion has a spiral shape see, e.g., an illustration in Figure 6.

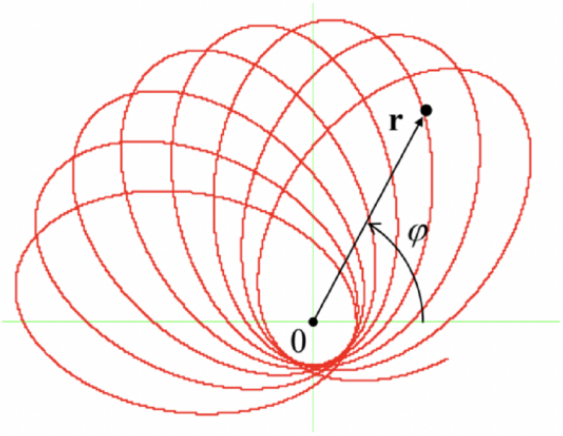

Figure 3.6. A typical open orbit of a particle moving in a non-Coulomb central field.

The situation is special, however, for a very important particular case, namely that of the Coulomb potential described by Eq. (49). Indeed, plugging this potential into Eq. (48), we get

$$\varphi = \pm\frac{L_z}{(2m)^{1/2}}\int \frac{dr}{r^2\left(E + \alpha/r - L_z^2/2mr^2\right)^{1/2}}. \tag{3.4.28}$$

This is a table integral, [17] giving

$$\varphi = \pm\cos^{-1}\frac{L_z^2/m\alpha r - 1}{\left(1 + 2EL_z^2/m\alpha^2\right)^{1/2}} + \text{const}. \tag{3.4.29}$$

The reciprocal function, $r(\varphi)$, is 2π-periodic:

$$r = \frac{p}{1 + e\cos(\varphi + \text{const})}, \tag{3.4.30}$$

so that at $E < 0$, the orbit is a closed line, [18] characterized by the following parameters: [19]

$$p \equiv \frac{L_z^2}{m\alpha}, \quad e \equiv \left(1 + \frac{2EL_z^2}{m\alpha^2}\right)^{1/2} \tag{3.4.31}$$

The physical meaning of these parameters is very simple. Indeed, the general Eq. (52), in the Coulomb potential for which $dU/dr = \alpha/r^2$, shows that p is just the circular orbit radius [20] for the given L_z : $r_0 = L_z^2/m\alpha \equiv p$, so that

$$\min\left[U_{\text{ef}}(r)\right] \equiv U_{\text{ef}}\left(r_0\right) = -\frac{\alpha^2 m}{2L_z^2}. \tag{3.4.32}$$

Using this equality together with the second of Eqs. (60), we see that the parameter e (called the eccentricity) may be represented just as

$$e = \left\{1 - \frac{E}{\min\left[U_{\text{ef}}(r)\right]}\right\}^{1/2}. \tag{3.4.33}$$

Analytical geometry tells us that Eq. (59), with $e < 1$, is one of the canonical representations of an ellipse, with one of its two focuses located at the origin. The fact that planets have such trajectories is known as the 1st Kepler law. Figure 7 shows the

relations between the dimensions of the ellipse and the parameters p and e. [21]

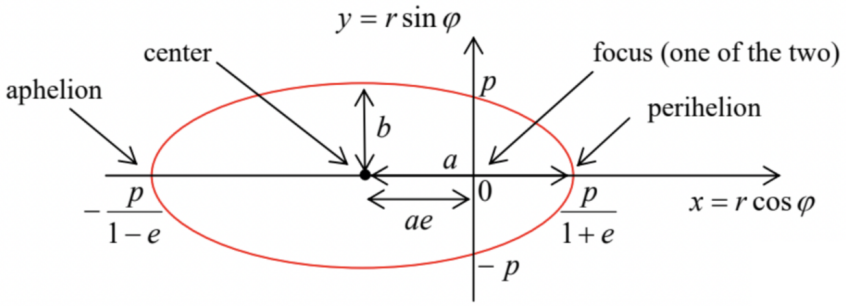

Figure 3.7. Ellipse, and its special points and dimensions.

In particular, the major semi-axis a and the minor semi-axis b are simply related to p and e and hence, via Eqs. (60), to the motion integrals E and L_z :

$$a = \frac{p}{1-e^2} = \frac{\alpha}{2|E|}, \quad b = \frac{p}{(1-e^2)^{1/2}} = \frac{L_z}{(2m|E|)^{1/2}}. \tag{3.4.34}$$

As was mentioned above, at $E \to \min[U_{\text{ef}}(r)]$ the orbit is almost circular, with $r(\varphi) \cong r_0 \approx p$. On the contrary, as E is increased to approach zero (its maximum value for the closed orbit), then $e \to 1$, so that the aphelion point $r_{\max} = p/(1-e)$ tends to infinity, i.e. the orbit becomes extremely extended – see the red lines in Figure 8 .

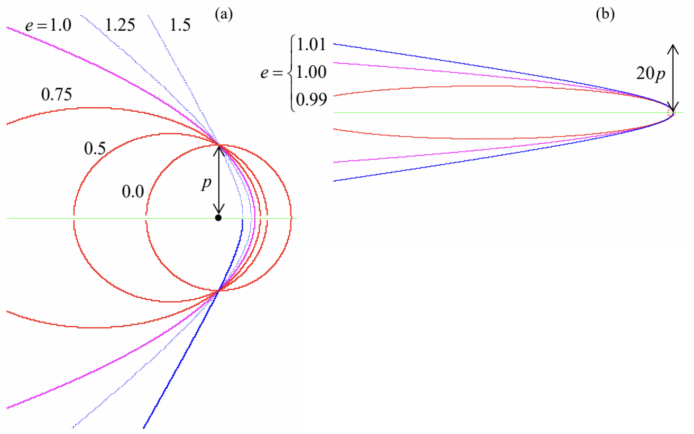

Figure 3.8. (a) Zoom-in and (b) zoom-out on the Coulombfield trajectories corresponding to the same parameter p (i.e., the same L_z), but different values of the eccentricity parameter e, i.e. of the energy E - see Eq. (60): ellipses ($e < 1$, red lines), a parabola ($e = 1$, magenta line), and hyperbolas ($e > 1$, blue lines). Note that the transition from closed to open trajectories at $e = 1$ is dramatic only at very large distances, $r >> p$.

The above relations enable, in particular, a ready calculation of the rotation period $T \equiv T_r = \tau_\varphi$. (In the case of a closed trajectory, τ_r and τ_φ coincide.) Indeed, it is well known that the ellipse area $A = \pi ab$. But according to the 2nd Kepler law (40), $dA/dt = L_z/2m = \text{const}$. Hence

$$\tau = \frac{A}{dA/dt} = \frac{\pi ab}{L_z/2m}. \tag{3.4.35}$$

Using Eqs. (60) and (63), this important result may be represented in several other forms:

$$\tau = \frac{\pi p^2}{(1-e^2)^{3/2}(L_z/2m)} = \pi\alpha\left(\frac{m}{2|E|^3}\right)^{1/2} = 2\pi a^{3/2}\left(\frac{m}{\alpha}\right)^{1/2}. \tag{3.4.36}$$

Since for the Newtonian gravity (1.15), $\alpha = Gm_1m_2 = GmM$, at $m_1 << m_2$ (i.e. $m << M$ this constant is proportional to m, and the last form of Eq. (64b) yields the 3rd Kepler law: periods of motion of different planets in the same central field, say that of our Sun, scale as $\tau \propto a^{3/2}$. Note that in contrast to the 2nd Kepler law (which is valid for any central field), the 1st and the 3rd Kepler laws are potentialspecific.

Now reviewing the above derivation of Eqs. (59)-(60), we see that they are also valid in the case of $E \geq 0$ - see the top horizontal line in Figure 5 and its discussion above, if we limit the results to the physically meaningful range $r \geq 0$. This means that if the energy is exactly zero, Eq. (59) (with $e = 1$) is still valid for all values of φ (except for one special point $\varphi = \pi$ where r becomes infinite) and describes a parabolic (i.e. open) trajectory - see the magenta lines in Figure 8.

Moreover, if $E > 0$, Eq. (59) is still valid within a certain sector of angles φ,

$$\Delta\varphi = 2\cos^{-1}\frac{1}{e} \equiv 2\cos^{-1}\left(1 + \frac{2EL_z^2}{m\alpha^2}\right)^{-1/2} < \pi, \quad \text{for } E > 0, \tag{3.4.37}$$

and describes an open, hyperbolic trajectory (see the blue lines in Figure 8). As was mentioned earlier, such trajectories are typical, in particular, for particle scattering.

---

[10] This name is very conditional, because this group of problems includes, for example, charged particle scattering (see Sec. 3.7 below).

[11] See, e.g., MA Eq. (10.8) with $\partial/\partial\theta = \partial/\partial\varphi = 0$.

[12] Here index z stands for the coordinate perpendicular to the motion plane. Since other components of the angular momentum equal zero, the index is not really necessary, but I will still use it - just to make a clear distinction between the angular momentum L_z and the Lagrangian function L.

[13] This is one of the three laws deduced, from the extremely detailed astronomical data collected by Tycho Brahe (1546-1601), by Johannes Kepler in the early 17^{th} century. In turn, the three Kepler laws have become the main basis for Newton's discovery, a few decades later, of the gravity law (1.15). That relentless march of physics...

[14] One may argue that this fact should have been evident from the very beginning because the effective particle of mass m moves in a potential field $U(r)$, which conserves energy.

[15] Note that this reduction has been done in a way different from that used for our testbed problem (shown in Figure 2.1) in Sec. 2 above. (The reader is encouraged to analyze this difference.) To emphasize this fact, I will keep writing E instead of H here, though for the planetary problem we are discussing now, these two notions coincide.

[16] In the opposite case when the interaction is repulsive, $U(r) > 0$, the addition of the positive angular energy term only increases the trend, and the scattering scenario is the only one possible.

[17] See, e.g., MA Eq. (6.3a).

[18] It may be proved that for the power-law interaction, $U \propto r^v$, the orbits are closed curves only if $v = -1$ (our current case of the Coulomb potential) or if $v = +2$ (the 3D harmonic oscillator) - the so-called Bertrand theorem.

[19] Let me hope that the difference between the parameter p and the particle momentum's magnitude is absolutely clear from the context, so that using the same (traditional) notation for both notions cannot lead to confusion.

[20] Mathematicians prefer a more solemn terminology: the parameter $2p$ is called the latus rectum of the ellipse.

[21] In this figure, the constant participating in Eqs. (58)-(59) is assumed to be zero. A different choice of the constant corresponds just to a different origin of φ, i.e. a constant turn of the ellipse about the origin.

3.5: Elastic Scattering

If $E > 0$, the motion is unbound for any realistic interaction potential. In this case, the two most important parameters of the particle trajectory are the impact parameter b and the scattering angle θ (Figure 9), and the main task for theory is to find the relation between them in the given potential $U(r)$.

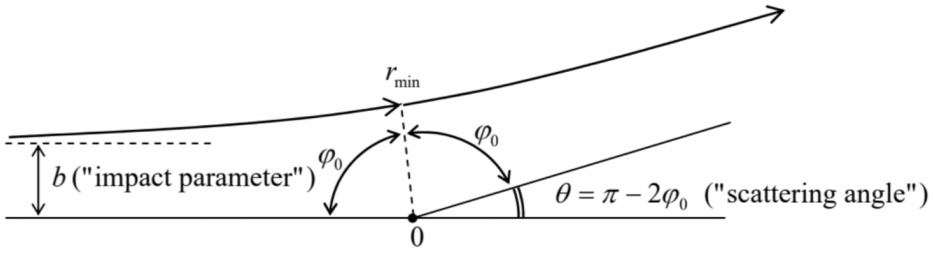

Figure 3.9. Main geometric parameters of the scattering problem.

For that, it is convenient to note that b is related to the two conserved quantities, particle's energy [22] E and its angular momentum L_z, in a simple way. Indeed, at $r \gg b$, the definition $\mathbf{L} = \mathbf{r} \times (m\mathbf{v})$ yields $L_z = bmv_\infty$, where $v_\infty = (2E/m)^{1/2}$ is the initial (and hence the final) velocity of the particle, so that

$$L_z = b(2mE)^{1/2}. \tag{3.5.1}$$

Hence the angular contribution to the effective potential (44) may be represented as

$$\frac{L_z^2}{2mr^2} = E\frac{b^2}{r^2}. \tag{3.5.2}$$

Second, according to Eq. (48), the trajectory sections going from infinity to the nearest approach point ($r = r_{\min}$) and from that point to infinity, have to be similar, and hence correspond to equal angle changes φ_0 – see Figure 9. Hence we may apply the general Eq. (48) to just one of the sections, say $[r_{\min}, \infty]$, to find the scattering angle:

$$\theta = \pi - 2\varphi_0 = \pi - 2\frac{L_z}{(2m)^{1/2}}\int_{r_{\min}}^{\infty}\frac{dr}{r^2\left[E - U(r) - L_z^2/2mr^2\right]^{1/2}} = \pi - 2\int_{r_{\min}}^{\infty}\frac{bdr}{r^2\left[1 - U(r)/E - b^2/r^2\right]^{1/2}}. \tag{3.5.3}$$

In particular, for the Coulomb potential (49), now with an arbitrary sign of α, we can apply the same table integral as in the previous section to get [23]

$$|\theta| = \left|\pi - 2\cos^{-1}\frac{\alpha/2Eb}{\left[1 + (\alpha/2Eb)^2\right]^{1/2}}\right|. \tag{3.5.4}$$

This result may be more conveniently rewritten as

$$\tan\frac{|\theta|}{2} = \frac{|\alpha|}{2Eb}. \tag{3.5.5}$$

Very clearly, the scattering angle's magnitude increases with the potential strength α, and decreases as either the particle energy or the impact parameter (or both) are increased.

The general result (68) and the Coulomb-specific relations (69) represent a formally complete solution of the scattering problem. However, in a typical experiment on elementary particle scattering, the impact parameter b of a single particle is unknown. In this case, our results may be used to obtain the statistics of the scattering angle θ, in particular, the so-called differential cross-section [24]

$$\frac{d\sigma}{d\Omega} \equiv \frac{1}{n}\frac{dN}{d\Omega}, \tag{3.5.6}$$

where n is the average number of the incident particles per unit area, and dN is the average number of the particles scattered into a small solid angle range $d\Omega$. For a uniform beam of initial particles, $d\sigma/d\Omega$ may be calculated by counting the average number of incident particles that have the impact parameters within a small range db :

$$dN = n2\pi b db. \tag{3.5.7}$$

and are scattered by a spherically-symmetric center, which provides an axially-symmetric scattering pattern, into the corresponding small solid angle range $d\Omega = 2\pi|\sin\theta d\theta|$. Plugging these two equalities into Eq. (70), we get the following general geometric relation:

$$\frac{d\sigma}{d\Omega} = b\left|\frac{db}{\sin\theta d\theta}\right|. \tag{3.5.8}$$

In particular, for the Coulomb potential (49), a straightforward differentiation of Eq. (69) yields the so-called Rutherford scattering formula (reportedly derived by Ralph Howard Fowler):

$$\frac{d\sigma}{d\Omega} = \left(\frac{\alpha}{4E}\right)^2 \frac{1}{\sin^4(\theta/2)} \tag{3.5.9}$$

This result, which shows a very strong scattering to small angles (so strong that the integral that expresses the total cross-section

$$\sigma \equiv \oint_{4\pi} \frac{d\sigma}{d\Omega} d\Omega \tag{3.5.10}$$

is diverging at $\theta \to 0$),[25] and very weak backscattering (to angles $\theta \approx \pi$) was historically extremely significant: in the early 1910s: its good agreement with α-particle scattering experiments carried out by Ernest Rutherford's group gave a strong justification for his introduction of the planetary model of atoms, with electrons moving around very small nuclei - just as planets move around stars.

Note that elementary particle scattering is frequently accompanied by electromagnetic radiation and/or other processes leading to the loss of the initial mechanical energy of the system. Such inelastic scattering may give significantly different results. (In particular, capture of an incoming particle becomes possible even for a Coulomb attracting center.) Also, quantum-mechanical effects may be important at the scattering of light particles with relatively low energies, [26] so that the above results should be used with caution.

---

[22] The energy conservation law is frequently emphasized by calling such process elastic scattering.

[23] Alternatively, this result may be recovered directly from the first form of Eq. (65), with the eccentricity e expressed via the same dimensionless parameter $(2Eb/\alpha)$: $e = \left[1 + (2Eb/\alpha)^2\right]^{1/2} > 1$.

[24] This terminology stems from the fact that an integral (74) of $d\sigma/d\Omega$ over the full solid angle, called the total cross-section σ, has the dimension of the area: $\sigma = N/n$, where N is the total number of scattered particles.

[25] This divergence, which persists at the quantum-mechanical treatment of the problem (see, e.g., QM Chapter 3), is due to particles with very large values of b, and disappears at an account, for example, of any non-zero concentration of the scattering centers.

[26] Their discussion may be found in QM Secs. 3.3 and 3.8.

3.6: Exercise Problems

3.1. For the system considered in Problem 2.6 (a bead sliding along a string with fixed tension $\mathscr{T}$, see the figure on the right), analyze small oscillations of the bead near the equilibrium.

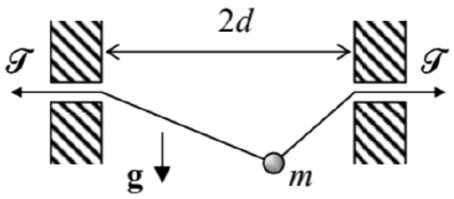

3.2. For the system considered in Problem 2.7 (a bead sliding along a string of a fixed length $2l$, see the figure on the right), analyze small oscillations near the equilibrium.

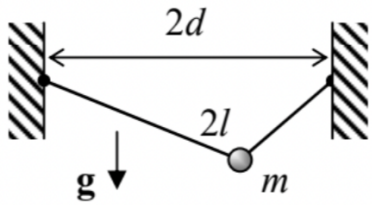

3.3. For a 1D particle of mass m, placed into potential $U(q) = \alpha q^{2n}$ (where $\alpha > 0$, and n is a positive integer), calculate the functional dependence of the particle oscillation period τ on its energy E. Explore the limit $n \to \infty$.

3.4. Explain why the term $mr^2\dot{\varphi}^2/2$, recast in accordance with Eq. (42), cannot be merged with $U(r)$ in Eq. (38), to form an effective 1D potential energy $U(r) - L_z^2/2mr^2$, with the second term's sign opposite to that given by Eq. (44). We have done an apparently similar thing for our testbed, bead-onrotating-ring problem at the very end of Sec. 1 - see Eq. (6); why cannot the same trick work for the planetary problem? Besides a formal explanation, discuss the physics behind this difference.

3.5. A system consisting of two equal masses m on a light rod of length l (frequently called a dumbbell) can slide without friction along a vertical ring of radius R, rotated about its vertical diameter with constant angular velocity ω– see the figure on the right. Derive the condition of stability of the lower horizontal position of the dumbbell.

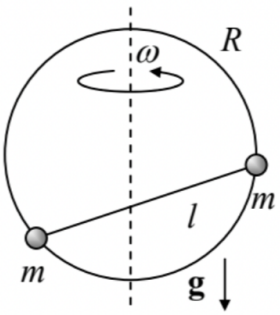

3.6. Analyze the dynamics of the so-called spherical pendulum - a point mass hung, in a uniform gravity field $\mathbf{g}$, on a light cord of length l, with no motion's confinement to a vertical plane. In particular:

(i) find the integrals of motion and reduce the problem to a 1D one,

(ii) calculate the time period of the possible circular motion around the vertical axis, and

(iii) explore small deviations from the circular motion. (Are the pendulum orbits closed?) [27]

3.7. The orbits of Mars and Earth around the Sun may be well approximated as circles, with a radii ratio of $3/2$. Use this fact, and the Earth's year duration (which you should know :-), to calculate the time of travel to Mars spending the least energy for spacecraft's launch. Neglect the planets' size and the effects of their gravitational fields.

3.8. Derive first-order and second-order differential equations for the reciprocal distance $u \equiv 1/r$ as a function of φ, describing the trajectory of particle's motion in a central potential $U(r)$. Spell out the latter equation for the particular case of the Coulomb

potential (49) and discuss the result.

3.9. For the motion of a particle in the Coulomb attractive field (with potential $U(r) = -\alpha/r$, with $\alpha > 0$), calculate and sketch the so-called hodograph [28] – the trajectory followed by the head of the velocity vector $\mathbf{v}$, provided that its tail is kept at the origin.

3.10. For motion in the following central potential:

$$U(r) = -\frac{\alpha}{r} + \frac{\beta}{r^2}, \tag{3.6.1}$$

(i) find the orbit $r(\varphi)$, for positive α and β, and all possible ranges of energy E;

(ii) prove that in the limit $\beta \to 0$, and for energy $E < 0$, the orbit may be represented as a slowly rotating ellipse;

(iii) express the angular velocity of this slow orbit rotation via the parameters α and β, the particle's mass m, its energy E, and the angular momentum L_z.

3.11. A particle is moving in the field of an attractive central force, with potential

$$U(r) = -\frac{\alpha}{r^n}, \quad \text{where } \alpha n > 0. \tag{3.6.2}$$

For what values of n is a circular orbit stable?

3.12. Determine the condition for a particle of mass m, moving under the effect of a central attractive force

$$\mathbf{F} = -\alpha \frac{\mathbf{r}}{r^3} \exp\left\{-\frac{r}{R}\right\}, \tag{3.6.3}$$

where α and R are positive constants, to have a stable circular orbit.

3.13. A particle of mass m, with angular momentum L_z, moves in the field of an attractive central force with a distance-independent magnitude F. If particle's energy E is slightly higher than the value $E_{\min}$ corresponding to the circular orbit of the particle, what is the time period of its radial oscillations? Compare the period with that of the circular orbit at $E = E_{\min}$.

3.14. For particle scattering by a repulsive Coulomb field, calculate the minimum approach distance $r_{\min}$ and the velocity $v_{\min}$ at that point, and analyze their dependence on the impact parameter b (see Figure 9) and the initial velocity v_∞ of the particle.

3.15. A particle is launched from afar, with impact parameter b, toward an attracting center with

$$U(r) = -\frac{\alpha}{r^n}, \quad \text{with } n > 2, \alpha > 0. \tag{3.6.4}$$

(i) Express the minimum distance between the particle and the center via b, if the initial kinetic energy E of the particle is barely sufficient for escaping its capture by the attracting center.

(ii) Calculate the capture's total cross-section; explore the limit $n \to 2$.

3.16. A meteorite with initial velocity v_∞ approaches an atmosphere-free planet of mass M and radius R.

(i) Find the condition on the impact parameter b for the meteorite to hit the planet's surface.

(ii) If the meteorite barely avoids the collision, what is its scattering angle?

3.17. Calculate the differential and total cross-sections of the classical, elastic scattering of small particles by a hard sphere of radius R.

3.18. The most famous [29] confirmation of Einstein's general relativity theory has come from the observation, by A. Eddington and his associates, of star light's deflection by the Sun, during the May 1919 solar eclipse. Considering light photons as classical particles propagating with the speed of light, $v_0 \to c \approx 3.00 \times 10^8$ m/s, and the astronomic data for Sun's mass, $M_S \approx 1.99 \times 10^{30}$ kg, and radius, $R_S \approx 6.96 \times 10^8$ m, calculate the non-relativistic mechanics' prediction for the angular deflection of the light rays grazing the Sun's surface.

---

[27] Solving this problem is a very good preparation for the analysis of symmetric top's rotation in the next chapter.

[28] The use of this notion for the characterization of motion may be traced back at least to an 1846 treatise by W. Hamilton. Nowadays, it is most often used in applied fluid mechanics, in particular meteorology.

[29] It was not the first confirmation, though. The first one came four years earlier from Albert Einstein himself, who showed that his theory may qualitatively explain the difference between the rate of Mercury orbit's precession, known from earlier observations, and the non-relativistic theory of that effect.

CHAPTER OVERVIEW

4: Rigid Body Motion

This chapter discusses the motion of rigid bodies, with a heavy focus on its most nontrivial part: the rotation. Some byproduct results of this analysis enable a discussion, at the end of the chapter, of the motion of point particles as observed from non-inertial reference frames.

4.1: Translation and Rotation

It is natural to start a discussion of many-particle systems from a (relatively :-) simple limit when the changes of distances $r_{kk'} \equiv |\mathbf{r}_k - \mathbf{r}_{k'}|$ between the particles are negligibly small. Such an abstraction is called the (absolutely) rigid body, and is a reasonable approximation in many practical problems, including the motion of solids. In other words, this model neglect deformations - which will be the subject of the next chapters. The rigid-body approximation reduces the number of degrees of freedom of the system of N particles from $3N$ to just six - for example, three Cartesian coordinates of one point (say, 0), and three angles of the system's rotation about three mutually perpendicular axes passing through this point - see Figure 1. [1]

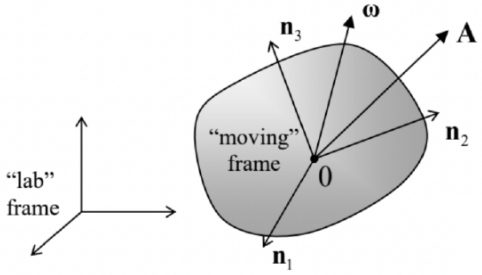

Figure 4.1. Deriving Eq. (8).

As it follows from the discussion in Secs. 1.1-3, any purely translational motion of a rigid body, at which the velocity vectors $\mathbf{v}$ of all points are equal, is not more complex than that of a point particle. Indeed, according to Eqs. (1.8) and (1.30), in an inertial reference frame such a body moves, upon the effect of the net external force $\mathbf{F}^{(\text{ext})}$, exactly as a point particle. However, the rotation is a bit more tricky.

Let us start by showing that an arbitrary elementary displacement of a rigid body may be always considered as a sum of the translational motion discussed above, and what is called a pure rotation. For that, consider a "moving" reference frame, firmly bound to the body, and an arbitrary vector A (Figure 1). The vector may be represented by its Cartesian components A_j in that moving frame:

$$\mathbf{A} = \sum_{j=1}^{3} A_j \mathbf{n}_j. \tag{4.1.1}$$

Let us calculate the time derivative of this vector as observed from a different ("lab") frame, taking into account that if the body rotates relative to this frame, the directions of the unit vectors $\mathbf{n}_j$, as seen from the lab frame, change in time. Hence, we have to differentiate both operands in each product contributing to the sum (1):

$$\left.\frac{d\mathbf{A}}{dt}\right|_{\text{in lab}} = \sum_{j=1}^{3} \frac{dA_j}{dt}\mathbf{n}_j + \sum_{j=1}^{3} A_j \frac{d\mathbf{n}_j}{dt}. \tag{4.1.2}$$

On the right-hand side of this equality, the first sum evidently describes the change of vector $\mathbf{A}$ as observed from the moving frame. In the second sum, each of the infinitesimal vectors $d\mathbf{n}_j$ may be represented by its Cartesian components:

$$d\mathbf{n}_j = \sum_{j'=1}^{3} d\varphi_{ij'} \mathbf{n}_{j'} \tag{4.1.3}$$

where $d\varphi_{ij'}$ are some dimensionless scalar coefficients. To find out more about them, let us scalarmultiply each side of Eq. (3) by an arbitrary unit vector $\mathbf{n}_{j''}$, and take into account the evident orthonormality condition:

$$\mathbf{n}_{j'} \cdot \mathbf{n}_{j''} = \delta_{jj''}, \tag{4.1.4}$$

where $\delta_{jj'}$ is the Kronecker delta symbol. [2] As a result, we get

$$d\mathbf{n}_j \cdot \mathbf{n}_{j''} = d\varphi_{ij''} \tag{4.1.5}$$

Now let us use Eq. (5) to calculate the first differential of Eq. (4):

$$d\mathbf{n}_{j'} \cdot \mathbf{n}_{j''} + \mathbf{n}_{j'} \cdot d\mathbf{n}_{j''} \equiv d\varphi_{jj''} + d\varphi_{j''} = 0; \quad \text{in particular, } 2d\mathbf{n}_j \cdot \mathbf{n}_j = 2d\varphi_{ij} = 0. \tag{4.1.6}$$

These relations, valid for any choice of indices j, j ', and j " of the set $\{1,2,3\}$, show that the matrix of $d\varphi_{ij}$ ' is antisymmetric with respect to the swap of its indices; this means that there are not nine just three non-zero independent coefficients $d\varphi_{ij}$, all with $j \neq j$ '. Hence it is natural to renumber them in a simpler way: $d\varphi_{ij'} = -d\varphi_{j'j} \equiv d\varphi_{j"}$, where the indices j, j ', and j " follow in the "correct" order - either $\{1,2,3\}$, or $\{2,3,1\}$, or $\{3,1,2\}$. It is easy to check (either just by a component-by-component comparison or using the Levi-Civita permutation symbol $\varepsilon_{ijj'}$ [1]) that in this new notation, Eq. (3) may be represented just as a vector product:

$$d\mathbf{n}_j = d\boldsymbol{\varphi} \times \mathbf{n}_j, \tag{4.1.7}$$

where $d\varphi$ is the infinitesimal vector defined by its Cartesian components $d\varphi_j$ in the rotating reference frame $\{\mathbf{n}_1, \mathbf{n}_2, \mathbf{n}_3\}$ - see Eq. (3).

This relation is the basis of all rotation kinematics. Using it, Eq. (2) may be rewritten as

$$\left.\frac{d\mathbf{A}}{dt}\right|_{\text{in lab}} = \left.\frac{d\mathbf{A}}{dt}\right|_{\text{in mov}} + \sum_{j=1}^{3} A_j \frac{d\boldsymbol{\varphi}}{dt} \times \mathbf{n}_j \equiv \left.\frac{d\mathbf{A}}{dt}\right|_{\text{in mov}} + \boldsymbol{\omega} \times \mathbf{A}, \quad \text{where } \boldsymbol{\omega} \equiv \frac{d\boldsymbol{\varphi}}{dt}. \tag{4.1.8}$$

To reveal the physical sense of the vector ω, let us apply Eq. (8) to the particular case when $\mathbf{A}$ is the radius vector $\mathbf{r}$ of a point of the body, and the lab frame is selected in a special way: its origin has the same position and moves with the same velocity as that of the moving frame in the particular instant under consideration. In this case, the first term on the right-hand side of Eq. (8) is zero, and we get

$$\left.\frac{d\mathbf{r}}{dt}\right|_{\text{in special lab frame}} = \boldsymbol{\omega} \times \mathbf{r}, \tag{4.1.9}$$

were vector $\mathbf{r}$ itself is the same in both frames. According to the vector product definition, the particle velocity described by this formula has a direction perpendicular to the vectors ω and $\mathbf{r}$ (Figure 2), and magnitude $\omega r \sin\theta$. As Figure 2 shows, the last expression may be rewritten as $\omega\rho$, where $\rho = r\sin\theta$ is the distance from the line that is parallel to the vector ω and passes through the point 0 . This is of course just the pure rotation about that line (called the instantaneous axis of rotation), with the angular velocity ω. Since according to Eqs. (3) and (8), the angular velocity vector ω is defined by the time evolution of the moving frame alone, it is the same for all points $\mathbf{r}$, i.e. for the rigid body as a whole. Note that nothing in our calculations forbids not only the magnitude but also the direction of the vector ω, and thus of the instantaneous axis of rotation, to change in time (and in many cases it does); hence the name.

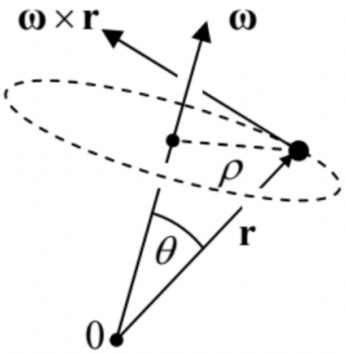

Figure 4.2. The instantaneous axis and the angular velocity of rotation.

Now let us generalize our result a step further, considering two reference frames that do not rotate versus each other: one ("lab") frame arbitrary, and another one selected in the special way described above, so that for it Eq. (9) is valid in it. Since their relative motion of these two reference frames is purely translational, we can use the simple velocity addition rule given by Eq. (1.6) to write

$$\mathbf{v}|_{\text{in lab}} = \mathbf{v}_0|_{\text{in lab}} + \mathbf{v}|_{\text{in special lab frame}} = \mathbf{v}_0|_{\text{in lab}} + \boldsymbol{\omega} \times \mathbf{r}, \tag{4.1.10}$$

where $\mathbf{r}$ is the radius vector of a point is measured in the body-bound ("moving") frame 0.

---

[1] An alternative way to arrive at the same number six is to consider three points of the body, which uniquely define its position. If movable independently, the points would have nine degrees of freedom, but since three distances r_{kk}, between them are now fixed, the resulting three constraints reduce the number of degrees of freedom to six.

[2] See, e.g., MA Eq. (13.1).

[3] See, e,g., MA Eq. (13.2). Using this symbol, we may write $d\varphi_{ij'} = -d\varphi_{jj} \equiv \varepsilon_{jjj} d\varphi_{j''}$ for any choice of j, j', and j ".

4.2: Inertia Tensor

Since the dynamics of each point of a rigid body is strongly constrained by the conditions r_{kk} ' = const, this is one of the most important fields of application of the Lagrangian formalism discussed in Chapter 2. For using this approach, the first thing we need to calculate is the kinetic energy of the body in an inertial reference frame. Since it is just the sum of the kinetic energies (1.19) of all its points, we can use Eq. (10) to write: [4]

$$T \equiv \sum \frac{m}{2}\mathbf{v}^2 = \sum \frac{m}{2}\left(\mathbf{v}_0 + \boldsymbol{\omega}\times\mathbf{r}\right)^2 = \sum \frac{m}{2}v_0^2 + \sum m\mathbf{v}_0\cdot(\boldsymbol{\omega}\times\mathbf{r}) + \sum \frac{m}{2}(\boldsymbol{\omega}\times\mathbf{r})^2. \tag{4.2.1}$$

Let us apply to the right-hand side of Eq. (11) two general vector analysis formulas listed in the Math Appendix: the so-called operand rotation rule MA Eq. (7.6) to the second term, and MA Eq. (7.7b) to the third term. The result is

$$T = \sum \frac{m}{2}v_0^2 + \sum m\mathbf{r}\cdot(\mathbf{v}_0\times\boldsymbol{\omega}) + \sum \frac{m}{2}\left[\omega^2 r^2 - (\boldsymbol{\omega}\cdot\mathbf{r})^2\right]. \tag{4.2.2}$$

This expression may be further simplified by making a specific choice of the point 0 (from that the radius vectors $\mathbf{r}$ of all particles are measured), namely by using for this point the center of mass of the body. As was already mentioned in Sec. 3.4 for the 2-point case, the radius vector $\mathbf{R}$ of this point is defined as

$$M\mathbf{R} \equiv \sum m\mathbf{r}, \quad M \equiv \sum m, \tag{4.2.3}$$

where M is the total mass of the body. In the reference frame centered as this point, $\mathbf{R} = 0$, so that the second sum in Eq. (12) vanishes, and the kinetic energy is a sum of just two terms:

$$T = T_{\text{tran}} + T_{\text{rot}}, \quad T_{\text{tran}} \equiv \frac{M}{2}V^2, \quad T_{\text{rot}} \equiv \sum \frac{m}{2}\left[\omega^2 r^2 - (\boldsymbol{\omega}\cdot\mathbf{r})^2\right] \tag{4.2.4}$$

where $\mathbf{V} \equiv d\mathbf{R}/dt$ is the center-of-mass velocity in our inertial reference frame, and all particle positions $\mathbf{r}$ are measured in the center-of-mass frame. Since the angular velocity vector ω is common for all points of a rigid body, it is more convenient to rewrite the rotational energy in a form in that the summation over the components of this vector is clearly separated from the summation over the points of the body:

$$T_{\text{rot}} = \frac{1}{2}\sum_{j,j'=1}^{3} I_{jj'}\omega_j\omega_{j'}, \tag{4.2.5}$$

where the 3×3 matrix with elements

$$I_{jj'} \equiv \sum m\left(r^2\delta_{jj'} - r_j r_{j'}\right) \tag{4.2.6}$$

is called the inertia tensor of the body. [5]

Actually, the term "tensor" for this matrix has to be justified, because in physics this term implies a certain reference-frame-independent notion, whose elements have to obey certain rules at the transfer between reference frames. To show that the matrix (16) indeed deserves its title, let us calculate another key quantity, the total angular momentum $\mathbf{L}$ of the same body. [6] Summing up the angular momenta of each particle, defined by Eq. (1.31), and then using Eq. (10) again, in our inertial reference frame we get

$$\mathbf{L} \equiv \sum \mathbf{r}\times\mathbf{p} = \sum m\mathbf{r}\times\mathbf{v} = \sum m\mathbf{r}\times(\mathbf{v}_0 + \boldsymbol{\omega}\times\mathbf{r}) \equiv \sum m\mathbf{r}\times\mathbf{v}_0 + \sum m\mathbf{r}\times(\boldsymbol{\omega}\times\mathbf{r}). \tag{4.2.7}$$

We see that the momentum may be represented as a sum of two terms. The first one,

$$\mathbf{L}_0 \equiv \sum m\mathbf{r}\times\mathbf{v}_0 = M\mathbf{R}\times\mathbf{v}_0, \tag{4.2.8}$$

describes the possible rotation of the center of mass around the inertial frame's origin. This term evidently vanishes if the moving reference frame's origin 0 is positioned at the center of mass (where $\mathbf{R} = 0$). In this case, we are left with only the second term, which describes a pure rotation of the body about its center of mass:

$$\mathbf{L} = \mathbf{L}_{\text{rot}} \equiv \sum m\mathbf{r}\times(\boldsymbol{\omega}\times\mathbf{r}) \tag{4.2.9}$$

Using one more vector algebra formula, the "bac minis cab" rule, [7] we may rewrite this expression as

$$\mathbf{L} = \sum m \left[\boldsymbol{\omega} r^2 - \mathbf{r} (\mathbf{r} \cdot \boldsymbol{\omega}) \right] . \tag{4.2.10}$$

Let us spell out an arbitrary Cartesian component of this vector:

$$L_j = \sum m \left[\omega_j r^2 - r_j \sum_{j'=1}^{3} r_{j'} \omega_{j'} \right] \equiv \sum m \sum_{j'=1}^{3} \omega_{j'} \left(r^2 \delta_{ij'} - r_j r_{j'} \right) . \tag{4.2.11}$$

By changing the summation order and comparing the result with Eq. (16), the angular momentum may be conveniently expressed via the same matrix elements I_{ij} ' as the rotational kinetic energy:

$$L_j = \sum_{j'=1}^{3} I_{jj'} \omega_{j'} . \tag{4.2.12}$$

Since $\mathbf{L}$ and ω are both legitimate vectors (meaning that they describe physical vectors independent of the reference frame choice), their connection, the matrix of elements I_{ij}, is a legitimate tensor. This fact, and the symmetry of the tensor $\left(I_{ij'} = I_{j'j} \right)$, which is evident from its definition (16), allow the tensor to be further simplified. In particular, mathematics tells us that by a certain choice of the axes' orientations, any symmetric tensor may be reduced to a diagonal form

$$I_{jj'} = I_j \delta_{jj'} , \tag{4.2.13}$$

where in our case

$$I_j = \sum m \left(r^2 - r_j^2 \right) = \sum m \left(r_{j'}^2 + r_{j'}^2 \right) \equiv \sum m \rho_j^2 , \tag{4.2.14}$$

being the distance of the particle from the j^{th} axis, i.e. the length of the perpendicular dropped from the point to that axis. The axes of such a special coordinate system are called the principal axes, while the diagonal elements I_j given by Eq. (24), the principal moments of inertia of the body. In such a special reference frame, Eqs. (15) and (22) are reduced to very simple forms:

$$T_{\text{rot}} = \sum_{j=1}^{3} \frac{I_j}{2} \omega_j^2 ,$$
$$L_j = I_j \omega_j .$$

Both these results remind the corresponding relations for the translational motion, $T_{\text{tran}} = MV^2/2$ and $\mathbf{P} = M\mathbf{V}$, with the angular velocity ω replacing the linear velocity $\mathbf{V}$, and the tensor of inertia playing the role of scalar mass M. However, let me emphasize that even in the specially selected reference frame, with axes pointing in principal directions, the analogy is incomplete, and rotation is generally more complex than translation, because the measures of inertia, I_j, are generally different for each principal axis.

Let me illustrate this fact on a simple but instructive system of three similar massive particles fixed in the vertices of an equilateral triangle (Figure 3).

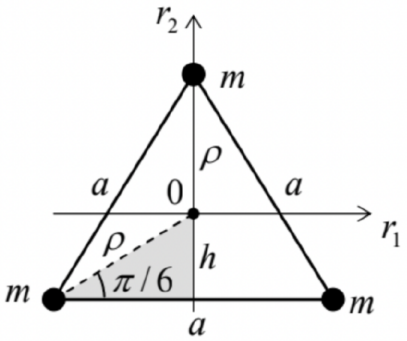

Figure 4.3. Principal moments of inertia: a simple case study.

Due to the symmetry of the configuration, one of the principal axes has to pass through the center of mass 0 and be normal to the plane of the triangle. For the corresponding principal moment of inertia, Eq. (24) readily yields $I_3 = 3m\rho^2$. If we want to express the result in terms of the triangle side a, we may notice that due to the system's symmetry, the angle marked in Figure 3 equals $\pi/6$, and from the shaded right triangle, $a/2 = \rho \cos(\pi/6) \equiv \rho\sqrt{3}/2$, giving $\rho = a/\sqrt{3}$, so that, finally, $I_3 = ma^2$.

Let me use this simple case to illustrate the following general axis shift theorem, which may be rather useful - especially for more complex systems. For that, let us relate the inertia tensor components $I_{jj'}$ and $I'_{jj'}$, calculated in two reference frames - one with the origin in the center of mass 0 , and another one $(0')$ displaced by a certain vector $\mathbf{d}$ (Figure 4a), so that for an arbitrary point, $\mathbf{r}' = \mathbf{r} + \mathbf{d}$. Plugging this relation into Eq. (16), we get

$$\begin{aligned} I''_{jj'} &= \sum m \left[(\mathbf{r}+\mathbf{d})^2 \delta_{jj'} - (r_j + d_j)\left(r_{j'} + d_{j'}\right) \right] \\ &= \sum m \left[\left(r^2 + 2\mathbf{r}\cdot\mathbf{d} + d^2\right)\delta_{jj'} - \left(r_j r_{j'} + r_j d_{j'} + r_{j'} d_j + d_j d_{j'}\right) \right]. \end{aligned}$$

Since in the center-of-mass frame, all sums $\sum m r_j$ equal zero, we may use Eq. (16) to finally obtain

$$I'_{jj'} = I_{jj'} + M\left(\delta_{jj'} d^2 - d_j d_{j'}\right). \tag{4.2.15}$$

In particular, this equation shows that if the shift vector $\mathbf{d}$ is perpendicular to one (say, j^{th}) of the principal axes (Figure 4 b), i.e. $d_j = 0$, then Eq. (28) is reduced to a very simple formula:

Principal axis'

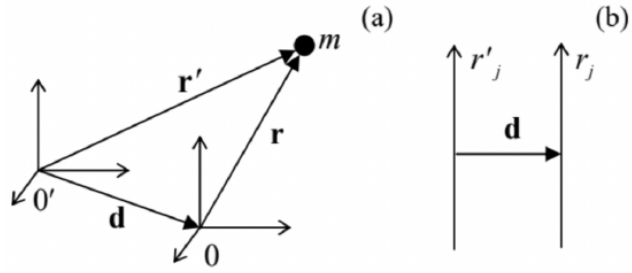

Figure 4.4. (a) A general reference frame's shift from the center of mass, and (b) a shift perpendicular to one of the principal axes.

Now returning to the system shown in Figure 3, let us perform such a shift to the new ("primed") axis passing through the location of one of the particles, still perpendicular to the particles' plane. Then the contribution of that particular mass to the primed moment of inertia vanishes, and $I'_3 = 2\mathrm{ma}^2$. Now, returning to the center of mass and applying Eq. (29), we get $I_3 = I_3 - M\rho^2 = 2ma^2 - (3m)(a/\sqrt{3})^2 = ma^2$, i.e. the same result as above.

The symmetry situation inside the triangle's plane is somewhat less evident, so let us start with calculating the moments of inertia for the axes shown vertical and horizontal in Figure 3. From Eq. (24) we readily get:

$$I_1 = 2mh^2 + m\rho^2 = m\left[2\left(\frac{a}{2\sqrt{3}}\right)^2 + \left(\frac{a}{\sqrt{3}}\right)^2\right] = \frac{ma^2}{2}, \quad I_2 = 2m\left(\frac{a}{2}\right)^2 = \frac{ma^2}{2}, \tag{4.2.16}$$

where h is the distance from the center of mass and any side of the triangle: $h = \rho\sin(\pi/6) = \rho/2 = a/2\sqrt{3}$. We see that $I_1 = I_2$, and mathematics tells us that in this case any in-plane axis (passing through the center-of-mass 0) may be considered as principal, and has the same moment of inertia. A rigid body Symmetric
top: with this property, $I_1 = I_2 \neq I_3$, is called the symmetric top. (The last direction is called the main principal with this property, $I_1 = I_2 \neq I_3$, is called the symmetric top. (The last direction is called the main principal axis of the system.)

Despite the symmetric top's name, the situation may be even more symmetric in the so-called spherical tops, i.e. highly symmetric systems whose principal moments of inertia are all equal,

$$I_1 = I_2 = I_3 \equiv I, \tag{4.2.17}$$

Mathematics says that in this case, the moment of inertia for rotation about any axis (but still passing through the center of mass) is equal to the same I. Hence Eqs. (25) and (26) are further simplified for any direction of the vector ω :

$$T_{\text{rot}} = \frac{I}{2}\omega^2, \quad \mathbf{L} = I\omega \tag{4.2.18}$$

thus making the analogy of rotation and translation complete. (As will be discussed in the next section, this analogy is also complete if the rotation axis is fixed by external constraints.)

Evident examples of a spherical top are a uniform sphere and a uniform spherical shell; a less obvious example is a uniform cube - with masses either concentrated in vertices, or uniformly spread over the faces, or uniformly distributed over the volume. Again, in

this case any axis passing through the center of mass is principal and has the same principal moment of inertia. For a sphere, this is natural; for a cube, rather surprising - but may be confirmed by a direct calculation.

---

[4] Actually, all symbols for particle masses, coordinates, and velocities should carry the particle's index, over which the summation is carried out. However, in this section, for the notation simplicity, this index is just implied.

[5] While the ABCs of the rotational dynamics were developed by Leonhard Euler in 1765 , an introduction of the inertia tensor's formalism had to wait very long - until the invention of the tensor analysis by Tullio Levi-Civita and Gregorio Ricci-Curbastro in 1900 - soon popularized by its use in Einstein's theory of general relativity.

[6] Hopefully, there is very little chance of confusing the angular momentum $\mathbf{L}$ (a vector) and its Cartesian components L_j (scalars with an index) on one hand, and the Lagrangian function L (a scalar without an index) on the other hand.

[7] See, e.g., MA Eq. (7.5).

4.3: Fixed-axis Rotation

Now we are well equipped for a discussion of rigid body's rotational dynamics. The general equation of this dynamics is given by Eq. (1.38), which is valid for dynamics of any system of particles - either rigidly connected or not:

$$\dot{\mathbf{L}} = \boldsymbol{\tau}, \tag{4.3.1}$$

where τ is the net torque of external forces. Let us start exploring this equation from the simplest case when the axis of rotation, i.e. the direction of vector ω, is fixed by some external constraints. Directing the z-axis along this vector, we have $\omega_x = \omega_y = 0$. According to Eq. (22), in this case, the z-component of the angular momentum,

$$L_z = I_{zz}\omega_z, \tag{4.3.2}$$

where I_{zz}, though not necessarily one of the principal moments of inertia, still may be calculated using Eq. (24):

$$I_{zz} = \sum m\rho_z^2 = \sum m\left(x^2 + y^2\right), \tag{4.3.3}$$

with ρ_z being the distance of each particle from the rotation axis z. According to Eq. (15), in this case the rotational kinetic energy is just

$$T_{\text{rot}} = \frac{I_{zz}}{2}\omega_z^2. \tag{4.3.4}$$

Moreover, it is straightforward to show that if the rotation axis is fixed, Eqs. (34)-(36) are valid even if the axis does not pass through the center of mass - provided that the distances ρ_z are now measured from that axis. (The proof is left for the reader's exercise.)

As a result, we may not care about other components of the vector $\mathbf{L}$, [8] and use just one component of Eq. (33),

$$\dot{L}_z = \tau_z, \tag{4.3.5}$$

because it, when combined with Eq. (34), completely determines the dynamics of rotation:

$$I_{zz}\dot{\omega}_z = \tau_z, \quad \text{i.e. } I_{zz}\ddot{\theta}_z = \tau_z, \tag{4.3.6}$$

where θ_z is the angle of rotation about the axis, so that $\omega_z = \dot{\theta}$. The scalar relations (34), (36) and (38), describing rotation about a fixed axis, are completely similar to the corresponding formulas of 1D motion of a single particle, with ω_z corresponding to the usual ("linear") velocity, the angular momentum component L_z - to the linear momentum, and I_z-to particle's mass.

The resulting motion about the axis is also frequently similar to that of a single particle. As a simple example, let us consider what is called the physical pendulum (Figure 5) - a rigid body free to rotate about a fixed horizontal axis that does not pass through the center of mass 0 , in a uniform gravity field $\mathbf{g}$.

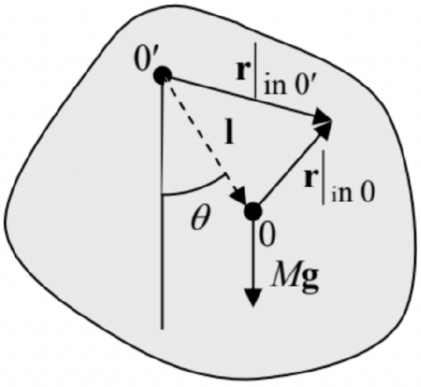

Figure 4.5. Physical pendulum: a body with a fixed (horizontal) rotation axis 0' that does not pass through the center of mass 0 . (The plane of drawing is normal to the axis.)

Let us drop the perpendicular from point 0 to the rotation axis, and call the oppositely directed vector $\mathbf{l}$ - see the dashed arrow in Figure 5. Then the torque (relative to the rotation axis 0 ') of the forces keeping the axis fixed is zero, and the only contribution to the net torque is due to gravity alone:

$$\boldsymbol{\tau}\big|_{\text{in } 0'} \equiv \sum \mathbf{r}\big|_{\text{in } 0'} \times \mathbf{F} = \sum (\mathbf{l} + \mathbf{r}\big|_{\text{in } 0}) \times m\mathbf{g} = \sum m(\mathbf{l} \times \mathbf{g}) + \sum m\mathbf{r}\big|_{\text{in } 0} \times \mathbf{g} = M\mathbf{l} \times \mathbf{g}. \tag{4.3.7}$$

(The last step used the facts that point 0 is the center of mass, so that the second term in the right-hand side equals zero, and that the vectors $\mathbf{l}$ and $\mathbf{g}$ are the same for all particles of the body.)

This result shows that the torque is directed along the rotation axis, and its (only) component τ_z is equal to $-Mgl\sin\theta$, where θ is the angle between the vectors $\mathbf{l}$ and $\mathbf{g}$, i.e. the angular deviation of the pendulum from the position of equilibrium - see Figure 5 again. As a result, Eq. (38) takes the form,

$$I'\ddot{\theta} = -Mgl\sin\theta, \tag{4.3.8}$$

where I' is the moment of inertia for rotation about the axis 0 ' rather than about the center of mass. This equation is identical to Eq. (1.18) for the point-mass (sometimes called "mathematical") pendulum, with the small-oscillation frequency

$$\Omega = \left(\frac{Mgl}{I'}\right)^{1/2} \tag{4.3.9}$$

As a sanity check, in the simplest case when the linear size of the body is much smaller than the suspension length l, Eq. (35) yields $I' = Ml^2$, and Eq. (41) reduces to the well-familiar formula $\Omega = (g/l)^{1/2}$ for the point-mass pendulum.

Now let us discuss the situations when a rigid body not only rotates but also moves as a whole. As we already know from our introductory chapter, the total linear momentum of the body,

$$\mathbf{P} \equiv \sum m\mathbf{v} = \sum m\dot{\mathbf{r}} = \frac{d}{dt}\sum m\mathbf{r} \tag{4.3.10}$$

satisfies the 2nd Newton law in the form (1.30). Using the definition (13) of the center of mass, the momentum may be represented as

$$\mathbf{P} = M\dot{\mathbf{R}} = M\mathbf{V},$$
$$M\dot{\mathbf{V}} = \mathbf{F},$$

where $\mathbf{F}$ is the vector sum of all external forces. This equation shows that the center of mass of the body moves exactly like a point particle of mass M, under the effect of the net force $\mathbf{F}$. In many cases, this fact makes the translational dynamics of a rigid body absolutely similar to that of a point particle.

The situation becomes more complex if some of the forces contributing to the vector sum $\mathbf{F}$ depend on the rotation of the same body, i.e. if its rotational and translational motions are coupled. Analysis of such coupled motion is rather straightforward if the direction of the rotation axis does not change in time, and hence Eqs. (35)-(36) are still valid. Possibly the simplest example is a round cylinder (say, a wheel) rolling on a surface without slippage (Figure 6). Here the no-slippage condition may be represented as the requirement of the net velocity of the particular wheel's point A that touches the surface to equal zero - in the reference frame connected to the surface. For the simplest case of plane surface (Figure 6a), this condition may be spelled out using Eq. (10), giving the following relation between the angular velocity ω of the wheel and the linear velocity V of its center:

$$V + r\omega = 0.$$

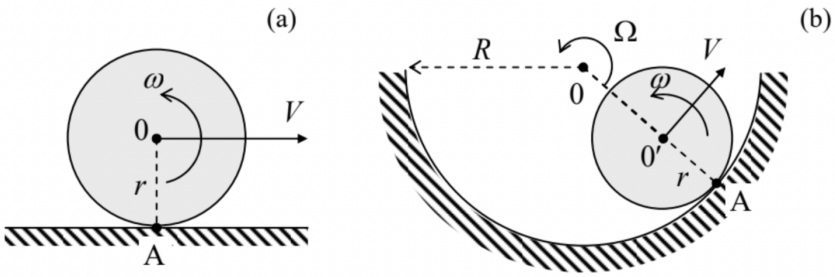

Figure 4.6. Round cylinder rolling over (a) a plane surface and (b) a concave surface.

Such kinematic relations are essentially holonomic constraints, which reduce the number of degrees of freedom of the system. For example, without the no-slippage condition (45), the wheel on a plane surface has to be considered as a system with two degrees of freedom, making its total kinetic energy (14) a function of two independent generalized velocities, say V and ω :

$$T = T_{\text{tran}} + T_{\text{rot}} = \frac{M}{2}V^2 + \frac{I}{2}\omega^2. \tag{4.3.11}$$

Using Eq. (45) we may eliminate, for example, the linear velocity and reduce Eq. (46) to

$$T = \frac{M}{2}(\omega r)^2 + \frac{I}{2}\omega^2 \equiv \frac{I_{\text{ef}}}{2}\omega^2, \quad \text{where } I_{\text{ef}} \equiv I + Mr^2. \tag{4.3.12}$$

This result may be interpreted as the kinetic energy of pure rotation of the wheel about the instantaneous rotation axis A, with I_{ef} being the moment of inertia about that axis, satisfying Eq. (29).

Kinematic relations are not always as simple as Eq. (45). For example, if a wheel is rolling on a concave surface (Figure 6b), we need to relate the angular velocities of the wheel's rotation about its axis 0 ' (say, ω) and that (say, Ω) of its axis' rotation about the center 0 of curvature of the surface. A popular error here is to write $\Omega = -(r/R)\omega$ [WRONG!]. A prudent way to derive the correct relation is to note that Eq. (45) holds for this situation as well, and on the other hand, the same linear velocity of the wheel's center may be expressed as $V = (R-r)\Omega$. Combining these formulas, we get the correct relation

$$\Omega = -\frac{r}{R-r}\omega. \tag{4.3.13}$$

Another famous example of the relation between the translational and rotational motion is given by the "sliding ladder" problem (Figure 7). Let us analyze it for the simplest case of negligible friction, and the ladder's thickness small in comparison with its length l.

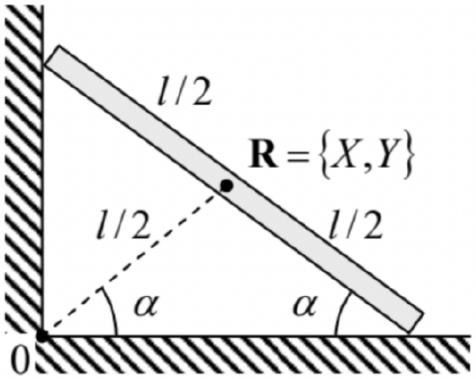

Figure 4.7. The sliding ladder problem.

To use the Lagrangian formalism, we may write the kinetic energy of the ladder as the sum (14) of its translational and rotational parts:

$$T = \frac{M}{2}\left(\dot{X}^2 + \dot{Y}^2\right) + \frac{I}{2}\dot{\alpha}^2, \tag{4.3.14}$$

where X and Y are the Cartesian coordinates of its center of mass in an inertial reference frame, and I is the moment of inertia for rotation about the z-axis passing through the center of mass. (For the uniformly distributed mass, an elementary integration of Eq. (35) yields $I = Ml^2/12$). In the reference frame with the center in the corner 0 , both X and Y may be simply expressed via the angle α :

$$X = \frac{l}{2}\cos\alpha, \quad Y = \frac{l}{2}\sin\alpha. \tag{4.3.15}$$

(The easiest way to obtain these relations is to notice that the dashed line in Figure 7 has length $l/2$, and the same slope α as the ladder.) Plugging these expressions into Eq. (49), we get

$$T = \frac{I_{\text{ef}}}{2}\dot{\alpha}^2, \quad I_{\text{ef}} \equiv I + M\left(\frac{l}{2}\right)^2 = \frac{1}{3}Ml^2. \tag{4.3.16}$$

Since the potential energy of the ladder in the gravity field may be also expressed via the same angle,

$$U = MgY = Mg\frac{l}{2}\sin\alpha, \tag{4.3.17}$$

α may be conveniently used as the (only) generalized coordinate of the system. Even without writing the Lagrange equation of motion for that coordinate, we may notice that since the Lagrangian function $L \equiv T - U$ does not depend on time explicitly, and the kinetic energy (51) is a quadratic-homogeneous function of the generalized velocity $\dot{\alpha}$, the full mechanical energy,

$$E \equiv T + U = \frac{I_{\text{ef}}}{2}\dot{\alpha}^2 + Mg\frac{l}{2}\sin\alpha = \frac{Mgl}{2}\left(\frac{l\dot{\alpha}^2}{3g} + \sin\alpha\right), \tag{4.3.18}$$

is conserved, giving us the first integral of motion. Moreover, Eq. (53) shows that the system's energy (and hence dynamics) is identical to that of a physical pendulum with an unstable fixed point $\alpha_1 = \pi/2$, a stable fixed point at $\alpha_2 = -\pi/2$, and frequency

$$\Omega = \left(\frac{3g}{2l}\right)^{1/2} \tag{4.3.19}$$

of small oscillations near the latter point. (Of course, this fixed point cannot be reached in the simple geometry shown in Figure 7, where the ladder's fall on the floor would change its equations of motion. Moreover, even before that, the left end of the ladder may detach from the wall. The analysis of this issue is left for the reader's exercise.)

---

[8] Note that according to Eq. (22), other Cartesian components of the angular momentum, L_x and L_y, may be different from zero, and may even evolve in time. The corresponding torques τ_x and τ_y, which obey Eq. (33), are automatically provided by the external forces that keep the rotation axis fixed.

4.4: Free Rotation

Now let us proceed to the more complex case when the rotation axis is not fixed. A good illustration of the complexity arising in this case comes from the case of a rigid body left alone, i.e. not subjected to external forces and hence with its potential energy U constant. Since in this case, according to Eq. (44), the center of mass moves (as measured from any inertial reference frame) with a constant velocity, we can always use a convenient inertial reference frame with the origin at that point. From the point of view of such a frame, the body's motion is a pure rotation, and $T_{\text{tran}} = 0$. Hence, the system's Lagrangian equals just the rotational energy (15), which is, first, a quadratic-homogeneous function of the components ω_j (which may be taken for generalized velocities), and, second, does not depend on time explicitly. As we know from Chapter 2, in this case the mechanical energy, here equal to T_{rot} alone, is conserved. According to Eq. (15), for the principal-axes components of the vector ω, this means

$$T_{\text{rot}} = \sum_{j=1}^{3} \frac{I_j}{2} \omega_j^2 = \text{const} \tag{4.4.1}$$

Next, as Eq. (33) shows, in the absence of external forces, the angular momentum $\mathbf{L}$ of the body is conserved as well. However, though we can certainly use Eq. (26) to represent this fact as

$$\mathbf{L} = \sum_{j=1}^{3} I_j \omega_j \mathbf{n}_j = \text{const}\,, \tag{4.4.2}$$

where $\mathbf{n}_j$ are the principal axes, this does not mean that all components ω_j are constant, because the principal axes are fixed relative to the rigid body, and hence may rotate with it.

Before exploring these complications, let us briefly mention two conceptually trivial, but practically very important, particular cases. The first is a spherical top $(I_1 = I_2 = I_3 = I)$. In this case, Eqs. (55) and (56) imply that all components of the vector $\omega = \mathbf{L}/\mathrm{I}$, i.e. both the magnitude and the direction of the angular velocity are conserved, for any initial spin. In other words, the body conserves its rotation speed and axis direction, as measured in an inertial frame. The most obvious example is a spherical planet. For example, our Mother Earth, rotating about its axis with angular velocity $\omega = 2\pi/(1\text{ day}) \approx 7.3 \times 10^{-5}\ \text{s}^{-1}$, keeps its axis at a nearly constant angle of $23^\circ 27'$ to the ecliptic pole, i.e. the axis normal to the plane of its motion around the Sun. (In Sec. 6 below, we will discuss some very slow motions of this axis, due to gravity effects.)

Spherical tops are also used in the most accurate gyroscopes, usually with gas-jet or magnetic suspension in vacuum. If done carefully, such systems may have spectacular stability. For example, the gyroscope system of the Gravity Probe B satellite experiment, flown in 2004-5, was based on quartz spheres - round with precision of about 10 nm and covered with superconducting thin films (which enabled their magnetic suspension and monitoring). The whole system was stable enough to measure that the so-called geodetic effect in general relativity (essentially, the space curving by Earth's mass), resulting in the axis' precession by only 6.6 arc seconds per year, i.e. with a precession frequency of just $\sim 10^{-11}\ \text{s}^{-1}$, agrees with theory with a record $\sim 0.3\%$ accuracy. [9]

The second simple case is that of the symmetric top $(I_1 = I_2 \neq I_3)$, with the initial vector $\mathbf{L}$ aligned with the main principal axis. In this case, $\omega = \mathbf{L}/\mathrm{I}_3 = $ const, so that the rotation axis is conserved. [10] Such tops, typically in the shape of a flywheel (heavy, flat rotor), and supported by a three-ring gimbal system (also called the "Cardan suspensions") that allow for torque-free rotation about three mutually perpendicular axes,[11] are broadly used in more common gyroscopes. Invented by Léon Foucault in the 1850s and made practical by H. Anschütz-Kaempfe, such gyroscopes have become core parts of automatic guidance systems, for example, in ships, airplanes, missiles, etc. Even if its support wobbles and/or drifts, the suspended gyroscope sustains its direction relative to an inertial reference frame.[12]

However, in the general case with no such special initial alignment, the dynamics of symmetric tops is more complicated. In this case, the vector $\mathbf{L}$ is still conserved, including its direction, but the vector ω is not. Indeed, let us direct the $\mathbf{n}_2$ axis normally to the common plane of vectors $\mathbf{L}$ and the current instantaneous direction $\mathbf{n}_3$ of the main principal axis (in Figure 8 below, the plane of the drawing); then, in that particular instant, $L_2 = 0$. Now let us recall that in a symmetric top, the axis $\mathbf{n}_2$ is a principal one. According to Eq. (26) with $j = 2$, the corresponding component ω_2 has to be equal to L_2/I_2, so it is equal to zero. This means that the vector ω lies in this plane (the common plane of vectors $\mathbf{L}$ and $\mathbf{n}_3$) as well - see Figure 8a.

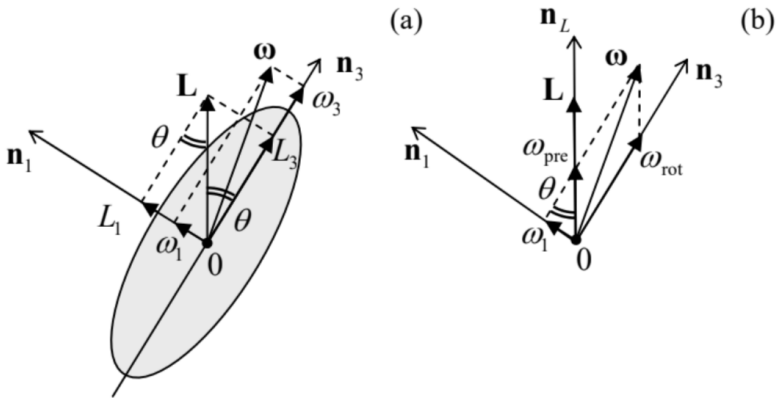

Figure 4.8. Free rotation of a symmetric top: (a) the general configuration of vectors, and (b) calculating the free precession frequency.

Now consider any point located on the main principal axis $\mathbf{n}_3$, and hence on the plane $[\mathbf{n}_3, \mathbf{L}]$. Since ω is the instantaneous axis of rotation, according to Eq. (9), the instantaneous velocity $\mathbf{v} = \omega \times \mathbf{r}$ of the point is directed normally to that plane. Since this is true for each point of the main axis (besides only one, with $\mathbf{r} = 0$, i.e. the center of mass, which does not move), this axis as a whole has to move perpendicular to the common plane of the vectors $\mathbf{L}, \omega$, and $\mathbf{n}_3$. Since this conclusion is valid for any moment of time, it means that the vectors ω and $\mathbf{n}_3$ rotate about the space-fixed vector $\mathbf{L}$ together, with some angular velocity ω_{pre}, at each moment staying within one plane. This effect is usually called the free precession (or "torque-free", or "regular") precession, and has to be clearly distinguished it from the completely different effect of the torque-induced precession, which will be discussed in the next section.To calculate ω_{pre}, let us represent the instant vector ω as a sum of not its Cartesian components (as in Figure 8a), but rather of two non-orthogonal vectors directed along $\mathbf{n}_3$ and $\mathbf{L}$ (Figure 8b):

$$\boldsymbol{\omega} = \omega_{\text{rot}} \mathbf{n}_3 + \omega_{\text{pre}} \mathbf{n}_L, \quad \mathbf{n}_L \equiv \frac{\mathbf{L}}{L}. \tag{4.4.3}$$

Figure 8b shows that ω_{rot} has the meaning of the angular velocity of rotation of the body about its main principal axis, while ω_{pre} is the angular velocity of rotation of that axis about the constant direction of the vector $\mathbf{L}$, i.e. the frequency of precession, i.e. exactly what we are trying to find. Now ω_{pre} may be readily calculated from the comparison of two panels of Figure 8, by noticing that the same angle θ between the vectors $\mathbf{L}$ and $\mathbf{n}_3$ participates in two relations:

$$\sin\theta = \frac{L_1}{L} = \frac{\omega_1}{\omega_{\text{pre}}}. \tag{4.4.4}$$

Since the $\mathbf{n}_1$-axis is a principal one, we may use Eq. (26) for $j = 1$, i.e. $L_1 = I_1 \omega_1$, to eliminate ω_1 from Eq. (58), and get a very simple formula

$$\omega_{\text{pre}} = \frac{L}{I_1}. \tag{4.4.5}$$

This result shows that the precession frequency is constant and independent of the alignment of the vector $\mathbf{L}$ with the main principal axis $\mathbf{n}_3$, while the amplitude of this motion (characterized by the angle θ) does depend on the alignment, and vanishes if $\mathbf{L}$ is parallel to $\mathbf{n}_3$. [13] Note also that if all principal moments of inertia are of the same order, ω_{pre} is of the same order as the total angular speed $\omega \equiv |\omega|$ of rotation.

Now let us briefly discuss the free precession in the general case of an "asymmetric top", i.e. a body with arbitrary $I_1 \neq I_2 \neq I_3$. In this case, the effect is more complex because here not only the direction but also the magnitude of the instantaneous angular velocity ω may evolve in time. If we are only interested in the relation between the instantaneous values of ω_j and L_j, i.e. the "trajectories" of the vectors ω and $\mathbf{L}$ as observed from the reference frame $\{\mathbf{n}_1, \mathbf{n}_2, \mathbf{n}_3\}$ of the principal axes of the body (rather than the explicit law of their time evolution), they may be found directly from the conservation laws. (Let me emphasize again that the vector $\mathbf{L}$, being constant in an inertial reference frame, generally evolves in the frame rotating with the body.) Indeed, Eq. (55) may be understood as the equation of an ellipsoid in Cartesian coordinates $\{\omega_1, \omega_2, \omega_3\}$, so that for a free body, the vector ω has to stay on the surface of that ellipsoid. [14] On the other hand, since the reference frame rotation preserves the length of any vector, the magnitude (but not the direction!) of the vector $\mathbf{L}$ is also an integral of motion in the moving frame, and we can write

$$L^2 \equiv \sum_{j=1}^{3} L_j^2 = \sum_{j=1}^{3} I_j^2 \omega_j^2 = \text{ const} \tag{4.4.6}$$

Hence the trajectory of the vector ω follows the closed curve formed by the intersection of two ellipsoids, (55) and (60). It is evident that this trajectory is generally "taco-edge-shaped", i.e. more complex than a planar circle, but never very complex either. [15]

The same argument may be repeated for the vector $\mathbf{L}$, for whom the first form of Eq. (60) descries a sphere, and Eq. (55), another ellipsoid:

$$T_{\text{rot}} = \sum_{j=1}^{3} \frac{1}{2I_j} L_j^2 = \text{const}. \tag{4.4.7}$$

On the other hand, if we are interested in the trajectory of the vector ω as observed from an inertial frame (in which the vector $\mathbf{L}$ stays still), we may note that the general relation (15) for the same rotational energy T_{rot} may also be rewritten as

$$T_{\text{rot}} = \frac{1}{2} \sum_{j=1}^{3} \omega_j \sum_{j'=1}^{3} I_{jj'} \omega_{j'}. \tag{4.4.8}$$

But according to the Eq. (22), the second sum on the right-hand side is nothing more than L_j, so that

$$T_{\text{rot}} = \frac{1}{2} \sum_{j=1}^{3} \omega_j L_j = \frac{1}{2} \boldsymbol{\omega} \cdot \mathbf{L}. \tag{4.4.9}$$

This equation shows that for a free body ($T_{\text{rot}} = \text{const}$, $\mathbf{L} = \text{const}$), even if the vector ω changes in time, its endpoint should stay within a plane perpendicular to the angular momentum $\mathbf{L}$. (Earlier, we have seen that for the particular case of the symmetric top - see Figure 8b, but for an asymmetric top, the trajectory of the endpoint may not be circular.)

If we are interested not only in the trajectory of the vector ω, but also the law of its evolution in time, it may be calculated using the general Eq. (33) expressed in the principal components ω_j. For that, we have to recall that Eq. (33) is only valid in an inertial reference frame, while the frame $\{\mathbf{n}_1, \mathbf{n}_2, \mathbf{n}_3\}$ may rotate with the body and hence is generally not inertial. We may handle this problem by applying, to the vector $\mathbf{L}$, the general kinematic relation (8):

$$\left.\frac{d\mathbf{L}}{dt}\right|_{\text{in lab}} = \left.\frac{d\mathbf{L}}{dt}\right|_{\text{in mov}} + \boldsymbol{\omega} \times \mathbf{L}. \tag{4.4.10}$$

Combining it with Eq. (33), in the moving frame we get

$$\frac{d\mathbf{L}}{dt} + \boldsymbol{\omega} \times \mathbf{L} = \boldsymbol{\tau}, \tag{4.4.11}$$

where τ is the external torque. In particular, for the principal-axis components L_j, related to the components ω_i by Eq. (26), the vector equation (65) is reduced to a set of three scalar Euler equations

$$I_j \dot{\omega}_j + \left(I_{j''} - I_{j'}\right) \omega_{j'} \omega_{j''} = \tau_j, \tag{4.4.12}$$

where the set of indices $\{j, j', j''\}$ has to follow the usual "right" order - e.g., $\{1, 2, 3\}$, etc. [16]

In order to get a feeling how do the Euler equations work, let us return to the particular case of a free symmetric top $(\tau_1 = \tau_2 = \tau_3 = 0, I_1 = I_2 \neq I_3)$. In this case, $I_1 - I_2 = 0$, so that Eq. (66) with $j = 3$ yields $\omega_3 = \text{const}$, while the equations for $j = 1$ and $j = 2$ take the following simple form:

$$\dot{\omega}_1 = -\Omega_{\text{pre}}\, \omega_2, \quad \dot{\omega}_2 = \Omega_{\text{pre}}\, \omega_1, \tag{4.4.13}$$

where Ω_{pre} is a constant determined by both the system parameters and the initial conditions:

$$\Omega_{\text{pre}} \equiv \omega_3 \frac{I_3 - I_1}{I_1}. \tag{4.4.14}$$

The system of two equations (67) has a sinusoidal solution with frequency Ω_{pre}, and describes a uniform rotation of the vector ω, with that frequency, about the main axis $\mathbf{n}_3$. This is just another representation of the torque-free precession analyzed above, this

time as observed from the rotating body. Evidently, $\Omega_{\rm pre}$ is substantially different from the frequency $\omega_{\rm pre}$ (59) of the precession as observed from the lab frame; for example, $\Omega_{\rm pre}$ vanishes for the spherical top (with $I_1 = I_2 = I_3$), while $\omega_{\rm pre}$, in this case, is equal to the rotation frequency.

Unfortunately, for the rotation of an asymmetric top (i.e., an arbitrary rigid body), when no component ω_j is conserved, the Euler equations (66) are strongly nonlinear even in the absence of any external torque, and a discussion of their solutions would take more time than I can afford. [17]

---

[9] Still, the main goal of this rather expensive ($750M) project, an accurate measurement of a more subtle relativistic effect, the so-called frame-dragging drift (also called "the Schiff precession"), predicted to be about 0.04 arc seconds per year, has not been achieved.

[10] This is also true for an asymmetric top, i.e. an arbitrary body (with, say, $I_1 < I_2 < I_3$), but in this case the alignment of the vector $\mathbf{L}$ with the axis $\mathbf{n}_2$ corresponding to the intermediate moment of inertia, is unstable: an infinitesimal initial misalignment of these vectors may lead to their large misalignment during the motion.

[11] See, for example, a very nice animation available online at http://en.Wikipedia.org/wiki/Gimbal.

[12] Much more compact (and much less accurate) gyroscopes used, for example, in smartphones and tablet computers, are based on a more subtle effect of rotation on mechanical oscillator's frequency, and are implemented as micro-electromechanical systems (MEMS) on silicon chip surfaces - see, e.g., Chapter 22 in V. Kaajakari, Practical MEMS, Small Gear Publishing, 2009.

[13] For our Earth, the free precession amplitude is so small (corresponding to sub-10-m linear displacements of the Earth surface) that this effect is of the same order as other, more irregular motions of the rotation axis, resulting from the turbulent fluid flow effects in planet's interior and its atmosphere.

[14] It is frequently called the Poinsot's ellipsoid, named after Louis Poinsot (1777-1859) who has made several important contributions to rigid body mechanics.

[15] Curiously, the "wobbling" motion along such trajectories was observed not only for macroscopic rigid bodies, but also for heavy atomic nuclei - see, e.g., N. Sensharma et al., Phys. Rev. Lett. 124, 052501 (2020).

[16] These equations are of course valid in the simplest case of the fixed rotation axis as well. For example, if $\omega = \mathbf{n}_z\omega$, i.e. $\omega_x = \omega_y = 0$, Eq. (66) is reduced to Eq. (38).

[17] For our Earth with its equatorial bulge (see Sec. 6 below), the ratio $(I_3 - I_1)/I_1$ is $\sim 1/300$, so that $2\pi/\Omega_{\rm pre}$ is about 10 months. However, due to the fluid flow effects mentioned above, the observed precession is not very regular.

[18] Such discussion may be found, for example, in Sec. 37 of L. Landau and E. Lifshitz, Mechanics, $3^{\rm rd}$ ed., Butterworth-Heinemann, 1976.

4.5: Torque-induced Precession

The dynamics of rotation becomes even more complex in the presence of external forces. Let us consider the most important and counter-intuitive effect of torque-induced precession, for the simplest case of an axially-symmetric body (which is a particular case of the symmetric top, $I_1 = I_2 \neq I_3$), supported at some point A of its symmetry axis, that does not coincide with the center of mass 0 - see Figure 9.

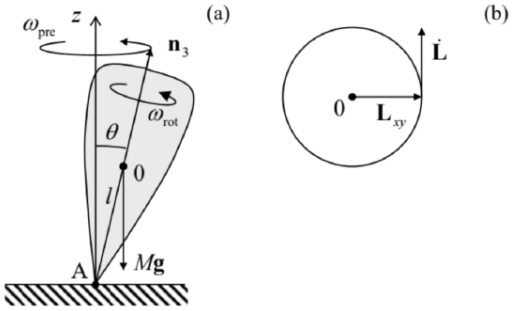

Figure 4.9. Symmetric top in the gravity field: (a) a side view at the system and (b) the top view at the evolution of the horizontal component of the angular momentum vector.

The uniform gravity field $\mathbf{g}$ creates bulk-distributed forces that, as we know from the analysis of the physical pendulum in Sec. 3, are equivalent to a single force $M\mathbf{g}$ applied in the center of mass - in Figure 9 , point 0 . The torque of this force relative to the support point A is

$$\boldsymbol{\tau} = \mathbf{r}_0|_{\text{in A}} \times M\mathbf{g} = Ml\mathbf{n}_3 \times \mathbf{g}. \tag{4.5.1}$$

Hence the general equation (33) of the angular momentum evolution (valid in any inertial frame, for example the one with an origin in point A) becomes

$$\dot{\mathbf{L}} = Ml\mathbf{n}_3 \times \mathbf{g}. \tag{4.5.2}$$

Despite the apparent simplicity of this (exact!) equation, its analysis is straightforward only in the limit when the top is launched spinning about its symmetry axis $\mathbf{n}_3$ with a very high angular velocity $\omega_{\text{rot.}}$. In this case, we may neglect the contribution to $\mathbf{L}$ due to a relatively small precession velocity ω_{pre} (still to be calculated), and use Eq. (26) to write

$$\mathbf{L} = I_3\boldsymbol{\omega} = I_3\omega_{\text{rot}}\mathbf{n}_3. \tag{4.5.3}$$

Then Eq. (70) shows that the vector $\mathbf{L}$ is perpendicular to both $\mathbf{n}_3$ (and hence $\mathbf{L}$) and $\mathbf{g}$, i.e. lies within the horizontal plane and is perpendicular to the horizontal component $\mathbf{L}_{xy}$ of the vector $\mathbf{L}-$ see Figure 9 b. Since, according to Eq. (70), the magnitude of this vector is constant, $|\mathbf{L}| = mgl\sin\theta$, the vector $\mathbf{L}$ (and hence the body's main axis) rotates about the vertical axis with the following angular velocity:

Torque-induced ecession: fintion limit

$$\omega_{\text{pre}} = \frac{|\dot{\mathbf{L}}|}{L_{xy}} = \frac{Mgl\sin\theta}{L\sin\theta} \equiv \frac{Mgl}{L} = \frac{Mgl}{I_3\omega_{\text{rot}}}.$$

Thus, very counter-intuitively, the fast-rotating top does not follow the external, vertical force and, in addition to fast spinning about the symmetry axis $\mathbf{n}_3$, performs a revolution, called the torqueinduced precession, about the vertical axis. Note that, similarly to the free-precession frequency (59), the torque-induced precession frequency (72) does not depend on the initial (and sustained) angle θ. However, the torque-induced precession frequency is inversely (rather than directly) proportional to ω_{rot} . This fact makes the above simple theory valid in many practical cases. Indeed, Eq. (71) is quantitatively valid if the contribution of the precession into $\mathbf{L}$ is relatively small: $I\omega_{\text{pre}} \ll I_3\omega_{\text{rot}}$, where I is a certain effective moment of inertia for the precession - to be calculated below. Using Eq. (72), this condition may be rewritten as

$$\omega_{\rm rot} >> \left(\frac{MglI}{I_3^2}\right)^{1/2}. \tag{4.5.4}$$

According to Eq. (16), for a body of not too extreme proportions, i.e. with all linear dimensions of the order of the same length scale l, all inertia moments are of the order of Ml^2, so that the right-hand side of Eq. (73) is of the order of $(g/l)^{1/2}$, i.e. comparable with the frequency of small oscillations of the same body as the physical pendulum, i.e. at the absence of its fast rotation.

To develop a qualitative theory that would be valid beyond such approximate treatment, the Euler equations (66) may be used, but are not very convenient. A better approach, suggested by the same L. Euler, is to introduce a set of three independent angles between the principal axes $\{\mathbf{n}_1, \mathbf{n}_2, \mathbf{n}_3\}$ bound to the rigid body, and the axes $\{\mathbf{n}_x, \mathbf{n}_y, \mathbf{n}_z\}$ of an inertial reference frame (Figure 10), and then express the basic equation (33) of rotation, via these angles. There are several possible options for the definition of such angles; Figure 10 shows the set of Euler angles, most convenient for analyses of fast rotation. [18] As one can see, the first Euler angle, θ, is the usual polar angle measured from the $\mathbf{n}_z$-axis to the $\mathbf{n}_3$-axis. The second one is the azimuthal angle φ, measured from the $\mathbf{n}_x$-axis to the so-called line of nodes formed by the intersection of planes $[\mathbf{n}_x, \mathbf{n}_y]$ and $[\mathbf{n}_1, \mathbf{n}_2]$. The last Euler angle, ψ, is measured Euler within the plane $[\mathbf{n}_1, \mathbf{n}_2]$, from the line of nodes to axis $\mathbf{n}_1$-axis. For example, in the simple picture of slow force-induced precession of a symmetric top, that was discussed above, the angle θ is constant, the angle ψ changes rapidly, with the rotation velocity $\omega_{\rm rot}$, while the angle φ evolves with the precession frequency $\omega_{\rm pre}$ (72).

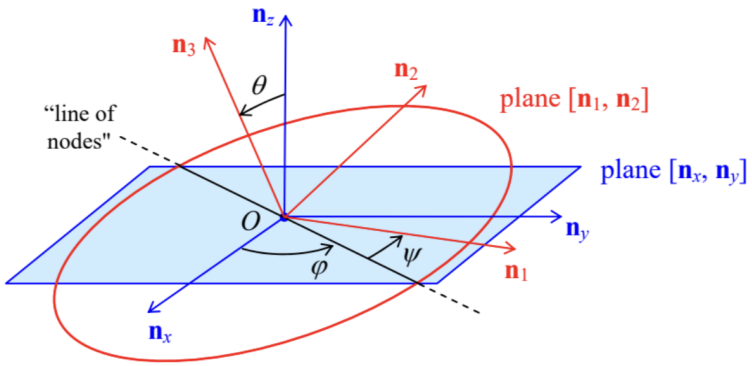

Fig. 4.10. Definition of the Euler angles.

Now we can express the principal-axes components of the instantaneous angular velocity vector, ω_1, ω_2, and ω_3, as measured in the lab reference frame, in terms of the Euler angles. This may be readily done by calculating, from Figure 10, the contributions of the Euler angles' evolution to the rotation about each principal axis, and then adding them up:

$$\begin{aligned}
\omega_1 &= \dot{\varphi}\sin\theta\sin\psi + \dot{\theta}\cos\psi \\
\omega_2 &= \dot{\varphi}\sin\theta\cos\psi - \dot{\theta}\sin\psi \\
\omega_3 &= \dot{\varphi}\cos\theta + \dot{\psi}
\end{aligned}$$

These relations enable the expression of the kinetic energy of rotation (25) and the angular momentum components (26) via the generalized coordinates θ, φ, and ψ and their time derivatives (i.e. the corresponding generalized velocities), and then using the powerful Lagrangian formalism to derive their equations of motion. This is especially simple to do in the case of symmetric tops (with $I_1 = I_2$), because plugging Eqs. (74) into Eq. (25) we get an expression,

$$T_{\rm rot} = \frac{I_1}{2}\left(\dot{\theta}^2 + \dot{\varphi}^2\sin^2\theta\right) + \frac{I_3}{2}(\dot{\varphi}\cos\theta + \dot{\psi})^2, \tag{4.5.5}$$

which does not include explicitly either φ or ψ. (This reflects the fact that for a symmetric top we can always select the $\mathbf{n}_1$-axis to coincide with the line of nodes, and hence take $\psi = 0$ at the considered moment of time. Note that this trick does not mean we can take $\dot{\psi} = 0$, because the $\mathbf{n}_1$-axis, as observed from an inertial reference frame, moves!) Now we should not forget that at the torque-induced precession, the center of mass moves as well (see, e.g., Figure 9), so that according to Eq. (14), the total kinetic energy of the body is the sum of two terms,

$$T = T_{\rm rot} + T_{\rm tran}, \quad T_{\rm tran} = \frac{M}{2}V^2 = \frac{M}{2}l^2\left(\dot{\theta}^2 + \dot{\varphi}^2\sin^2\theta\right), \tag{4.5.6}$$

while its potential energy is just

$$U = Mgl\cos\theta + \text{ const}\,. \tag{4.5.7}$$

Now we could readily write the Lagrange equations of motion for the Euler angles, but it is simpler to immediately notice that according to Eqs. (75)-(77), the Lagrangian function, $T-U$, does not depend explicitly on the "cyclic" coordinates φ and ψ, so that the corresponding generalized momenta (2.31) are conserved:

$$p_\varphi \equiv \frac{\partial T}{\partial \dot\varphi} = I_{\rm A}\dot\varphi\sin^2\theta + I_3(\dot\varphi\cos\theta + \dot\psi)\cos\theta = \text{const},$$

$$p_\psi \equiv \frac{\partial T}{\partial \dot\psi} = I_3(\dot\varphi\cos\theta + \dot\psi) = \text{const},$$

where $I_{\rm A} \equiv I_1 + Ml^2$. (According to Eq. (29), $I_{\rm A}$ is just the body's moment of inertia for rotation about a horizontal axis passing through the support point A.) According to the last of Eqs. (74), p_ψ is just L_3, i.e. the angular momentum's component along the precessing axis $\mathbf{n}_3$. On the other hand, by its very definition (78), p_φ is L_z, i.e. the same vector $\mathbf{L}$'s component along the static axis z. (Actually, we could foresee in advance the conservation of both these components of $\mathbf{L}$ for our system, because the vector (69) of the external torque is perpendicular to both $\mathbf{n}_3$ and $\mathbf{n}_z$.) Using this notation, and solving the simple system of linear equations (78)-(79) for the angle derivatives, we get

$$\dot\varphi = \frac{L_z - L_3\cos\theta}{I_{\rm A}\sin^2\theta}, \quad \dot\psi = \frac{L_3}{I_3} - \frac{L_z - L_3\cos\theta}{I_{\rm A}\sin^2\theta}\cos\theta. \tag{4.5.8}$$

One more conserved quantity in this problem is the full mechanical energy [19]

$$E \equiv T + U = \frac{I_{\rm A}}{2}\left(\dot\theta^2 + \dot\varphi^2\sin^2\theta\right) + \frac{I_3}{2}(\dot\varphi\cos\theta + \dot\psi)^2 + Mgl\cos\theta. \tag{4.5.9}$$

Plugging Eqs. (80) into Eq. (81), we get a first-order differential equation for the angle θ, which may be represented in the following physically transparent form:

$$\frac{I_{\rm A}}{2}\dot\theta^2 + U_{\rm ef}(\theta) = E, \quad U_{\rm ef}(\theta) \equiv \frac{(L_z - L_3\cos\theta)^2}{2I_{\rm A}\sin^2\theta} + \frac{L_3^2}{2I_3} + Mgl\cos\theta + \text{ const} \tag{4.5.10}$$

Thus, similarly to the planetary problems considered in Sec. 3.4, the torque-induced precession of a symmetric top has been reduced (without any approximations!) to a 1D problem of the motion of one of its degrees of freedom, the polar angle θ, in the effective potential $U_{\rm ef}(\theta)$. According to Eq. (82), very similar to Eq. (3.44) for the planetary problem, this potential is the sum of the actual potential energy U given by Eq. (77), and a contribution from the kinetic energy of motion along two other angles. In the absence of rotation about the axes $\mathbf{n}_z$ and $\mathbf{n}_3$ (i.e., $L_z = L_3 = 0$), Eq. (82) is reduced to the first integral of the equation (40) of motion of a physical pendulum, with $I' = I_{\rm A}$. If the rotation is present, then (besides the case of very special initial conditions when $\theta(0) = 0$ and $L_z = L_3$), [20] the first contribution to $U_{\rm ef}(\theta)$ diverges at $\theta \to 0$ and π, so that the effective potential energy has a minimum at some non-zero value θ_0 of the polar angle θ - see Figure 11 .

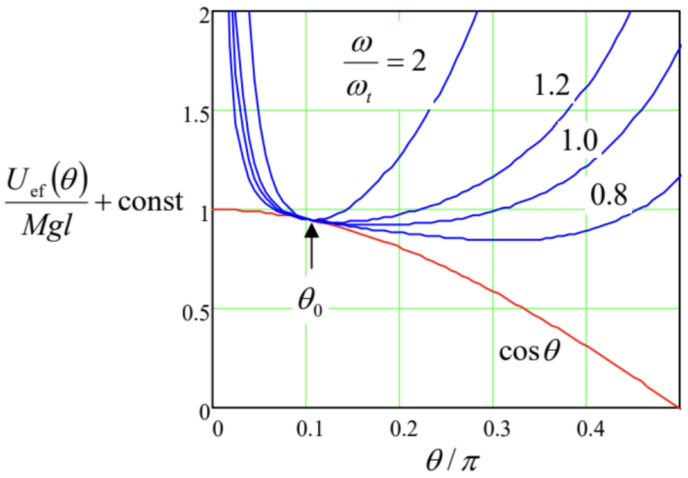

Figure 4.11. The effective potential energy U_{ef} of the symmetric top, given by Eq. (82), as a function of the polar angle θ, for a particular value (0.95) of the ratio $r \equiv L_z/L_3$ (so that at $\omega_{rot} >> \omega_h, \theta_0 = \cos^{-1} r \approx 0.1011\pi$), and several values of the ratio ω_{rot}/ω_{th}.

If the initial angle $\theta(0)$ is equal to this value θ_0, i.e. if the initial effective energy is equal to its minimum value $U_{ef}(\theta_0)$, the polar angle remains constant through the motion: $\theta(t) = \theta_0$. This corresponds to the pure torque-induced precession whose angular velocity is given by the first of Eqs. (80):

$$\omega_{pre} \equiv \dot{\varphi} = \frac{L_z - L_3 \cos\theta_0}{I_A \sin^2\theta_0}. \tag{4.5.11}$$

The condition for finding θ_0, $dU_{ef}/d\theta = 0$, is a transcendental algebraic equation that cannot be solved analytically for arbitrary parameters. However, in the high spinning speed limit (73), this is possible. Indeed, in this limit the Mgl-proportional contribution to U_{ef} is small, and we may analyze its effect by successive approximations. In the 0^{th} approximation, i.e. at $Mgl = 0$, the minimum of U_{ef} is evidently achieved at $\cos\theta_0 = L_z/L_3$, turning the precession frequency (83) to zero. In the next, 1^{st} approximation, we may require that at $\theta = \theta_0$, the derivative of the first term of Eq. (82) for U_{ef} over $\cos\theta$, equal to $L_z(L_z - L_3\cos\theta)/I_A \sin^2\theta$,[21] is canceled with that of the gravity-induced term, equal to Mgl. This immediately yields $\omega_{pre} = (L_z - L_3\cos\theta_0)/I_A \sin^2\theta_0 = Mgl/L_3$, so that identifying ω_{rot} with $\omega_3 \equiv L_3/I_3$ (see Figure 8), we recover the simple expression (72).

The second important result that may be readily obtained from Eq. (82) is the exact expression for the threshold value of the spinning speed for a vertically rotating top ($\theta = 0, L_z = L_3$). Indeed, in the limit $\theta \to 0$ this expression may be readily simplified:

$$U_{ef}(\theta) \approx \text{const} + \left(\frac{L_3^2}{8I_A} - \frac{Mgl}{2}\right)\theta^2. \tag{4.5.12}$$

This formula shows that if $\omega_{rot} \equiv L_3/I_3$ is higher than the following threshold value,

$$\text{Threshold rotation speed} \qquad \omega_{th} \equiv 2\left(\frac{MglI_A}{I_3^2}\right)^{1/2}, \tag{4.5.13}$$

then the coefficient at θ^2 in Eq. (84) is positive, so that U_{ef} has a stable minimum at $\theta_0 = 0$. On the other hand, if ω_3 is decreased below ω_{th}, the fixed point becomes unstable, so that the top falls. As the plots in Figure 11 show, Eq. (85) for the threshold frequency works very well even for non-zero but small values of the precession angle θ_0. Note that if we take $I = I_A$ in the condition (73) of the approximate treatment, it acquires a very simple sense: $\omega_{rot} >> \omega_{th}$.

Finally, Eqs. (82) give a natural description of one more phenomenon. If the initial energy is larger than $U_{ef}(\theta_0)$, the angle θ oscillates between two classical turning points on both sides of the fixed point θ_0-see also Figure 11. The law and frequency of these oscillations may be found exactly as in Sec. 3.3 - see Eqs. (3.27) and (3.28). At $\omega_3 \gg \omega_h$, this motion is a fast rotation of the symmetry axis $\mathbf{n}_3$ of the body about its average position performing the slow torque-induced precession. Historically, these

oscillations are called nutations, but their physics is similar to that of the free precession that was analyzed in the previous section, and the order of magnitude of their frequency is given by Eq. (59).

It may be proved that small friction (not taken into account in the above analysis) leads first to decay of these nutations, then to a slower drift of the precession angle θ_0 to zero and, finally, to a gradual decay of the spinning speed $\omega_{\rm rot}$ until it reaches the threshold (85) and the top falls.

---

[19] Of the several choices more convenient in the absence of fast rotation, the most common is the set of so-called Tait-Brian angles (called the yaw, pitch, and roll), which are broadly used for aircraft and maritime navigation.

[20] Indeed, since the Lagrangian does not depend on time explicitly, $H = \text{const}$, and since the full kinetic energy T (75)-(76) is a quadratic-homogeneous function of the generalized velocities, $E = H$.

[21] In that simple case, the body continues to rotate about the vertical symmetry axis: $\theta(t) = 0$. Note, however, that such motion is stable only if the spinning speed is sufficiently high - see Eq. (85) below.

[22] Indeed, the derivative of the fraction $1/2I_{\rm A}\sin^2\theta$, taken at the point $\cos\theta = L_z/L_3$, is multiplied by the numerator, $(L_z - L_3\cos\theta)^2$, which turns to zero at this point.

4.6: Non-inertial Reference Frames

To complete this chapter, let us use the results of our analysis of the rotation kinematics in Sec. 1 to complete the discussion of the transfer between two reference frames, started in the introductory Chapter 1. As Figure 12 (which reproduces Figure 1.2 in a more convenient notation) shows, even if the "moving" frame 0 rotates relative to the "lab" frame 0 ', the radius vectors observed from these two frames are still related, at any moment of time, by the simple Eq. (1.5). In our new notation:

$$\mathbf{r}' = \mathbf{r}_0 + \mathbf{r}. \tag{4.6.1}$$

between two reference frames.

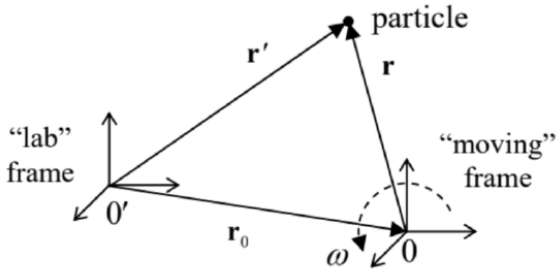

Figure 4.12. The general case of transfer

However, as was mentioned in Sec. 1, for velocities the general addition rule is already more complex. To find it, let us differentiate Eq. (86) over time:

$$\frac{d}{dt}\mathbf{r}' = \frac{d}{dt}\mathbf{r}_0 + \frac{d}{dt}\mathbf{r}. \tag{4.6.2}$$

The left-hand side of this relation is evidently the particle's velocity as measured in the lab frame, and the first term on the right-hand side is the velocity $\mathbf{v}_0$ of the point 0 , as measured in the same lab frame. The last term is more complex: due to the possible mutual rotation of the frames 0 and 0 ', that term may not vanish even if the particle does not move relative to the rotating frame 0 - see Figure 12 .

Fortunately, we have already derived the general Eq. (8) to analyze situations exactly like this one. Taking $\mathbf{A} = \mathbf{r}$ in it, we may apply the result to the last term of Eq. (87), to get

$$\mathbf{v}|_{\text{in lab}} = \mathbf{v}_0|_{\text{in lab}} + (\mathbf{v} + \boldsymbol{\omega} \times \mathbf{r}), \tag{4.6.3}$$

where ω is the instantaneous angular velocity of an imaginary rigid body connected to the moving reference frame (or we may say, of this frame as such), as measured in the lab frame 0', while $\mathbf{v}$ is $d\mathbf{r}/dt$ as measured in the moving frame 0 . The relation (88), on one hand, is a natural generalization of Eq. (10) for $\mathbf{v} \neq 0$; on the other hand, if $\omega = 0$, it is reduced to simple Eq. (1.8) for the translational motion of the frame 0 .

To calculate the particle's acceleration, we may just repeat the same trick: differentiate Eq. (88) over time, and then use Eq. (8) again, now for the vector $\mathbf{A} = \mathbf{v} + \omega \times \mathbf{r}$. The result is

$$\mathbf{a}|_{\text{in lab}} \equiv \mathbf{a}_0|_{\text{in lab}} + \frac{d}{dt}(\mathbf{v} + \boldsymbol{\omega} \times \mathbf{r}) + \boldsymbol{\omega} \times (\mathbf{v} + \boldsymbol{\omega} \times \mathbf{r}). \tag{4.6.4}$$

Carrying out the differentiation in the second term, we finally get the goal relation,

$$\mathbf{a}|_{\text{in lab}} \equiv \mathbf{a}_0|_{\text{in lab}} + \mathbf{a} + \dot{\boldsymbol{\omega}} \times \mathbf{r} + 2\boldsymbol{\omega} \times \mathbf{v} + \boldsymbol{\omega} \times (\boldsymbol{\omega} \times \mathbf{r}), \tag{4.6.5}$$

where $\mathbf{a}$ is particle's acceleration, as measured in the moving frame. This result is a natural generalization of the simple Eq. (1.9) to the rotating frame case.

Now let the lab frame 0 ' be inertial; then the 2^{nd} Newton law for a particle of mass m is

$$m\mathbf{a}|_{\text{in lab}} = \mathbf{F}, \tag{4.6.6}$$

where $\mathbf{F}$ is the vector sum of all forces exerted on the particle. This is simple and clear; however, in many cases it is much more convenient to work in a non-inertial reference frame; for example, describing most phenomena on Earth's surface, it is rather inconvenient to use a reference frame resting on the Sun (or in the galactic center, etc.). In order to understand what we should pay for the convenience of using a moving frame, we may combine Eqs. (90) and (91) to write

$$m\mathbf{a} = \mathbf{F} - m\mathbf{a}_0|_{\text{in lab}} - m\boldsymbol{\omega} \times (\boldsymbol{\omega} \times \mathbf{r}) - 2m\boldsymbol{\omega} \times \mathbf{v} - m\dot{\boldsymbol{\omega}} \times \mathbf{r}. \tag{4.6.7}$$

This result means that if we want to use a 2^{nd} Newton law's analog in a non-inertial reference frame, we have to add, to the actual net force $\mathbf{F}$ exerted on a particle, four pseudo-force terms, called inertial forces, all proportional to particle's mass. Let us analyze them one by one, always remembering that these are just mathematical terms, not actual forces. (In particular, it would be futile to seek for the 3^{rd} Newton law's counterpart for any inertial force.)

The first term, $-m\mathbf{a}_0|_{\text{in lab}}$, is the only one not related to rotation and is well known from the undergraduate mechanics. (Let me hope the reader remembers all these weight-in-the-moving-elevator problems.) However, despite its simplicity, this term has more subtle consequences. As an example, let us consider, semi-qualitatively, the motion of a planet, such as our Earth, orbiting a star and also rotating about its own axis - see Figure 13. The bulk-distributed gravity forces, acting on a planet from its star, are not quite uniform, because they obey the $1/r^2$ gravity law (1.15), and hence are equivalent to a single force applied to a point A slightly offset from the planet's center of mass 0 , toward the star. For a spherically-symmetric planet, the direction from 0 to A would be exactly aligned with the direction toward the star. However, real planets are not absolutely rigid, so that, due to the centrifugal "force" (to be discussed imminently), the rotation about their own axis makes them slightly ellipsoidal - see Figure 13. (For our Earth, this equatorial bulge is about 10 km.) As a result, the net gravity force does create a small torque relative to the center of mass 0 . On the other hand, repeating all the arguments of this section for a body (rather than a point), we may see that, in the reference frame moving with the planet, the inertial force $-M\mathbf{a}_0$ (with the magnitude of the total gravity force, but directed from the star) is applied exactly to the center of mass and hence does not create a torque about it. As a result, this pair of forces creates a torque τ perpendicular to both the direction toward the star and the vector 0A. (In Figure 13 , the torque vector is perpendicular to the plane of the drawing). If the angle δ between the planet's "polar" axis of rotation and the direction towards the star was fixed, then, as we have seen in the previous section, this torque would induce a slow axis precession about that direction.

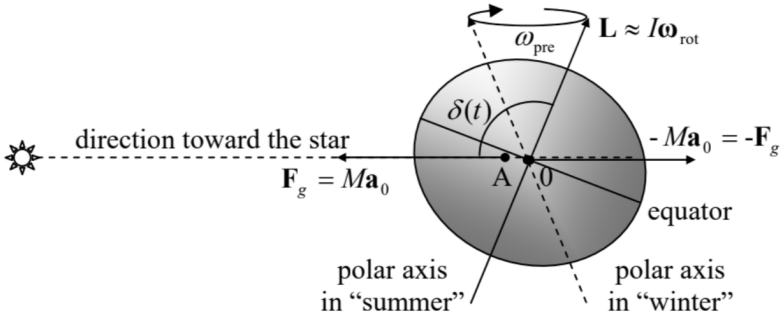

Figure 4.13. The axial precession of a planet (with the equatorial bulge and the 0A-offset strongly exaggerated).

However, as a result of the orbital motion, the angle δ oscillates in time much faster (once a year) between values $(\pi/2 + \varepsilon)$ and $(\pi/2 - \varepsilon)$, where ε is the axis tilt, i.e. angle between the polar axis (the direction of vectors $\mathbf{L}$ and ω_{rot}) and the normal to the ecliptic plane of the planet's orbit. (For the Earth, $\varepsilon \approx 23.4^\circ$.) A straightforward averaging over these fast oscillations [22] shows that the torque leads to the polar axis' precession about the axis perpendicular to the ecliptic plane, keeping the angle ε constant – see Figure 13. For the Earth, the period $T_{\text{pre}} = 2\pi/\omega_{\text{pre}}$ of this precession of the equinoxes, corrected to a substantial effect of Moon's gravity, is close to 26,000 years. [23]

Returning to Eq. (92), the direction of the second term of its right-hand side,

$$\mathbf{F}_{\text{cf}} \equiv -m\boldsymbol{\omega} \times (\boldsymbol{\omega} \times \mathbf{r}), \tag{4.6.8}$$

called the centrifugal force, is always perpendicular to, and directed out of the instantaneous rotation axis - see Figure 14. Indeed, the vector $\omega \times \mathbf{r}$ is perpendicular to both ω and $\mathbf{r}$ (in Figure 14, normal to the drawing plane and directed from the reader) and has the magnitude $\omega r \sin\theta = \omega\rho$, where ρ is the distance of the particle from the rotation axis. Hence the outer vector product, with the account of the minus sign, is normal to the rotation axis ω, directed from this axis, and is equal to $\omega^2 r \sin\theta = \omega^2\rho$. The "centrifugal force" is of course just the result of the fact that the centripetal acceleration $\omega^2\rho$, explicit in the inertial reference frame, disappears in the rotating frame. For a typical location of the Earth $\left(\rho \sim R_{\text{E}} \approx 6 \times 10^6 \text{ m}\right)$, with its angular velocity

$\omega_E \approx 10^{-4}$ s^{-1} , the acceleration is rather considerable, of the order of 3 cm/s^2, i.e. ~ 0.003 g, and is responsible, in particular, for the largest part of the equatorial bulge mentioned above.

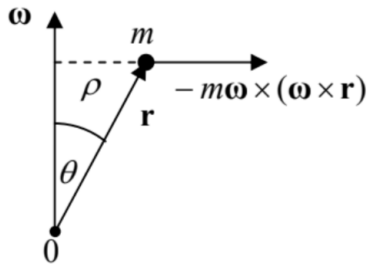

Fig. 4.14. The centrifugal force.

As an example of using the centrifugal force concept, let us return again to our "testbed" problem on the bead sliding along a rotating ring - see Figure 2.1. In the non-inertial reference frame attached to the ring, we have to add, to the actual forces $m\mathbf{g}$ and $\mathbf{N}$ acting on the bead, the horizontal centrifugal force [24] directed from the rotation axis, with the magnitude $m\omega^2\rho$. Its component tangential to the ring equals $\left(m\omega^2\rho\right)\cos\theta = m\omega^2 R\sin\theta\cos\theta$, and hence the component of Eq. (92) along this direction is $ma = -mg\sin\theta + m\omega^2 R\sin\theta\cos\theta$. With $a = R\ddot{\theta}$, this gives us an equation of motion equivalent to Eq. (2.25), which had been derived in Sec. 2.2 (in the inertial frame) using the Lagrangian formalism.

The third term on the right-hand side of Eq. (92),

$$\mathbf{F}_C \equiv -2m\boldsymbol{\omega}\times\mathbf{v}, \tag{4.6.9}$$

is the so-called Coriolis force [25] which is different from zero only if the particle moves in the rotating reference frame. Its physical sense may be understood by considering a projectile fired horizontally, say from the North Pole - see Figure 15.

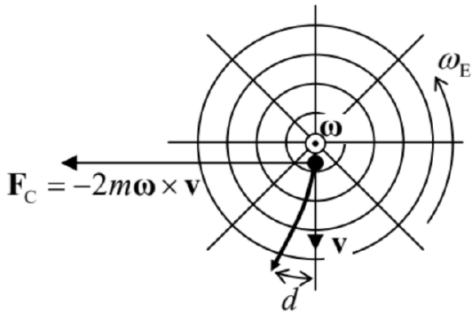

Figure 4.15. The trajectory of a projectile fired horizontally from the North Pole, from the point of view of an Earth-bound observer looking down. The circles show parallels, while the straight lines mark meridians.

From the point of view of the Earth-based observer, the projectile will be affected by an additional Coriolis force (94), directed westward, with magnitude $2m\omega_E v$, where $\mathbf{v}$ is the main, southward component of the velocity. This force would cause the westward acceleration $a = 2\omega_E v$, and hence the westward deviation growing with time as $d = at^2/2 = \omega_E v t^2$. (This formula is exact only if d is much smaller than the distance $r = vt$ passed by the projectile.) On the other hand, from the point of view of an inertial-frame observer, the projectile's trajectory in the horizontal plane is a straight line. However, during the flight time t, the Earth surface slips eastward from under the trajectory by the distance $d = r\varphi = (vt)(\omega_E t) = \omega_E v t^2$, where $\varphi = \omega_E t$ is the azimuthal angle of the Earth rotation during the flight). Thus, both approaches give the same result - as they should.

Hence, the Coriolis "force" is just a fancy (but frequently very convenient) way of description of a purely geometric effect pertinent to the rotation, from the point of view of the observer participating in it. This force is responsible, in particular, for the higher right banks of rivers in the Northern hemisphere, regardless of the direction of their flow - see Figure 16. Despite the smallness of the Coriolis force (for a typical velocity of the water in a river, $v \sim 1$ m/s, it is equivalent to acceleration $a_C \sim 10^{-2}$ cm/s$^2 \sim 10^{-5}$ g), its multi-century effects may be rather prominent. [26]

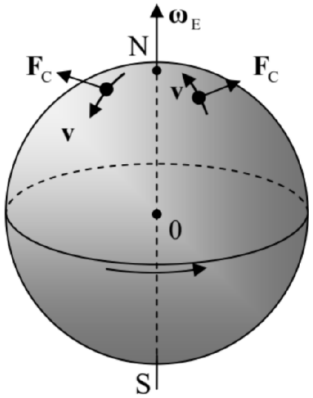

Figure 4.16. Coriolis forces due to Earth's rotation, in the Northern hemisphere.

Finally, the last, fourth term of Eq. (92), $-m\dot{\boldsymbol{\omega}}\times\mathbf{r}$, exists only when the rotation frequency changes in time, and may be interpreted as a local-position-specific addition to the first term.The key relation (92), derived above from the Newton equation (91), may be alternatively obtained from the Lagrangian approach, which gives, as a by-product, some important insights on the momentum, as well as on the relation between E and H, at rotation. Let us use Eq. (88) to represent the kinetic energy of the particle in an inertial "lab" frame in terms of $\mathbf{v}$ and $\mathbf{r}$ measured in a rotating frame:

$$T=\frac{m}{2}\left[\mathbf{v}_0|_{\text{in lab}}+(\mathbf{v}+\boldsymbol{\omega}\times\mathbf{r})\right]^2, \tag{4.6.10}$$

and use this expression to calculate the Lagrangian function. For the relatively simple case of a particle's motion in the field of potential forces, measured from a reference frame that performs a pure rotation (so that $\mathbf{v}_0$ |in lab $=0$) [27] with a constant angular velocity ω, we get

$$L\equiv T-U=\frac{m}{2}v^2+m\mathbf{v}\cdot(\boldsymbol{\omega}\times\mathbf{r})+\frac{m}{2}(\boldsymbol{\omega}\times\mathbf{r})^2-U\equiv\frac{m}{2}v^2+m\mathbf{v}\cdot(\boldsymbol{\omega}\times\mathbf{r})-U_{\text{ef}}, \tag{4.6.11}$$

where the effective potential energy,[28]

$$U_{\text{ef}}\equiv U+U_{\text{cf}},\qquad \text{with } U_{\text{cf}}\equiv-\frac{m}{2}(\boldsymbol{\omega}\times\mathbf{r})^2, \tag{4.6.12}$$

is just the sum of the actual potential energy U of the particle and the so-called centrifugal potential energy, associated with the centrifugal force (93):

$$\mathbf{F}_{\text{cf}}=-\nabla U_{\text{cf}}=-\nabla\left[-\frac{m}{2}(\boldsymbol{\omega}\times\mathbf{r})^2\right]=-m\boldsymbol{\omega}\times(\boldsymbol{\omega}\times\mathbf{r}) \tag{4.6.13}$$

It is straightforward to verify that the Lagrangian equations of motion derived from Eqs. (96), considering the Cartesian components of $\mathbf{r}$ and $\mathbf{v}$ as generalized coordinates and velocities, coincide with Eq. (92) (with $\mathbf{a}_0|_{\text{in lab}}=0,\dot{\boldsymbol{\omega}}=0$, and $\mathbf{F}=-\nabla U$). Now it is very informative to have a look at a byproduct of this calculation, the generalized momentum (2.31) corresponding to the particle's coordinate $\mathbf{r}$ as measured in the rotating reference frame, [29]

$$\boldsymbol{h}\equiv\frac{\partial L}{\partial\mathbf{v}}=m(\mathbf{v}+\boldsymbol{\omega}\times\mathbf{r}) \tag{4.6.14}$$

According to Eq. (88) with $\mathbf{v}_0|_{\text{in lab}}=0$, the expression in the parentheses is just $\mathbf{v}|_{\text{in lab. However, from}}$ the point of view of the moving frame, i.e. not knowing about the simple physical sense of the vector $\boldsymbol{p}$, we would have a reason to speak about two different linear momenta of the same particle, the so-called kinetic momentum $\mathbf{p}=m\mathbf{v}$ and the canonical momentum $\boldsymbol{\mu}=\mathbf{p}+m\omega\times\mathbf{r}$. [30]

Now let us calculate the Hamiltonian function H, defined by Eq. (2.32), and the energy E as functions of the same moving-frame variables:

$$H\equiv\sum_{j=1}^{3}\frac{\partial L}{\partial v_j}v_j-L=\boldsymbol{\mu}\cdot\mathbf{v}-L=m(\mathbf{v}+\boldsymbol{\omega}\times\mathbf{r})\cdot\mathbf{v}-\left[\frac{m}{2}v^2+m\mathbf{v}\cdot(\boldsymbol{\omega}\times\mathbf{r})-U_{\text{ef}}\right]=\frac{mv^2}{2}+U_{\text{ef}},$$

$$E\equiv T+U=\frac{m}{2}v^2+m\mathbf{v}\cdot(\boldsymbol{\omega}\times\mathbf{r})+\frac{m}{2}(\boldsymbol{\omega}\times\mathbf{r})^2+U=\frac{m}{2}v^2+U_{\text{ef}}+m\mathbf{v}\cdot(\boldsymbol{\omega}\times\mathbf{r})+m(\boldsymbol{\omega}\times\mathbf{r})^2.$$

These expressions clearly show that E and H are not equal. [31] In hindsight, this is not surprising, because the kinetic energy (95), expressed in the moving-frame variables, includes a term linear in $\mathbf{v}$, and hence is not a quadratic-homogeneous function of this generalized velocity. The difference of these functions may be represented as

$$E - H = m\mathbf{v}\cdot(\boldsymbol{\omega}\times\mathbf{r}) + m(\boldsymbol{\omega}\times\mathbf{r})^2 \equiv m(\mathbf{v}+\boldsymbol{\omega}\times\mathbf{r})\cdot(\boldsymbol{\omega}\times\mathbf{r}) = m\mathbf{v}|_{\text{in lab}}\cdot(\boldsymbol{\omega}\times\mathbf{r}). \tag{4.6.15}$$

Now using the operand rotation rule again, we may transform this expression into a simpler form: [32]

$$E - H = \boldsymbol{\omega}\cdot(\mathbf{r}\times m\mathbf{v}|_{\text{in lab}}) = \boldsymbol{\omega}\cdot(\mathbf{r}\times\boldsymbol{\mu}) = \boldsymbol{\omega}\cdot\mathbf{L}|_{\text{in lab}}\,. \tag{4.6.16}$$

As a sanity check, let us apply this general expression to the particular case of our testbed problem - see Figure 2.1. In this case, the vector ω is aligned with the z-axis, so that of all Cartesian components of the vector $\mathbf{L}$, only the component L_z is important for the scalar product in Eq. (102). This component evidently equals $\omega I_z = \omega m\rho^2 = \omega m(R\sin\theta)^2$, so that

$$E - H = m\omega^2 R^2 \sin^2\theta, \tag{4.6.17}$$

i.e. the same result that follows from the subtraction of Eqs. (2.40) and (2.41).

---

[23] Details of this calculation may be found, e.g., in Sec. 5.8 of the textbook by H. Goldstein et al., Classical Mechanics, 3rd ed., Addison Wesley, 2002 .

[24] This effect is known from antiquity, apparently discovered by Hipparchus of Rhodes (190-120 BC)

[25] For this problem, all other inertial "forces", besides the Coriolis force (see below) vanish, while the latter force is directed perpendicular to the ring and does not affect the bead's motion along it.

[26] Named after G.-G. de Coriolis (already reverently mentioned in Chapter 1) who described its theory and applications in detail in 1835, though the first semi-quantitative analyses of this effect were given by Giovanni Battista Riccioli and Claude François Dechales already in the mid-1600s, and all basic components of the Coriolis theory may be traced to a 1749 work by Leonard Euler.

[27] The same force causes the counter-clockwise circulation in the "Nor'easter" storms on the US East Coast, having an the air velocity component directed toward the cyclone's center, due to lower pressure in its middle.

[28] A similar analysis of the cases with $\mathbf{v}_0|_{\text{in lab}} \neq 0$, for example, of a translational relative motion of the reference frames, is left for reader's exercise.

[29] For the attentive reader who has noticed the difference between the negative sign in the expression for U_{cf}, and the positive sign before the similar second term in Eq. (3.44): as was already discussed in Chapter 3, this difference is due to the difference of assumptions. In the planetary problem, the angular momentum $\mathbf{L}$ (and hence its component L_z) is fixed, while the corresponding angular velocity $\dot{\varphi}$ is not. On the opposite, in our current discussion, the angular velocity ω of the reference frame is assumed to be fixed, i.e. is independent of $\mathbf{r}$ and $\mathbf{v}$.

[30] Here $\partial L/\partial\mathbf{v}$ is just a shorthand for a vector with Cartesian components $\partial L/\partial v_j$. In a more formal language, this is the gradient of the scalar function L in the velocity space.

[31] A very similar situation arises at the motion of a particle with electric charge q in magnetic field $\mathscr{B}$. In that case, the role of the additional term $\boldsymbol{\mu} - \mathbf{p} = m\omega\times\mathbf{r}$ is played by the product $q\mathscr{A}$, where $\mathscr{A}$ is the vector potential of the field $(\mathscr{B} = \nabla\times\mathscr{A})$ - see, e.g., EM Sec. 9.7, and in particular Eqs. (9.183) and (9.192).

[32] Please note the last form of Eq. (99), which shows the physical sense of the Hamiltonian function of a particle in the rotating frame very clearly, as the sum of its kinetic energy (as measured in the moving frame), and the effective potential energy (96b), including that of the centrifugal "force".

4.7: Exercise Problems

4.1. Calculate the principal moments of inertia for the following uniform rigid bodies:

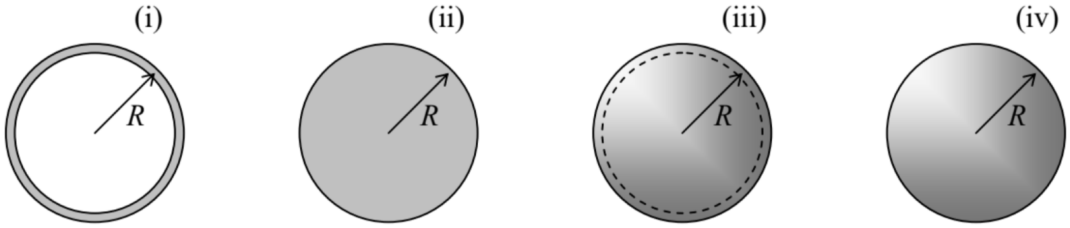

(i) a thin, planar, round hoop, (ii) a flat round disk, (iii) a thin spherical shell, and (iv) a solid sphere Compare the results, assuming that all the bodies have the same radius R and mass M.

4.2. Calculate the principal moments of inertia for the rigid bodies shown in the figure below:

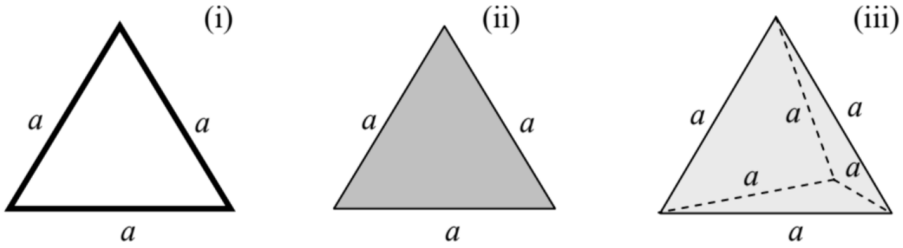

(i) an equilateral triangle made of thin rods with a uniform linear mass density μ,

(ii) a thin plate in the shape of an equilateral triangle, with a uniform areal mass density σ, and

[32] Note that by the definition (1.36), the angular momenta $\mathbf{L}$ of particles merely add up. As a result, the final form of Eq. (102) is valid for an arbitrary system of particles. (iii) a tetrahedron made of a heavy material with a uniform bulk mass density ρ.

Assuming that the total mass of the three bodies is the same, compare the results and give an interpretation of their difference.

4.3. Prove that Eqs. (34)-(36) are valid for rotation of a rigid body about a fixed axis z, even if it does not pass through its center of mass.

4.4. The end of a uniform thin rod of length $2l$ and mass m, initially at rest, is hit by a bullet of mass m', flying with velocity v_0 (see the figure on the right), which gets stuck in the rod. Use two different approaches to calculate the velocity of the opposite end of the rod right after the collision.

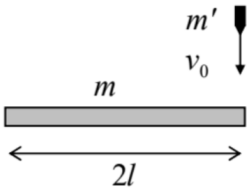

4.5. A uniform ball is placed on a horizontal plane, while rotating with an angular velocity ω_0, but having no initial linear velocity. Calculate the angular velocity after the ball's slippage stops, assuming the Coulomb approximation for the kinetic friction force: $F_f = \mu N$, where N is a pressure between the surfaces, and μ is a velocity-independent coefficient.

4.6. A body may rotate about a fixed horizontal axis A− see Figure 5. Find the frequency of its small oscillations, in a uniform gravity field, as a function of the distance l of the axis from the body's center of mass 0 , and analyze the result.

4.7. Calculate the frequency, and sketch the mode of oscillations of a round uniform cylinder of radius R and the mass M, that may roll, without slipping, on a horizontal surface of a block of mass M '. The block, in turn, may move in the same direction, without friction, on a horizontal surface, being connected to it with an elastic spring - see the figure on the right.

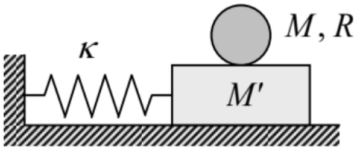

4.8. A thin uniform bar of mass M and length l is hung on a light thread of length l ' (like a "chime" bell - see the figure on the right). Derive the equations of motion of the system within the plane of the drawing.

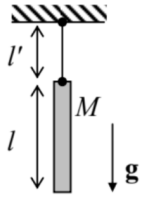

4.9. A solid, uniform, round cylinder of mass M can roll, without slipping, over a concave, round cylindrical surface of a block of mass M', in a uniform gravity field - see the figure on the right. The block can slide without friction on a horizontal surface. Using the Lagrangian formalism,

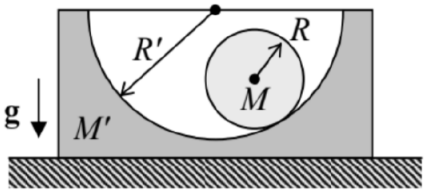

(i) find the frequency of small oscillations of the system near the equilibrium, and

(ii) sketch the oscillation mode for the particular case $M' = M, R' = 2R$.

4.10. A uniform solid hemisphere of radius R is placed on a horizontal plane – see the figure on the right. Find the frequency of its small oscillations within a vertical plane, for two ultimate cases:

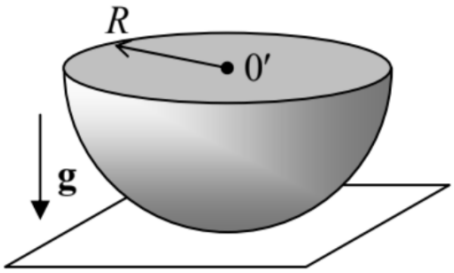

(i) there is no friction between the hemisphere and plane surfaces, and

(ii) the static friction is so strong that there is no slippage between these surfaces.

4.11. For the "sliding ladder" problem, started in Sec. 3 (see Figure 7), find the critical value α_c of the angle α at that the ladder loses its contact with the vertical wall, assuming that it starts sliding from the vertical position, with a negligible initial velocity.

4.12. Six similar, uniform rods of length l and mass m are connected by light joints so that they may rotate, without friction, versus each other, forming a planar polygon. Initially, the polygon was at rest, and had the correct hexagon shape – see the figure on the right. Suddenly, an external force $\mathbf{F}$ is applied to the middle of one rod, in the direction of the hexagon's symmetry center. Calculate the accelerations: of the rod to which the force is applied (a), and of the opposite rod (a'), immediately after the application of the force.

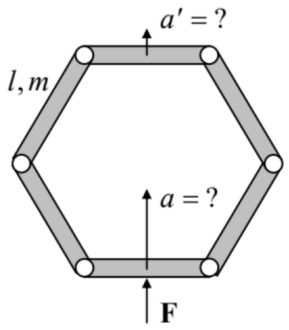

4.13. A rectangular cuboid (parallelepiped) with sides a_1, a_2, and a_3, made of a material with a constant mass density ρ, is rotated, with a constant angular velocity ω, about one of its space diagonals - see the figure on the right. Calculate the torque τ necessary to sustain such rotation.

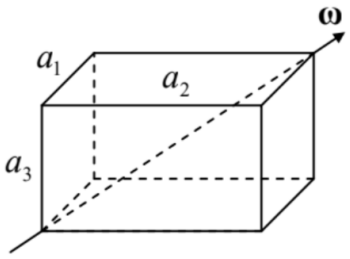

4.14. One end of a light shaft of length l is firmly attached to the center of a thin uniform solid disk of radius $R << l$ and mass M, whose plane is perpendicular to the shaft. Another end of the shaft is attached to a vertical axis (see the figure on the right) so that the shaft may rotate about the axis without friction. The disk rolls, without slippage, over a horizontal surface, so that the whole system rotates about the vertical axis with a constant angular velocity ω. Calculate the (vertical) supporting force N exerted on the disk by the surface.

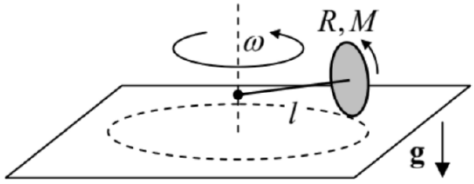

4.15. An air-filled balloon is placed inside a water-filled container, which moves by inertia in free space, at negligible gravity. Suddenly, force $\mathbf{F}$ is applied to the container, pointing in a certain direction. What direction does the balloon move relative to the container?

4.16. Two planets are in a circular orbit around their common center of mass. Calculate the effective potential energy of a much lighter body (say, a spacecraft) rotating with the same angular velocity, on the line connecting the planets. Sketch the plot of the radial dependence of U_{ef} and find out the number of so-called Lagrange points is which the potential energy has local maxima. Calculate their position explicitly in the limit when one of the planets is much more massive than the other one.

4.17. A small body is dropped down to the surface of Earth from height $h < R_{\text{E}}$, without initial velocity. Calculate the magnitude and direction of its deviation from the vertical, due to the Earth rotation. Estimate the effect's magnitude for a body dropped from the Empire State Building. 4.18. Calculate the height of solar tides on a large ocean, using the following simplifying assumptions: the tide period ($1/2$ of Earth's day) is much longer than the period of all ocean waves, the Earth (of mass M_{E}) is a sphere of radius R_{E}, and its distance r_{S} from the Sun (of mass M_{S}) is constant and much larger than R_{E}.

4.19. A coin of radius r is rolled, with velocity V, on a horizontal surface without slippage. What should be the coin's tilt angle θ (see the figure on the right) for it to roll on a circle of radius $R \ggg r$? Modeling the coin as a very thin, uniform disk, and assuming that the angle θ is small, solve this problem in:

(i) an inertial ("lab") reference frame, and

(ii) the non-inertial reference frame moving with the coin's center (but not rotating with it).

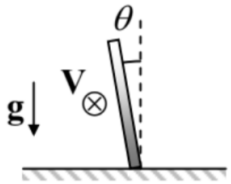

4.20. A satellite is on a circular orbit of radius R, around the Earth.

(i) Write the equations of motion of a small body as observed from the satellite, and simplify them for the case when the motion is limited to the satellite's close vicinity.

(ii) Use the equations to prove that the body may be placed on an elliptical trajectory around the satellite's center of mass, within its plane of rotation about Earth. Calculate the ellipse's orientation and eccentricity.

4.21. A non-spherical shape of an artificial satellite may ensure its stable angular orientation relative to Earth's surface, advantageous for many practical goals. Modeling the satellite as a strongly elongated, axially-symmetric body, moving around the Earth on a circular orbit of radius R, find its stable orientation.

4.22. * A rigid, straight, uniform rod of length l, with the lower end on a pivot, falls in a uniform gravity field - see the figure on the right. Neglecting friction, calculate the distribution of the bending torque τ along its length, and analyze the result.

Hint: The bending torque is the net torque of the force $\mathbf{F}$ acting between two parts of the rod, mentally separated by its cross-section, about a certain "neutral axis". [33] As will be discussed in detail in Sec. 7.5, at the proper definition of this axis, the bending torque's gradient along the rod's length is equal to $(-F)$, where F is the rod-normal ("shear") component of the force exerted by the top part of the rod on its lower part.

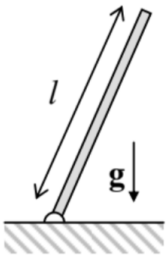

4.23. Let $\mathbf{r}$ be the radius vector of a particle, as measured in a possibly non-inertial but certainly non-rotating reference frame. Taking its Cartesian components for the generalized coordinates, calculate the corresponding generalized momentum $\boldsymbol{\mu}$ of the particle, and its Hamiltonian function H. Compare $\boldsymbol{\mu}$ with $m\mathbf{v}$, and H with the particle's energy E. Derive the Lagrangian equation of motion in this approach, and compare it with Eq. (92).

[34] Inadequate definitions of this torque are the main reason for numerous wrong solutions of this problem, posted online - readers beware!

CHAPTER OVERVIEW

5: Oscillations

In this course, oscillations and waves are discussed in detail, because of their importance for fundamental and applied physics. This chapter starts with a discussion of the so-called "linear" (or "harmonic") oscillator, whose differential equation of motion is linear and hence allows the full analytical solution, and then proceed to "nonlinear" and parametric systems whose dynamics may be only explored by either approximate analytical or numerical methods.

5.1: Free and Forced Oscillations

In Sec. 3.2 we briefly discussed oscillations in a keystone Hamiltonian system - a 1D harmonic oscillator described by a very simple Lagrangian [1]

$$L \equiv T(\dot{q}) - U(q) = \frac{m}{2}\dot{q}^2 - \frac{\kappa}{2}q^2, \tag{5.1.1}$$

whose Lagrange equation of motion, [2]

Harmonic oscillator: equation $\quad m\ddot{q} + \kappa q = 0, \quad$ i.e. $\ddot{q} + \omega_0^2 q = 0, \quad$ with $\omega_0^2 \equiv \frac{\kappa}{m} \geq 0$,

is a linear homogeneous differential equation. Its general solution is given by (3.16), which is frequently recast into another, amplitude-phase form:

$$q(t) = u\cos\omega_0 t + v\sin\omega_0 t = A\cos(\omega_0 t - \varphi), \tag{5.1.2}$$

where A is the amplitude and φ the phase of the oscillations, which are determined by the initial conditions. Mathematically, it is frequently easier to work with sinusoidal functions as complex exponents, by rewriting the last form of Eq. (3a) in one more form: [3]

$$q(t) = \mathrm{Re}\left[Ae^{-i(\omega_0 t - \varphi)}\right] = \mathrm{Re}\left[ae^{-i\omega_0 t}\right], \tag{5.1.3}$$

$$a \equiv Ae^{i\varphi}, \quad |a| = A, \quad \mathrm{Re}\, a = A\cos\varphi = u, \quad \mathrm{Im}\, a = A\sin\varphi = v. \tag{5.1.4}$$

For an autonomous, Hamiltonian oscillator, Eq. (3) gives the full classical description of its dynamics. However, it is important to understand that this free-oscillation solution, with a constant amplitude A, is due to the conservation of the energy $E \equiv T + U = \kappa A^2/2$ of the oscillator. If its energy changes for any reason, the description needs to be generalized.

First of all, if the energy leaks out of the oscillator to its environment (the effect usually called the energy dissipation), the free oscillations decay with time. The simplest model of this effect is represented by an additional linear drag (or "kinematic friction") force, proportional to the generalized velocity and directed opposite to it:

$$F_v = -\eta\dot{q}, \tag{5.1.5}$$

where constant η is called the drag coefficient. [4] The inclusion of this force modifies the equation of motion (2) to become

$$m\ddot{q} + \eta\dot{q} + \kappa q = 0. \tag{5.1.6}$$

This equation is frequently rewritten in the form

$$\ddot{q} + 2\delta\dot{q} + \omega_0^2 q = 0, \quad \text{with } \delta \equiv \frac{\eta}{2m}, \tag{5.1.7}$$

where the parameter δ is called the damping coefficient (or just "damping"). Note that Eq. (6) is still a linear homogeneous second-order differential equation, and its general solution still has the form of the sum (3.13) of two exponents of the type $\exp\{\lambda t\}$, with arbitrary pre-exponential coefficients. Plugging such an exponent into Eq. (6), we get the following algebraic characteristic equation for λ :

$$\lambda^2 + 2\delta\lambda + \omega_0^2 = 0. \tag{5.1.8}$$

Solving this quadratic equation, we get

$$\lambda_\pm = -\delta \pm i\omega_0', \quad \text{where } \omega_0' \equiv \left(\omega_0^2 - \delta^2\right)^{1/2}, \tag{5.1.9}$$

so that for not very high damping $(\delta < \omega_0)$ [5] we get the following generalization of Eq. (3):

$$q_{\text{free}}(t) = c_+ e^{\lambda_+ t} + c_- e^{\lambda_- t} = \left(u_0\cos\omega_0' t + v_0\sin\omega_0' t\right)e^{-\delta t} = A_0 e^{-\delta t}\cos\left(\omega_0' t - \varphi_0\right). \tag{5.1.10}$$

The result shows that, besides a certain correction to the free oscillation frequency (which is very small in the most interesting low damping limit, $\delta << \omega_0$), the energy dissipation leads to an exponential decay of oscillation amplitude with the time constant $\tau = 1/\delta$:

$$A = A_0 e^{-t/\tau}, \quad \text{where } \tau \equiv \frac{1}{\delta} = \frac{2m}{\eta} \tag{5.1.11}$$

A very popular dimensionless measure of damping is the so-called quality factor Q (or just the Q-factor) that is defined as $\omega_0/2\delta$, and may be rewritten in several other useful forms:

$$Q \equiv \frac{\omega_0}{2\delta} = \frac{m\omega_0}{\eta} = \frac{(m\kappa)^{1/2}}{\eta} = \pi\frac{\tau}{\tau} = \frac{\omega_0\tau}{2}, \tag{5.1.12}$$

where $\tau = 2\pi/\omega_0$ is the oscillation period in the absence of damping - see Eq. (3.29). Since the oscillation energy E is proportional to A^2, i.e. decays as $\exp\{-2t/\tau\}$, with the time constant $\tau/2$, the last form of Eq. (11) may be used to rewrite the Q-factor in one more form:

$$Q = \omega_0 \frac{E}{(-\dot{E})} \equiv \omega_0 \frac{E}{\mathscr{P}}, \tag{5.1.13}$$

where $\mathscr{P}$ is the dissipation power. (Two other practical ways to measure Q will be discussed below.) The range of Q-factors of important oscillators is very broad, all the way from $Q \sim 10$ for a human leg (with relaxed muscles), to $Q \sim 10^4$ of the quartz crystals used in electronic clocks and watches, all the way up to $Q \sim 10^{12}$ for carefully designed microwave cavities with superconducting walls.

In contrast to the decaying free oscillations, the forced oscillations, induced by an external force $F(t)$, may maintain their amplitude (and hence energy) infinitely, even at non-zero damping. This process may be described using a still linear but now inhomogeneous differential equation

$$m\ddot{q} + \eta\dot{q} + \kappa q = F(t), \tag{5.1.14}$$

or, more conveniently for analysis, the following generalization of Eq. (6b):

Forced oscillator with damping	$\ddot{q} + 2\delta\dot{q} + \omega_0^2 q = f(t), \quad$	where $f(t) \equiv F(t)/m.$

For a mechanical linear, dissipative 1D oscillator (6), under the effect of an additional external force $F(t)$, Eq. (13a) is just an expression of the 2nd Newton law. However, according to Eq. (1.41), Eq. (13) is valid for any dissipative, linear 6 1D system whose Gibbs potential energy (1.39) has the form $U_G(q,t) = \kappa q^2/2 - F(t)q$.

The forced-oscillation solutions may be analyzed by two mathematically equivalent methods whose relative convenience depends on the character of function $f(t)$.

(i) Frequency domain. Representing the function $f(t)$ as a Fourier sum of sinusoidal harmonics: [7]

$$f(t) = \sum_{\omega} f_\omega e^{-i\omega t}, \tag{5.1.15}$$

and using the linearity of Eq. (13), we may represent its general solution as a sum of the decaying free oscillations (9) with the frequency ω_0', independent of the function $f(t)$, and forced oscillations due to each of the Fourier components of the force: [8]

$$q(t) = q_{\text{free}}(t) + q_{\text{forced}}(t), \quad q_{\text{forced}}(t) = \sum_{\omega} a_\omega e^{-i\omega t} \tag{5.1.16}$$

Plugging Eq. (15) into Eq. (13), and requiring the factors before each $e^{-i\omega t}$ on both sides to be equal, we get

$$a_\omega = f_\omega \chi(\omega), \tag{5.1.17}$$

where the complex function $\chi(\omega)$, in our particular case equal to

$$\chi(\omega) = \frac{1}{(\omega_0^2 - \omega^2) - 2i\omega\delta}, \tag{5.1.18}$$

is called either the response function or (especially for non-mechanical oscillators) the generalized susceptibility. From here, and Eq. (4), the amplitude of the oscillations under the effect of a sinusoidal force is

$$A_\omega \equiv |a_\omega| = |f_\omega||\chi(\omega)|\,, \quad \text{with } |\chi(\omega)| = \frac{1}{\left[\left(\omega_0^2-\omega^2\right)^2+(2\omega\delta)^2\right]^{1/2}} \tag{5.1.19}$$

This formula describes, in particular, an increase of the oscillation amplitude A_ω at $\omega \to \omega_0-$ see the left panel in Figure 1. In particular, at the exact equality of these two frequencies,

$$|\chi(\omega)|_{\omega=\omega_0} = \frac{1}{2\omega_0\delta}, \tag{5.1.20}$$

so that, according to Eq. (11), the ratio of the response magnitudes at $\omega = \omega_0$ and $\omega = 0$ ($|\chi(\omega)|_{\omega=0} = 1/{\omega_0}^2$) is exactly equal to the Q-factor of the oscillator. Thus, the response increase is especially strong in the low damping limit ($\delta << \omega_0$, i.e. $Q >> 1$); moreover at $Q \to \infty$ and $\omega \to \omega_0$ the response diverges. (This fact is very useful for the methods to be discussed later in this section.) This is the classical description of the famous phenomenon of resonance, so ubiquitous in physics.

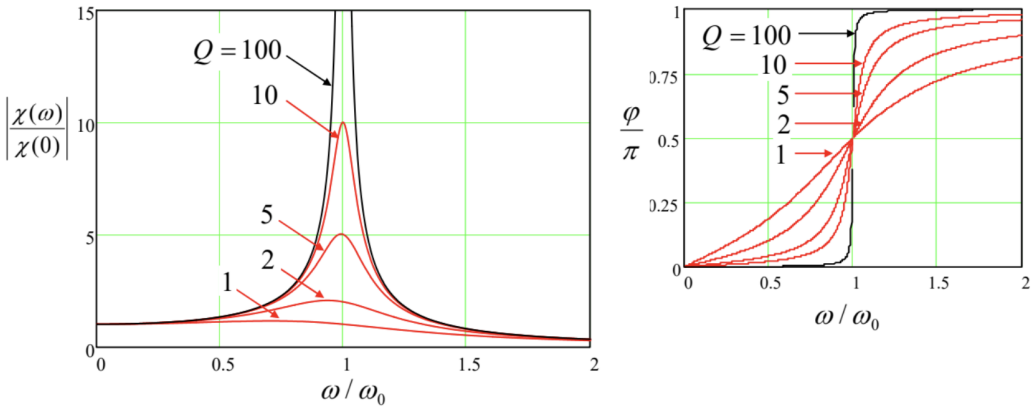

Figure 5.1. Resonance in the linear oscillator, for several values of Q.

Due to the increase of the resonance peak height, its width is inversely proportional to Q. Quantitatively, in the most interesting low-damping limit, i.e. at $Q >> 1$, the reciprocal Q-factor gives the normalized value of the so-called full-width at half-maximum (FWHM) of the resonance curve: [9]

$$\frac{\Delta\omega}{\omega_0} = \frac{1}{Q}. \tag{5.1.21}$$

Indeed, this $\Delta\omega$ is defined as the difference $(\omega_+ - \omega_-)$ between the two values of ω at that the square of the oscillator response function, $|\chi(\omega)|^2$ (which is proportional to the oscillation energy), equals a half of its resonance value (19). In the low damping limit, both these points are very close to ω_0, so that in the linear approximation in $|\omega^- \omega_0| << \omega_0$, we may write $\left({\omega_0}^{2-}\omega^2\right) \equiv -(\omega+\omega_0)(\omega^-\omega_0) \approx -2\omega\xi \approx -2\omega_0\xi$, where

$$\xi \equiv \omega - \omega_0 \tag{5.1.22}$$

is a very convenient parameter called detuning, which will be repeatedly used later in this chapter. In this approximation, the second of Eqs. (18) is reduced to [10]

$$|\chi(\omega)|^2 = \frac{1}{4\omega_0^2\left(\delta^2+\xi^2\right)}. \tag{5.1.23}$$

As a result, the points $\omega_\pm$correspond to $\xi^2 = \delta^2$, i.e. $\omega_\pm = \omega_0 \pm \delta = \omega_0(1 \pm 1/2Q)$, so that $\Delta\omega \equiv \omega_+ - \omega_- = \omega_0/Q$, thus proving Eq. (20).

(ii) Time domain. Returning to arbitrary external force $f(t)$, one may argue that Eqs. (9), (15)-(17) provide a full solution of the forced oscillation problem even in this general case. This is formally correct, but this solution may be very inconvenient if the external force is far from a sinusoidal function of time, especially if it is not periodic at all. In this case, we should first calculate the complex amplitudes f_ω participating in the Fourier sum (14). In the general case of a non-periodic $f(t)$, this is actually the Fourier integral, [11]

$$f(t)=\int_{-\infty}^{+\infty} f_\omega e^{-i\omega t}\,dt, \tag{5.1.24}$$

so that f_ω should be calculated using the reciprocal Fourier transform,

$$f_\omega=\frac{1}{2\pi}\int_{-\infty}^{+\infty} f\left(t'\right)e^{i\omega t'}\,dt' \tag{5.1.25}$$

Now we may use Eq. (16) for each Fourier component of the resulting forced oscillations, and rewrite the last of Eqs. (15) as

$$\begin{aligned} q_{\text{forced}}\left(t\right) &= \int_{-\infty}^{+\infty} a_\omega e^{-i\omega t}\,d\omega=\int_{-\infty}^{+\infty}\chi(\omega)f_\omega e^{-i\omega t}\,d\omega=\int_{-\infty}^{+\infty}d\omega\chi(\omega)\frac{1}{2\pi}\int_{-\infty}^{+\infty}dt' f\left(t'\right)e^{i\omega(t'-t)} \\ &=\int_{-\infty}^{+\infty}dt' f\left(t'\right)\left[\frac{1}{2\pi}\int_{-\infty}^{+\infty}d\omega\chi(\omega)e^{i\omega(t'-t)}\right] \end{aligned}$$

with the response function $\chi(\omega)$ given, in our case, by Eq. (17). Besides requiring two integrations, Eq. (25) is conceptually uncomforting: it seems to indicate that the oscillator's coordinate at time t depends not only on the external force exerted at earlier times t ' $<t$, but also at future times. This would contradict one of the most fundamental principles of physics (and indeed, science as a whole), the causality: no effect may precede its cause.

Fortunately, a straightforward calculation (left for the reader's exercise) shows that the response function (17) satisfies the following rule: [12]

$$\int_{-\infty}^{+\infty}\chi(\omega)e^{-i\omega\tau}\,d\omega=0,\qquad \text{for } \tau<0. \tag{5.1.26}$$

This fact allows the last form of Eq. (25) to be rewritten in either of the following equivalent forms:

$$q_{\text{forced}}\left(t\right)=\int_{-\infty}^{t} f\left(t'\right)G\left(t-t'\right)dt'\equiv\int_{0}^{\infty} f(t-\tau)G(\tau)d\tau, \tag{5.1.27}$$

where $G(\tau)$, defined as the Fourier transform of the response function,

$$G(\tau)\equiv\frac{1}{2\pi}\int_{-\infty}^{+\infty}\chi(\omega)e^{-i\omega\tau}d\omega, \tag{5.1.28}$$

is called the (temporal) Green's function of the system. According to Eq. (26), $G(\tau)=0$ for all $\tau<0$.

While the second form of Eq. (27) is frequently more convenient for calculations, its first form is more suitable for physical interpretation of the Green's function. Indeed, let us consider the particular case when the force is a delta function

$$f(t)=\delta\left(t-t'\right),\qquad \text{with } t'<t, \text{ i.e. } \tau\equiv t-t'>0, \tag{5.1.29}$$

representing an ultimately short pulse at the moment t ', with unit "area" $\int f(t)dt$. Substituting Eq. (29a) into Eq. (27), [13] we get

$$q(t)=G\left(t-t'\right). \tag{5.1.30}$$

Thus the Green's function $G\left(t-t'\right)$ is just the oscillator's response, as measured at time t, to a short force pulse of unit "area", exerted at time t '. Hence Eq. (27) expresses the linear superposition principle in the time domain: the full effect of the force $f(t)$ on a linear system is a sum of effects of short pulses of duration dt ' and magnitude $f\left(t'\right)$, each with its own "weight" $G\left(t-t'\right)$ - see Figure 2 .

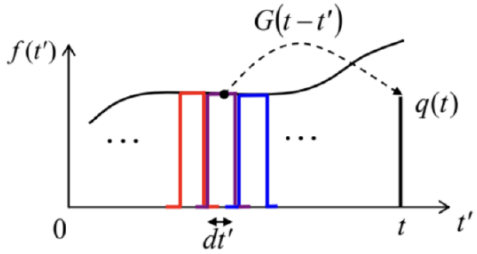

Figure 5.2. A schematic, finite-interval representation of a force $f(t)$ as a sum of short pulses at all times $t' < t$, and their contributions to the linear system's response $q(t)$, as given by Eq. (27).

This picture may be used for the calculation of Green's function for our particular system. Indeed, Eqs. (29)-(30) mean that $G(\tau)$ is just the solution of the differential equation of motion of the system, in our case, Eq. (13), with the replacement $t \to \tau$, and a δ-functional right-hand side:

$$\frac{d^2G(\tau)}{d\tau^2} + 2\delta\frac{dG(\tau)}{d\tau} + \omega_0^2 G(\tau) = \delta(\tau). \tag{5.1.31}$$

Since Eqs. (27) describes only the second term in Eq. (15), i.e. only the forced, rather than free oscillations, we have to exclude the latter by solving Eq. (31) with zero initial conditions:

$$G(-0) = \frac{dG}{d\tau}(-0) = 0, \tag{5.1.32}$$

where $\tau = -0$ means the instant immediately preceding $\tau = 0$.

This calculation may be simplified even further. Let us integrate both sides of Eq. (31) over an infinitesimal interval including the origin, e.g. [- $d\tau/2, +d\tau/2$], and then follow the limit $d\tau \to 0$. Since the Green's function has to be continuous because of its physical sense as the (generalized) coordinate, all terms on the left-hand side but the first one vanish, while the first term yields $dG/d\tau|_{+0} - dG/d\tau|_{-0}$. Due to the second of Eqs. (32), the last of these two derivatives equals zero, while the right-hand side of Eq. (31) yields 1 upon the integration. Thus, the function $G(\tau)$ may be calculated for $\tau > 0$ (i.e. for all times when it is different from zero) by solving the homogeneous version of the system's equation of motion for $\tau > 0$, with the following special initial conditions:

$$G(0) = 0, \quad \frac{dG}{d\tau}(0) = 1. \tag{5.1.33}$$

This approach gives us a convenient way for the calculation of Green's functions of linear systems. In particular for the oscillator with not very high damping $(\delta < \omega_0$, i.e. $Q > 1/2)$, imposing the boundary conditions (33) on the homogeneous equation's solution (9), we immediately get

$$G(\tau) = \frac{1}{\omega_0'} e^{-\delta\tau} \sin\omega_0'\tau \tag{5.1.34}$$

(The same result may be obtained directly from Eq. (28) with the response function $\chi(\omega)$ given by Eq. (19). This way is, however, a little bit more cumbersome, and is left for the reader's exercise.)

Relations (27) and (34) provide a very convenient recipe for solving many forced oscillations problems. As a very simple example, let us calculate the transient process in an oscillator under the effect of a constant force being turned on at $t = 0$, i.e. proportional to the theta-function of time:

$$f(t) = f_0\theta(t) \equiv \begin{cases} 0, & \text{for } t < 0, \\ f_0, & \text{for } t > 0, \end{cases} \tag{5.1.35}$$

provided that at $t < 0$ the oscillator was at rest, so that in Eq. (15), $q_{\text{free}}(t) \equiv 0$. Then the second form of Eq. (27), and Eq. (34), yield

$$q(t) = \int_0^\infty f(t-\tau)G(\tau)d\tau = f_0\int_0^t \frac{1}{\omega_0'} e^{-\delta\tau} \sin\omega_0'\tau d\tau. \tag{5.1.36}$$

The simplest way to work out such integrals is to represent the sine function under it as the imaginary part of $\exp\{i\omega_0' t\}$, and merge the two exponents, getting

$$q(t) = f_0 \frac{1}{\omega_0'} \mathrm{Im}\left[\frac{1}{-\delta + i\omega_0'} e^{-\delta\tau + i\omega_0'\tau}\right]_0^t = \frac{F_0}{k}\left[1 - e^{-\delta t}\left(\cos\omega_0' t + \frac{\delta}{\omega_0'}\sin\omega_0' t\right)\right] \tag{5.1.37}$$

This result, plotted in Figure 3, is rather natural: it describes nothing more than the transient from the initial position $q = 0$ to the new equilibrium position $q_0 = f_0/{\omega_0}^2 = F_0/\kappa$, accompanied by decaying oscillations. For this particular simple function $f(t)$, the same result might be also obtained by introducing a new variable $\tilde{q}(t) \equiv q(t) - q_0$ and solving the resulting homogeneous equation for $\tilde{q}$ (with appropriate initial condition $\tilde{q}(0) = -q_0$. However, for more complicated functions $f(t)$ the Green's function approach is irreplaceable.

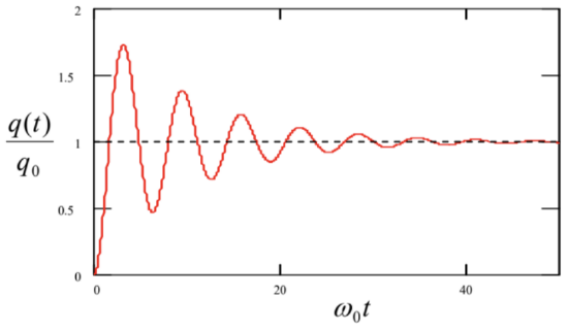

Figure 5.3. The transient process in a linear oscillator, induced by a step-like force $f(t)$, for the particular case $\delta/\omega_0 = 0.1$ (i.e., $Q = 5$).

Note that for any particular linear system, its Green's function should be calculated only once, and then may be repeatedly used in Eq. (27) to calculate the system response to various external forces either analytically or numerically. This property makes the Green's function approach very popular in many other fields of physics − with the corresponding generalization or re-definition of the function. [14]

---

[1] For the notation brevity, in this chapter I will drop indices "ef" in the energy components T and U, and parameters like m, κ, etc. However, the reader should still remember that T and U do not necessarily coincide with the actual kinetic and potential energies (even if those energies may be uniquely identified) - see Sec. 3.1.

[2] ω_0 is usually called the own frequency of the oscillator. In quantum mechanics, the Germanized version of the same term, eigenfrequency, is used more. In this series, I will use either of the terms, depending on the context.

[3] Note that this is the so-called physics convention. Most engineering texts use the opposite sign in the imaginary exponent, $\exp\{-i\omega t\} \to \exp\{i\omega t\}$, with the corresponding sign implications for intermediate formulas, but (of course) similar final results for real variables.

[4] Here Eq. (5) is treated as a phenomenological model, but in statistical mechanics, such dissipative term may be derived as an average force exerted upon a system by its environment, at very general assumptions. As discussed in detail elsewhere in this series (SM Chapter 5 and QM Chapter 7), due to the numerous degrees of freedom of a typical environment (think about the molecules of air surrounding the usual mechanical pendulum), its force also has a random component; as a result, the dissipation is fundamentally related to fluctuations. The latter effects may be neglected (as they are in this course) only if E is much higher than the energy scale of the random fluctuations of the oscillator - in the thermal equilibrium at temperature T, the larger of $k_B T$ and $\hbar\omega_0/2$.

[5] Systems with high damping $(\delta > \omega_0)$ can hardly be called oscillators, and though they are used in engineering and physics experiment (e.g., for the shock, vibration, and sound isolation), for their detailed discussion I have to refer the interested reader to special literature - see, e.g., C. Harris and A. Piersol, Shock and Vibration Handbook, 5^{th} ed., McGraw Hill, 2002. Let me only note that dynamics of systems with very high damping $(\delta \gg \omega_0)$ has two very different time scales: a relatively short "momentum relaxation time" $1/\lambda \approx 1/2\delta = m/\eta$, and a much longer "coordinate relaxation time" $1/\lambda_+ \approx 2\delta/{\omega_0}^2 = \eta/\kappa$.

[6] This is a very unfortunate, but common jargon, meaning "the system described by linear equations of motion".

[7] Here, in contrast to Eq. (3b), we may drop the operator Re, assuming that $f_{-\omega} = f_{\omega}{}^{*}$, so that the imaginary components of the sum compensate each other.

[8] In physics, this mathematical property of linear equations is frequently called the linear superposition principle.

[9] Note that the phase shift $\varphi \equiv \arg[\chi(\omega)]$ between the oscillations and the external force (see the right panel in Figure 1) makes its steepest change, by $\pi/2$, within the same frequency interval $\Delta\omega$.

[10] Such function of frequency is met in many branches of science, frequently under special names, including the "Cauchy distribution", "the Lorentz function" (or "Lorentzian line", or "Lorentzian distribution"), "the BreitWigner function" (or "the Breit-Wigner distribution"), etc.

[11] Let me hope that the reader knows that Eq. (23) may be used for periodic functions as well; in such a case, f_{ω} is a set of equidistant delta functions. (A reminder of the basic properties of the Dirac δ-function may be found, for example, in MA Sec. 14.)

[12] Eq. (26) remains true for any linear physical systems in which $f(t)$ represents a cause, and $q(t)$ its effect. Following tradition, I discuss the frequency-domain expression of this causality relation (called the KramersKronig relations) in the Classical Electrodynamics part of this lecture series - see EM Sec. 7.2.

[13] Technically, for this integration, t ' in Eq. (27) should be temporarily replaced with another letter, say t ".

[14] See, e.g., EM Sec. 2.7, and QM Sec. 2.2.

5.2: Weakly Nonlinear Oscillations

In comparison with systems discussed in the last section, which are described by linear differential equations with constant coefficients and thus allow a complete and exact analytical solution, oscillations in nonlinear systems (very unfortunately but commonly called nonlinear oscillations) present a complex and, generally, analytically intractable problem. However, much insight on possible processes in such systems may be gained from a discussion of an important case of weakly nonlinear systems, which may be explored analytically. An important example of such systems is given by an anharmonic oscillator - a 1D system whose higher terms in the potential expansion (3.10) cannot be neglected, but are small and may be accounted for approximately. If, in addition, damping is low (or negligible), and the external harmonic force exerted on the system is not too large, the equation of motion is a slightly modified version of Eq. (13):

$$\ddot{q} + \omega^2 q = f(t, q, \dot{q}, \ldots), \tag{5.2.1}$$

where $\omega \approx \omega_0$ is the anticipated frequency of oscillations (whose choice is to a certain extent arbitrary see below), and the right-hand side f is small (say, scales as some small dimensionless parameter $\varepsilon << 1$), and may be considered as a small perturbation.

Since at $\varepsilon = 0$ this equation has the sinusoidal solution given by Eq. (3), one might naïvely think that at a nonzero but small ε, the approximate solution to Eq. (38) should be sought in the form

$$q(t) = q^{(0)} + q^{(1)} + q^{(2)} + \ldots, \quad \text{where } q^{(n)} \propto \varepsilon^n, \tag{5.2.2}$$

with $q^{(0)} = A\cos(\omega_0 t - \varphi) \propto \varepsilon^0$. This is a good example of apparently impeccable mathematical reasoning that would lead to a very inefficient procedure. Indeed, let us apply it to the problem we already know the exact solution for, namely the free oscillations in a linear but damped oscillator, for this occasion assuming the damping to be very low, $\delta/\omega_0 \sim \varepsilon << 1$. The corresponding equation of motion, Eq. (6), may be represented in form (38) if we take $\omega = \omega_0$ and

$$f = -2\delta\dot{q}, \quad \text{with } \delta \propto \varepsilon. \tag{5.2.3}$$

The naïve approach described above would allow us to find small corrections, of the order of δ, to the free, non-decaying oscillations $A\cos(\omega_0 t - \varphi)$. However, we already know from Eq. (9) that the main effect of damping is a gradual decrease of the free oscillation amplitude to zero, i.e. a very large change of the amplitude, though at low damping, $\delta << \omega_0$, this decay takes large time $t \sim \tau >> 1/\omega_0$. Hence, if we want our approximate method to be productive (i.e. to work at all time scales, in particular for forced oscillations with stationary amplitude and phase), we need to account for the fact that the small righthand side of Eq. (38) may eventually lead to essential changes of oscillation's amplitude A (and sometimes, as we will see below, also of oscillation's phase φ) at large times, because of the slowly accumulating effects of the small perturbation. [15]

This goal may be achieved [16] by the account of these slow changes already in the " 0^{th} approximation", i.e. the basic part of the solution in the expansion (39):

$$q^{(0)} = A(t)\cos[\omega t - \varphi(t)], \quad \text{with } \dot{A}, \dot{\varphi} \to 0 \quad \text{at } \varepsilon \to 0 \tag{5.2.4}$$

(It is evident that Eq. (9) is a particular case of this form.) Let me discuss this approach using a simple but representative example of a dissipative (but high- Q) pendulum driven by a weak sinusoidal external force with a nearly-resonant frequency:

$$\ddot{q} + 2\delta\dot{q} + \omega_0^2 \sin q = f_0 \cos\omega t, \tag{5.2.5}$$

with $|\omega - \omega_0|$, $\delta << \omega_0$, and the force amplitude f_0 so small that $|q| << 1$ at all times. From what we know about the forced oscillations from Sec. 1, in this case it is natural to identify ω on the left-hand side of Eq. (38) with the force's frequency. Expanding $\sin q$ into the Taylor series in small q, keeping only the first two terms of this expansion, and moving all small terms to the right-hand side, we can rewrite Eq. (42) in the following popular form (38): [17]

$$\ddot{q} + \omega^2 q = -2\delta\dot{q} + 2\xi\omega q + \alpha q^3 + f_0\cos\omega t \equiv f(t, q, \dot{q}). \tag{5.2.6}$$

Here $\alpha = \omega_0^2/6$ in the case of the pendulum (though the calculations below will be valid for any α), and the second term on the right-hand side was obtained using the approximation already employed in Sec. 1 : $\left(\omega^2 - \omega_0^2\right) q \approx 2\omega\left(\omega - \omega_0\right) q = 2\omega\xi q$, where $\xi \equiv \omega - \omega_0$ is the detuning parameter that was already used earlier - see Eq. (21).

Now, following the general recipe expressed by Eqs. (39) and (41), in the 1^{st} approximation in $f \propto \varepsilon$ we may look for the solution to Eq. (43) in the following form: [18]

$$q(t) = A\cos\Psi + q^{(1)}(t), \quad \text{where } \Psi \equiv \omega t - \varphi, \quad q^{(1)} \sim \varepsilon. \tag{5.2.7}$$

Let us plug this solution into both parts of Eq. (43), keeping only the terms of the first order in ε. Thanks to our (smart :-) choice of ω on the left-hand side of that equation, the two zero-order terms in that part cancel each other. Moreover, since each term on the right-hand side of Eq. (43) is already of the order of ε, we may drop $q^{(1)} \propto \varepsilon$ from the substitution into that part at all, because this would give us only terms $O\left(\varepsilon^2\right)$ or higher. As a result, we get the following approximate equation:

$$\ddot{q}^{(1)} + \omega^2 q^{(1)} = f^{(0)} \equiv -2\delta\frac{d}{dt}(A\cos\Psi) + 2\xi\omega(A\cos\Psi) + \alpha(A\cos\Psi)^3 + f_0\cos\omega t. \tag{5.2.8}$$

According to Eq. (41), generally, A and φ should be considered (slow) functions of time. However, let us leave the analyses of the transient process and system's stability until the next section, and use Eq. (45) to find stationary oscillations in the system, that are established after an initial transient. For that limited task, we may take $A = \text{const}$, $\varphi = \text{const}$, so that $q^{(0)}$ represents sinusoidal oscillations of frequency ω. Sorting the terms on the right-hand side according to their time dependence, [19] we see that it has terms with frequencies ω and 3ω:

$$f^{(0)} = \left(2\xi\omega A + \frac{3}{4}\alpha A^3 + f_0\cos\varphi\right)\cos\Psi + (2\delta\omega A - f_0\sin\varphi)\sin\Psi + \frac{1}{4}\alpha A^3\cos 3\Psi. \tag{5.2.9}$$

Now comes the main punch of the van der Pol approach: mathematically, Eq. (45) may be viewed as the equation of oscillations in a linear, dissipation-free harmonic oscillator of frequency ω (not ω_0!) under the action of an external force $f(t)$ represented by the right-hand side of the equation. In our particular case, it has three terms: two "quadrature" components at that very frequency ω, and the third one at frequency 3ω. As we know from our analysis of this problem in Sec. 1, if any of the first two components is not equal to zero, $q^{(1)}$ grows to infinity - see Eq. (19) with $\delta = 0$. At the same time, by the very structure of the van der Pol approximation, $q^{(1)}$ has to be finite – moreover, small! The only way out of this contradiction is to require that the amplitudes of both quadrature components of $f^{(0)}$ with frequency ω are equal to zero:

$$2\xi\omega A + \frac{3}{4}\alpha A^3 + f_0\cos\varphi = 0, \quad 2\delta\omega A - f_0\sin\varphi = 0. \tag{5.2.10}$$

These two harmonic balance equations enable us to find both parameters of the forced oscillations: their amplitude A and phase φ. The phase may be readily eliminated from this system (most easily, by expressing $\sin\varphi$ and $\cos\varphi$ from Eqs. (47), and then requiring the sum $\sin^2\varphi + \cos^2\varphi$ to equal 1), and the solution for A recast in the following implicit but convenient form:

$$A^2 = \frac{f_0^2}{4\omega^2}\frac{1}{\xi^2(A) + \delta^2}, \quad \text{where } \xi(A) \equiv \xi + \frac{3}{8}\frac{\alpha A^2}{\omega} = \omega - \left(\omega_0 - \frac{3}{8}\frac{\alpha A^2}{\omega}\right). \tag{5.2.11}$$

This expression differs from Eq. (22) for the linear resonance in the low-damping limit only by the replacement of the detuning ξ with its effective amplitude-dependent value $\xi(A)$ - or, equivalently, the replacement of the frequency ω_0 of the oscillator with its effective, amplitude-dependent value

$$\omega_0(A) = \omega_0 - \frac{3}{8}\frac{\alpha A^2}{\omega}. \tag{5.2.12}$$

The physical meaning of $\omega_0(A)$ is simple: this is just the frequency of free oscillations of amplitude A in a similar nonlinear system, but with zero damping. [20] Indeed, for $\delta = 0$ and $f_0 = 0$ we could repeat our calculations, assuming that ω is an amplitude-dependent eigenfrequency $\omega_0(A)$. Then the second of Eqs. (47) is trivially satisfied, while the second of them gives Eq. (49). The implicit relation (48) enables us to draw the curves of this nonlinear resonance just by bending the linear resonance plots (Figure 1) according to the so-called skeleton curve expressed by Eq. (49). Figure 4 shows the result of this procedure. Note that at small amplitude, $\omega(A) \to \omega_0$, i.e. we return to the usual, "linear" resonance (22).

To bring our solution to its logical completion, we should still find the first perturbation $q^{(1)}(t)$ from what is left of Eq. (45). Since the structure of this equation is similar to Eq. (13) with the force of frequency 3ω and zero damping, we may use Eqs. (16)-(17) to obtain

$$q^{(1)}(t) = -\frac{1}{32\omega^2}\alpha A^3\cos 3(\omega t - \varphi). \tag{5.2.13}$$

Adding this perturbation (note the negative sign!) to the sinusoidal oscillation (41), we see that as the amplitude A of oscillations in a system with $\alpha > 0$ (e.g., a pendulum) grows, their waveform becomes a bit more "blunt" near the largest deviations from the

equilibrium.

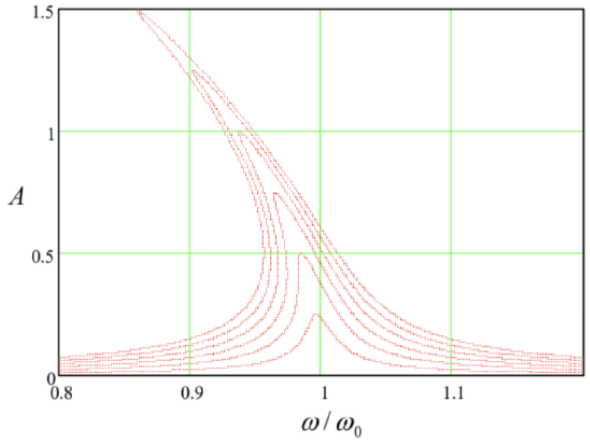

Figure 5.4. The nonlinear resonance in the Duffing oscillator, as described by Eq. (48), for the particular case $\alpha = \omega_0^2/6, \delta/\omega = 0.01$ (i.e. $Q = 50$), and several values of the parameter ${f_0}/{\omega_0}^2$, increased by equal steps of 0.005 from 0 to 0.03.

The same Eq. (50) also enables an estimate of the range of validity of our first approximation: since it has been based on the assumption $\left|q^{(1)}\right| << \left|q^{(0)}\right| \leq A$, for this particular problem we have to require $\alpha A^2/32\omega^2 << 1$. For a pendulum (i.e. for $\alpha = \omega_0^2/6$), this condition becomes $A^2 << 192$. Though numerical coefficients in such strong inequalities should be taken with a grain of salt, the large magnitude of this particular coefficient gives a good hint that the method may give very accurate results even for relatively large oscillations with $A \sim 1$. In Sec. 7 below, we will see that this is indeed the case.

From the mathematical viewpoint, the next step would be to write the next approximation as

$$q(t) = A\cos\Psi + q^{(1)}(t) + q^{(2)}(t), \quad q^{(2)} \sim \varepsilon^2, \tag{5.2.14}$$

and plug it into the Duffing equation (43), which (thanks to our special choice of $q^{(0)}$ and $q^{(1)}$) would retain only the sum $\ddot{q}^{(2)} + \omega^2 q^{(2)}$ on its left-hand side. Again, requiring the amplitudes of two quadrature components of the frequency ω on the right-hand side to vanish, we may get second-order corrections to A and φ. Then we may use the remaining part of the equation to calculate $q^{(2)}$, and then go after the third-order terms, etc. However, for most purposes, the sum $q^{(0)} + q^{(1)}$, and sometimes even just the crudest approximation $q^{(0)}$ alone, are completely sufficient. For example, according to Eq. (50), for a simple pendulum swinging as much as between the opposite horizontal positions $(A = \pi/2)$, the 1^{st} order correction $q^{(1)}$ is of the order of 0.5%. (Soon beyond this value, completely new dynamic phenomena start – see Sec. 7 below – but they cannot be described by these successive approximations at all.) Due to such reasons, higher approximations are rarely pursued for particular systems.

---

[15] The same flexible approach is necessary to approximations used in quantum mechanics. The method discussed here is much closer in spirit (though not completely identical) to the WKB approximation (see, e.g., QM Sec. 2.4) rather than most perturbative approaches (QM Ch. 6).

[16] The basic idea of this approach was reportedly suggested in 1920 by Balthasar van der Pol, and its first approximation (on which I will focus) is frequently called the van der Pol method. However, in optics and quantum mechanics, it is most commonly called the Rotating Wave Approximation (RWA). In math-oriented texts, this approach, especially its extensions to higher approximations, is usually called either the small parameter method or the asymptotic method. The list of other scientists credited for the development of this method, its variations, and extensions includes, most notably, N. Krylov, N. Bogolyubov, and Yu. Mitroplolsky.

[17] This equation is frequently called the Duffing equation (or the equation of the Duffing oscillator), after Georg Duffing who carried out its first (rather incomplete) analysis in 1918.

[18] For a mathematically rigorous treatment of higher approximations, see, e.g., Yu. Mitropolsky and N. Dao, Applied Asymptotic Methods in Nonlinear Oscillations, Springer, 2004. A more laymen (and, by today's standards, somewhat verbose) discussion of various oscillatory phenomena may be found in the classical text A. Andronov, A. Vitt, and S. Khaikin, Theory of Oscillators, Dover, 2011.

[19] Using the second of Eqs. (44), $\cos\omega t$ may be rewritten as $\cos(\Psi+\varphi)\equiv\cos\Psi\cos\varphi-\sin\Psi\sin\varphi$. Then using the identity given, for example, by MA Eq. (3.4): $\cos^3\Psi=(3/4)\cos\Psi+(1/4)\cos 3\Psi$, we get Eq. (46).

[20] The effect of pendulum's frequency dependence on its oscillation amplitude was observed as early as 1673 by Christiaan Huygens - who by the way had invented the pendulum clock, increasing the timekeeping accuracy by about three orders of magnitude (and also discovered the largest of Saturn's moons, Titan).

5.3: Reduced Equations

A much more important issue is the stability of the solutions described by Eq. (48). Indeed, Figure 4 shows that within a certain range of parameters, these equations give three different values for the oscillation amplitude (and phase), and it is important to understand which of these solutions are stable. Since these solutions are not the fixed points in the sense discussed in Sec. 3.2 (each point in Figure 4 represents a nearly-sinusoidal oscillation), their stability analysis needs a more general approach that would be valid for oscillations with amplitude and phase slowly evolving in time. This approach will also enable the analysis of non-stationary (especially the initial transient) processes, which are of importance for some dynamic systems.

First of all, let us formalize the way the harmonic balance equations, such as Eqs. (47), are obtained for the general case (38) - rather than for the particular Eq. (43) considered in the last section. After plugging in the 0^{th} approximation (41) into the right-hand side of equation (38) we have to require the amplitudes of both quadrature components of frequency ω to vanish. From the standard Fourier analysis, we know that these requirements may be represented as

$$\overline{f^{(0)}\sin\Psi}=0,\ \overline{f^{(0)}\cos\Psi}=0, \tag{5.3.1}$$

where the top bar means the time averaging - in our current case, over the period $2\pi/\omega$ of the right-hand side of Eq. (52), with the arguments calculated in the 0^{th} approximation:

$$f^{(0)}\equiv f\left(t,q^{(0)},\dot{q}^{(0)},\ldots\right)\equiv f(t,A\cos\Psi,-A\omega\sin\Psi,\ldots),\quad \text{with } \Psi=\omega t-\varphi. \tag{5.3.2}$$

Now, for a transient process the contribution of $q^{(0)}$ to the left-hand side of Eq. (38) is not zero any longer, because its amplitude and phase may be both slow functions of time - see Eq. (41). Let us calculate this contribution. The exact result would be

$$\begin{aligned}\ddot{q}^{(0)}+\omega^2 q^{(0)} &\equiv \left(\frac{d^2}{dt^2}+\omega^2\right)A\cos(\omega t-\varphi)\\ &=\left(\ddot{A}+2\dot{\varphi}\omega A-\dot{\varphi}^2 A\right)\cos(\omega t-\varphi)-2\dot{A}(\omega-\dot{\varphi})\sin(\omega t-\varphi).\end{aligned}$$

However, in the first approximation in ε, we may neglect the second derivative of A, and also the squares and products of the first derivatives of A and φ (which are all of the second order in ε), so that Eq. (54) is reduced to

$$\ddot{q}^{(0)}+\omega^2 q^{(0)}\approx 2A\dot{\varphi}\omega\cos(\omega t-\varphi)-2\dot{A}\omega\sin(\omega t-\varphi). \tag{5.3.3}$$

On the right-hand side of Eq. (53), we can neglect the time derivatives of the amplitude and phase at all, because this part is already proportional to the small parameter. Hence, in the first order in ε, Eq. (38) becomes

$$\ddot{q}^{(1)}+\omega^2 q^{(1)}=f_{\text{ef}}^{(0)}\equiv f^{(0)}-(2A\dot{\varphi}\omega\cos\Psi-2\dot{A}\omega\sin\Psi). \tag{5.3.4}$$

Now, applying Eqs. (52) to the function $f_{\text{ef}}^{(0)}$, and taking into account that the time averages of $\sin^2\Psi$ and $\cos^2\Psi$ are both equal to $1/2$, while the time average of the product $\sin\Psi\cos\Psi$ vanishes, we get a pair of so-called reduced equations (alternatively called "truncated", or "RWA", or "van der Pol" equations) for the time evolution of the amplitude and phase:

$$\dot{A}=-\frac{1}{\omega}\overline{f^{(0)}\sin\Psi},\quad \dot{\varphi}=\frac{1}{\omega A}\overline{f^{(0)}\cos\Psi} \tag{5.3.5}$$

Extending the definition (4) of the complex amplitude of oscillations to their slow evolution in time, $a(t)\equiv A(t)\exp\{i\varphi(t)\}$, and differentiating this relation, the two equations (57a) may be also rewritten in the form of either one equation for a :

$$\dot{a}=\frac{i}{\omega}\overline{f^{(0)}e^{i(\Psi+\varphi)}}\equiv\frac{i}{\omega}\overline{f^{(0)}e^{i\omega t}} \tag{5.3.6}$$

or two equations for the real and imaginary parts of $a(t)=u(t)+iv(t)$:

$$\dot{u}=-\frac{1}{\omega}\overline{f^{(0)}\sin\omega t},\quad \dot{v}=\frac{1}{\omega}\overline{f^{(0)}\cos\omega t}. \tag{5.3.7}$$

The first-order harmonic balance equations (52) are evidently just the particular case of the reduced equations (57) for stationary oscillations ($\dot{A}=\dot{\varphi}=0$). [21]

Superficially, the system (57a) of two coupled, first-order differential equations may look more complex than the initial, second-order differential equation (38), but actually, it is usually much simpler. For example, let us spell them out for the easy case of free oscillations a linear oscillator with damping. For that, we may reuse the ready Eq. (46) by taking $\alpha = f_0 = 0$, and thus turning Eqs. (57a) into

$$\dot{A} = -\frac{1}{\omega}\overline{f^{(0)}\sin\Psi} \equiv -\frac{1}{\omega}\overline{(2\xi\omega A\cos\Psi + 2\delta\omega A\sin\Psi)\sin\Psi} \equiv -\delta A,$$
$$\dot{\varphi} = \frac{1}{\omega A}\overline{f^{(0)}\cos\Psi} \equiv \frac{1}{\omega A}\overline{(2\xi\omega A\cos\Psi + 2\delta\omega A\sin\Psi)\cos\Psi} \equiv \xi.$$

The solution of Eq. (58a) gives us the same "envelope" law $A(t) = A(0)e^{-\delta t}$ as the exact solution (10) of the initial differential equation, while the elementary integration of Eq. (58b) yields $\varphi(t) = \xi t +$ const $\equiv \omega t - \omega_0 t + \varphi(0)$. This means that our approximate solution,

$$q^{(0)}(t) = A(t)\cos[\omega t - \varphi(t)] = A(0)e^{-\delta t}\cos[\omega_0 t - \varphi(0)], \tag{5.3.8}$$

agrees with the exact Eq. (9), and misses only the correction (8) of the oscillation frequency. (This correction is of the second order in δ, i.e. of the order of ε^2, and hence is beyond the accuracy of our first approximation.) It is remarkable how nicely do the reduced equations recover the proper frequency of free oscillations in this autonomous system - in which the very notion of ω is ambiguous.

The result is different at forced oscillations. For example, for the (generally, nonlinear) Duffing oscillator described by Eq. (43) with $f_0 \neq 0$, Eqs. (57a) yield the reduced equations,

$$\dot{A} = -\delta A + \frac{f_0}{2\omega}\sin\varphi, \quad A\dot{\varphi} = \xi(A)A + \frac{f_0}{2\omega}\cos\varphi, \tag{5.3.9}$$

which are valid for an arbitrary function $\xi(A)$, provided that this nonlinear detuning remains much smaller than the oscillation frequency. Here (after a transient), the amplitude and phase tend to the stationary states described by Eqs. (47). This means that φ becomes a constant, so that $q^{(0)} \to A\cos(\omega t -$ const), i.e. the reduced equations again automatically recover the correct frequency of the solution, in this case equal to the external force frequency.

Note that each stationary oscillation regime, with certain amplitude and phase, corresponds to a fixed point of the reduced equations, so that the stability of those fixed points determines that of the oscillations. In the next three sections, we will carry out such an analysis for several simple systems of key importance for physics and engineering.

---

[21] One may ask why cannot we stick to just one, most compact, complex-amplitude form (57b) of the reduced equations. The main reason is that when the function $f(q, \dot{q}, t)$ is nonlinear, we cannot replace its real arguments, such as $q = A\cos(\omega t - \varphi)$, with their complex-function representations like $a\exp\{-i\omega t\}$ (as could be done in the linear problems considered in Sec. 5.1), and need to use real variables, such as either $\{A, \varphi\}$ or $\{u, v\}$, anyway.

5.4: Self-oscillations and Phase Locking

The motivation for B. van der Pol to develop his method was the analysis of one more type of oscillatory motion: self-oscillations. Several systems, e.g., electronic rf amplifiers with positive feedback, and optical media with quantum level population inversion, provide convenient means for the compensation, and even over-compensation of the intrinsic energy losses in oscillators. Phenomenologically, this effect may be described as the change of sign of the damping coefficient δ from positive to negative. Since for small oscillations the equation of motion is still linear, we may use Eq. (9) to describe its general solution. This equation shows that at $\delta < 0$, even infinitesimal deviations from equilibrium (say, due to unavoidable fluctuations) lead to oscillations with exponentially growing amplitude. Of course, in any real system such growth cannot persist infinitely, and shall be limited by this or that effect - e.g., in the above examples, respectively, by amplifier's saturation and quantum level population's exhaustion.

In many cases, the amplitude limitation may be described reasonably well by making the following replacement:

$$2\delta\ddot{q} \to 2\delta\dot{q} + \beta\dot{q}^3, \tag{5.4.1}$$

with $\beta > 0$. Let us analyze the effects of such nonlinear damping, applying the van der Pol's approach to the corresponding homogeneous differential equation (which is also known under his name):

$$\ddot{q} + 2\delta\dot{q} + \beta\dot{q}^3 + \omega_0^2 q = 0. \tag{5.4.2}$$

Carrying out the dissipative and detuning terms to the right-hand side, and taking them for f in the canonical Eq. (38), we can easily calculate the right-hand sides of the reduced equations (57a), getting 22

$$\dot{A} = -\delta(A)A, \quad \text{where } \delta(A) \equiv \delta + \frac{3}{8}\beta\omega^2 A^2,$$
$$A\dot{\varphi} = \xi A.$$

The last of these equations has exactly the same form as Eq. (58b) for the case of decaying oscillations and hence shows that the self-oscillations (if they happen, i.e. if $A \neq 0$) have the own frequency ω_0 of the oscillator - cf. Eq. (59). However, Eq. (63a) is more substantive. If the initial damping δ is positive, it has only the trivial fixed point, $A_0 = 0$ (that describes the oscillator at rest), but if δ is negative, there is also another fixed point,

$$A_1 = \left(\frac{8|\delta|}{3\beta\omega^2}\right)^{1/2}, \quad \text{for } \delta < 0 \tag{5.4.3}$$

which describes steady self-oscillations with a non-zero amplitude A_1.

Let us apply the general approach discussed in Sec. 3.2, the linearization of equations of motion, to this reduced equation. For the trivial fixed point $A_0 = 0$, the linearization of Eq. (63a) is reduced to discarding the nonlinear term in the definition of the amplitude-dependent damping $\delta(A)$. The resulting linear equation evidently shows that the system's equilibrium point, $A = A_0 = 0$, is stable at $\delta > 0$ and unstable at $\delta < 0$. (We have already discussed this self-excitation condition above.) On the other hand, the linearization of near the non-trivial fixed point A_1 requires a bit more math: in the first order in $\widetilde{A} \equiv A - A_1 \to 0$, we get

$$\dot{\widetilde{A}} \equiv \dot{A} = -\delta\left(A_1 + \widetilde{A}\right) - \frac{3}{8}\beta\omega^2\left(A_1 + \widetilde{A}\right)^3 \approx -\delta\widetilde{A} - \frac{3}{8}\beta\omega^2 3A_1^2\widetilde{A} = (-\delta + 3\delta)\widetilde{A} = 2\delta\widetilde{A}, \tag{5.4.4}$$

where Eq. (64) has been used to eliminate A_1. We see that the fixed point A_1 (and hence the whole process) is stable as soon as it exists $(\delta < 0)-$ similarly to the situation in our "testbed problem" (Figure 2.1), besides that in our current, dissipative system, the stability is "actual" rather than "orbital" - see Sec. 6 for more on this issue.

Now let us consider another important problem: the effect of an external sinusoidal force on a self-excited oscillator. If the force is sufficiently small, its effects on the self-excitation condition and the oscillation amplitude are negligible. However, if the frequency ω of such a weak force is close to the own frequency ω_0 of the oscillator, it may lead to a very important effect of phase locking [23] - also called the "synchronization", though the latter term also has a much broader meaning. At this effect, the oscillation frequency deviates from ω_0, and becomes exactly equal to the external force's frequency ω, within a certain range

$$-\Delta \leq \omega - \omega_0 < +\Delta. \tag{5.4.5}$$

To prove this fact, and also to calculate the phase-locking range width 2Δ, we may repeat the calculation of the right-hand sides of the reduced equations (57a), adding the term $f_0 \cos\omega t$ to the righthand side of Eq. (62) - cf. Eqs. (42)-(43). This addition modifies Eqs. (63) as follows: 24

$$\dot{A} = -\delta(A)A + \frac{f_0}{2\omega}\sin\varphi,$$
$$A\dot{\varphi} = \xi A + \frac{f_0}{2\omega}\cos\varphi.$$

If the system is self-excited, and the external force is weak, its effect on the oscillation amplitude is small, and in the first approximation in f_0 we can take A to be constant and equal to the value A_1 given by Eq. (64). Plugging this approximation into Eq. (67b), we get a very simple equation [25]

$$\text{Phase locking equation} \qquad \dot{\varphi} = \xi + \Delta\cos\varphi \tag{5.4.6}$$

where in our current case

$$\Delta \equiv \frac{f_0}{2\omega A_1}. \tag{5.4.7}$$

Within the range $-|\Delta| < \xi < +|\Delta|$, Eq. (68) has two fixed points on each 2π-segment of the variable φ :

$$\varphi_\pm = \pm\cos^{-1}\left(-\frac{\xi}{\Delta}\right) + 2\pi n. \tag{5.4.8}$$

It is easy to linearize Eq. (68) near each point to analyze their stability in our usual way; however, let me use this case to demonstrate another convenient way to do this in 1D systems, using the so-called phase plane - the plot of the right-hand side of Eq. (68) as a function of φ - see Figure 5 .

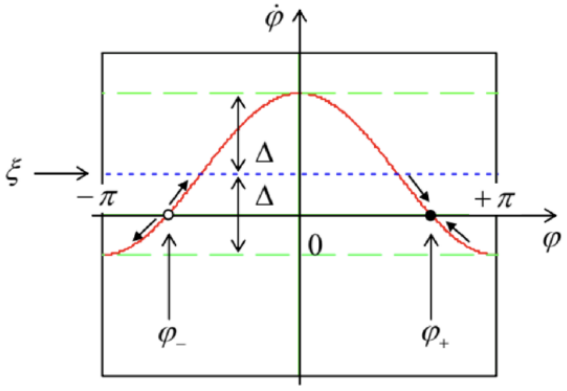

Figure 5.5. The phase plane of a phaselocked oscillator, for the particular case $\xi = \Delta/2$, $f_0 > 0$.

Since according to Eq. (68), positive values of this function correspond to the growth of φ in time and vice versa, we may draw the arrows showing the direction of phase evolution. From this graphics, it is clear that one of these fixed points (for $f_0 > 0, \varphi_+$) is stable, while its counterpart (in this case, φ.) is unstable. Hence the magnitude of Δ given by Eq. (69) is indeed the phase-locking range (or rather it half) that we wanted to find. Note that the range is proportional to the amplitude of the phaselocking signal - perhaps the most important feature of this effect.

To complete our simple analysis, based on the assumption of fixed oscillation amplitude, we need to find the condition of its validity. For that, we may linearize Eq. (67a), for the stationary case, near the value A_1, just as we have done in Eq. (65) for the transient process. The stationary result,

$$\widetilde{A} \equiv A - A_1 = \frac{1}{2|\delta|}\frac{f_0}{2\omega}\sin\varphi_\pm \approx A_1\left|\frac{\Delta}{2\delta}\right|\sin\varphi_\pm, \tag{5.4.9}$$

shows that our assumption, $|\widetilde{A}| << A_1$, and hence the final result (69), are valid if the calculated phaselocking range 2Δ is much smaller than $4|\delta|$.

[22] For that, one needs to use the trigonometric identity $\sin^3\Psi = (3/4)\sin\Psi - (1/4)\sin 3\Psi -$ see, e.g., MA Eq. (3.4).

[23] Apparently, the mutual phase locking of two pendulum clocks was first noticed by the same C. Huygens.

[24] Actually, this result should be evident, even without calculations, from the comparison of Eqs. (60) and (63).

[25] This equation is ubiquitous in phase-locking systems, including even some digital electronic circuits used for that purpose - at the proper re-definition of the phase difference φ.

5.5: Parametric Excitation

In both problems solved in the last section, the stability analysis was easy because it could be carried out for just one slow variable, either amplitude or phase. More generally, such an analysis of the reduced equations involves both these variables. A classical example of such a situation is provided by one important physical phenomenon - the parametric excitation of oscillations. A simple example of such excitation is given by a pendulum with a variable parameter, for example, the suspension length $l(t)$ - see Figure 6. Experiments (including those with playground swings :-) and numerical simulations show that if the length is changed (modulated) periodically, with some frequency 2ω that is close to $2\omega_0$, and a sufficiently large swing Δl, the equilibrium position of the pendulum becomes unstable, and it starts oscillating with frequency ω equal exactly to the half of the modulation frequency (and hence only approximately equal to the average frequency ω_0 of the oscillator).

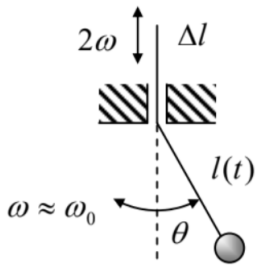

Figure 5.6. Parametric excitation of a pendulum.

For an elementary analysis of this effect, we may consider the simplest case when the oscillations are small. At the lowest point $(\theta = 0)$, where the pendulum moves with the highest velocity $v_{\max}$, the suspension string's tension $\mathcal{T}$ is higher than mg by the centripetal force: $\mathcal{T}_{\max} = mg + mv_{\max}^2/l$. On the contrary, at the maximum deviation of the pendulum from the equilibrium, the force is lower than mg, because of the string's tilt: $\mathcal{T}_{\min} = mg\cos\theta_{\max}$. Using the energy conservation, $E = mv_{\max}^2/2 = mgl\,(1-\cos\theta_{\max})$, we may express these values as $\mathcal{T}_{\max} = mg + 2E/l$ and $\mathcal{T}_{\min} = mg - E/l$. Now, if during each oscillation period the string is pulled up slightly by Δl (with $|\Delta l| << l$) at each of its two passages through the lowest point, and is let to go down by the same amount at each of two points of the maximum deviation, the net work of the external force per period is positive:

$$\mathcal{W} \approx 2\,(\mathcal{T}_{\max} - \mathcal{T}_{\min})\,\Delta l \approx 6\frac{\Delta l}{l}E, \tag{5.5.1}$$

and hence increases the oscillator's energy. If the parameter swing Δl is sufficient, this increase may overcompensate the energy drained out by damping during the same period. Quantitatively, Eq. (10) shows that low damping $(\delta < \omega_0)$ leads to the following energy decrease,

$$\Delta E \approx -4\pi\frac{\delta}{\omega_0}E, \tag{5.5.2}$$

per oscillation period. Comparing Eqs. (72) and (73), we see that the net energy flow into the oscillations is positive, $\mathcal{W} + \Delta E > 0$, i.e. oscillation amplitude has to grow if [26]

$$\frac{\Delta l}{l} > \frac{2\pi\delta}{3\omega_0} \equiv \frac{\pi}{3Q}. \tag{5.5.3}$$

Since this result is independent of the oscillation energy E, the growth of energy and amplitude is exponential (until E becomes so large that some of our assumptions fail), so that Eq. (74) is the condition of parametric excitation - in this simple model.

However, this result does not account for a possible difference between the oscillation frequency ω and the eigenfrequency ω_0, and also does not clarify whether the best phase shift between the oscillations and parameter modulation, assumed in the above calculation, may be sustained automatically. To address these issues, we may apply the van der Pol approach to a simple but reasonable model:

$$\ddot{q} + 2\delta\dot{q} + \omega_0^2(1 + \mu\cos 2\omega t)q = 0, \tag{5.5.4}$$

describing the parametric excitation in a linear oscillator with a sinusoidal modulation of the parameter $\omega_0^2(t)$. Rewriting this equation in the canonical form (38),

$$\ddot{q} + \omega^2 q = f(t, q, \dot{q}) \equiv -2\delta\dot{q} + 2\xi\omega q - \mu\omega_0^2 q\cos 2\omega t, \tag{5.5.5}$$

and assuming that the dimensionless ratios δ/ω and $|\xi|/\omega$, and the modulation depth μ are all much less than 1, we may use general Eqs. (57a) to get the following reduced equations:

$$\dot{A} = -\delta A - \frac{\mu\omega}{4} A \sin 2\varphi,$$
$$A\dot{\varphi} = A\xi - \frac{\mu\omega}{4} A \cos 2\varphi.$$

These equations evidently have a fixed point, with $A_0 = 0$, but its stability analysis (though possible) is not absolutely straightforward, because the phase φ of oscillations is undetermined at that point. In order to avoid this (technical rather than conceptual) difficulty, we may use, instead of the real amplitude and phase of oscillations, either their complex amplitude $a = A\exp\{i\varphi\}$, or its Cartesian components u and v-see Eqs. (4). Indeed, for our function f, Eq. (57b) gives

$$\dot{a} = (-\delta + i\xi)a - i\frac{\mu\omega}{4} a^*, \tag{5.5.6}$$

while Eqs. (57c) yield

$$\dot{u} = -\delta u - \xi v - \frac{\mu\omega}{4} v,$$
$$\dot{v} = -\delta v + \xi u - \frac{\mu\omega}{4} u.$$

We see that in contrast to Eqs. (77), in the Cartesian coordinates $\{u, v\}$ the trivial fixed point $a_0 = 0$ (i.e. $u_0 = v_0 = 0$) is absolutely regular. Moreover, equations (78)-(79) are already linear, so they do not require any additional linearization. Thus we may use the same approach as was already used in Secs. 3.2 and 5.1, i.e. look for the solution of Eqs. (79) in the exponential form $\exp\{\lambda t\}$. However, now we are dealing with two variables and should allow them to have, for each value of λ, a certain ratio u/v. For that, we may take the partial solution in the form

$$u = c_u e^{\lambda t}, \quad v = c_v e^{\lambda t}. \tag{5.5.7}$$

where the constants c_u and c_v are frequently called the distribution coefficients. Plugging this solution into Eqs. (79), we get from them the following system of two linear algebraic equations:

$$(-\delta - \lambda)c_u + \left(-\xi - \frac{\mu\omega}{4}\right) c_v = 0,$$
$$\left(+\xi - \frac{\mu\omega}{4}\right) c_u + (-\delta - \lambda)c_v = 0.$$

The characteristic equation of this system, i.e. the condition of compatibility of Eqs. (81),

$$\begin{vmatrix} -\delta - \lambda & -\xi - \frac{\mu\omega}{4} \\ \xi - \frac{\mu\omega}{4} & -\delta - \lambda \end{vmatrix} \equiv \lambda^2 + 2\delta\lambda + \delta^2 + \xi^2 - \left(\frac{\mu\omega}{4}\right)^2 = 0 \tag{5.5.8}$$

has two roots:

$$\lambda_\pm = -\delta \pm \left[\left(\frac{\mu\omega}{4}\right)^2 - \xi^2\right]^{1/2} \tag{5.5.9}$$

Requiring the fixed point to be unstable, $\mathrm{Re}\,\lambda_+ > 0$, we get the parametric excitation condition

$$\frac{\mu\omega}{4} > \left(\delta^2 + \xi^2\right)^{1/2}. \tag{5.5.10}$$

Thus the parametric excitation may indeed happen without any external phase control: the arising oscillations self-adjust their phase to pick up energy from the external source responsible for the periodic parameter variation.

Our key result (84) may be compared with two other calculations. First, in the case of negligible damping $(\delta = 0)$, Eq. (84) turns into the condition $\mu\omega/4 > |\xi|$. This result may be compared with the well-developed theory of the so-called Mathieu equation, whose canonical form is

$$\frac{d^2y}{dv^2} + (a - 2b\cos 2v)y = 0. \tag{5.5.11}$$

With the substitutions $y \to q, v \to \omega t, a \to (\omega_0/\omega)^2$, and $b/a \to -\mu/2$, this equation is just a particular case of Eq. (75) for $\delta = 0$. In terms of Eq. (85), our result (84) may be re-written just as $b > |a-1|$, and is supposed to be valid for $b << 1$. The boundaries given by this condition are shown with dashed lines in Figure 7 together with the numerically calculated [27] stability boundaries for the Mathieu equation.

One can see that the van der Pol approximation works just fine within its applicability limit (and a bit beyond :-), though it fails to predict some other important features of the Mathieu equation, such as the existence of higher, more narrow regions of parametric excitation (at $a \approx n^2$, i.e. $\omega_0 \approx \omega/n$, for all integer n), and some spill-over of the stability region into the lower half-plane $a < 0$. [28] The reason for these failures is the fact that, as can be seen in Figure 7, these phenomena do not appear in the first approximation in the parameter modulation amplitude $\mu \propto \varepsilon$, which is the realm of applicability of the reduced equations (79).

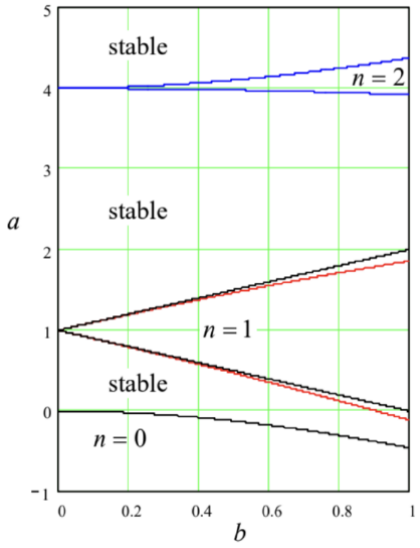

Figure 5.7. Stability boundaries of the Mathieu equation (85), as calculated: numerically (solid curves) and using the reduced equations (dashed straight lines). In the regions numbered by various n, the trivial solution $y = 0$ of the equation is unstable, i.e. its general solution $y(v)$ includes an exponentially growing term.

In the opposite case of non-zero damping but exact tuning $(\xi = 0, \omega \approx \omega_0)$, Eq. (84) becomes

$$\mu > \frac{4\delta}{\omega_0} \equiv \frac{2}{Q}. \tag{5.5.12}$$

This condition may be compared with Eq. (74) by taking $\Delta l/l = 2\mu$. The comparison shows that while the structure of these conditions is similar, the numerical coefficients are different by a factor close to 2 . The first reason for this difference is that the instant parameter change at optimal moments of time is more efficient than the smooth, sinusoidal variation described by (75). Even more significantly, the change of pendulum's length modulates not only its frequency $\omega_0 \equiv (g/l)^{1/2}$ as Eq. (75) implies but also its mechanical impedance $Z \equiv (gl)^{1/2}-$ the notion to be discussed in detail in the next chapter. (The analysis of the general case of the simultaneous modulation of ω_0 and Z is left for the reader's exercise.)

Before moving on, let me summarize the most important differences between the parametric and forced oscillations:

(i) Parametric oscillations completely disappear outside of their excitation range, while the forced oscillations have a non-zero amplitude for any frequency and amplitude of the external force see Eq. (18).

(ii) Parametric excitation may be described by a linear homogeneous equation - e.g., Eq. (75) which cannot predict any finite oscillation amplitude within the excitation range, even at finite damping. In order to describe stationary parametric oscillations, some nonlinear effect has to be taken into account. (I am leaving analyses of such effects for the reader's exercise - see Problems 13 and 14.)

One more important feature of the parametric oscillations will be discussed at the end of the next section.

---

[26] A modulation of the pendulum's mass (say, by periodic pumping water in and out of a suspended bottle) gives a qualitatively similar result. Note, however, that parametric oscillations cannot be excited by modulating any oscillator's parameter - for example,

oscillator's damping coefficient (at least if it stays positive at all times), because its does not change the system's energy, just the energy drain rate.

[27] Such calculations are substantially simplified by the use of the so-called Floquet theorem, which is also the mathematical basis for the discussion of wave propagation in periodic media – see the next chapter.

[28] This region (for $b < 1, -b^2/2 < a < 0$) describes, in particular, the counter-intuitive stability of the so-called Kapitza pendulum - an inverted pendulum with the suspension point oscillated fast in the vertical direction - the effect first observed by Andrew Stephenson in 1908 .

5.6: Fixed Point Classification

The reduced equations (79) give us a good pretext for a brief discussion of an important general topic of dynamics: fixed points of a system described by two time-independent, first-order differential equations with time-independent coefficients. [29] After their linearization near a fixed point, the equations for deviations can always be expressed in the form similar to Eq. (79):

$$\dot{\tilde{q}}_1 = M_{11}\tilde{q}_1 + M_{12}\tilde{q}_2,$$
$$\dot{\tilde{q}}_2 = M_{21}\tilde{q}_1 + M_{22}\tilde{q}_2,$$

where $M_{jj'}$ (with $j, j' = 1, 2$) are some real scalars, which may be viewed as the elements of a 2×2 matrix M. Looking for an exponential solution of the type (80),

$$\tilde{q}_1 = c_1 e^{\lambda t}, \quad \tilde{q}_2 = c_2 e^{\lambda t}, \tag{5.6.1}$$

we get a general system of two linear equations for the distribution coefficients $c_{1,2}$:

$$(M_{11} - \lambda)\, c_1 + M_{12} c_2 = 0,$$
$$M_{21} c_1 + (M_{22} - \lambda)\, c_2 = 0.$$

These equations are consistent if

$$\begin{vmatrix} M_{11} - \lambda & M_{12} \\ M_{21} & M_{22} - \lambda \end{vmatrix} = 0 \tag{5.6.2}$$

giving us a quadratic characteristic equation:

$$\lambda^2 - \lambda\,(M_{11} + M_{22}) + (M_{11}M_{22} - M_{12}M_{21}) = 0. \tag{5.6.3}$$

Its solution, [30]

$$\lambda_\pm = \frac{1}{2}(M_{11} + M_{22}) \pm \frac{1}{2}\left[(M_{11} - M_{22})^2 + 4M_{12}M_{21}\right]^{1/2}, \tag{5.6.4}$$

shows that the following situations are possible:

A. The expression under the square root, $(M_{11} - M_{22})^2 + 4M_{12}M_{21}$, is positive. In this case, both characteristic exponents $\lambda_\pm$ are real, and we can distinguish three sub-cases:

(i) Both λ_+ and λ_- are negative. As Eqs. (88) show, in this case the deviations $\tilde{q}$ tend to zero at $t \to \infty$, i.e. fixed point is stable. Because of generally different magnitudes of the exponents $\lambda_\pm$, the process represented on the phase plane $[\tilde{q}_1, \tilde{q}_2]$ (see Figure 8a, with the solid arrows, for an example) may be seen as consisting of two stages: first, a faster (with the rate $|\lambda_-| > |\lambda_+|$) relaxation to a linear asymptote, [31] and then a slower decline, with the rate $|\lambda_+|$, along this line, i.e. at a virtually fixed ratio of the variables. Such a fixed point is called the stable node.

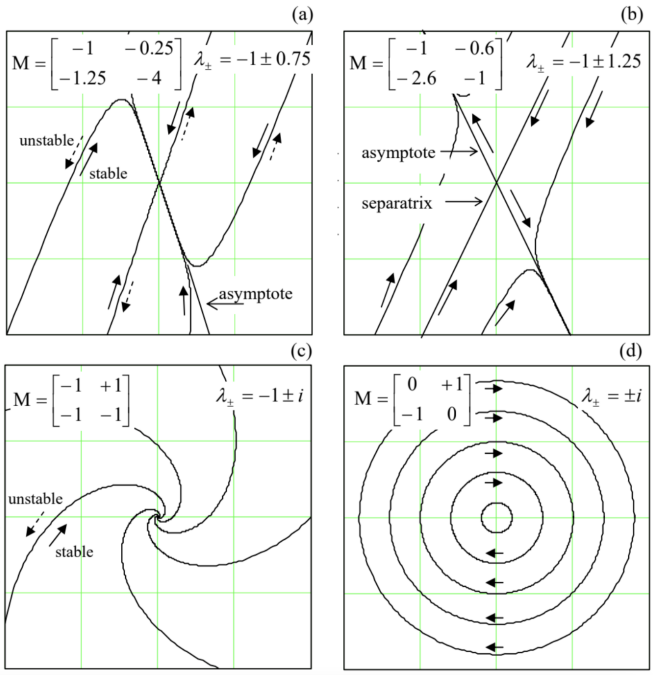

Figure 5.8. Typical trajectories on the phase plane $[\tilde{q}_1, \tilde{q}_2]$ near fixed points of different types: (a) node, (b) saddle, (c) focus, and (d) center. The particular elements of the matrix M, used in the first three panels, correspond to Eqs. (81) for the parametric excitation, with $\xi = \delta$ and three different values of the ratio $\mu\omega/4\delta$: (a) 1.25, (b) 1.6, and (c) 0 .

(ii) Both $\lambda_+$and $\lambda_{\text{are positive. This case of an unstable node differs from the previous}}$ one only by the direction of motion along the phase plane trajectories - see the dashed arrows in Figure 8a. Here the variable ratio is also approaching a constant soon, now the one corresponding to $\lambda_+ > \lambda$.

(iii) Finally, in the case of a saddle $(\lambda_+ > 0, \lambda_- < 0)$, the system's dynamics is different (Figure 8b): after the rate- $\lambda_-|$relaxation to an asymptote, the perturbation starts to grow, with the rate λ_+, along one of two opposite directions. (The direction is determined on which side of another straight line, called the separatrix, the system has been initially.) So the saddle [32] is an unstable fixed point.

B. The expression under the square root in Eq. (92), $(M_{11} - M_{22})^2 + 4M_{12}M_{21}$, is negative. In this case, the square root is imaginary, making the real parts of both roots equal, $\mathrm{Re}\,\lambda_\pm = (M_{11} + M_{22})/2$, and their imaginary parts equal but opposite. As a result, here there can be just two types of fixed points:

(i) Stable focus, at $(M_{11} + M_{22}) < 0$. The phase plane trajectories are spirals going to the origin (i.e. toward the fixed point) - see Figure 8c with the solid arrow.

(ii) Unstable focus, taking place at $(M_{11} + M_{22}) > 0$, differs from the stable one only by the direction of motion along the phase trajectories - see the dashed arrow in the same Figure 8c.

C. Frequently, the border case, $M_{11} + M_{22} = 0$, corresponding to the orbital ("indifferent") stability already discussed in Sec. 3.2, is also distinguished, and the corresponding fixed point is referred to as the center (Figure 8d). Considering centers as a separate category makes sense because such fixed points are typical for Hamiltonian systems, whose first integral of motion may be frequently represented as the distance of the phase point from a fixed point. For example, introducing new variables $\tilde{q}_1 \equiv \tilde{q}, \tilde{q}_2 \equiv m\dot{\tilde{q}}_1$, we may rewrite Eq. (3.12) of a harmonic oscillator without dissipation (again, with indices "ef" dropped for brevity), as a system of two first-order differential equations:

$$\dot{\tilde{q}}_1 = \frac{1}{m}\tilde{q}_2, \quad \dot{\tilde{q}}_2 = -\kappa\tilde{q}_1, \tag{5.6.5}$$

i.e. as a particular case of Eq. (87), with $M_{11} = M_{22} = 0$, and $M_{12}M_{21} = -\kappa/m \equiv -\omega_0^2 < 0$, and hence $(M_{11} - M_{22})^2 + 4M_{12}M_{21} = -4\omega_0^2 < 0$, and $M_{11} + M_{22} = 0$. On the symmetrized phase plane $[\tilde{q}_1, \tilde{q}_2/Z]$, where the parameter $Z \equiv (\kappa m)^{1/2} \equiv m\omega_0$ is the oscillator's impedance, the sinusoidal oscillations of amplitude A are represented by a circle of radius A about the center-type fixed point $A = 0$. In the case when $\tilde{q}_1 \equiv \tilde{q}$ is the linear coordinate q of an actual mechanical oscillator, so

that $\tilde{q}_2 \equiv m\dot{\tilde{q}}_1$ is its linear momentum $p = m\dot{q}$, such a circular trajectory corresponds to the conservation of the oscillator's energy

$$E \equiv T + U \equiv \frac{p^2}{2m} + \frac{\kappa q^2}{2} \equiv \frac{\kappa}{2}\left[\tilde{q}_1^2 + \left(\frac{\tilde{q}_2}{Z}\right)^2\right] = \frac{\kappa A^2}{2} = \text{const} \tag{5.6.6}$$

This is a convenient moment for a brief discussion of the so-called Poincaré (or "slow-variable", or "stroboscopic") plane. [33] From the point of view of the basic Eq. (41), the sinusoidal oscillations $q(t) = A\cos(\omega t - \varphi)$, described by a circular trajectory on the actual (symmetrized) phase plane, correspond to a fixed point $\{A, \varphi\}$, which may be conveniently represented by a stationary geometric point on the plane with these polar coordinates - see Figure 9a. (As follows from Eq. (4), the Cartesian coordinates of the point on that plane are just the variables $u \equiv A\cos\varphi$ and $v \equiv A\cos\varphi$ that were used, in particular, in the last section.) The quasi-sinusoidal process (41), with slowly changing A and φ, may be represented by a slow motion of that point on this Poincaré plane.

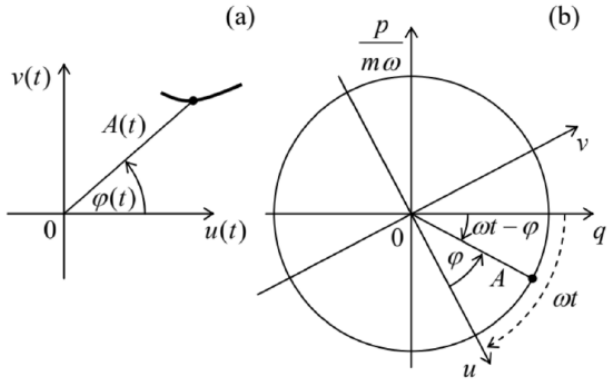

Figure 5.9. (a) Representation of a sinusoidal oscillation (point) and a slow transient process (line) on the Poincaré plane, and (b) the relation between the "fast" phase plane and the "slow" (Poincaré) plane.

Figure 9 b shows a convenient way to visualize the relation between the actual phase plane of an oscillator, with the "fast" symmetrized coordinates q and $p/m\omega$, and the Poincaré plane with the "slow" coordinates u and v : the latter plane rotates relative to the former one, about the origin, clockwise, with the angular velocity ω. [34] Another, "stroboscopic" way to generate the Poincare plane pattern is to have a fast glance at the "real" phase plane just once during the oscillation period $T = 2\pi/\omega$.

In many cases, the representation on the Poincaré plane is more convenient than that on the "real" phase plane. In particular, we have already seen that the reduced equations for such important phenomena as the phase locking and the parametric oscillations, whose original differential equations include time explicitly, are time-independent - cf., e.g., (75) and (79) describing the latter effect. This simplification brings the equations into the category considered earlier in this section, and enables an easy classification of their fixed points, which may shed additional light on their dynamic properties.

In particular, Figure 10 shows the classification of the only (trivial) fixed point $A_1 = 0$ on the Poincaré plane of the parametric oscillator, which follows from Eq. (83). As the parameter modulation depth μ is increased, the type of this fixed point changes from a stable focus (pertinent to a simple oscillator with damping) to a stable node and then to a saddle describing the parametric excitation. In the last case, the two directions of the perturbation growth, so prominently featured in Figure 8 b, correspond to the two possible values of the oscillation phase φ, with the phase choice determined by initial conditions.

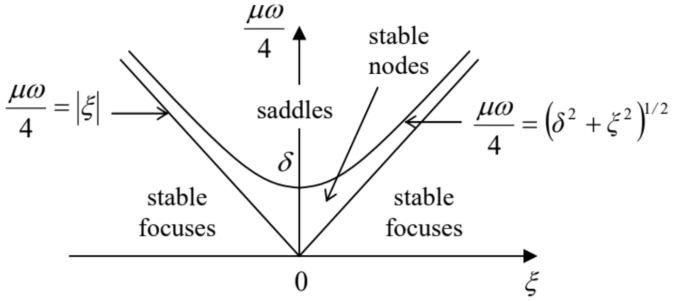

Fig. 5.10. Types of the trivial fixed point of a parametric oscillator.

This double degeneracy of the parametric oscillation's phase could already be noticed from Eqs. (77), because they are evidently invariant with respect to the replacement $\varphi \to \varphi + \pi$. Moreover, the degeneracy is not an artifact of the van der Pol approximation, because the initial equation (75) is already invariant with respect to the corresponding replacement $q(t) \to q(t - \pi/\omega)$. This invariance means that all other characteristics (including the amplitude) of the parametric oscillations excited with either of the two phases are exactly similar. At the dawn of the computer age (in the late 1950s and early 1960 s), there were substantial attempts, especially in Japan, to use this property for storage and processing digital information coded in the phase-binary form. Though these attempts have not survived the competition with simpler approaches based on voltage-binary coding, some current trends in the development of prospective reversible and quantum computers may be traced back to that idea.

---

[29] Autonomous systems described by a single, second-order homogeneous differential equation, say $F(q, \dot{q}, \ddot{q}) = 0$, also belong to this class, because we may always treat the generalized velocity $\dot{q} \equiv v$ as a new variable, and use this definition as one first-order differential equation, while the initial equation, in the form $F(q, v, \dot{v}) = 0$, as the second first-order equation.

[30] In the language of linear algebra, $\lambda_{\pm}$are the eigenvalues, and the corresponding sets of the distribution coefficients $[c_1, c_2]_{\pm}$are the eigenvectors of the matrix M with elements M_{jj} '.

[31] The asymptote direction may be found by plugging the value λ_{+}back into Eq. (89) and finding the corresponding ratio c_1/c_2. Note that the separation of the system's evolution into the two stages is conditional, being most vivid in the case of a large difference between the exponents $\lambda_{+}$and λ.

[32] The term "saddle" is due to the fact that in this case, the system's dynamics is qualitatively similar to that of a heavily damped motion in a 2D potential $U(\tilde{q}_1, \tilde{q}_2)$ having the shape of a horse saddle (or a mountain pass).

[33] Named after Jules Henri Poincaré $(1854 - 1912)$, who is credited, among many other achievements in physics and mathematics, for his contributions to special relativity (see, e.g., EM Chapter 9), and the basic idea of unstable trajectories responsible for the deterministic chaos - to be discussed in Chapter 9 of this course.

[34] This notion of phase plane rotation is the origin of the term "Rotating Wave Approximation", mentioned above. (The word "wave" is an artifact of this method's wide application in classical and quantum optics.)

5.7: Numerical Approaches

If the amplitude of oscillations, for whatever reason, becomes so large that nonlinear terms in the equation describing an oscillator become comparable with its linear terms, numerical methods are virtually the only avenue available for their theoretical studies. In Hamiltonian 1D systems, such methods may be applied directly to Eq. (3.26), but dissipative and/or parametric systems typically lack such first integrals of motion, so that the initial differential equation has to be solved.

Let us discuss the general idea of such methods on the example of what mathematicians call the Cauchy problem (finding the solution for all moments of time, starting from the known initial conditions) for the first-order differential equation

$$\dot{q} = f(t, q). \tag{5.7.1}$$

(The generalization to a system of several such equations is straightforward.) Breaking the time axis into small, equal steps h (Figure 11) we can reduce the equation integration problem to finding the function's value at the next time point, $q_{n+1} \equiv q(t_{n+1}) \equiv q(t_n + h)$ from the previously found value $q_n = q(t_n) -$ and, if necessary, the values of q at other previous time steps.

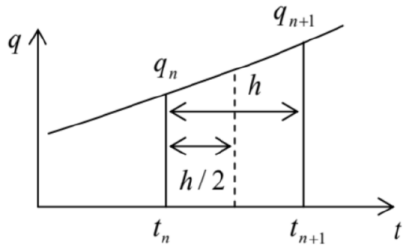

Figure 5.11. The basic notions used at numerical integration of ordinary differential equations.

In the simplest approach (called the Euler method), q_{n+1} is found using the following formula:

$$q_{n+1} = q_n + k,$$
$$k \equiv h f(t_n, q_n).$$

This approximation is equivalent to the replacement of the genuine function $q(t)$, on the segment $[t_n, t_{n+1}]$, with the two first terms of its Taylor expansion in point t_n :

$$q(t_n + h) \approx q(t_n) + \dot{q}(t_n) h \equiv q(t_n) + h f(t_n, q_n). \tag{5.7.2}$$

This approximation has an error proportional to h^2. One could argue that making the step h sufficiently small, the Euler method's error might be made arbitrarily small, but even with all the number-crunching power of modern computer platforms, the CPU time necessary to reach sufficient accuracy may be too large for large problems. [35] Besides that, the increase of the number of time steps, which is necessary at $h \to 0$ at a fixed total time interval, increases the total rounding errors and eventually may cause an increase, rather than the reduction of the overall error of the computed result.

A more efficient way is to modify Eq. (96) to include the terms of the second order in h. There are several ways to do this, for example using the 2^{nd} -order Runge-Kutta method:

$$q_{n+1} = q_n + k_2,$$
$$k_2 \equiv h f\left(t_n + \frac{h}{2}, q_n + \frac{k_1}{2}\right), \quad k_1 \equiv h f(t_n, q_n).$$

One can readily check that this method gives the exact result if the function $q(t)$ is a quadratic polynomial, and hence in the general case its errors are of the order of h^3. We see that the main idea here is to first break the segment $[t_n, t_{n+1}]$ in half (see Figure 11), evaluate the right-hand side of the differential equation (95) at the point intermediate (in both t and q) between the points number n and $(n+1)$, and then use this information to predict q_{n+1}.

The advantage of the Runge-Kutta approach over other second-order methods is that it may be readily extended to the 4^{th} order, without an additional breakup of the interval $[t_n, t_{n+1}]$. :

$$q_{n+1} = q_n + \frac{1}{6}(k_1 + 2k_2 + 2k_3 + k_4),$$
$$k_4 \equiv hf(t_n + h, q_n + k_3), k_3 \equiv hf\left(t_n + \frac{h}{2}, q_n + \frac{k_2}{2}\right), k_2 \equiv hf\left(t_n + \frac{h}{2}, q_n + \frac{k_1}{2}\right), k_1 \equiv hf(t_n, q_n).$$

This method has a much lower error, $O\left(h^5\right)$, without being not too cumbersome. These features have made the 4^{th} -order Runge-Kutta the default method in most numerical libraries. Its extension to higher orders is possible, but requires more complex formulas, and is justified only for some special cases, e.g., very abrupt functions $q(t)$. [36] The most frequent enhancement of the method is an automatic adjustment of the step h to reach the pre-specified accuracy, but not make more calculations than necessary.

Figure 12 shows a typical example of an application of that method to the very simple problem of a damped linear oscillator, for two values of fixed time step h (expressed in terms of the number N of such steps per oscillation period). The black straight lines connect the adjacent points obtained by the 4^{th} -order Runge-Kutta method, while the points connected with the green straight lines represent the exact analytical solution (22). The plots show that a-few-percent errors start to appear only at as few as ~ 10 time steps per period, so that the method is indeed very efficient.

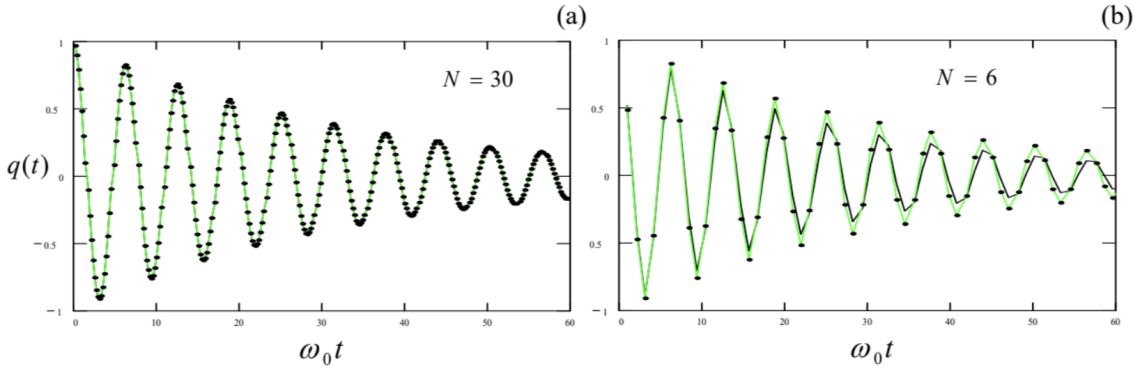

Figure 5.12. Results of the Runge-Kutta solution of Eq. (6) (with $\delta/\omega_0 = 0.03$) for: (a) 30 and (b) 6 points per oscillation period. The results are shown by points; the black and green lines are only the guides for the eye.

Let me hope that the discussion in the next section will make the conveniences and the handicaps of the numerical approach to problems of nonlinear dynamics very clear.

---

[35] In addition, the Euler method is not time-reversible - the handicap that may be essential for the integration of Hamiltonian systems described by systems of second-order differential equations. However, this drawback may be partly overcome by the so-called leapfrogging - the overlap of time steps h for a generalized coordinate and the corresponding generalized velocity.

[36] The most popular approaches in such cases are the Richardson extrapolation, the Bulirsch-Stoer algorithm, and a set of so-called prediction-correction techniques, e.g. the Adams-Bashforth-Moulton method - see the literature recommended in MA Sec. 16(iii).

5.8: Harmonic and Subharmonic Oscillations

Figure 13 shows the numerically calculated [37] transient process and stationary oscillations in a linear oscillator and a very representative nonlinear system, the pendulum described by Eq. (42), both with the same ω_0. Both systems are driven by a sinusoidal external force of the same amplitude and frequency - in this illustration, equal to the small-oscillation own frequency ω_0 of both systems. The plots show that despite a very substantial amplitude of the pendulum oscillations (the angle amplitude of about one radian), their waveform remains almost exactly sinusoidal. [38] On the other hand, the nonlinearity affects the oscillation amplitude very substantially. These results imply that the corresponding reduced equations (60), which are based on the assumption (41), may work very well far beyond its formal restriction $|q| << 1$.

Still, the waveform of oscillations in a nonlinear system always differs from that of the applied force – in our case, from the sine function of frequency ω. This fact is frequently formulated as the generation, by the system, of higher harmonics. Indeed, the Fourier theorem tells us that any nonsinusoidal periodic function of time may be represented as a sum of its basic harmonic of frequency ω and higher harmonics with frequencies $n\omega$, with integer $n > 1$.

Note that an effective generation of higher harmonics is only possible with adequate nonlinearity of the system. For example, consider the nonlinear term αq^3 used in the equations explored in Secs. 2 and 3. If the waveform $q(t)$ is sinusoidal, such term will have only the basic (1^{st}) and the 3^{rd} harmonics see, e.g., Eq. (50). As another example, the "pendulum nonlinearity" $\sin q$ cannot produce, without a time-independent component ("bias") in $q(t)$, any even harmonic, including the 2^{nd} one. The most efficient generation of harmonics may be achieved using systems with the sharpest nonlinearities - e.g., semiconductor diodes whose current may follow an exponential dependence on the applied voltage through several orders of magnitude. [39]

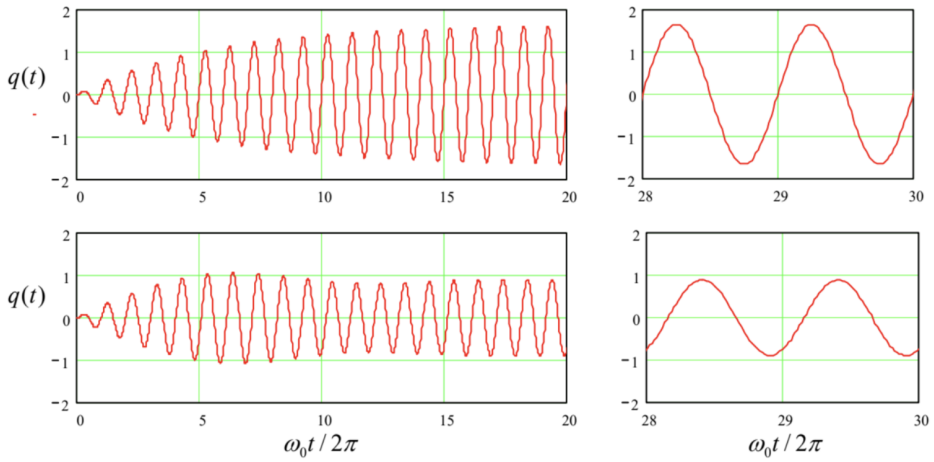

Figure 5.13. The oscillations induced by a similar sinusoidal external force (turned on at $t = 0$) in two systems with the same small-oscillation frequency ω_0 and low damping: a linear oscillator (two top panels) and a pendulum (two bottom panels). In all cases, $\delta/\omega_0 = 0.03$, $f_0 = 0.1$, and $\omega = \omega_0$.

Another way to increase the contents of an n^{th} higher harmonic in a nonlinear oscillator is to reduce the excitation frequency ω to $\sim \omega_0/n$, so that the oscillator resonated at the frequency $n\omega \approx \omega_0$ of the desired harmonic. For example, Figure 14a shows the oscillations in a pendulum described by the same Eq. (42), but driven at frequency $\omega = \omega_0/3$. One can see that the 3^{rd} harmonic amplitude may be comparable with that of the basic harmonic, especially if the external frequency is additionally lowered (Figure 14b) to accommodate for the deviation of the effective frequency $\omega_0(A)$ of own oscillations from its small-oscillation value ω_0 – see Eq. (49), Figure 4, and their discussion in Sec. 2 above.

However, numerical modeling of nonlinear oscillators, as well as experiments with their physical implementations, bring more surprises. For example, the bottom panel of Figure 15 shows oscillations in a pendulum under the effect of a strong sinusoidal force with a frequency ω close to $3\omega_0$. One can see that at some parameter values and initial conditions, the system's oscillation spectrum is heavily contributed (almost dominated) by the 3^{rd} subharmonic, i.e. the Fourier component of frequency $\omega/3 \approx \omega_0$.

This counter-intuitive phenomenon of such subharmonic generation may be explained as follows. Let us assume that subharmonic oscillations of frequency $\omega/3 \approx \omega_0$ have somehow appeared, and coexist with the forced oscillations of frequency 3ω:

$$q(t) \approx A\cos\Psi + A_{\rm sub}\,\cos\Psi_{\rm sub}\,, \qquad \text{where } \Psi \equiv \omega t - \varphi, \quad \Psi_{\rm sub} \equiv \frac{\omega t}{3} - \varphi_{\rm sub}\,. \tag{5.8.1}$$

Then the leading nonlinear term, αq^3, of the Taylor expansion of the pendulum's nonlinearity $\sin q$, is proportional to

$$\begin{aligned} q^3 &= (A\cos\Psi + A_{\rm sub}\,\cos\Psi_{\rm sub}\,)^3 \\ &\equiv A^3\cos^3\Psi + 3A^2A_{\rm sub}\,\cos^2\Psi\cos\Psi_{\rm sub} + 3AA_{\rm sub}^2\,\cos\Psi\cos^2\Psi_{\rm sub} + A_{\rm sub}^3\,\cos^3\Psi_{\rm sub} \end{aligned}$$

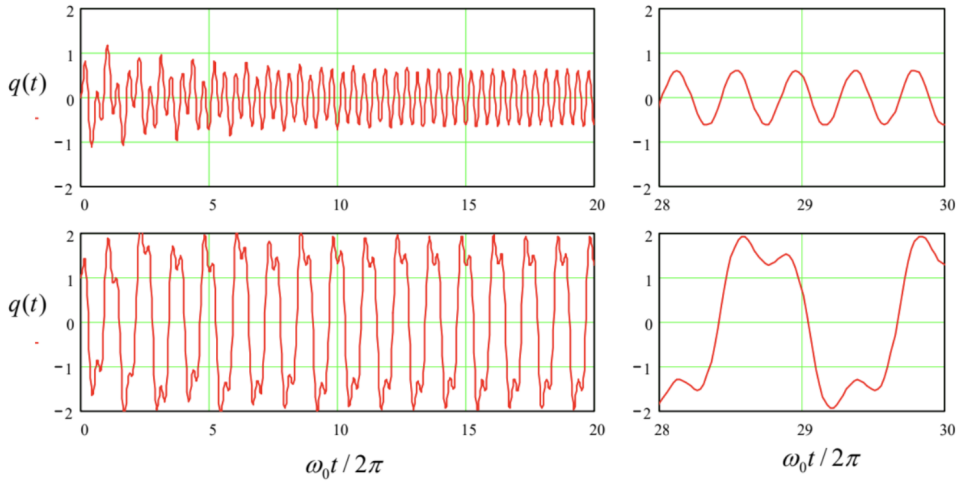

Figure 5.14. The oscillations induced in a pendulum, with damping $\delta/\omega_0 = 0.03$, by a sinusoidal external force of amplitude $f_0 = 0.75$, and frequencies $\omega_0/3$ (top panel) and $0.8 \times \omega_0/3$ (bottom panel).

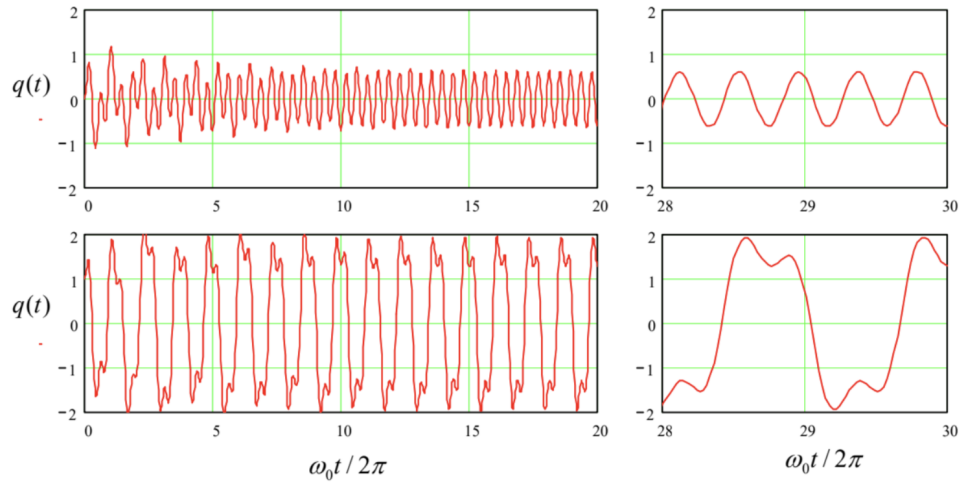

Fig. 5.15. The oscillations of a pendulum with $\delta/\omega_0 = 0.03$, driven by a sinusoidal external force of amplitude $f_0 = 3$ and frequency $0.8 \times 3\omega_0$, at initial conditions $q(0) = 0$ (the top row) and $q(0) = 1$ (the bottom row), with $dq/dt(0) = 0$ in both cases.

While the first and the last terms of the last expression depend only of the amplitudes of the individual components of oscillations, the two middle terms are more interesting, because they produce so-called combinational frequencies of the two components. For our case, the third term,

$$3AA_{\rm sub}^2\,\cos\Psi\cos^2\Psi_{\rm sub} = \frac{3}{4}AA_{\rm sub}^2\,\cos(\Psi - 2\Psi_{\rm sub}\,) + \ldots, \tag{5.8.2}$$

is of special importance, because it produces, besides other combinational frequencies, the subharmonic component with the total phase

$$\Psi - 2\Psi_{\rm sub} = \frac{\omega t}{3} - \varphi + 2\varphi_{\rm sub} \tag{5.8.3}$$

Thus, within a certain range of the mutual phase shift between the Fourier components, this nonlinear contribution is synchronous with the subharmonic oscillations, and describes the interaction that can deliver to it the energy from the external force, so that the oscillations may be sustained. Note, however, that the amplitude of the term describing this energy exchange is proportional to the square of $A_{\rm sub}$, and vanishes at the linearization of the equations of motion near the trivial fixed point. This means that the point is always stable, i.e., the $3^{\rm rd}$ subharmonic cannot be self-excited and always needs an initial "kickoff" - compare the two panels of Figure 15. The same is true for higher-order subharmonics.

Only the second subharmonic is a special case. Indeed, let us make a calculation similar to Eq. (102), by replacing Eq. (101) with

$$q(t) \approx A\cos\Psi + A_{\rm sub}\,\cos\Psi_{\rm sub}\,, \qquad \text{where } \Psi \equiv \omega t - \varphi, \quad \Psi_{\rm sub} \equiv \frac{\omega t}{2} - \varphi_{\rm sub}\,, \tag{5.8.4}$$

for a nonlinear term proportional to q^2 :

$$q^2 = \left(A\cos\Psi + A_{\rm sub}\,\cos\Psi_{\rm sub}\right)^2 = A^2\cos^2\Psi + 2AA_{\rm sub}\,\cos\Psi\cos\Psi_{\rm sub} + A_{\rm sub}^2\,\cos^2\Psi_{\rm sub}\,. \tag{5.8.5}$$

Here the combinational-frequency term capable of supporting the $2^{\rm nd}$ subharmonic,

$$2AA_{\rm sub}\,\cos\Psi\cos\Psi_{\rm sub} = AA_{\rm sub}\,\cos(\Psi - \Psi_{\rm sub}) = AA_{\rm sub}\,\cos(\omega t - \varphi + \varphi_{\rm sub}) + \ldots, \tag{5.8.6}$$

is linear in the subharmonic's amplitude, i.e. survives the linearization near the trivial fixed point. This means that the second subharmonic may arise spontaneously, from infinitesimal fluctuations.

Moreover, such excitation of the second subharmonic is very similar to the parametric excitation that was discussed in detail in Sec. 5, and this similarity is not coincidental. Indeed, let us redo the expansion (106) making a somewhat different assumption - that the oscillations are a sum of the forced oscillations at the external force's frequency ω and an arbitrary but weak perturbation:

$$q(t) = A\cos(\omega t - \varphi) + \tilde{q}(t), \qquad \text{with } |\tilde{q}| << A. \tag{5.8.7}$$

Then, neglecting the small term proportional to $\tilde{q}^2$, we get

$$q^2 \approx A^2\cos^2(\omega t - \varphi) + 2\tilde{q}(t)A\cos(\omega t - \varphi). \tag{5.8.8}$$

Besides the inconsequential phase φ, the second term in the last formula is exactly similar to the term describing the parametric effects in Eq. (75). This fact means that for a weak perturbation, a system with a quadratic nonlinearity in the presence of a strong "pumping" signal of frequency ω is equivalent to a system with parameters changing in time with frequency ω. This fact is broadly used for the parametric excitation at high (e.g., optical) frequencies, where the mechanical means of parameter modulation (see, e.g., Figure 5) are not practicable. The necessary quadratic nonlinearity at optical frequencies may be provided by a non-centrosymmetric nonlinear crystal, e.g., the β-phase barium borate ($\mathrm{BaB_2O_4}$).

Before finishing this chapter, let me elaborate a bit on a general topic: the relation between the numerical and analytical approaches to problems of dynamics - and physics as a whole. We have just seen that sometimes numerical solutions, like those shown in Figure 15b, may give vital clues for previously unanticipated phenomena such as the excitation of subharmonics. (The phenomenon of deterministic chaos, which will be discussed in Chapter 9 below, presents another example of such "numerical discoveries".) One might also argue that in the absence of exact analytical solutions, numerical simulations may be the main theoretical tool for the study of such phenomena. These hopes are, however, muted by the general problem that is frequently called the curse of dimensionality [40] in which the last word refers to the number of parameters of the problem to be solved. [41]

Indeed, let us have another look at Figure 15. OK, we have been lucky to find a new phenomenon, the $3^{\rm rd}$ subharmonic generation, for a particular set of parameters – in that case, five of them: $\delta/\omega_0 = 0.03, \omega/\omega_0 = 2.4, f_0 = 3, q(0) = 1$, and $dq/dt(0) = 0$. Could we tell anything about how common this effect is? Are subharmonics with different n possible in this system? The only way to address these questions computationally is to carry out similar numerical simulations in many points of the d dimensional (in this case, $d = 5$) space of parameters. Say, we have decided that breaking the reasonable range of each parameter to $N = 100$ points is sufficient. (For many problems, even more points are necessary - see, e.g., Sec. 9.1.) Then the total number of numerical experiments to carry out is $N^d = \left(10^2\right)^5 = 10^{10}$ - not a simple task even for the powerful modern computing facilities. (Besides the pure number of required CPU cycles, consider the storage and analysis of the results.) For many important problems of nonlinear dynamics, e.g., turbulence, the parameter dimensionality d is substantially larger, and the computer resources necessary even for one numerical experiment, are much greater.

In the view of the curse of dimensionality, approximate analytical considerations, like those outlined above for the subharmonic excitation, are invaluable. More generally, physics used to stand on two legs: experiment and analytical theory. The enormous progress of computer performance during a few last decades has provided it with one more point of support (a tail? :-) - numerical simulation. This does not mean we can afford to discard any of the legs we are standing on.

---

[37] All numerical results shown in this section have been obtained by the 4^{th}-order Runge-Kutta method with the automatic step adjustment that guarantees the relative error of the order of 10^{-4} – much smaller than the pixel size in the shown plots.

[38] In this particular case, the higher harmonic content is about 0.5%, dominated by the 3^{rd} harmonic, whose amplitude and phase are in a very good agreement with Eq. (50).

[39] This method is used in practice, for example, for the generation of electromagnetic waves with frequencies in the terahertz range $\left(10^{12} - 10^{13}\text{ Hz}\right)$, which still lacks efficient electronic self-oscillators that could be used as practical generators.

[40] This term had been coined in 1957 by Richard Bellman in the context of the optimal control theory (where the dimensionality means the number of parameters affecting the system under control), but gradually has spread all over quantitative sciences using numerical methods.

[41] In EM Sec. 1.2, I discuss implications of the curse implications for a different case, when both analytical and numerical solutions to the same problem are possible.

5.9: Exercise Problems

5.1. For a system with the response function given by Eq. (17), prove Eq. (26) and use an approach different from the one used in Sec. 1, to derive Eq. (34).

Hint: You may like to use the Cauchy integral theorem and the Cauchy integral formula for analytical functions of a complex variable [42]

5.2. A square-wave pulse of force (see the figure on the right) is exerted on a linear oscillator with eigenfrequency ω_0 (with no damping), initially at rest. Calculate the law of motion $q(t)$, sketch it, and interpret the result.

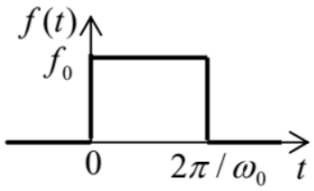

5.3. At $t = 0$, a sinusoidal external force $F(t) = F_0 \cos \omega t$, is exerted on a linear oscillator with eigenfrequency ω_0 and damping δ, which was at rest at $t \leq 0$.

(i) Derive the general expression for the time evolution of the oscillator's coordinate, and interpret the result.

(ii) Spell out the result for the exact resonance $(\omega = \omega_0)$ in a system with low damping $(\delta << \omega_0)$, and, in particular, explore the limit $\delta \to 0$.

5.4. A pulse of external force $F(t)$, with a finite duration τ, is exerted on a linear oscillator, initially at rest in its equilibrium position. Neglecting dissipation, calculate the change of oscillator's energy, using two different approaches, and compare the results.

5.5. For a system with the following Lagrangian function:

$$L = \frac{m}{2}\dot{q}^2 - \frac{\kappa}{2}q^2 + \frac{\varepsilon}{2}\dot{q}^2 q^2, \tag{5.9.1}$$

calculate the frequency of free oscillations as a function of their amplitude A, at $A \to 0$, using two different approaches.

5.6. For a system with the Lagrangian function

$$L = \frac{m}{2}\dot{q}^2 - \frac{\kappa}{2}q^2 + \varepsilon\dot{q}^4, \tag{5.9.2}$$

with small parameter ε, use the van der Pol method to find the frequency of free oscillations as a function of their amplitude.

5.7. On the plane $[a_1, a_2]$ of two real, time-independent parameters a_1 and a_2, find the regions in which the fixed point of the following system of equations,

$$\dot{q}_1 = a_1 (q_2 - q_1),$$
$$\dot{q}_2 = a_2 q_1 - q_2,$$

is unstable, and sketch the regions of each fixed point type − stable and unstable nodes, focuses, etc.

5.8. Solve Problem 3(ii) using the reduced equations (57), and compare the result with the exact solution.

5.9. Use the reduced equations to analyze forced oscillations in an oscillator with weak nonlinear damping, described by the following equation:

$$\ddot{q} + 2\delta\dot{q} + \omega_0^2 q + \beta\dot{q}^3 = f_0 \cos \omega t, \tag{5.9.3}$$

with $\omega \approx \omega_0$; $\beta, \delta > 0$; and $\beta\omega A^2 << 1$. In particular, find the stationary amplitude of the forced oscillations and analyze their stability. Discuss the effect(s) of the nonlinear term on the resonance.

5.10. Within the approach discussed in Sec. 4, calculate the average frequency of a self-oscillator outside of the range of its phase-locking by an external sinusoidal force.

5.11.* Use the reduced equations to analyze the stability of the forced nonlinear oscillations described by the Duffing equation (43). Relate the result to the slope of resonance curves (Figure 4).

5.12. Use the van der Pol method to find the condition of parametric excitation of the oscillator described by the following equation:

$$\ddot{q} + 2\delta\dot{q} + \omega_0^2(t)q = 0, \tag{5.9.4}$$

where $\omega_0^2(t)$ is the square-wave function shown in the figure on the right, with $\omega \approx \omega_0$.

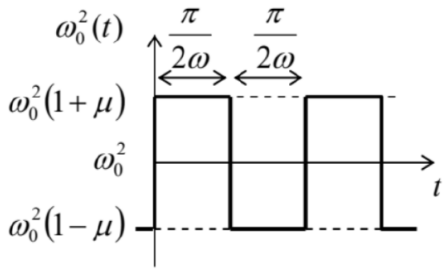

5.13. Use the van der Pol method to analyze parametric excitation of an oscillator with weak nonlinear damping, described by the following equation:

$$\ddot{q} + 2\delta\ddot{q} + \beta\dot{q}^3 + {\omega_0}^2(1 + \mu\cos 2\omega t)q = 0, \tag{5.9.5}$$

with $\omega \approx \omega_0; \beta, \delta > 0;$ and $\mu, \beta\omega A^2 << 1$. In particular, find the amplitude of stationary oscillations and analyze their stability.

5.14. * Adding nonlinear term αq^3 to the left-hand side of Eq. (75),

(i) find the corresponding addition to the reduced equations,

(ii) calculate the stationary amplitude A of the parametric oscillations,

(iii) find the type and stability of each fixed point of the reduced equations,

(iv) sketch the Poincare phase planes of the system in major parameter regions.

5.15. Use the van der Pol method to find the condition of parametric excitation of an oscillator with weak modulation of both the effective mass $m(t) = m_0\,(1 + \mu_m \cos 2\omega t)$ and the effective spring constant $\kappa(t) = \kappa_0\,[1 + \mu_\kappa \cos(2\omega t - \psi)]$, with the same frequency $2\omega \approx 2\omega_0$, at arbitrary modulation depths ratio μ_m/μ_k and phase shift ψ. Interpret the result in terms of modulation of the instantaneous frequency $\omega(t) \equiv [\kappa(t)/m(t)]^{1/2}$ and the mechanical impedance $Z(t) \equiv [\kappa(t)m(t)]^{1/2}$ of the oscillator.

5.16. * Find the condition of parametric excitation of a nonlinear oscillator described by the following equation:

$$\ddot{q} + 2\delta\dot{q} + \omega_0^2 q + \gamma q^2 = f_0 \cos 2\omega t, \tag{5.9.6}$$

with sufficiently small δ, γ, f_0, and $\xi \equiv \omega - \omega_0$.

5.17. Find the condition of stability of the equilibrium point $q = 0$ of a parametric oscillator described by Eq. (75), in the limit when $\delta << |\omega_0| << \omega$ and $\mu << 1$. Use the result to analyze stability of the Kapitza pendulum mentioned in Sec. 5.

---

[42] See, e.g., MA Eq. (15.1).

CHAPTER OVERVIEW

6: From Oscillations to Waves

In this chapter, the discussion of oscillations is extended to systems with two and more degrees of freedom. This extension naturally leads to another key notion of physics - the waves, in particular those in uniform $1D$ systems. (A more general discussion of elastic waves in continua is deferred until the next chapter.) However, even the limited scope of the models analyzed in this chapter will still enable us to discuss such important general aspects of waves as their dispersion, phase and group velocities, impedance, reflection, and attenuation.

6.1: Two Coupled Oscillators

Let us discuss oscillations in systems with several degrees of freedom, starting from the simplest case of two linear (harmonic), dissipation-free, 1D oscillators. If the oscillators are independent of each other, the Lagrangian function of their system may be represented as a sum of two independent terms of the type (5.1):

$$L = L_1 + L_2, \quad L_{1,2} = T_{1,2} - U_{1,2} = \frac{m_{1,2}}{2}\dot{q}_{1,2}^2 - \frac{\kappa_{1,2}}{2}q_{1,2}^2. \tag{6.1.1}$$

Correspondingly, Eqs. (2.19) for $q_j = q_{1,2}$ yields two independent equations of motion of the oscillators, each one being similar to Eq. (5.2):

$$m_{1,2}\ddot{q}_{1,2} + m_{1,2}\Omega_{1,2}^2 q_{1,2} = 0, \quad \text{where } \Omega_{1,2}^2 = \frac{\kappa_{1,2}}{m_{1,2}}. \tag{6.1.2}$$

(In the context of what follows, $\Omega_{1,2}$ are sometimes called the partial frequencies.) This means that in this simplest case, an arbitrary motion of the system is just a sum of independent sinusoidal oscillations at two frequencies equal to the partial frequencies (2).

However, as soon as the oscillators are coupled (i.e. interact), the full Lagrangian L contains an additional mixed term L_{int} depending on both generalized coordinates q_1 and q_2 and/or generalized velocities. As a simple example, consider the system shown in Figure 1, there two small masses $m_{1,2}$ are constrained to move in only one direction (shown horizontal), and are kept between two stiff walls with three springs.

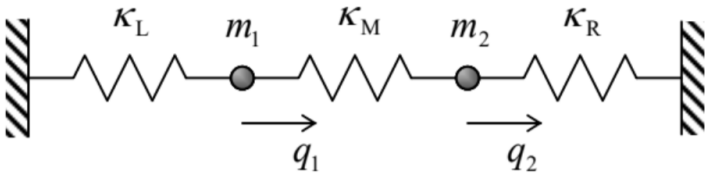

Fig. 6.1. A simple system of two coupled linear oscillators.

In this case, the kinetic energy is still separable, $T = T_1 + T_2$, but the total potential energy, consisting of the elastic energies of three springs, is not:

$$U = \frac{\kappa_{\text{L}}}{2}q_1^2 + \frac{\kappa_{\text{M}}}{2}(q_1 - q_2)^2 + \frac{\kappa_{\text{R}}}{2}q_2^2, \tag{6.1.3}$$

where $q_{1.2}$ are the horizontal displacements of the particles from their equilibrium positions. It is convenient to rewrite this expression as

$$U = \frac{\kappa_1}{2}q_1^2 + \frac{\kappa_2}{2}q_2^2 - \kappa q_1 q_2, \quad \text{where } \kappa_1 \equiv \kappa_{\text{L}} + \kappa_{\text{M}}, \quad \kappa_2 \equiv \kappa_{\text{R}} + \kappa_{\text{M}}, \quad \kappa \equiv \kappa_{\text{M}}, \tag{6.1.4}$$

showing that the Lagrangian function $L = T - U$ of this system contains, besides the partial terms (1), a bilinear interaction term:

$$L = L_1 + L_2 + L_{\text{int}}, \quad L_{\text{int}} = \kappa q_1 q_2. \tag{6.1.5}$$

The resulting Lagrange equations of motion are

$$m_1\ddot{q}_1 + m_1\Omega_1^2 q_1 = \kappa q_2,$$
$$m_2\ddot{q}_2 + m_2\Omega_2^2 q_2 = \kappa q_1.$$

Thus the interaction leads to an effective generalized force κq_2 exerted on subsystem 1 by subsystem 2 , and the reciprocal effective force κq_1.

Please note two important aspects of this (otherwise rather simple) system of equations. First, in contrast to the actual physical interaction forces (such as $F_{12} = -F_{21} = \kappa_{\text{M}}(q_2 - q_1)$ for our system [1]) the effective forces on the right-hand sides of Eqs. (5) do not obey the 3rd Newton law. Second, the forces are proportional to the same coefficient κ, this feature is a result of the general bilinear structure (4) of the interaction energy, rather than of any special symmetry.

From our prior discussions, we already know how to solve Eqs. (5), because it is still a system of linear and homogeneous differential equations, so that its general solution is a sum of particular solutions of the form similar to Eqs. (5.88),

$$q_1 = c_1 e^{\lambda t}, \quad q_2 = c_2 e^{\lambda t}, \tag{6.1.6}$$

with all possible values of λ. These values may be found by plugging Eq. (6) into Eqs. (5), and requiring the resulting system of two linear, homogeneous algebraic equations for the distribution coefficients $c_{1,2}$,

$$m_1\lambda^2 c_1 + m_1\Omega_1^2 c_1 = \kappa c_2$$
$$m_2\lambda^2 c_2 + m_2\Omega_2^2 c_2 = \kappa c_1$$

to be self-consistent. In our particular case, we get a characteristic equation,

$$\begin{vmatrix} m_1\left(\lambda^2+\Omega_1^2\right) & -\kappa \\ -\kappa & m_2\left(\lambda^2+\Omega_2^2\right) \end{vmatrix} = 0, \tag{6.1.7}$$

that is quadratic in λ^2, and thus allows a simple analytical solution:

$$\left(\lambda^2\right)_{\pm} = -\frac{1}{2}\left(\Omega_1^2+\Omega_2^2\right) \mp \left[\frac{1}{4}\left(\Omega_1^2+\Omega_2^2\right)^2 - \Omega_1^2\Omega_2^2 + \frac{\kappa^2}{m_1 m_2}\right]^{1/2} \tag{6.1.8}$$

$$\equiv -\frac{1}{2}\left(\Omega_1^2+\Omega_2^2\right) \mp \left[\frac{1}{4}\left(\Omega_1^2-\Omega_2^2\right)^2 + \frac{\kappa^2}{m_1 m_2}\right]^{1/2}. \tag{6.1.9}$$

According to Eqs. (2) and (3b), for any positive values of spring constants, the product $\Omega_1\Omega_2 = \left(\kappa_L+\kappa_M\right)\left(\kappa_R+\kappa_M\right)/\left(m_1 m_2\right)^{1/2}$ is always larger than $\kappa/\left(m_1 m_2\right)^{1/2} = \kappa_M/\left(m_1 m_2\right)^{1/2}$, so that the square root in Eq. (9) is always smaller than $\left(\Omega_1{}^2+\Omega_2{}^2\right)/2$. As a result, both values of λ^2 are negative, i.e. the general solution to Eq. (5) is a sum of four terms, each proportional to $\exp\{\pm i\omega_{\pm}t\}$, where both own frequencies ("eigenfrequencies") $\omega_{\pm} \equiv i\lambda_{\pm}$ are real:

Anticrossing description

$$\omega_{\pm}^2 \equiv -\lambda_{\pm}^2 = \frac{1}{2}\left(\Omega_1^2+\Omega_2^2\right) \pm \left[\frac{1}{4}\left(\Omega_1^2-\Omega_2^2\right)^2 + \frac{\kappa^2}{m_1 m_2}\right]^{1/2}. \tag{6.1.10}$$

A plot of these eigenfrequencies as a function of one of the partial frequencies (say, Ω_1), with the other partial frequency fixed, gives us the famous anticrossing (also called the "avoided crossing" or "non-crossing") diagram - see Figure 2. One can see that at weak coupling, frequencies $\omega_{\pm}$ are close to the partial frequencies $\Omega_{1,2}$ everywhere besides a narrow range near the anticrossing point $\Omega_1 = \Omega_2$. Most remarkably, at passing through this region, ω_+ smoothly "switches" from following Ω_2 to following Ω_1 and vice versa.

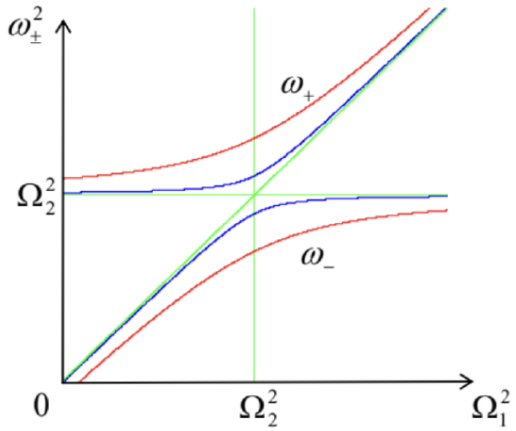

Figure 6.2. The anticrossing diagram for two values of the normalized coupling strength $\kappa/\left(m_1 m_2\right)^{1/2}\Omega_2^2$: 0.3 (red lines) and 0.1 (blue lines). In this plot, Ω_1 is assumed to be changed by varying κ_1 rather than m_1, but in the opposite case, the diagram is qualitatively similar.

The reason for this counterintuitive behavior may be found by examining the distribution coefficients $c_{1,2}$ corresponding to each branch of the diagram, which may be obtained by plugging the corresponding value of $\lambda_{\pm} = -i\omega_{\pm}$ back into Eqs. (7). For example, at the anticrossing point $\Omega_1 = \Omega_2 \equiv \Omega$, Eq. (10) is reduced to

$$\omega_{\pm}^2 = \Omega^2 \pm \frac{\kappa}{(m_1 m_2)^{1/2}} = \Omega^2 \left(1 \pm \frac{\kappa}{(\kappa_1 \kappa_2)^{1/2}} \right). \tag{6.1.11}$$

Plugging this expression back into any of Eqs. (7), we see that for the two branches of the anticrossing diagram, the distribution coefficient ratio is the same by magnitude but opposite by sign:

$$\left(\frac{c_1}{c_2} \right)_{\pm} = \mp \left(\frac{m_2}{m_1} \right)^{1/2}, \text{ at } \Omega_1 = \Omega_2. \tag{6.1.12}$$

In particular, if the system is symmetric $(m_1 = m_2, \kappa_L = \kappa_R)$, then at the upper branch, corresponding to $\omega_+ > \omega_-$, we get $c_1 = -c_2$. This means that in this so-called hard mode, [2] masses oscillate in anti-phase: $q_1(t) \equiv -q_2(t)$. The resulting substantial extension/compression of the middle spring (see Figure 1 again) yields additional returning force which increases the oscillation frequency. On the contrary, at the lower branch, corresponding to ω_-, the particle oscillations are in phase: $c_1 = c_2$, i.e. $q_1(t) \equiv q_2(t)$, so that the middle spring is neither stretched nor compressed at all. As a result, in this soft mode, the oscillation frequency ω_- is lower than ω_+, and does not depend on κ_M:

$$\omega_-^2 = \Omega^2 - \frac{\kappa}{m} = \frac{\kappa_L}{m} = \frac{\kappa_R}{m}. \tag{6.1.13}$$

Note that for both modes, the oscillations equally engage both particles.

Far from the anticrossing point, the situation is completely different. Indeed, a similar calculation of $c_{1,2}$ shows that on each branch of the diagram, the magnitude of one of the distribution coefficients is much larger than that of its counterpart. Hence, in this limit, any particular mode of oscillations involves virtually only one particle. A slow change of system parameters, bringing it through the anticrossing, results, first, in a maximal delocalization of each mode at $\Omega_1 = \Omega_2$, and then in the restoration of the localization, but in a different partial degree of freedom.

We could readily carry out similar calculations for the case when the systems are coupled via their velocities, $L_{int} = m\dot{q}_1\dot{q}_2$, where m is a coupling coefficient – not necessarily a certain physical mass. [3] The results are generally similar to those discussed above, again with the maximum level splitting at $\Omega_1 = \Omega_2 \equiv \Omega$:

$$\omega_{\pm}^2 = \frac{\Omega^2}{1 \mp |m|/(m_1 m_2)^{1/2}} \approx \Omega^2 \left[1 \pm \frac{|m|}{(m_1 m_2)^{1/2}} \right], \tag{6.1.14}$$

the last relation being valid for weak coupling. The generalization to the case of both coordinate and velocity coupling is also straightforward - see the next section.

Note that the anticrossing diagram, shown in Figure 2, is even more ubiquitous in quantum mechanics, because, due to the time-oscillatory character of the Schrödinger equation solutions, a weak coupling of any two quantum states leads to qualitatively similar behavior of the eigenfrequencies $\omega_{\pm}$of the system, and hence of its eigenenergies ("energy levels") $E_{\pm} = \hbar\omega_{\pm}$ of the system.

One more property of weakly coupled oscillators, a periodic slow transfer of energy from one oscillator to the other and back, especially well pronounced at or near the anticrossing point $\Omega_1 = \Omega_2$, is also more important for quantum than for classical mechanics. This is why I refer the reader to the QM part of this series for a detailed discussion of this phenomenon.

---

[1] Using these expressions, Eqs. (5) may be readily obtained from the Newton laws, but the Lagrangian approach used above will make their generalization, in the next section, more straightforward.

[2] In physics, the term "mode" is typically used to describe the distribution of a variable in space, at its oscillations with a single frequency. In our current case, when the notion of space is reduced to two oscillator numbers, the "mode" means just a set of two distribution coefficients $c_{1,2}$ for a particular eigenfrequency.

[3] In mechanics, with $q_{1,2}$ standing for the actual linear displacements of particles, such coupling is not very natural, but there are many dynamic systems of non-mechanical nature in which such coupling is the most natural one. The simplest example is the system of two LC ("tank") circuits, with either capacitive or inductive coupling. Indeed, as was discussed in Sec. 2.2, for such a system, the very notions of the potential and kinetic energies are conditional and interchangeable.

6.2: N Coupled Oscillators

The calculations of the previous section may be readily generalized to the case of an arbitrary number (say, N) coupled harmonic oscillators, with an arbitrary type of coupling. It is evident that in this case Eq. (4) should be replaced with

$$L=\sum_{j=1}^{N} L_j+\sum_{j,j'=1}^{N} L_{jj'} \tag{6.2.1}$$

Moreover, we can generalize the above expression for the mixed terms L_{jj}, taking into account their possible dependence not only on the generalized coordinates but also on the generalized velocities, in a bilinear form similar to Eq. (4). The resulting Lagrangian may be represented in a compact form,

$$L=\sum_{j,j'=1}^{N}\left(\frac{m_{ij'}}{2}\dot{q}_j\dot{q}_{j'}-\frac{\kappa_{ij'}}{2}q_jq_{j'}\right), \tag{6.2.2}$$

where the off-diagonal terms are index-symmetric: $m_{jj'}=m_{j'j}, \kappa_{jj'}=\kappa_{jj}$, and the factors $1/2$ compensate the double counting of each term with $j\neq j$ ', taking place at the summation over two independently running indices. One may argue that Eq. (16) is quite general if we still want to keep the equations of motion linear - as they always are if the oscillations are small enough.

Plugging Eq. (16) into the general form (2.19) of the Lagrange equation, we get N equations of motion of the system, one for each value of the index $j'=1,2,\ldots,N$:

$$\sum_{j=1}^{N}\left(m_{ijj}\ddot{q}_j+\kappa_{jj'}q_j\right)=0. \tag{6.2.3}$$

Just as in the previous section, let us look for a particular solution to this system in the form

$$q_j=c_je^{\lambda t}. \tag{6.2.4}$$

As a result, we are getting a system of N linear, homogeneous algebraic equations,

$$\sum_{j=1}^{N}\left(m_{ij'}\lambda^2+\kappa_{jj'}\right)c_j=0, \tag{6.2.5}$$

for the set of N distribution coefficients c_j. The condition that this system is self-consistent is that the determinant of its matrix equals zero:

$$\mathrm{Det}\left(m_{ij'}\lambda^2+\kappa_{ij'}\right)=0. \tag{6.2.6}$$

This characteristic equation is an algebraic equation of degree N for λ^2, and so has N roots $\left(\lambda^2\right)_n$. For any Hamiltonian system with stable equilibrium, the matrices m_{ij} ' and κ_{ij} ' ensure that all these roots are real and negative. As a result, the general solution to Eq. (17) is the sum of $2N$ terms proportional to $\exp\left\{\pm i\omega_n t\right\}, n=1,2,\ldots,N$, where all N eigenfrequencies ω_n are real.

Plugging each of these $2N$ values of $\lambda=\pm i\omega_n$ back into a particular set of linear equations (17), one can find the corresponding set of distribution coefficients $c_{j\pm}$. Generally, the coefficients are complex, but to keep $q_j(t)$ real, the coefficients c_{j+} corresponding to $\lambda=+i\omega_n$, and c_j - corresponding to $\lambda=-i\omega_n$ have to be complex-conjugate of each other. Since the sets of the distribution coefficients may be different for each λ_n, they should be marked with two indices, j and n. Thus, at general initial conditions, the time evolution of the j^{th} coordinate may be represented as

$$q_j=\frac{1}{2}\sum_{n=1}^{N}\left(c_{jn}\exp\{+i\omega_n t\}+c_{jn}^{*}\exp\{-i\omega_n t\}\right)\equiv\mathrm{Re}\sum_{n=1}^{N}c_{jn}\exp\{i\omega_n t\} \tag{6.2.7}$$

This formula shows very clearly again the physical sense of the distribution coefficients c_{jn} : a set of these coefficients, with different values of index j but the same n, gives the complex amplitudes of oscillations of the coordinates for the special initial conditions that ensure purely sinusoidal motion of all the system, with frequency ω_n.

The calculation of the eigenfrequencies and distribution coefficients of a particular coupled system with many degrees of freedom from Eqs. (19)-(20) is a task that frequently may be only done numerically. [4] Let us discuss just two particular but very important cases. First, let all the coupling coefficients be small in the following sense: $|m_{jj'}| << m_j \equiv m_{jj}$ and $|\kappa_{ij'}| << \kappa_j \equiv \kappa_{jj}$, for all $j \neq j$, and all partial frequencies $\Omega_j \equiv (\kappa_j/m_j)^{1/2}$ be not too close to each other:

$$\frac{\left|\Omega_j^2 - \Omega_{j'}^2\right|}{\Omega_j^2} >> \frac{|\kappa_{jj'}|}{\kappa_j}, \frac{|m_{jj'}|}{m_j}, \quad \text{for all } j \neq j'. \tag{6.2.8}$$

(Such situation frequently happens if parameters of the system are "random" in the sense that they do not follow any special, simple rule - for example, resulting from some simple symmetry of the system.) Results of the previous section imply that in this case, the coupling does not produce a noticeable change of oscillation frequencies: $\{\omega_n\} \approx \{\Omega_j\}$. In this situation, oscillations at each eigenfrequency are heavily concentrated in one degree of freedom, i.e. in each set of the distribution coefficients c_{jn} (for a given n), one coefficient's magnitude is much larger than all others.

Now let the conditions (22) be valid for all but one pair of partial frequencies, say Ω_1 and Ω_2, while these two frequencies are so close that coupling of the corresponding partial oscillators becomes essential. In this case, the approximation $\{\omega_n\} \approx \{\Omega_j\}$ is still valid for all other degrees of freedom, and the corresponding terms may be neglected in Eqs. (19) for $j = 1$ and 2. As a result, we return to Eqs. (7) (perhaps generalized for velocity coupling) and hence to the anticrossing diagram (Figure 2) discussed in the previous section. As a result, an extended change of only one partial frequency (say, Ω_1) of a weakly coupled system produces a sequence of eigenfrequency anticrossings - see Figure 3.

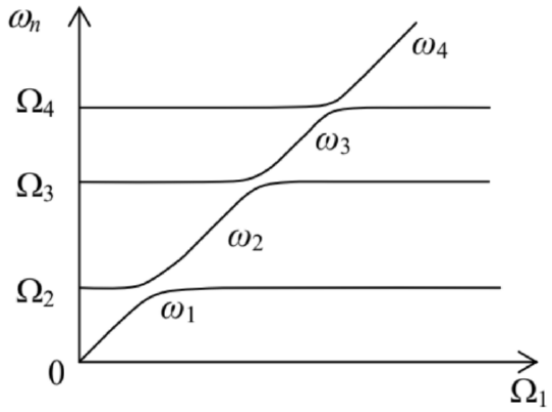

Figure 6.3. The level anticrossing in a system of N weakly coupled oscillators - schematically.

[4] Fortunately, very effective algorithms have been developed for this matrix diagonalization task - see, e.g., references in MA Sec. 16(iii)-(iv). For example, the popular MATLAB software package was initially created exactly for this purpose. ("MAT" in its name stands for "matrix" rather than "mathematics".)

6.3: 1D Waves

The second case when the general results of the last section may be simplified are coupled systems with a considerable degree of symmetry. Perhaps the most important of them are uniform systems that may sustain traveling and standing waves. Figure 4a shows a simple example of such a system - a long uniform chain of particles, of mass m, connected with light, elastic springs, prestretched with the tension force $\mathscr{T}$ to have equal lengths d. (To some extent, this is a generalization of the two-particle system considered in Sec. 1– cf. Figure 1.)

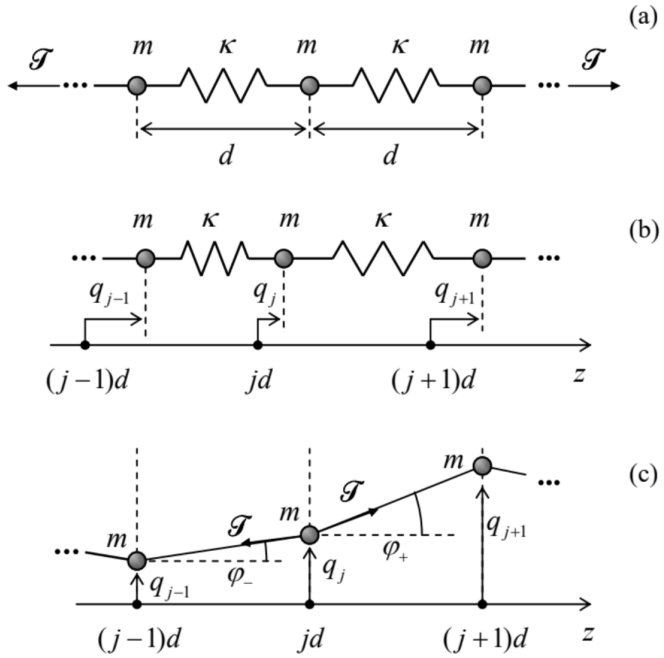

Fig. 6.4. (a) A uniform 1D chain of elastically coupled particles, and their small (b) longitudinal and (c) transverse displacements (much exaggerated for clarity).

The spring's pre-stretch does not affect small longitudinal oscillations q_j of the particles about their equilibrium positions $z_j = jd$ (where the integer j numbers the particles sequentially) – see Figure 4 b. [5] Indeed, in the 2nd Newton law for such a longitudinal motion of the j^{th} particle, the forces $\mathscr{T}$ and $-\mathscr{T}$ exerted by the springs on the right and the left of it, cancel. However, elastic additions, $\kappa\Delta q$, to these forces are generally different:

$$m\ddot{q}_j = \kappa\left(q_{j+1} - q_j\right) - \kappa\left(q_j - q_{j-1}\right). \tag{6.3.1}$$

On the contrary, for transverse oscillations within one plane (Figure 4c), the net transverse component of the pre-stretch force exerted on the j^{th} particle, $\mathscr{T}_{\text{t}} = \mathscr{T}\left(\sin\varphi_+ - \sin\varphi_-\right)$, where $\varphi_\pm$are the force direction angles, does not vanish. As a result, direct contributions into this force from small transverse oscillations, with $|q_j| << d$, $\mathscr{T}\kappa$, are negligible. Also, due to the first of these strong conditions, the angles $\varphi_\pm$are small, and hence may be approximated, respectively, as $\varphi_+ \approx \left(q_{j+1} - q_j\right)/d$ and $\varphi_- \approx \left(q_j - q_{j-1}\right)/d$. Plugging these expressions into a similar approximation, $\mathscr{T}_{\text{t}} \approx \mathscr{T}\varphi_+ - \varphi_-$) for the transverse force, we see that it may be expressed as $\mathscr{T}\left(q_{j+1} - q_j\right)/d - \mathscr{T}\left(q_j - q_{j-1}\right)/d$, i.e. is absolutely similar to that in the longitudinal case, just with the replacement $\kappa \to \mathscr{T}/d$. As a result, we may write the equation of motion of the j^{th} particle for these two cases in the same form:

$$m\ddot{q}_j = \kappa_{\text{ef}}\left(q_{j+1} - q_j\right) - \kappa_{\text{ef}}\left(q_j - q_{j-1}\right), \tag{6.3.2}$$

where κ_{ef} is the "effective spring constant", equal to κ for the longitudinal oscillations, and to $\mathscr{T}/d$ for the transverse oscillations. [6] Apart from the (formally) infinite size of the system, Eq. (24) is just a particular case of Eq. (17), and thus its particular solution may be looked for in the form (18), where in the light of our previous experience, we may immediately take $\lambda^2 \equiv -\omega^2$. With this substitution, Eq. (24) gives the following simple form of the general system of equations (17) for the distribution coefficients c_j :

$$\left(-m\omega^2 + 2\kappa_{\text{ef}}\right)c_j - \kappa_{\text{ef}}c_{j+1} - \kappa_{\text{ef}}c_{j-1} = 0. \tag{6.3.3}$$

Now comes the most important conceptual step toward the wave theory. The translational symmetry of Eq. (25), i.e. its invariance to the replacement $j \to j+1$, allows it to have particular solutions of the following form:

$$c_j = ae^{i\alpha j} \tag{6.3.4}$$

where the coefficient α may depend on ω (and system's parameters), but not on the particle number j. Indeed, plugging Eq. (26) into Eq. (25) and canceling the common factor $e^{i\alpha j}$, we see that it is indeed identically satisfied, provided that α obeys the following algebraic equation:

$$\left(-m\omega^2 + 2\kappa_{\text{ef}}\right) - \kappa_{\text{ef}} e^{+i\alpha} - \kappa_{\text{ef}} e^{-i\alpha} = 0. \tag{6.3.5}$$

The physical sense of the solution (26) becomes clear if we use it and Eq. (18) with $\lambda = \mp i\omega$, to write

$$q_j(t) = \text{Re}[a \exp\{i\,(kz_j \mp \omega t)\}] = \text{Re}[a \exp\{ik\,(z_j \mp v_{\text{ph}} t)\}] \tag{6.3.6}$$

where the wave number k is defined as $k \equiv \alpha/d$. Eq. (28) describes a sinusoidal [7] traveling wave of particle displacements, which propagates, depending on the sign before v_{ph}, to the right or the left along the particle chain, with the so-called phase velocity

$$v_{\text{ph}} \equiv \frac{\omega}{k}. \tag{6.3.7}$$

Perhaps the most important characteristic of a wave system is the so-called dispersion relation, i.e. the relation between the wave's frequency ω and its wave number k– one may say, between the temporal and spatial frequencies of the wave. For our current system, this relation is given by Eq. (27) with $\alpha \equiv kd$. Taking into account that $\left(2 - e^{+i\alpha} - e^{-i\alpha}\right) \equiv 2(1-\cos\alpha) \equiv 4\sin^2(\alpha/2)$, the dispersion relation may be rewritten in a simpler form:

$$\omega = \pm\omega_{\max} \sin\frac{\alpha}{2} \equiv \pm\omega_{\max} \sin\frac{kd}{2}, \quad \text{where } \omega_{\max} \equiv 2\left(\frac{\kappa_{\text{ef}}}{m}\right)^{1/2} \tag{6.3.8}$$

This result, sketched in Figure 5, is rather remarkable in several aspects. I will discuss them in detail, because most of these features are typical for waves of any type (including even the "de Broglie waves", i.e. wavefunctions, in quantum mechanics), propagating in periodic structures.

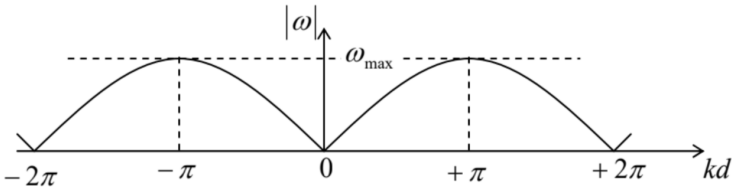

Fig. 6.5. The dispersion relation (30).

First, at low frequencies, $\omega << \omega_{\max}$, the dispersion relation (31) is linear:

$$\omega = \pm vk, \quad \text{where } v \equiv \left|\frac{d\omega}{dk}\right|_{k=0} = \frac{\omega_{\max} d}{2} = \left(\frac{\kappa_{\text{ef}}}{m}\right)^{1/2} d. \tag{6.3.9}$$

Plugging Eq. (31) into Eq. (29), we see that the constant v plays, in the low-frequency limit, the role of the same phase velocity for waves of any frequency. Due to its importance, this acoustic wave limit will with the subject of the special next section.

Second, when the wave frequency is comparable with $\omega_{\max}$, the dispersion relation is not linear, and the system is dispersive. This means that as a wave, whose Fourier spectrum has several essential components with frequencies of the order of $\omega_{\max}$, travels along the structure, its waveform (which may be defined as the shape of the line connecting all points $q_j(z)$, at the same time) changes. [9] This effect may be analyzed by representing the general solution of Eq. (24) as the sum (more generally, an integral) of the components (28) with different complex amplitudes a :

$$q_j(t) = \text{Re} \int_{-\infty}^{+\infty} a_k \exp\{i\,[kz_j - \omega(k)t]\} dk. \tag{6.3.10}$$

This notation emphasizes the dependence of the component wave amplitudes a_k and frequencies ω on the wave number k. While the latter dependence is given by the dispersion relation (in our current case by Eq. (30)), the function a_k is determined by the initial conditions. For applications, the case when a_k is substantially different from zero only in a narrow interval, of a width

$\Delta k << k_0$ around some central value k_0, is of special importance. The Fourier transform reciprocal to Eq. (32) shows that this is true, in particular, for the so-called wave packet - a sinusoidal wave modulated by a spatial envelope function of a large width $\Delta z \sim 1/\Delta k >> 1/k_0$ – see, e.g., Figure 6 .

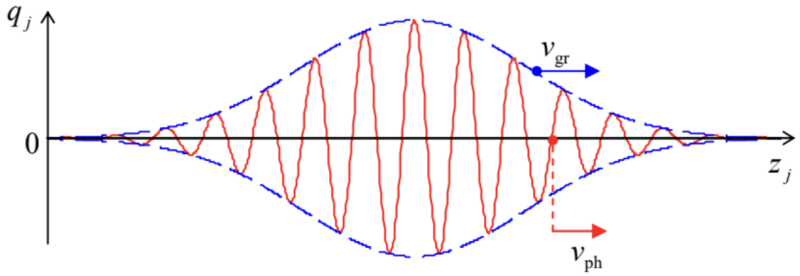

Figure 6.6. The phase and group velocities of a wave packet.

Using the strong inequality $\Delta k << k_0$, the wave packet's propagation may be analyzed by expending the dispersion relation $\omega(k)$ into the Taylor series at point k_0, and, in the first approximation in $\Delta k/k_0$, restricting the expansion to its first two terms:

$$\omega(k) \approx \omega_0 + \left.\frac{d\omega}{dk}\right|_{k=k_0} \tilde{k}, \quad \text{where } \omega_0 \equiv \omega(k_0), \text{ and } \tilde{k} \equiv k - k_0. \tag{6.3.11}$$

In this approximation, Eq. (32) yields

$$\begin{aligned} q_j(t) &\approx \mathrm{Re} \int_{-\infty}^{+\infty} a_k \exp\left\{ i \left[\left(k_0 + \tilde{k}\right) z_j - \left(\omega_0 + \frac{d\omega}{dk} \mid k = k_0 \tilde{k} \right) t \right] \right\} dk \\ &\equiv \mathrm{Re} \left[\exp\{i (k_0 z_j - \omega_0 t)\} \int_{-\infty}^{+\infty} a_k \exp\left\{ i\tilde{k} \left(z_j - \left.\frac{d\omega}{dk}\right|_{k=k_0} t \right) \right\} dk \right]. \end{aligned}$$

Comparing the last expression with the initial form of the wave packet,

$$q_j(0) = \mathrm{Re} \int_{-\infty}^{+\infty} a_k e^{ikz_j} dk \equiv \mathrm{Re} \left[\exp\{ik_0 z_j\} \int_{-\infty}^{+\infty} a_k \exp\left\{\tilde{k} z_j\right\} dk \right], \tag{6.3.12}$$

and taking into account that the phase factors before the integrals in the last forms of Eqs. (34) and (35) do not affect its envelope, we see that in this approximation the envelope sustains its initial form and propagates along the system with the so-called group velocity

$$v_{\mathrm{gr}} \equiv \left.\frac{d\omega}{dk}\right|_{k=k_0}. \tag{6.3.13}$$

Except for the acoustic wave limit (31), this velocity, which characterizes the propagation of waveform's envelope, is different from the phase velocity (29), which describes the propagation of the "carrier" sinusoidal wave, e.g., the position of one of its zeros - see the red and blue arrows in Figure 6 . (Taking into account the next term in the Taylor expansion of the function $\omega(q)$, proportional to $d^2\omega/dq^2$, we would find that the dispersion leads to a gradual change of the envelope's form. Such changes play an important role in quantum mechanics, so that they are discussed in detail in the QM part of these lecture notes.) Next, for our particular dispersion relation (30), the difference between v_{ph} and v_{gr} increases as ω approaches $\omega_{\max}$, with the group velocity (36) tending to zero, while the phase velocity staying almost constant. The physics of such a maximum frequency available for the wave propagation may be readily understood by noticing that according to Eq. (30), at $\omega = \omega_{\max}$, the wave number k equals $n\pi/d$, where n is an odd integer, and hence the phase shift $\alpha \equiv kd$ is an odd multiple of π. Plugging this value into Eq. (28), we see that at $\omega = \omega_{\max}$, the oscillations of two adjacent particles are in anti-phase, for example:

$$q_0(t) = \mathrm{Re}[a \exp\{-i\omega t\}], \quad q_1(t) = \mathrm{Re}[a \exp\{i\pi - i\omega t\}] = -q_0(t). \tag{6.3.14}$$

It is clear, especially from Figure 4 b for longitudinal oscillations, that at such a phase shift, all the springs are maximally stretched/compressed (just as in the hard mode of the two coupled oscillators analyzed in Sec. 1), so that it is natural that this mode has the highest possible frequency.

This fact invites a natural question: what happens with the system if it is agitated at a frequency $\omega > \omega_{\max}$, say by an external force applied at its boundary? Reviewing the calculations that have led to the dispersion relation (30), we see that they are all valid not only for real but also any complex values of k. In particular, at $\omega > \omega_{\max}$ it gives

$$k = \frac{(2n-1)\pi}{d} \pm \frac{i}{\Lambda}, \quad \text{where } n = 1, 2, 3, \ldots, \quad \Lambda \equiv \frac{d}{2\cosh^{-1}(\omega/\omega_{\max})}. \tag{6.3.15}$$

Plugging this relation into Eq. (28), we see that the wave's amplitude becomes an exponential function of the particle's position:

$$|q_j| = |a|e^{\pm j\,\mathrm{Im}\,kd} \propto \exp\{\pm z_j/\Lambda\}. \tag{6.3.16}$$

Physically this means that penetrating into the structure, the wave decays exponentially (from the excitation point), dropping by a factor of $e \approx 3$ at the so-called penetration depth Λ. (According to Eq. (38), at $\omega \sim \omega_{\max}$ this depth is of the order of the distance d between the adjacent particles, and decreases but rather slowly as the frequency is increased beyond $\omega_{\max}$.) Such a limited penetration is a very common property of waves, including the electromagnetic waves penetrating into various plasmas and superconductors, and the quantum-mechanical de Broglie waves penetrating into classically-forbidden regions of space. Note that this effect of "wave expulsion" from a medium does not require any energy dissipation.

Finally, one more fascinating feature of the dispersion relation (30) is its periodicity: if the relation is satisfied by some wave number $k_0(\omega)$, it is also satisfied at any $k_n(\omega) = k_0(\omega) + 2\pi n/d$, where n is an integer. This property is independent of the particular dynamics of the system and is a common property of all systems that are d-periodic in the usual ("direct") space. It has especially important implications for the quantum de Broglie waves in periodic systems - for example, crystals - leading, in particular, to the famous band/gap structure of their energy spectrum. [10]

---

[5] Note the need a clear distinction between the equilibrium position z_j of the j^{th} point and its deviation from it, q_j. Such distinction has to be sustained in the continuous limit (see below), where it is frequently called the Eulerian description - named after L. Euler, even though it was introduced to mechanics by J. d'Alembert. In this course, the distinction is emphasized by using different letters - respectively, z and q. (In the 3D case, $\mathbf{r}$ and $\mathbf{q}$.)

[6] The re-derivation of Eq. (24) from the Lagrangian formalism, with the simultaneous strict proof that the small oscillations in the longitudinal direction and the two mutually perpendicular transverse directions are all independent of each other, is a very good exercise, left for the reader.

[7] In optics and quantum mechanics, such waves are usually called monochromatic; I will not use this term until the corresponding parts (EM and QM) of my series.

[8] This term is purely historical. Though the usual sound waves in air belong to this class, the waves we are discussing may have frequencies both well below and well above the human ear's sensitivity range.

[9] The waveform deformation due to dispersion (which we are considering now) should be clearly distinguished from its possible change due to attenuation, i.e. energy loss - which is not taken into account is our current energy-conserving model - cf. Sec. 6 below.

[10] For more detail see, e.g., QM Sec. 2.5.

6.4: Acoustic Waves

Now let us return to the limit of low-frequency, dispersion-free acoustic waves, with $|\omega| << \omega_0$, propagating with the frequency-independent velocity (31). Such waves are the general property of any elastic continuous medium and obey a simple (and very important) partial differential equation. To derive it, let us note that in the acoustic wave limit, $|kd| << 1$, [11] the phase shift $\alpha \equiv kd$ is very close to $2\pi n$. This means that the differences $q_{j+1}(t) - q_j(t)$ and $q_j(t) - q_{j-1}(t)$, participating in Eq. (25), are relatively small and may be approximated with $\partial q/\partial j \equiv \partial q/\partial(z/d) \equiv d(\partial q/\partial z)$, with the derivatives taken at middle points between the particles: respectively, $z_+ \equiv (z_{j+1} - z_j)/2$ and $z_- \equiv (z_j - z_{j-1})/2$. Let us now consider z as a continuous argument, and introduce the particle displacement $q(z,t)$– a continuous function of space and time, satisfying the requirement $q(z_j, t) = q_j(t)$. In this notation, in the limit kd $\to 0$, the sum of the last two terms of Eq. (24) becomes $-\kappa d\left[\partial q/\partial z(z_+) - \partial q/\partial z(z_-)\right]$, and hence may be approximated as $-\kappa d^2\left(\partial^2 q/\partial z^2\right)$, with the second derivative taken at point $(z_+ - z_-)/2 \equiv z_j$, i.e. exactly at the same point as the time derivative. As the result, the whole set of ordinary differential equations (24), for different j, is reduced to just one partial differential equation

$$m\frac{\partial^2 q}{\partial t^2} - \kappa_{\text{ef}}\, d^2 \frac{\partial^2 q}{\partial z^2} = 0. \tag{6.4.1}$$

Using Eq. (31), we may rewrite this $1D$ wave equation in a more general form

$$\left(\frac{1}{v^2}\frac{\partial^2}{\partial t^2} - \frac{\partial^2}{\partial z^2}\right) q(z,t) = 0 \tag{6.4.2}$$

The most important property of the wave equation (40), which may be verified by an elementary substitution, is that it is satisfied by either of two traveling wave solutions (or their linear superposition):

$$q_+(z,t) = f_+(t - z/v), \quad q_-(z,t) = f_-(t + z/v), \tag{6.4.3}$$

where $f_\pm$are any smooth functions of one argument. The physical sense of these solutions may be revealed by noticing that the displacements $q_\pm$do not change at the addition of an arbitrary change Δt to their time argument, provided that it is accompanied by an addition of the proportional addition of $\mp v\Delta t$ to their space argument. This means that with time, the waveforms just move (respectively, to the left or the right), with the constant speed v, retaining their form - see Figure 7. [12]

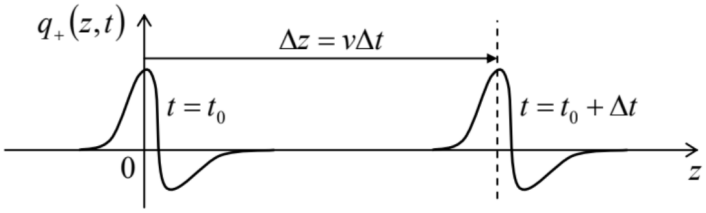

Fig. 6.7. Propagation of a traveling wave in a dispersion-free 1D system.

Returning to the simple model shown in Figure 4, let me emphasize that the acoustic-wave velocity v is different for the waves of two types: for the longitudinal waves (with $\kappa_{\text{ef}} = \kappa$, see Figure 4b),

$$v = v_l \equiv \left(\frac{\kappa}{m}\right)^{1/2} d, \tag{6.4.4}$$

while for the transverse waves (with $\kappa_{\text{ef}} = \mathscr{T}/d$, see Figure 4c):

$$v = v_t = \left(\frac{\mathscr{T}}{md}\right)^{1/2} d \equiv \left(\frac{\mathscr{J} d}{m}\right)^{1/2} \equiv \left(\frac{\mathscr{T}}{\mu}\right)^{1/2} \tag{6.4.5}$$

where the constant $\mu \equiv m/d$ has a simple physical sense of the particle chain's mass per unit length. Evidently, these velocities, in the same system, may be rather different.The wave equation (40), with its only parameter v, may conceal the fact that any wavesupporting system is characterized by one more key parameter. In our current model (Figure 4), this parameter may be revealed by calculating the forces $F_\pm(z,t)$ accompanying any of the traveling waves (41) of particle displacements. For example, in the acoustic wave limit $kd \to 0$ we are considering now, the force exerted by the j^{th} particle on its right neighbor may be approximated as

$$F(z_j,t) \equiv \kappa_{\rm ef}\left[q_j(t) - q_{j+1}(t)\right] \approx -\kappa_{\rm ef}\frac{\partial q}{\partial z}\Big|_{z=z_j} d, \tag{6.4.6}$$

where, as was discussed above, $\kappa_{\rm ef}$ equals κ for the longitudinal waves, and to $\mathscr{T}/d$ for the transverse waves. But for the traveling waves (41), the partial derivatives $\partial q_\pm/\partial z$ are equal to $\mp(df_\pm/dt)/v$, so that the corresponding forces are equal to

$$F_\pm = \mp\frac{\kappa_{\rm ef} d}{v}\frac{df_\pm}{dt}, \tag{6.4.7}$$

i.e. are proportional to the particle's velocities $u = \partial q/\partial t$ in these waves, [13] $u_\pm = df_\pm/dt$, for the same z and t. This means that the ratio

$$\frac{F_\pm(z,t)}{u_\pm(z,t)} = -\kappa_{\rm ef} d\frac{\partial q_\pm/\partial z}{\partial q_\pm/\partial t} = -\kappa_{\rm ef} d\frac{(\mp df_\pm/dt)/v}{df_\pm/dt} \equiv \pm\frac{\kappa_{\rm ef} d}{v}, \tag{6.4.8}$$

depends only on the wave propagation direction, but is independent of z and t, and also of the propagating waveform. Its magnitude,

$$Z \equiv \left|\frac{F_\pm(z,t)}{u_\pm(z,t)}\right| = \frac{\kappa_{\rm ef} d}{v} = (\kappa_{\rm ef} m)^{1/2}, \tag{6.4.9}$$

characterizing the dynamic "stiffness" of the system for the propagating waves, is called the wave impedance. [14] Note that the impedance is determined by the product of the system's generic parameters $\kappa_{\rm ef}$ and m, while the wave velocity (31) is proportional to their ratio, so that these two parameters are completely independent, and both are important. According to Eq. (47), the wave impedance, just as the wave velocity, is also different for the longitudinal and transverse waves:

$$Z_l = \frac{\kappa d}{\nu_l} \equiv (\kappa m)^{1/2}, \quad Z_t = \frac{\mathscr{T}}{\nu_t} \equiv (\mathscr{T}\mu)^{1/2}. \tag{6.4.10}$$

(Note that the first of these expressions for Z coincides with the one used for a single oscillator in Sec. 5.6. In that case, Z may be also recast in a form similar to Eq. (46), namely, as the ratio of the force and velocity amplitudes at free oscillations.)

One of the wave impedance's key functions is to scale the power carried by a traveling wave:

$$\mathscr{P}_\pm \equiv F_\pm(z,t)u_\pm(z,t) = -\kappa_{\rm ef} d\frac{\partial q_\pm}{\partial z}\frac{\partial q_\pm}{\partial t} = \pm\frac{\kappa_{\rm ef} d}{v}\left(\frac{df_\pm}{dt}\right)^2 \equiv \pm Z\left(\frac{df_\pm}{dt}\right)^2. \tag{6.4.11}$$

Two remarks about this important result. First, the sign of $\mathscr{P}$ depends only on the direction of the wave propagation, but not on the waveform. Second, the instant value of the power does not change if we move with the wave in question, i.e. measure $\mathscr{P}$ at points with $z \pm vt =$ const. This is natural because in the Hamiltonian system we are considering, the wave energy is conserved. Hence, the wave impedance Z characterizes the energy transfer along the system rather than its dissipation.

Another important function of the wave impedance notion becomes clear when we consider waves in nonuniform systems. Indeed, our previous analysis assumed that the 1D system supporting the waves (Figure 4) is exactly periodic, i.e. macroscopically uniform, and extends all the way from $-\infty$ to $+\infty$. Now let us examine what happens when this is not true. The simplest, and very important example of such nonuniform systems is a sharp interface, i.e. a point (say, $z = 0$) at which system parameters experience a jump while remaining constant on each side of the interface – see Figure 8.

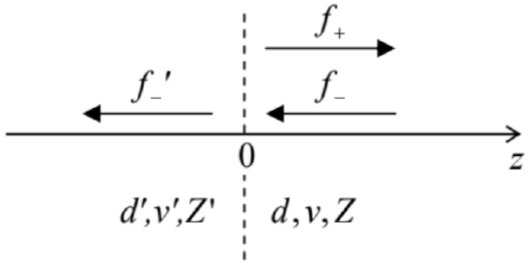

Figure 6.8. Partial reflection of a wave from a sharp interface.

In this case, the wave equation (40) and its partial solutions (41) are is still valid for $z\langle 0$ and $z\rangle$ 0 - in the former case, with primed parameters. However, the jump of parameters at the interface leads to a partial reflection of the incident wave from the interface, so that at least on the side of the incidence (in the case shown in Figure 8, for $z \geq 0$), we need to use two such terms, one describing the incident wave and another one, the reflected wave:

$$q(z,t)=\begin{cases} f'_-\left(t+z/v'\right), & \text{for } z\le 0,\\ f_-(t+z/v)+f_+(t-z/v), & \text{for } z\ge 0.\end{cases} \tag{6.4.12}$$

To find the relations between the functions f_-, f_+, and f_-' (of which the first one, describing the incident wave, may be considered known), we may use two boundary conditions at $z=0$. First, the displacement $q_0(t)$ of the particle at the interface has to be the same whether it is considered a part of the left or right sub-system, and it participates in Eqs. (50) for both $z\le 0$ and $z\ge 0$. This gives us the first boundary condition:

$$f'_-(t)=f_-(t)+f_+(t). \tag{6.4.13}$$

On the other hand, the forces exerted on the interface from the left and the right should also have equal magnitude, because the interface may be considered as an object with a vanishing mass, and any nonzero net force would give it an infinite (and hence unphysical) acceleration. Together with Eqs. (45) and (47), this gives us the second boundary condition:

$$Z'\frac{df'_-(t)}{dt}=Z\left[\frac{df_-(t)}{dt}-\frac{df_+(t)}{dt}\right]. \tag{6.4.14}$$

Integrating both parts of this equation over time, and neglecting the integration constant (which describes a common displacement of all particles rather than their oscillations), we get

$$Z'f'_-(t)=Z\left[f_-(t)-f_+(t)\right]. \tag{6.4.15}$$

Now solving the system of two linear equations (51) and (53) for $f_+(t)$ and $f'_+(t)$, we see that both these functions are proportional to the incident waveform:

$$f_+(t)=Rf_-(t),\quad f'_-(t)=\tau f_-(t), \tag{6.4.16}$$

with the following reflection (R) and transmission (T) coefficients:

$$R=\frac{Z-Z'}{Z+Z'},\quad \tau=\frac{2Z}{Z+Z'}. \tag{6.4.17}$$

Later in this series, we will see that with the appropriate re-definition of the impedance, these relations are also valid for waves of other physical nature (including the de Broglie waves in quantum mechanics) propagating in 1D continuous structures, and also in continua of higher dimensions, at the normal wave incidence upon the interface. [15] Note that the coefficients R and T give the ratios of wave amplitudes, rather than their powers. Combining Eqs. (49) and (55), we get the following relations for the powers - either at the interface or at the corresponding points of the reflected and transmitted waves:

$$\mathscr{P}_+=\left(\frac{Z-Z'}{Z+Z'}\right)^2\mathscr{P}_-,\quad \mathscr{P}'_-=\frac{4ZZ'}{\left(Z+Z'\right)^2}\mathscr{P}_-. \tag{6.4.18}$$

Note that $\mathscr{P}_-+\mathscr{P}_+=\mathscr{P}'_-$, , again reflecting the wave energy conservation.

Perhaps the most important corollary of Eqs. (55)-(56) is that the reflected wave completely vanishes, i.e. the incident wave is completely transmitted through the interface $\left(\mathscr{P}'_+=\mathscr{P}_+\right)$, if the socalled impedance matching condition $Z'=Z$ is satisfied, even if the wave velocities $v(32)$ are different on the left and the right sides of it. On the contrary, the equality of the acoustic velocities in the two continua does not guarantee the full transmission of their interface. Again, this is a very general result.

Finally, let us note that for the important particular case of a sinusoidal incident wave: [16]

$$f_-(t)=\mathrm{Re}\left[ae^{-i\omega t}\right],\quad \text{so that } f_+(t)=\mathrm{Re}\left[\mathrm{R}a\,e^{-i\omega t}\right], \tag{6.4.19}$$

where a is its complex amplitude, the total wave (50) on the right of the interface is

$$q(z,t)=\mathrm{Re}\left[ae^{-i\omega(t+z/v)}+\mathrm{R}\,ae^{-i\omega(t-z/v)}\right]\equiv\mathrm{Re}\left[a\left(e^{-ikz}+\mathrm{Re}^{+ikz}\right)e^{-i\omega t}\right],\ \text{for } z\ge 0 \tag{6.4.20}$$

while according to Eq. (45), the corresponding force distribution is

$$F(z,t)=F_-(z,t)+F_+(z,t)=-Z\frac{\partial f_-(t-z/v)}{\partial t}+Z\frac{\partial f_-(t-z/v)}{\partial t}=\mathrm{Re}\left[i\omega Za\left(e^{-ikz}-Re^{+ikz}\right)e^{-i\omega t}\right]. \tag{6.4.21}$$

These expressions will be used in the next section.

[11] Strictly speaking, per the discussion at the end of the previous section, in this reasoning k means the distance of the wave number from the closest point $2\pi n/d$ – see Figure 5 again.

[12] From the point of view of Eq. (40), the only requirement to the "smoothness" of the functions $f_{\pm}$is to be doubly differentiable. However, we should not forget that in our case the wave equation is only an approximation of the discrete Eq. (24), so that according to Eq. (30), the traveling waveform conservation is limited by the acoustic wave limit condition $\omega << \omega_{\max}$, which should be fulfilled for any Fourier component of these functions.

[13] Of course, the particle's velocity u (which proportional to the wave amplitude) should not be confused with the wave's velocity v (which is independent of this amplitude).

[14] This notion is regretfully missing from many physics (but not engineering!) textbooks.

[15] See, the corresponding parts of the lecture notes: QM Sec. 2.3 and EM Sec. 7.3.

[16] In the acoustic wave limit, when the impedances Z and Z', and hence the reflection coefficient R, are real, R and Z may be taken from under the Re operators in Eqs. (57)-(59). However, in the current, more general form of these relations they are also valid for the case of arbitrary frequencies, $\omega \sim \omega_{\max}$, when R and Z may be complex.

6.5: Standing Waves

Now let us consider the two limits in which Eqs. (55) predicts a total wave reflection $(\tau = 0)$: $Z'/Z \to \infty$ (when $R = -1$) and $Z'/Z \to 0$ (when $R = +1$). According to Eq. (53), the former limit corresponds to $f(t) + f_+(t) \equiv q(0,t) = 0$, i.e. to vanishing oscillations at the interface. This means that this particular limit describes a perfectly rigid boundary, not allowing the system's end to oscillate at all. In this case, Eqs. (58)-(59) yield

$$q(z,t) = \mathrm{Re}\left[a\left(e^{-ikz} - e^{+ikz}\right)e^{-i\omega t}\right] \equiv -2\,\mathrm{Re}\left[ae^{-i\omega t}\right]\sin kz,$$
$$F(z,t) = \mathrm{Re}\left[i\omega Za\left(e^{-ikz} + e^{+ikz}\right)e^{-i\omega t}\right] \equiv 2\omega Z\,\mathrm{Re}\left[ae^{-i(\omega t - \pi/2)}\right]\cos kz.$$

These equalities mean that we may interpret the process on the right of the interface using two mathematically equivalent, but physically different languages: either as the sum of two traveling waves (the incident one and the reflected one, traveling in opposite directions), or as a single standing wave. Note that in contrast with the traveling wave (Figure 9a, cf. Figure 7), in the standing sinusoidal wave (Figure 9b) all particles oscillate in time with one phase.

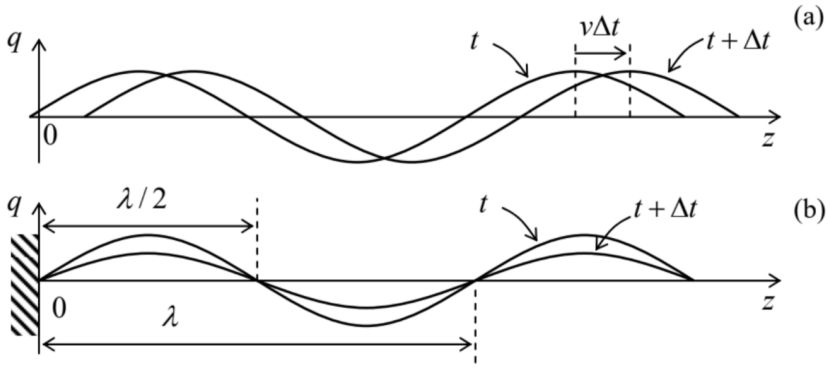

Figure 6.9. The time evolution of (a) a traveling sinusoidal wave, and (b) a standing sinusoidal wave at a rigid boundary.

Note also that the phase of the force oscillations (61) is shifted, both in space and in time, by $\pi/2$ relatively to the particle displacement oscillations. (In particular, at the rigid boundary the force amplitude reaches its maximum.) As a result, the average power flow vanishes, so that the average energy of the standing wave does not change, though its instant energy still oscillates, at each spatial point, between its kinetic and potential components - just as at the usual harmonic oscillations of one particle. A similar standing wave, but with a maximum of the displacement q, and with a zero ("node") of the force F, is formed at the open boundary, with $\mathrm{Z}'/\mathrm{Z} \to 0$, and hence $\mathrm{R} = +1$. Now I have to explain why I have used the sinusoidal waveform for the wave reflection analysis. Let us consider a 1D wave system, which obeys Eq. (40), of a finite length l, limited by two rigid walls (located, say, at $z = 0$ and $z = l$), which impose the corresponding boundary conditions,

$$q(0,t) = q(l,t) = 0, \tag{6.5.1}$$

on its motion. Naturally, a sinusoidal traveling wave, induced in the system, will be reflected from both ends, forming the standing wave patterns of the type (60) near each of them. These two patterns are compatible if l is exactly equal to an integer number (say, n) of $\lambda/2$, where $\lambda \equiv 2\pi/k$ is the wavelength:

$$l = n\frac{\lambda}{2} \equiv n\frac{\pi}{k}. \tag{6.5.2}$$

This requirement yields the following spectrum of possible wave numbers:

$$k_n = n\frac{\pi}{l}, \tag{6.5.3}$$

where the list of possible integers n may be limited to non-negative values: $n = 1, 2, 3, \ldots$ (Indeed, negative values give absolutely similar waves (60), while $n = 0$ yields $k_n = 0$, and the corresponding wave vanishes at all points: $\sin(0 \cdot z) \equiv 0$.) In the acoustic wave limit we are discussing, Eq. (31), $\omega = \pm vk$, may be used to translate this wave-number spectrum into an equally simple spectrum of possible standing-wave frequencies: [17]

$$\omega_n = vk_n = n\frac{\pi v}{l}, \quad \text{with } n = 1, 2, 3, \ldots \tag{6.5.4}$$

Now let us notice that this spectrum, and the corresponding standing-wave patterns, [18]

$$q^{(n)}(z,t) = 2\,\mathrm{Re}[a_n \exp\{-i\omega_n t\}] \sin k_n z, \quad \text{for } 0 \le z \le l, \tag{6.5.5}$$

may be obtained in a different way, by a direct solution of the wave equation (41) with the boundary conditions (62). Indeed, let us look for the general solution of this partial differential equation in the socalled variable-separated form [19]

$$q(z,t) = \sum_n Z_n(z) T_n(t), \tag{6.5.6}$$

where each partial product $Z_n(z)T_n(t)$ is supposed to satisfy the equation on its own. Plugging such partial solution into Eq. (40), and then dividing all its terms by the same product, $Z_n T_n$, we may rewrite the result as

$$\frac{1}{v^2}\frac{1}{T_n}\frac{d^2T_n}{dt^2} = \frac{1}{Z_n}\frac{d^2Z_n}{dz^2}. \tag{6.5.7}$$

Here comes the punch line of the variable separation method: since the left-hand side of the equation may depend only on t, while its right-hand side, only on z, Eq. (68) may be valid only if both its sides are constant. Denoting this constant as $-k_n{}^2$, we get two similar ordinary differential equations,

$$\frac{d^2Z_n}{dz^2} + k_n^2 Z_n = 0, \quad \frac{d^2T_n}{dt^2} + \omega_n^2 T_n = 0, \quad \text{where } \omega_n^2 \equiv v^2 k_n^2, \tag{6.5.8}$$

with well-known (and similar) sinusoidal solutions

$$Z_n = c_n \cos k_n z + s_n \sin k_n z, \quad T_n = u_n \cos \omega_n t + v_n \sin \omega_n z \equiv \mathrm{Re}[a_n \exp\{-i\omega_n t\}], \tag{6.5.9}$$

where $c_n, v_n, u_n,$ and v_n (or, alternatively, $a_n \equiv u_n + iv_n$) are constants. The first of these relations, with all k_n different, may satisfy the boundary conditions only if for all $n, c_n = 0$, and $\sin k_n l = 0$, giving the same wave number spectrum (64) and hence the own frequency spectrum (65), so that the general solution (67) of the so-called boundary problem, given by Eqs. (40) and (62), takes the form

$$q(z,t) = \mathrm{Re} \sum_n a_n \exp\{-i\omega_n t\} \sin k_n z, \tag{6.5.10}$$

where the complex amplitudes a_n are determined by the initial conditions.

Hence such sinusoidal standing waves (Figure 10a) are not just an assumption, but a natural property of the 1D wave equation. It is also easy to verify that the result (71) is valid for the same system with different boundary conditions, though with a modified wave number spectrum. For example, if the rigid boundary condition $(q = 0)$ is implemented at $z = 0$, and the so-called free (or "open") boundary conditions $(F = 0$, i.e. $\partial q/\partial z = 0)$ is imposed at $z = l$, the spectrum becomes

$$k_n = \left(n - \frac{1}{2}\right)\frac{\pi}{l}, \quad \text{with } n = 1, 2, 3, \ldots, \tag{6.5.11}$$

so that the lowest standing waves look like Figure 10b shows. [20]

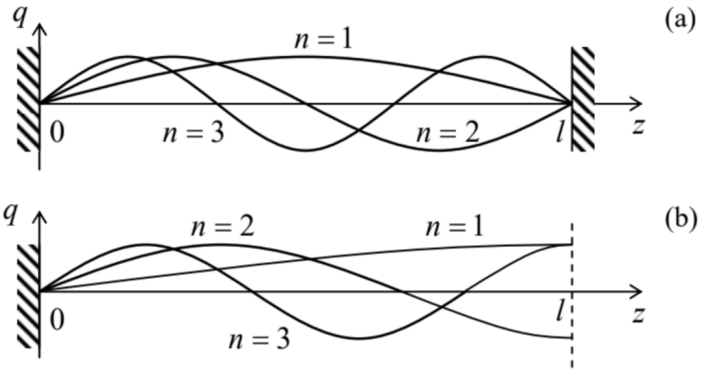

Figure 6.10. The lowest standing wave modes for the 1D systems with (a) two rigid boundaries, and (b) one rigid and one open boundary.

Note that the difference between the sequential values of k_n is still constant:

$$k_{n+1} - k_n = \frac{\pi}{l}, \tag{6.5.12}$$

i.e. the same as for the spectrum (64). This is natural because in both cases the transfer from the n^{th} mode to the $(n+1)^{\text{th}}$ mode corresponds just to an addition of one more half-wave - see Figure 10. (This conclusion is valid for any combination of rigid and free boundary conditions.) As was discussed above, for the discrete-particle chain we have started with (Figure 4), the wave equation (40), and hence the above derivation of Eq. (71), are only valid in the acoustic wave limit, i.e. when the distance d between the particles is much less than the wavelengths $\lambda_n \equiv 2\pi/k_n$ of the mode under analysis. For a chain of length l, this means that the number of particles, $N \sim l/d$, has to be much larger than 1 . However, a remarkable property of Eq. (71) is that it remains valid, with the same wave number spectrum (64), not only in the acoustic limit but also for arbitrary $N > 0$. Indeed, since $\sin k_n z \equiv (\exp\{+ik_n z\} - \exp\{-ik_n z\})/2$, each n^{th} term of Eq. (71) may be represented as a sum of two traveling waves with equal but opposite wave vectors. As was discussed in Sec. 3, such a wave is a solution of equation (24) describing the discreteparticle system for any k_n, with the only condition that its frequency obeys the general dispersion relation (30), rather than its acoustic limit (65).

Moreover, the expressions for k_n (with appropriate boundary conditions), such as Eq. (64) or Eq. (72), also survive the transition to arbitrary N, because their derivation above was based only on the sinusoidal form of the standing wave. The only new factor arising in the case of arbitrary N is that due to the equidistant property (73) of the wave number spectrum, as soon as n exceeds N, the waveforms (71), at particle locations $z_j = jd$, start to repeat. For example,

$$\sin k_{n+N} z_j = \sin(k_n + N\Delta k)jd = \sin\left(k_n + N\frac{\pi}{d}\right)jd = \sin(k_n z_j + \pi jN) = \pm \sin k_n z_j. \tag{6.5.13}$$

Hence the system has only N different (linearly-independent) modes. But this result is in full compliance with the general conclusion made in Sec. 2, that any system of N coupled 1D oscillators has exactly N own frequencies and corresponding oscillation modes. So, our analysis of a particular system, shown in Figure 4, just exemplifies this general conclusion. Figure 11 below illustrates this result for a particular finite value of N; the curve connecting the points shows exactly the same dispersion relation as was shown in Figure 5 , but now it is just a guide for the eye, because for a system with a finite length l, the wave number spectrum is discrete, and the intermediate values of k and ω do not have an immediate physical sense. [21] Note that the own frequencies of the system are not equidistant, while the wave numbers are.

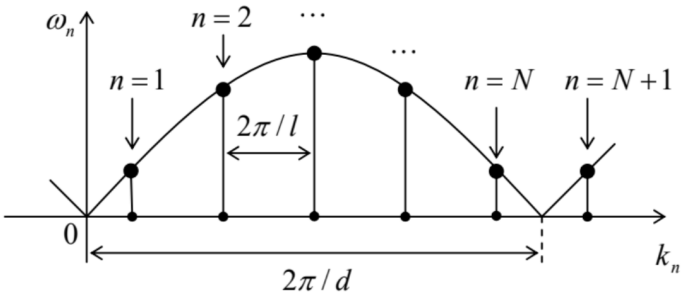

Figure 6.11. The wave numbers and own frequencies of a chain of a finite number N of particles in a chain with one rigid and one open boundary - schematically.

This insensitivity of the spacing (73) between the adjacent wave numbers to the particular physics of a macroscopically uniform system is a very general fact, common for waves of any nature, and is broadly used for analyses of systems with a very large number of particles (such as human-size crystals, with $N \sim 10^{23}$). For N so large, the effect of the boundary conditions, e.g., the difference between the spectra (64) and (72) is negligible, and they may be summarized as the following rule for the number of different standing waves within some interval $\Delta k \gg \pi/l$:

$$\Delta N \equiv \frac{\Delta k|_{\text{standing}}}{k_{n+1} - k_n} = \frac{l}{\pi}\Delta k\Big|_{\text{standing}}. \tag{6.5.14}$$

For such analyses, it is frequently more convenient to work with traveling waves rather than the standing ones. In this case, we have to take into account that (as was just discussed above) each standing wave (66) may be decomposed to two traveling waves with wave numbers $\pm k_n$, so that size of the interval Δk doubles, and Eq. (75a) becomes [22]

$$\Delta N = \frac{l}{2\pi}\Delta k\Big|_{\text{traveling}} \tag{6.5.15}$$

Note that this counting rule is valid for waves of just one type. As was discussed above, for the model system we have studied (Figure 4), there are 3 types of such waves - one longitudinal and two transverse, so that if we need to count them all, ΔN should be multiplied by 3 .

---

[17] Again, negative values of ω may be dropped, because they give similar real functions $q(z,t)$.

[18] They describe, in particular, the well-known transverse standing waves on a guitar string.

[19] This variable separation method is very general and is discussed in all parts of this series, especially in EM Chapter 2.

[20] The lowest standing wave of the system, with the smallest k_n and ω_n, is usually called its fundamental mode.

[21] Note that Figure 11 shows the case of one rigid and one open boundary (see Figure 10b), where $l = Nd$; for a conceptually simpler system with two rigid boundaries (Figure 10a) we would need to take $l = (N+1)d$, because neither of the end points can oscillate.

[22] Note that this simple, but very important relation is frequently derived using the so-called Born-Carman boundary condition $q_0(t) \equiv q_N(t)$, which implies bending the system of interest into a closed loop. For a 1D system with $N >> 1$, such mental exercise may be somehow justified, but for systems of higher dimension, it is hardly physically plausible – and is unnecessary.

6.6: Wave Decay and Attenuation

Now let us discuss the effects of dissipation on the 1D waves, on the example of the same uniform system shown in Figure 4. The effects are simplest for a linear drag that may be described, as it was done for a single oscillator in Sec.5.1, by adding the term $\eta dq_j/dt$, to Eq. (24) for each particle:

$$m\ddot{q}_j + \eta\dot{q}_j - \kappa_{\text{ef}}\left(q_{j+1} - q_j\right) + \kappa_{\text{ef}}\left(q_j - q_{j-1}\right) = 0. \tag{6.6.1}$$

(In a uniform system, the drag coefficient η should be similar for all particles, though it may be different for the longitudinal and transverse oscillations.)

To analyze the dissipation effect on the standing waves, we may again use the variable separation method, i.e. look for the solution of Eq. (76) in the form similar to Eq. (67), naturally readjusting it for our current discrete case:

$$q\left(z_j, t\right) = \sum_n Z_n\left(z_j\right) T_n(t). \tag{6.6.2}$$

After dividing all terms by $mZ_n\left(z_j\right)T_n(t)$, and separating the time-dependent and space-dependent terms, we get

$$\frac{\ddot{T}_n}{T_n} + \frac{\eta}{m}\frac{\dot{T}_n}{T_n} = \frac{\kappa_{\text{ef}}}{m}\left[\frac{Z_n\left(z_{j+1}\right)}{Z_n\left(z_j\right)} + \frac{Z_n\left(z_{j+1}\right)}{Z_n\left(z_j\right)} - 2\right] = \text{const} \tag{6.6.3}$$

As we know from the previous section, the resulting equation for the function $Z_n\left(z_j\right)$ is satisfied if the variable separation constant is equal to $-{\omega_n}^2$, where ω_n obeys the dispersion relation (30) for the wave number k_n, properly calculated for the dissipation-free system, with the account of the given boundary conditions - see, e.g. Eqs. (62) and (72). Hence for the function $T_n(t)$ we are getting the ordinary differential equation

$$\ddot{T}_n + 2\delta\dot{T}_n + \omega_n^2 T_n = 0, \qquad \text{with } \delta \equiv \frac{\eta}{2m}, \tag{6.6.4}$$

which is absolutely similar to Eq. (5.6b) for a single linear oscillator, which was studied in Sec. 5.1. As we already know, it has the solution (5.9), describing the free oscillation decay with the relaxation time given by $(5.10), \tau = 1/\delta$, and hence similar for all modes. [23]

Hence, the above analysis of the dissipation effect on the free standing waves has not brought any surprises, but it gives us a hint of how their forced oscillations, induced by some external forces $F_j(t)$ exerted on the particles, may be analyzed. Indeed, representing the force as a sum of spatial harmonics proportional to the system's modes,

$$F_j(t) = m\sum_n f_n(t) Z_n\left(z_j\right) \tag{6.6.5}$$

and using the variable separation (77), we arrive at the equation

$$\ddot{T}_n + 2\delta\dot{T}_n + \omega_n^2 T_n = f_n(t), \tag{6.6.6}$$

similar to Eq. (5.13b) for a single oscillator. This fact enables using all the methods discussed in Sec. 5.1 for the forced oscillation analysis, besides that the temporal Green's function, defined by either of the equivalent equations (5.27) and (5.28), now acquires the index n, i.e. becomes mode-dependent: $G(\tau) \to G_n(\tau)$. Performing the weighed summation similar to Eq. (80),

$$G_j(\tau) = \sum_n G_n(\tau) Z_n\left(z_j\right), \tag{6.6.7}$$

we get the spatial-temporal Green's function of the system - in this case, for a discrete, 1D set of spatial points $z_j = jd$. As in the single-oscillator case, it has a simple physical sense of the oscillations induced by a delta-functional force (i.e. a very short pulse), exerted on the j^{th} particle. We will meet (and use) such spatial-temporal Green's functions in other parts of this series as well.

Now let us discuss the dissipation effects on the traveling waves, where they may take a completely different form of attenuation. Let us discuss it on a simple example when one end (located at $z = 0$) of a very long chain $(l \to \infty)$ is externally-forced to perform sinusoidal oscillations of a certain frequency ω and a fixed amplitude A_0. In this case, it is natural to look for the particular solution of Eq. (76) in a form very different from Eq. (77):

$$q_j(z, t) = \text{Re}\left[c_j e^{-i\omega t}\right] \tag{6.6.8}$$

with time-independent but generally complex amplitudes c_j. As our discussion of a single oscillator in Sec. 5.1 implies, this is not the general, but rather a partial solution, which describes forced oscillations in the system, to which it settles after some initial transient process. (At non-zero damping, we may be sure that this process fades after a finite time, and thus may be ignored for most purposes.)

Plugging Eq. (83) into Eq. (76), we reduce it to an equation for the amplitudes c_j,

$$\left(-m\omega^2 - i\omega\eta + 2\kappa_{\rm ef}\right) c_j - \kappa_{\rm ef} c_{j+1} - \kappa_{\rm ef} c_{j-1} = 0, \tag{6.6.9}$$

which is a natural generalization of Eq. (25). As a result, partial solutions of the set of these equations (for $j = 0, 1, 2, \dots$) may be looked for in the form (26) again, but now, because of the new, imaginary term in Eq. (84), we should be ready to get a complex phase shift α, and hence a complex wave number $k \equiv \alpha/d$.[24] Indeed, the resulting characteristic equation for k,

$$\sin^2 \frac{kd}{2} = \frac{\omega^2}{\omega_{\rm max}^2} + i\frac{2\omega\delta}{\omega_{\rm max}^2} \tag{6.6.10}$$

(where $\omega_{\rm max}$ is defined by Eq. (30), and the damping coefficient is defined just as in a single oscillator, $\delta \equiv \eta/2m$), does not have a real solution even at $\omega < \omega_{\rm max}$. Using the well-known expressions for the sine function of a complex argument [25] Eq. (85) may be readily solved in the most important low-damping limit $\delta << \omega$. In the linear approximation in δ, it does not affect the real part of k, but makes its imaginary part different from zero:

$$k = \pm\frac{2}{d}\left(\sin^{-1}\frac{\omega}{\omega_{\rm max}} + i\frac{\delta}{\omega_{\rm max}}\right) \equiv \pm\left(\frac{2}{d}\sin^{-1}\frac{\omega}{\omega_{\rm max}} + i\frac{\delta}{v}\right), \quad \text{for } -\pi \le \mathrm{Re}\, k \le \pi, \tag{6.6.11}$$

with a periodic extension to other periods - see Figure 5. Just as was done in Eq. (28), due to two values of the wave number, generally we have to take c_j in the form of not a single wave (26), but of a linear superposition of two partial solutions:

$$c_j = \sum_{\pm} c_{\pm} \exp\left\{\pm i\, \mathrm{Re}\, k z_j \mp \frac{\delta}{v} z_j\right\} \tag{6.6.12}$$

where the constants $c_{\pm}$should be found from the boundary conditions. In our particular case, $|c_0| = A_0$ and $c_\infty = 0$, so that only one of these two waves, namely the wave exponentially decaying at its penetration into the system, is different from zero: $|c_+| = A_0, c_- = 0$. Hence our solution describes a single wave, with the real amplitude and the oscillation energy decreasing as

$$A_j \equiv |c_j| = A_0 \exp\left\{-\frac{\delta}{v} z_j\right\}, \quad E_j \propto A_j^2 \propto \exp\{-\alpha z_j\}, \quad \text{with } \alpha = \frac{2\delta}{v}, \tag{6.6.13}$$

i.e. with a frequency-independent attenuation constant $\alpha = 2\delta/v$,[26] so that the spatial scale of wave penetration into a dissipative system is given by $l_d \equiv 1/\alpha$. Certainly, our simple solution (88) is only valid for a system of length $l >> l_d$; otherwise, we would need the second term in the sum (87) to describe the wave reflected from its opposite end.

---

[23] Even an elementary experience with acoustic guitars shows that for their strings this particular conclusion of our theory is not valid: higher modes ("overtones") decay substantially faster, leaving the fundamental mode oscillations for a slower decay. This is a result of another important energy loss (i.e. the wave decay) mechanism, not taken into account in Eq. (76) - the radiation of the sound into the guitar's body through the string supports, mostly through the bridge. Such radiation may be described by a proper modification of the boundary conditions (62), in terms of the ratio of the wave impedance (47) of the string and those of the supports.

[24] As a reminder, we have already met such a situation in the absence of damping, but at $\omega > \omega_{\rm max}$ – see Eq. (38).

[25] See, e.g., MA Eq. (3.5).

[26] I am sorry to use for the attenuation the same letter α as for the phase shift in Eq. (26) and a few of its corollaries, but both notations are traditional.

6.7: Nonlinear and Parametric Effects

Now let me discuss (because of the lack of time, very briefly, on a semi-quantitative level), the new nonlinear and parametric phenomena that appear in oscillatory systems with more than one degree of freedom - cf. Secs. 5.4-5.8. One important new effect here is the mutual phase locking of (two or more) weakly coupled self-excited oscillators with close frequencies: if the own frequencies of the oscillators are sufficiently close, their oscillation frequencies "stick together" to become exactly equal. Though its dynamics of this process is very close to that of the phase locking of a single oscillator by an external signal, which was discussed in Sec. 5.4, it is rather counter-intuitive in the view of the results of Sec. 1, and in particular, the anticrossing diagram shown in Figure 2. The analysis of the effect using the van der Pol method (which is highly recommended to the reader, see Problem 16) shows that the origin of the difference is the oscillators' nonlinearity, which makes oscillation amplitudes virtually independent of the phase evolution - see Eq. (5.68) and its discussion.

One more new effect is the so-called non-degenerate parametric excitation. It may be illustrated on the example of just two coupled oscillators - see Sec. 1 above. Let us assume that the coupling constant κ, participating in Eqs. (5), is not constant, but oscillates in time - say with some frequency ω_p. In this case, the forces acting on each oscillator from its counterpart, described by the right-hand side of Eqs. (5), will be proportional to $\kappa q_{2,1}(1+\mu\cos\omega_p t)$. Assuming that the oscillations of q_1 and q_2 are close to sinusoidal ones, with certain frequencies $\omega_{1,2}$, we see that the force exerted on each oscillator will contain the so-called combinational frequencies

$$\omega_p \pm \omega_{2,1} \tag{6.7.1}$$

If one of these frequencies is close to the own oscillation frequency of the oscillator, we can expect a substantial parametric interaction between the oscillators (on top of the constant coupling effects discussed in Sec. 1). According to Eq. (89), this may happen in two cases:

$$\omega_p = \omega_1 + \omega_2,$$
$$\omega_p = \omega_1 - \omega_2.$$

The quantitative analysis (also highly recommended to the reader, see Problem 18) shows that in the case (90a), the parameter modulation indeed leads to energy "pumping" into the oscillations. As a result, a sufficiently large μ, at sufficiently small damping coefficients $\delta_{1,2}$ and the effective detuning

$$\xi \equiv \omega_p - (\Omega_1 + \Omega_2), \tag{6.7.2}$$

may lead to a simultaneous self-excitation of two frequency components $\omega_{1,2}$. These frequencies, while being approximately equal to the corresponding own frequencies $\Omega_{1,2}$ of the system, are related to the pumping frequency ω_p by the exact relation (90a), but otherwise are arbitrary, e.g., may be incommensurate (Figure 12a), thus justifying the term non-degenerate parametric excitation. [27] (The parametric excitation of a single oscillator, that was analyzed in Sec. 5.5, is a particular, degenerate case of such excitation, with $\omega_1 = \omega_2 = \omega_p/2$.) On the other hand, for the case described by Eq. (90b), the parameter modulation always pumps energy from the oscillations, effectively increasing the system's damping.

Somewhat counter-intuitively, this difference between two cases (90) may be simpler interpreted using the basic notions of quantum mechanics. Namely, the equality $\omega_p = \omega_1 + \omega_2$ enables a decay of an external photon of energy $\hbar\omega_0$ into two photons of energies $\hbar\omega_1$ and $\hbar\omega_2$ of the oscillators. (On the contrary, the complementary relation (90b), meaning that $\omega_1 = \omega_p + \omega_2$, results in a pumping-induced decay of photons of frequency ω_1.)

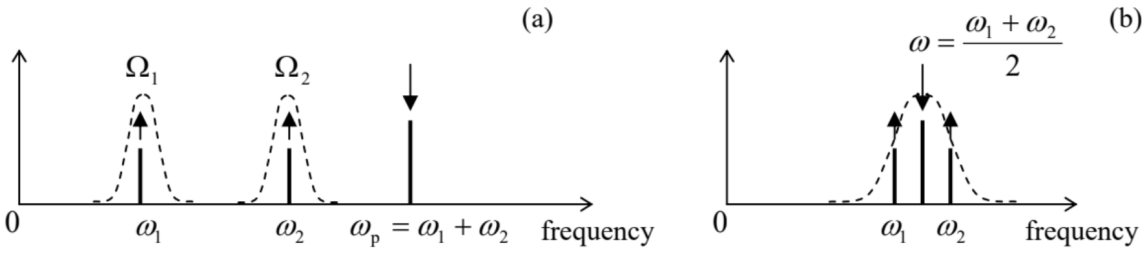

Figure 6.12. Spectra of oscillations at (a) the non-degenerate parametric excitation, and (b) the fourwave mixing. The arrow directions symbolize the energy flows into and out of the system.

Note that even if the frequencies ω_1 and ω_2 of the parametrically excited oscillations are incommensurate, the oscillations are highly correlated. Indeed, the quantum mechanical theory of this effect [28] shows that the generated photons are entangled. This fact makes the parametric excitation very popular for a broad class of experiments in several currently active fields including quantum computation and encryption, and the Bell inequality/local reality studies. [29]

Proceeding to nonlinear phenomena, let us note, first of all, that the simple reasoning that accompanied Eq. (5.108) in Sec. 5.8, is also valid in the case when oscillations consist of two (or more) sinusoidal components with incommensurate frequencies. Replacing the notation 2ω with ω_p, we see that the non-degenerate parametric excitation of the type (90a) is possible in a system of two coupled oscillators with a quadratic nonlinearity (of the type γq^2), "pumped" by an intensive external signal at frequency $\omega_p \approx \Omega_1 + \Omega_2$. In optics, it is often more convenient to have all signals within the same, relatively narrow frequency range. A simple calculation, similar to the one made in Eqs. (5.107)-(5.108), shows that this may be done using the cubic nonlinearity [30] of the type αq^3, which allows a similar parametric energy exchange at the frequency relation shown in Figure 12b:

$$2\omega = \omega_1 + \omega_2, \qquad \text{with } \omega \approx \omega_1 \approx \omega_2. \tag{6.7.3}$$

This process is often called the four-wave mixing, because it may be interpreted quantummechanically as the transformation of two externally-delivered photons, each with energy $\hbar\omega$, into two other photons of energies $\hbar\omega_1$ and $\hbar\omega_2$. The word "wave" in this term stems from the fact that at optical frequencies, it is hard to couple a sufficient volume of a nonlinear medium with lumped-type resonators. It is much easier to implement the parametric excitation (as well as other nonlinear phenomena such as the higher harmonic generation) of light in distributed systems of a linear size much larger than the involved wavelengths. In such systems, the energy transfer from the incoming wave of frequency ω to generated waves of frequencies ω_1 and ω_2 is gradually accumulated at their joint propagation along the system. From the analogy between Eq. (85) (describing the evolution of the wave's amplitude in space), and the usual equation of the linear oscillator (describing its evolution in time), it is clear that this energy transfer accumulation requires not only the frequencies ω, but also the wave numbers k be in similar relations. For example, the four-wave mixing requires that not only the frequency balance (92a), but also a similar relation

$$2k = k_1 + k_2, \tag{6.7.4}$$

to be fulfilled. Since all three frequencies are close, this relation is easy to arrange. Unfortunately, due to the lack of time/space, for more discussion of this very interesting subject, called nonlinear optics, I have to refer the reader to special literature. [31]

It may look like a dispersion-free media, with $\omega/k = v =$ const, is the perfect solution for arranging the parametric interaction of waves, because in such media, for example, Eq. (92b) automatically follows from Eq. (92a). However, in such a media not only the desirable three parametrically interacting waves but also all their harmonics, have the same velocity. At these conditions, the energy transfer rates between all harmonics are of the same order. Perhaps the most important result of such a multi-harmonic interaction is that intensive incident traveling waves, interacting with a nonlinear medium, may develop sharply non-sinusoidal waveforms, in particular those with an almost instant change of the field at a certain moment. Such shock waves, especially those of mechanical nature, are of large interest for certain applications - some of them not quite innocent, e.g., the dynamics of explosion in the usual (chemical) and nuclear bombs. [32]

To conclude this chapter, let me note that the above discussion of 1D acoustic waves will be extended, in Sec. 7.7, to elastic 3D media. There we will see that generally, the waves obey a more complex equation than the apparently natural generalization of Eq. (40):

$$\left(\frac{1}{v^2} \frac{\partial^2}{\partial t^2} - \nabla^2 \right) q(\mathbf{r}, t) = 0, \tag{6.7.5}$$

where ∇^2 is the Laplace operator. This fact adds to the complexity of traveling-wave and standing-wave phenomena in higher dimensions. Moreover, in multi-dimensional systems, including such pseudo-1D systems as thin rods and pseudo-2D systems such as thin membranes, even static elastic deformations may be very nontrivial. A brief introduction to the general theory of small deformations, with a focus on elastic continua, will be the subject of the next chapter.

---

[27] Note that in some publications, the term parametric down-conversion (PDC) is used instead.

[28] Which is, surprisingly, not much more complex than the classical theory - see, e.g., QM Sec.5.5

[29] See, e.g., QM Secs. 8.5 and 10.3, respectively.

[30] In optics, such nonlinearity is implemented using transparent crystals such as lithium niobate $(\mathrm{LiNbO_3})$, with the cubic-nonlinear dependence of the electric polarization on the applied electric field: $\mathscr{P} \propto \mathscr{E} + \alpha \mathscr{E}^3$.

[31] See, e.g., N. Bloembergen, Nonlinear Optics, 4^{th} ed., World Scientific, 1996, or a more modern treatment by R. Boyd, Nonlinear Optics, 3^{rd} ed., Academic Press, 2008. This field is currently very active. As just a single example, let me mention the recent experiments with parametric amplification of ultrashort (20 -fs) optical pulses to peak power as high as $\sim 5 \times 10^{12}$ W – see X. Zeng et al., Optics Lett. 42, 2014 (2017).

[32] The classical (and perhaps still the best) monograph on the subject is Ya. Zeldovich, Physics of Shock Waves and High-Temperature Phenomena, Dover, 2002.

6.8: Exercise Problems

For each of the systems specified in Problems 6.1-6.6:

(i) introduce convenient generalized coordinates q_j of the system,

(ii) calculate the frequencies of its small harmonic oscillations near the equilibrium,

(iii) calculate the corresponding distribution coefficients, and

(iv) sketch the oscillation modes.

6.1. Two elastically coupled pendula, confined to a vertical plane, with the parameters shown in the figure on the right (see also Problems 1.8 and 2.9).

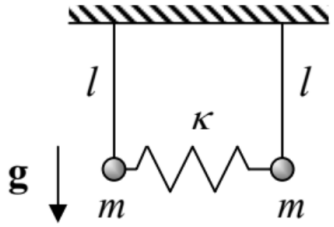

6.2. The double pendulum, confined to a vertical plane containing the support point (considered in Problem 2.1), with $m' = m$ and $l = l' -$ see the figure on the right.

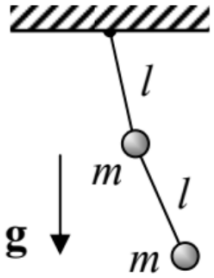

6.3. The chime bell considered in Problem 4.8 (see the figure on the right), for the particular case $l = l'$.

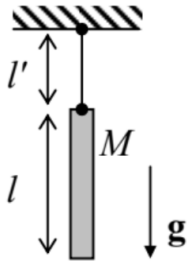

6.4. The triple pendulum shown in the figure on the right, with the motion confine to a vertical plane containing the support point.

Hint: You may use any (e.g., numerical) method to calculate the characteristic equation's roots.

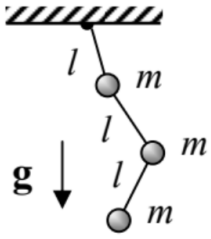

6.5. A linear, symmetric system of three particles, shown in the figure on the right, where the connections between the particles not only act as usual elastic springs (giving potential energies $U = \kappa(\Delta l)^2/2$) but also resist bending, giving additional potential energy $U' = \kappa'(l\theta)^2/2$, where θ is the (small) bending angle. [33]

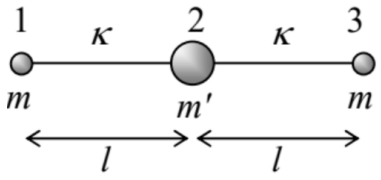

6.6. Three similar beads of mass m, which may slide along a circle of radius R without friction, connected with similar springs with elastic constants κ and equilibrium lengths l_0 - see the figure on the right.

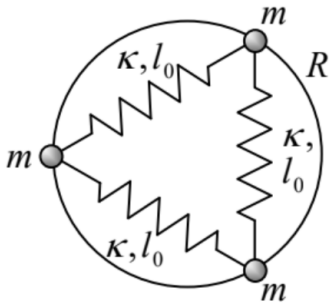

6.7. An external longitudinal force $F(t)$ is applied to the right particle of the system shown in Figure 1, with $\kappa_L = \kappa_R = \kappa'$ and $m_1 = m_2 \equiv m$ (see the figure on the right), and the response $q_1(t)$ of the left N particle to this force is being measured.

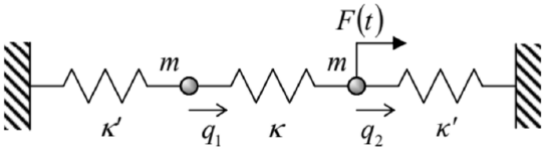

(i) Calculate the temporal Green's function for this response.

(ii) Use this function to calculate the response to the following force:

$$F(t) = \begin{cases} 0, & \text{for } t < 0 \\ F_0 \sin \omega t, & \text{for } 0 \le t \end{cases} \tag{6.8.1}$$

with constant amplitude F_0 and frequency ω.

6.8. Use the Lagrangian formalism to re-derive Eqs. (24) for both the longitudinal and the transverse oscillations in the system shown in Figure 4a.

6.9. Calculate the energy (per unit length) of a sinusoidal traveling wave propagating in the 1D system shown in Figure 4a. Use your result to calculate the average power flow created by the wave, and compare it with Eq. (49) valid in the acoustic wave limit.

6.10. Calculate the spatial distributions of the kinetic and potential energies in a standing, sinusoidal, 1D acoustic wave, and analyze their evolution in time.

6.11. The midpoint of a guitar string of length l has been slowly pulled off by distance $h << l$ from its equilibrium position, and then let go. Neglecting dissipation, use two different approaches to calculate the midpoint's displacement as a function of time.

Hint: You may like to use the following table series:

$$\sum_{m=1}^{\infty} \frac{\cos(2m-1)\xi}{(2m-1)^2} = \frac{\pi^2}{8}\left(1 - \frac{\xi}{\pi/2}\right), \quad \text{for } 0 \le \xi \le \pi. \tag{6.8.2}$$

6.12. Calculate the dispersion law $\omega(k)$ and the maximum and minimum frequencies of small longitudinal waves in a long chain of similar, spring-coupled pendula - see the figure on the right.

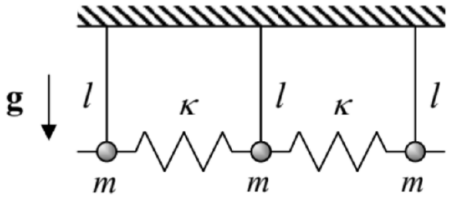

6.13. Calculate and analyze the dispersion relation $\omega(k)$ for small waves in a long chain of elastically coupled particles with alternating masses - see the figure on the right. In particular, discuss the dispersion relation's period Δk, and its evolution at $m' \to m$.

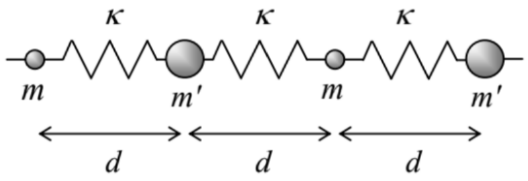

6.14. Analyze the traveling wave's reflection from a "point inhomogeneity": a single particle with a different mass $m_0 \neq m$, within an otherwise uniform 1D chain - see the figure on the right.

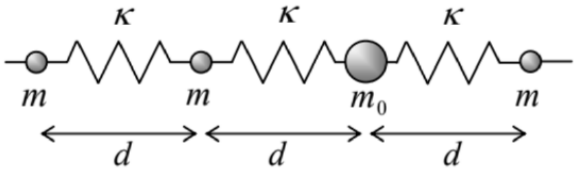

6.15*

(i) Explore an approximate way to analyze waves in a continuous 1D system with parameters slowly varying along its length.

(ii) Apply this method to calculate the frequencies of transverse standing waves on a freely hanging heavy rope of length l, with a constant mass μ per unit length - see the figure on the right.

(iii) For the three lowest standing wave modes, compare the results with those obtained in the solution of Problem 4 for the triple pendulum.

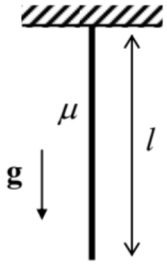

Hint: The reader familiar with the WKB approximation in quantum mechanics (see, e.g., QM Sec. 2.4) is welcome to adapt it for this classical application. Another possible starting point is the van der Pol approximation discussed in Sec. 5.3, which should be translated from the time domain to the space domain.

6.16. * Use the van der Pol approximation to analyze the mutual phase locking of two weakly coupled self-oscillators with the dissipative nonlinearity, for the cases of:

(i) the direct coordinate coupling, described by Eq. (5), and

(ii) a bilinear but otherwise arbitrary coupling of two similar oscillators.

Hint: In Task (ii), describe the coupling by a linear operator, and express the result via its Fourier image.

6.17. * Extend the second task of the previous problem to the mutual phase locking of N similar self-oscillators. In particular, explore the in-phase mode's stability for the case of the so-called global coupling via a single force F contributed equally by all oscillators.

6.18. * Find the condition of non-degenerate parametric excitation in a system of two coupled oscillators, described by Eqs. (5), but with a time-dependent coupling: $\kappa \to \kappa\left(1+\mu\cos\omega_{\mathrm{p}}t\right)$, with $\omega_{\mathrm{p}} \approx \Omega_1+\Omega_2$, and $\kappa/m << \left|\Omega_2-\Omega_1\right|$.

Hint: Assuming the modulation depth μ, static coupling κ, and detuning $\xi \equiv \omega_{\mathrm{p}}-\left(\Omega_1+\Omega_2\right)$ sufficiently small, use the van der Pol approximation for each of the coupled oscillators.

6.19. Show that the cubic nonlinearity of the type αq^3 indeed enables the parametric interaction ("four-wave mixing") of oscillations with incommensurate frequencies related by Eqs. (92a).

6.20. Calculate the velocity of the transverse waves propagating on a thin, planar, elastic membrane, with mass m per unit area, pre-stretched with force τ per unit width.

---

[33] This is a good model for small oscillations of linear molecules such as the now-infamous CO_2.

CHAPTER OVERVIEW

7: Deformations and Elasticity

The objective of this chapter is a brief discussion of small deformations of $3D$ continua, with a focus on the elastic properties of solids. The reader will see that such deformations are nontrivial even in the absence of their time evolution, so that several key problems of statics will need to be discussed before proceeding to such dynamic phenomena as elastic waves in infinite media and thin rods.

7.1: Strain

As was discussed in Chapters 4 and 6, in a continuum, i.e. a system of particles so close to each other that the system discreteness may be neglected, the particle displacement $\mathbf{q}$ may be considered as a continuous function of space and time. In this chapter, we will consider only small deviations from the rigid-body approximation discussed in Chapter 4, i.e. small deformations. The deformation smallness allows one to consider the displacement vector $\mathbf{q}$ as a function of the initial (pre-deformation) position of the particle, $\mathbf{r}$, and time t - just as was done in Chapter 6 for 1D waves.

The first task of the deformation theory is to exclude from consideration the types of motion considered in Chapter 4, namely the translation and rotation, unrelated to deformations. This means, first of all, that the variables describing deformations should not depend on the part of displacement distribution, that is independent of the position $\mathbf{r}$ (i.e. is common for the whole media), because that part corresponds to a translational shift rather than to a deformation (Figure 1a). Moreover, even certain nonuniform displacements do not contribute to deformation. For example, Eq. (4.9) (with $d\mathbf{r}$ replaced with $d\mathbf{q}$ to comply with our current notation) shows that a small displacement of the type

$$d\mathbf{q}_{\text{rotation}} = d\varphi \times \mathbf{r}, \tag{7.1.1}$$

where $d\varphi = \omega dt$ is an infinitesimal vector common for the whole continuum, corresponds to its rotation about the direction of that vector, and has nothing to do with its deformation (Figure 1b).

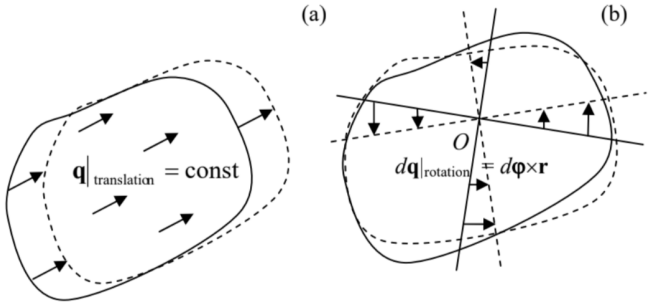

Figure 7.1. Two types of displacement vector distributions that are unrelated to deformation: (a) translation and (b) rotation.

This is why to develop an adequate quantitative characterization of deformation, we should start with finding suitable functions of the spatial distribution of displacements, $\mathbf{q}(\mathbf{r})$, that exist only due to deformations. One of such measures is the change of the distance $dl = |d\mathbf{r}|$ between two close points:

$$(dl)^2\big|_{\text{after deformation}} - (dl)^2\big|_{\text{before deformation}} = \sum_{j=1}^{3} (dr_j + dq_j)^2 - \sum_{j=1}^{3} (dr_j)^2 \tag{7.1.2}$$

where dq_j is the j^{th} Cartesian component of the difference $d\mathbf{q}$ between the displacements $\mathbf{q}$ of these close points. If the deformation is small in the sense $|d\mathbf{q}| << |d\mathbf{r}| = dl$, we may keep in Eq. (2) only the terms proportional to the first power of the infinitesimal vector $d\mathbf{q}$:

$$(dl)^2\big|_{\text{after deformation}} - (dl)^2\big|_{\text{before deformation}} = \sum_{j=1}^{3} \left[2dr_j dq_j + (dq_j)^2\right] \approx 2\sum_{j=1}^{3} dr_j dq_j. \tag{7.1.3}$$

Since q_j is a function of three independent scalar arguments r_j, its full differential (at fixed time) may be represented as

$$dq_j = \sum_{j'=1}^{3} \frac{\partial q_j}{\partial r_{j'}} dr_{j'} \tag{7.1.4}$$

The coefficients $\partial q_j / \partial r_j$, may be considered as elements of a tensor [1] providing a linear relation between the vectors d$\mathbf{r}$ and d$\mathbf{q}$. Plugging Eq. (4) into Eq. (2), we get

$$(dl)^2\big|_{\text{after deformation}} - (dl)^2_{|\text{before deformation}} = 2\sum_{j,j'=1}^{3} \frac{\partial q_j}{\partial r_{j'}} dr_j dr_{j'}. \tag{7.1.5}$$

The convenience of the tensor $\partial q_j/\partial r_j$, for characterizing deformations is that it automatically excludes the translation displacement (Figure 1a), which is independent of r_j. Its drawback is that its particular components are still affected by the rotation of the body (though the sum (5) is not). Indeed, according to the vector product definition, Eq. (1) may be represented in Cartesian coordinates as

$$dq_j|_{\text{rotation}} = \left(d\varphi_{j'} r_{j''} - d\varphi_{j''} r_{j'}\right) \varepsilon_{jj'j''}, \tag{7.1.6}$$

where ε_{ijij} is the Levi-Civita symbol. Differentiating Eq. (6) over a particular Cartesian coordinate of vector $\mathbf{r}$, and taking into account that this partial differentiation (∂) is independent of (and hence may be swapped with) the differentiation (d) over the rotation angle φ, we get the amounts,

$$d\left(\frac{\partial q_j}{\partial r_{j'}}\right)_{\text{rotation}} = -\varepsilon_{ijj''} d\varphi_{j''}, \quad d\left(\frac{\partial q_{j'}}{\partial r_j}\right)_{\text{rotation}} = -\varepsilon_{ji'j''} d\varphi_{j''} = \varepsilon_{jj'j''} d\varphi_{j''}, \tag{7.1.7}$$

which may differ from 0 . However, notice that the sum of these two differentials equals zero for any $d\varphi$, which is possible only if [2]

$$\left(\frac{\partial q_{j'}}{\partial r_j} + \frac{\partial q_j}{\partial r_{j'}}\right)_{\text{rotation}} = 0, \quad \text{for } j \neq j'. \tag{7.1.8}$$

This is why it is convenient to rewrite Eq. (5) in a mathematically equivalent form,

$$(dl)^2\big|_{\text{affer deformation}} - (dl)^2 \mid \ |\text{before deformation} = 2\sum_{j,j'=1}^{3} s_{ij'} dr_j dr_{j'}, \tag{7.1.9}$$

where s_{jj} ' are the elements of the so-called symmetrized strain tensor, defined as

$$s_{ij'} \equiv \frac{1}{2}\left(\frac{\partial q_j}{\partial r_{j'}} + \frac{\partial q_{j'}}{\partial r_j}\right). \tag{7.1.10}$$

(Note that this modification does not affect the diagonal elements: $s_{jj} = \partial q_j/\partial r_j$.). The advantage of the symmetrized tensor (9 b) over the initial tensor with elements $\partial q_j/\partial r_j$, is that according to Eq. (8), at pure rotation, all elements of the symmetrized strain tensor vanish.

Now let us discuss the physical meaning of this tensor. As was already mentioned in Sec. 4.2, any symmetric tensor may be diagonalized by an appropriate selection of the reference frame axes. In such principal axes, $s_{jj} = s_{jj}\delta_{jj}$, so that Eq. (4) takes a simple form:

$$dq_j = \frac{\partial q_j}{\partial r_j} dr_j = s_{jj} dr_j. \tag{7.1.11}$$

We may use this expression to calculate the change of each side of an elementary cuboid (parallelepiped) with sides dq_j parallel to the principal axes:

$$dr_j|_{\text{after deformation}} - dr_j|_{\text{before deformation}} \equiv dq_j = s_{jj} dr_j, \tag{7.1.12}$$

and of cuboid's volume $dV = dr_1 dr_2 dr_3$:

$$dV|_{\text{after deformation}} - dV|_{\text{before deformation}} = \prod_{j=1}^{3}(dr_j + s_{jj} dr_j) - \prod_{j=1}^{3} dr_j = dV\left[\prod_{j=1}^{3}(1 + s_{jj}) - 1\right] \tag{7.1.13}$$

Since all our analysis is only valid in the linear approximation in small s_{jj}, Eq. (12) is reduced to

$$dV|_{\text{after deformation}} - dV|_{\text{before deformation}} \approx dV \sum_{j=1}^{3} s_{jj} \equiv dV\,\mathrm{Tr(s)}, \tag{7.1.14}$$

where $\mathrm{Tr}(\text{ trace })$[3] of any matrix (in particular, any tensor) is the sum of its diagonal elements; in our current case [4]

$$\mathrm{Tr(s)} \equiv \sum_{j=1}^{3} s_{jj} \tag{7.1.15}$$

So, the diagonal components of the tensor characterize the medium's compression/extension; then what is the meaning of its off-diagonal components? It may be illustrated on the simplest example of purely shear deformation, shown in Figure 2 (the geometry is assumed to be uniform along the z-axis normal to the plane of the drawing). In this case, all displacements (assumed small) have just one Cartesian component, in Figure 2 along the x-axis: $\mathbf{q} = \mathbf{n}_x \alpha y$ (with $\alpha < 1$), so that the only nonzero component of the initial strain tensor $\partial q_j / \partial r_j$, is $\partial q_x / \partial y = \alpha$, and the symmetrized tensor (9 b) is

$$\mathrm{s} = \begin{pmatrix} 0 & \alpha/2 & 0 \\ \alpha/2 & 0 & 0 \\ 0 & 0 & 0 \end{pmatrix}. \tag{7.1.16}$$

Evidently, the change of volume, given by Eq, (13), vanishes in this case. Thus, off-diagonal elements of the tensor s characterize shear deformations.

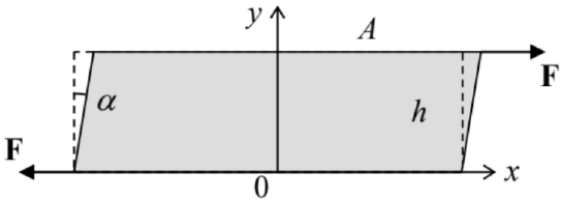

Figure 7.2. An example of pure shear.

To conclude this section, let me note that Eq. (9) is only valid in Cartesian coordinates. For the solution of some important problems with the axial or spherical symmetry, it is frequently convenient to express six different components of the symmetric strain tensor via three components of the displacement vector $\mathbf{q}$ in either cylindrical or spherical coordinates. A straightforward differentiation of the definitions of these curvilinear coordinates, similar to that used to derive the well-known expressions for spatial derivatives, [5] yields, in particular, the following formulas for the diagonal elements of the tensor:

(i) in the cylindrical coordinates:

$$s_{\rho\rho} = \frac{\partial q_\rho}{\partial \rho}, \quad s_{\varphi\varphi} = \frac{1}{\rho}\left(q_r + \frac{\partial q_\varphi}{\partial \varphi}\right), \quad s_{zz} = \frac{\partial q_z}{\partial z}. \tag{7.1.17}$$

(ii) in the spherical coordinates:

$$s_{rr} = \frac{\partial q_r}{\partial r}, \quad s_{\theta\theta} = \frac{1}{r}\left(q_r + \frac{\partial q_\theta}{\partial \theta}\right), \quad s_{\varphi\varphi} = \frac{1}{r}\left(q_r + q_\theta \frac{\cos\theta}{\sin\theta} + \frac{1}{\sin\theta}\frac{\partial q_\varphi}{\partial \varphi}\right). \tag{7.1.18}$$

These expressions, which will be used below for the solution of some problems for symmetrical geometries, may be a bit counter-intuitive. Indeed, Eq. (16) shows that even for a purely radial, axiallysymmetric deformation, $\mathbf{q} = \mathbf{n}_\rho q(\rho)$, the angular component of the strain tensor does not vanish: $s_{\varphi\varphi} = q/\rho$. (According to Eq. (17), in the spherical coordinates, both angular components of the tensor exhibit the same property.) Note, however, that this relation describes a very simple geometric effect: the change of the lateral distance $\rho d\varphi << \rho$ between two close points with the same distance from the symmetry axis, at a small change of ρ, that keeps the angle $d\varphi$ between the directions towards these two points constant.

---

[1] Since both $d\mathbf{q}$ and $d\mathbf{r}$ are legitimate physical vectors (whose Cartesian components are properly transformed as the transfer between reference frames), the 3×3 matrix with elements $\partial q_j / \partial r_j$, is indeed a legitimate physical tensor - see the discussion in Sec. 4.2.

[2] As a result, the full sum (5), which includes three partial sums (8), is not affected by rotation - as we already know.

[3] The traditional European notation for Tr is Sp (from the German Spur meaning "trace" or "track").

[4] Actually, the tensor theory shows that the trace does not depend on the particular choice of the coordinate axes.

[5] See, e.g., MA Eqs. (10.1)-(10.12).

7.2: Stress

Now let us discuss the forces that cause the strain - or, from an alternative point of view, are caused by the strain. Internal forces acting inside (i.e. between arbitrarily defined parts of) a continuum may be also characterized by a tensor. This stress tensor, [6] with elements $\sigma_{jj'}$, relates the Cartesian components of the vector $d\mathbf{F}$ of the force acting on an elementary area dA of an (in most cases, imagined) interface between two parts of a continuum, with the components of the elementary vector $d\mathbf{A} = \mathbf{n}dA$ normal to the area – see Figure 3:

$$dF_j = \sum_{j'=1}^{3} \sigma_{ij'} dA_{j'}. \tag{7.2.1}$$

The usual sign convention here is to take the outer normal $d\mathbf{n}$, i.e. to direct $d\mathbf{A}$ out of "our" part of the continuum, i.e. the part on which the calculated force $d\mathbf{F}$ is exerted - by the complementary part.

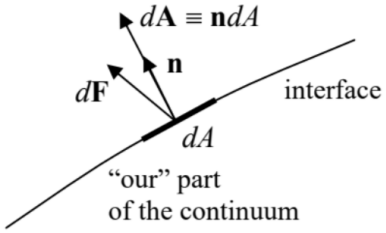

Figure 7.3. The definition of vectors $d\mathbf{A}$ and $d\mathbf{F}$.

In some cases, the stress tensor's structure is very simple. For example, as will be discussed in detail in the next chapter, static and ideal fluids (i.e. liquids and gases) may only provide forces normal to any interface, and usually directed toward "our" part of the body, so that

$$d\mathbf{F} = -\mathcal{P}d\mathbf{A}, \quad \text{i.e. } \sigma_{ij'} = -\mathcal{P}\delta_{jj'}, \tag{7.2.2}$$

where the scalar $\mathcal{P}$ (in most cases positive) is called pressure, and generally may depend on both the spatial position and time. This type of stress, with $\mathcal{P} > 0$, is frequently called hydrostatic compressioneven if it takes place in solids, as it may.

However, in the general case, the stress tensor also has off-diagonal terms, which characterize the shear stress. For example, if the shear strain, shown in Figure 2, is caused by a pair of forces $\pm\mathbf{F}$, they create internal forces $F_x\mathbf{n}_x$, with $F_x > 0$ if we speak about the force acting upon a part of the sample below the imaginary horizontal interface we are discussing. To avoid a horizontal acceleration of each horizontal slice of the sample, the forces should not depend on y, i.e. $F_x = \text{const} = F$. Superficially, it may look that in this case, the only nonzero component of the stress tensor is $dF_x/dA_y = F/A = \text{const}$, so that tensor is asymmetric, in contrast to the strain tensor (15) of the same system. Note, however, that the pair of forces $\pm\mathbf{F}$ creates not only the shear stress but also a nonzero rotating torque $\tau = -Fh\mathbf{n}_z = -(dF_x/dA_y)Ah\mathbf{n}_z = -(dF_x/dA_y)V\mathbf{n}_z$, where $V = Ah$ is sample's volume. So, if we want to perform a static stress experiment, i.e. avoid sample's rotation, we need to apply some other forces, e.g., a pair of vertical forces creating an equal and opposite torque $\tau' = (dF_y/dA_x)V\mathbf{n}_z$, implying that $dF_y/dA_x = dF_x/dA_y = F/A$. As a result, the stress tensor becomes symmetric, and similar in structure to the symmetrized strain tensor (15):

$$\sigma = \begin{pmatrix} 0 & F_0/A & 0 \\ F_0/A & 0 & 0 \\ 0 & 0 & 0 \end{pmatrix}. \tag{7.2.3}$$

In many situations, the body may be stressed not only by forces applied to their surfaces but also by some volume-distributed (bulk) forces $d\mathbf{F} = \mathbf{f}dV$, whose certain effective bulk density $\mathbf{f}$. (The most evident example of such forces is gravity. If its field is uniform as described by Eq. (1.16), then $\mathbf{f} = \rho\mathbf{g}$, where ρ is the mass density.) Let us derive the key formula describing the summation of the interface and bulk forces. For that, consider again an elementary cuboid with sides dr_j parallel to the corresponding coordinate axes (Figure 4) - now not necessarily the principal axes of the stress tensor.

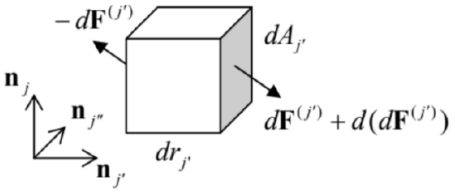

Figure 7.4. Deriving Eq. (23).

If elements $\sigma_{ij'}$ of the tensor do not depend on position, the force $d\mathbf{F}^{(j)}$ acting on the j' '-th face of the cuboid is exactly balanced by the equal and opposite force acting on its opposite face, because the vectors $d\mathbf{A}^{(j')}$ at these faces are equal and opposite. However, if σ_{ij} is a function of $\mathbf{r}$, then the net force $d\left(d\mathbf{F}^{(j)}\right)$ does not vanish. (In this expression, the first differential sign refers to the elementary shift dr_j, while the second one, to the elementary area $dA_{j'}$.) Using the expression $\sigma_{ij}dA_j$, for to the j, th contribution to the sum (18), in the first order in $d\mathbf{r}$ the j^{th} components of the vector $d\left(d\mathbf{F}^{(j)}\right)$ is

$$d\left(dF_j^{(j')}\right) = d\left(\sigma_{ij'}dA_{j'}\right) = \frac{\partial\sigma_{jj'}}{\partial r_{j'}}dr_{j'}dA_{j'} \equiv \frac{\partial\sigma_{ij'}}{\partial r_{j'}}dV, \tag{7.2.4}$$

where the cuboid's volume $dV = dr_j \cdot dA_j$ ' evidently does not depend on the index j '. The addition of these force components for all three pairs of cuboid faces, i.e. the summation of Eqs. (21) over all three values of the upper index j ', yields the following relation for the j^{th} Cartesian component of the net force exerted on the cuboid:

$$d\left(dF_j\right) = \sum_{j'=1}^{3} d\left(dF_j^{(j')}\right) = \sum_{j'=1}^{3} \frac{\partial\sigma_{ij'}}{\partial r_{j'}}dV. \tag{7.2.5}$$

Since any volume may be broken into such infinitesimal cuboids, Eq. (22) shows that the space-varying stress is equivalent to a volume-distributed force $d\mathbf{F}_{\text{ef}} = \mathbf{f}_{\text{ef}}\,dV$, whose effective (not real!) bulk density $\mathbf{f}_{\text{ef}}$ has the following Cartesian components

$$\left(f_{\text{ef}}\right)_j = \sum_{j'=1}^{3} \frac{\partial\sigma_{ij'}}{\partial r_{j'}}, \tag{7.2.6}$$

so that in the presence of genuinely bulk forces $d\mathbf{F} = \mathbf{f}dV$, densities $\mathbf{f}_{\text{ef}}$ and $\mathbf{f}$ just add up. This the socalled Euler-Cauchy stress principle.

Let us use this addition rule to spell out the 2^{nd} Newton law for a unit volume of a continuum:

$$\rho\frac{\partial^2\mathbf{q}}{\partial t^2} = \mathbf{f}_{\text{ef}} + \mathbf{f}. \tag{7.2.7}$$

Using Eq. (23), the j^{th} Cartesian component of Eq. (24) may be represented as

$$\rho\frac{\partial^2 q_j}{\partial t^2} = \sum_{j'=1}^{3} \frac{\partial\sigma_{ij'}}{\partial r_{j'}} + f_j. \tag{7.2.8}$$

This is the key equation of the continuum's dynamics (and statics), which will be repeatedly used below.

For the solution of some problems, it is also convenient to have a general expression for the work $\delta\mathscr{W}$ of the stress forces at a virtual deformation $\delta\mathbf{q}$ - understood in the same variational sense as the virtual displacements $\delta\mathbf{r}$ in Sec. 2.1. Using the Euler-Cauchy principle (23), for any volume V of a medium not affected by volume-distributed forces, we may write [7]

$$\delta\mathscr{W} = -\int_V \mathbf{f}_{\text{ef}} \cdot \delta\mathbf{q}\,d^3r = -\sum_{j=1}^{3}\int_V \left(f_{\text{ef}}\right)_j \delta q_j d^3r = -\sum_{j,j'=1}^{3}\int_V^{\partial\sigma_{ij'}} \frac{\partial r_{j'}}{\partial q_j}d^3r. \tag{7.2.9}$$

Let us work out this integral by parts for a volume so large that the deformations δq_j on its surface are negligible. Then, swapping the operations of the variation and the spatial differentiation (just like it was done with the time derivative in Sec. 2.1), we get

$$\delta\mathscr{W} = \sum_{j,j'=1}^{3}\int_V \sigma_{ij'}\delta\frac{\partial q_j}{\partial r_{j'}}d^3r. \tag{7.2.10}$$

Assuming that the tensor σ_{ij}, is symmetric, we may rewrite this expression as

$$\delta \mathscr{W} = \frac{1}{2} \sum_{j,j'=1}^{3} \int_V \left(\sigma_{jj'} \delta \frac{\partial q_j}{\partial r_{j'}} + \sigma_{jj} \delta \frac{\partial q_j}{\partial r_{j'}} \right) d^3 r. \tag{7.2.11}$$

Now, swapping indices j and j ' in the second expression, we finally get

$$\delta \mathscr{H} = \frac{1}{2} \sum_{j,j'=1}^{3} \int_V \delta \left(\frac{\partial q_j}{\partial r_{j'}} \sigma_{ij'} + \frac{\partial q_{j'}}{\partial r_j} \sigma_{jj'} \right) d^3 r = - \sum_{j,j'=1}^{3} \int_V \sigma_{ij'} \delta s_{jj'} d^3 r, \tag{7.2.12}$$

where s_{jj} ' are the components of the strain tensor (9b). It is natural to rewrite this important formula as

$$\delta \mathscr{W} = \int_V \delta w(\mathbf{r}) d^3 r, \quad \text{where } \delta w(\mathbf{r}) \equiv \sum_{j,j'=1}^{3} \sigma_{ij'} \delta s_{jj}, \tag{7.2.13}$$

and interpret the locally-defined scalar function $\delta_{rc}(\mathbf{r})$ as the work of the stress forces per unit volume, at a small variation of the deformation.

As a sanity check, for the pure pressure (19), Eq. (30) is reduced to the evidently correct result $\delta \mathscr{W} = -\mathcal{P} \delta V$, where V is the volume of "our" part of the continuum.

---

[6] It is frequently called the Cauchy stress tensor, partly to honor Augustin-Louis Cauchy who introduced this notion (and is responsible for the development, mostly in the 1820s, much of the theory described in this chapter), and partly to distinguish it from and other possible definitions of the stress tensor, including the 1^{st} and 2^{nd} PiolaKirchhoff tensors. For the small deformations discussed in this course, all these notions coincide.

[7] Here the sign corresponds to the work of the "external" stress force $d\mathbf{F}$, exerted on "our" part of the continuum by its counterpart - see Figure 3. Note that some texts consider the opposite definition of $\delta \mathscr{H}$, leading to its opposite sign.

7.3: Hooke's Law

In order to form a complete system of equations describing the continuum's dynamics, one needs to complement Eq. (25) with an appropriate constitutive equation describing the relation between the forces described by the stress tensor σ_{ij}, and the deformations $\mathbf{q}$ described (in the small deformation limit) by the strain tensor s_{jj}. This relation depends on the medium, and generally may be rather complex. Even leaving alone various anisotropic solids (e.g., crystals) and macroscopicallyinhomogeneous materials (like ceramics or sand), strain typically depends not only on the current value of stress (possibly in a nonlinear way), but also on the previous history of stress application. Indeed, if strain exceeds a certain plasticity threshold, atoms (or nanocrystals) may slip to their new positions and never come back even if the strain is reduced. As a result, deformations become irreversible - see Figure 5 .

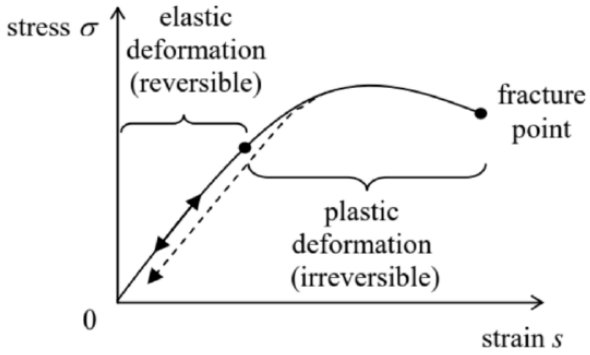

Figure 7.5. A typical relation between the stress and strain in solids (schematically).

Only below the thresholds of nonlinearity and plasticity (which are typically close to each other), the strain is nearly proportional to stress, i.e. obeys the famous Hooke's law. [8] However, even in this elastic range, the law is not quite simple, and even for an isotropic medium is described not by one but by two constants, called the elastic moduli. The reason for that is that most elastic materials resist the strain accompanied by a volume change (say, the hydrostatic compression) differently from how they resist a shear deformation.

To describe this difference, let us first represent the symmetrized strain tensor $(9b)$ in the following mathematically equivalent form:

$$s_{ij'} = \left(s_{jj'} - \frac{1}{3}\delta_{ij'}\,\mathrm{Tr(s)}\right) + \left(\frac{1}{3}\delta_{jj'}\,\mathrm{Tr(s)}\right). \tag{7.3.1}$$

According to Eq. (13), the traceless tensor in the first parentheses of Eq. (31) does not give any contribution to the volume change, e.g., may be used to characterize a purely shear deformation, while the second term describes the hydrostatic compression alone. Hence we may expect that the stress tensor may be represented (again, within the elastic deformation range only!) as

$$\sigma_{ij'} = 2\mu\left(s_{ij'} - \frac{1}{3}\mathrm{Tr(s)}\delta_{jj'}\right) + 3K\left(\frac{1}{3}\mathrm{Tr(s)}\delta_{jj'}\right) \tag{7.3.2}$$

where K and μ are constants. (The inclusion of coefficients 2 and 3 into Eq. (32) is justified by the simplicity of some of its corollaries - see, e.g., Eqs. (36) and (41) below.) Indeed, experiments show that Hooke's law in this form is followed, at small strain, by all isotropic materials. In accordance with the above discussion, the constant μ (in some texts, denoted as G) is called the shear modulus, while the constant K (sometimes denoted B), the bulk modulus. The two left columns of Table 1 show the approximate values of these moduli for typical representatives of several major classes of materials. [9]

Table 7.1. Elastic moduli, density, and sound velocities of a few representative materials (approximate values)

	K(GPa)	μ(GPa)	E(GPa)	v	$\rho\,(\mathrm{kg/m^3})$	$v_1(\mathrm{\ m/s})$	$v_t(\mathrm{m/s})$
Diamond [a]	600	450	1,100	0.20	3,500	1,830	1,200
Hardened steel	170	75	200	0.30	7,800	5,870	3,180
Water [b]	2.1	0	0	0.5	1,000	1,480	0
Air [b]	0.00010	0	0	0.5	1.2	332	0

(a) Averages over crystallographic directions (10% anisotropy).

(b) At the so-called ambient conditions $(T = 20^\circ\mathrm{C}, P = 1\ \text{bar} \equiv 10^5\ \text{Pa})$.

To better appreciate these values, let us first discuss the quantitative meaning of K and μ, using two simple examples of elastic deformation. However, in preparation for that, let us first solve the set of nine (or rather six different) linear equations (32) for s_{jj}. This is easy to do, due to the simple structure of these equations: they relate the components $\sigma_{ij'}$ and $s_{ij'}$ ' with the same indices, besides the involvement of the tensor's trace. This slight complication may be readily overcome by noticing that according to Eq. (32),

$$\mathrm{Tr}(\sigma) \equiv \sum_{j=1}^{3} \sigma_{jj} = 3K\,\mathrm{Tr}(\mathrm{s}), \quad \text{so that } \mathrm{Tr}(\mathrm{s}) = \frac{1}{3K}\mathrm{Tr}(\sigma). \tag{7.3.3}$$

Plugging this result into Eq. (32) and solving it for s_{jj}, we readily get the reciprocal relation, which may be represented in a similar form:

$$s_{ij'} = \frac{1}{2\mu}\left(\sigma_{jj'} - \frac{1}{3}\mathrm{Tr}(\sigma)\delta_{jj'}\right) + \frac{1}{3K}\left(\frac{1}{3}\mathrm{Tr}(\sigma)\delta_{jj'}\right). \tag{7.3.4}$$

Now let us apply Hooke's law, in the form of Eqs. (32) or (34), to two simple situations in which the strain and stress tensors may be found without using the full differential equation of the elasticity theory and boundary conditions for them. (That will be the subject of the next section.) The first situation is the hydrostatic compression when the stress tensor is diagonal, and all its diagonal components are equal - see Eq. (19). [10] For this case Eq. (34) yields

$$s_{jj'} = -\frac{\mathcal{P}}{3K}\delta_{jj'}, \tag{7.3.5}$$

i.e. regardless of the shear modulus, the strain tensor is also diagonal, with all diagonal components equal. According to Eqs. (11) and (13), this means that all linear dimensions of the body are reduced by a similar factor, so that its shape is preserved, while the volume is reduced by

$$\frac{\Delta V}{V} = \sum_{j=1}^{3} s_{jj} = -\frac{\mathcal{P}}{K}. \tag{7.3.6}$$

This formula clearly shows the physical sense of the bulk modulus K as the reciprocal compressibility. As Table 1 shows, the values of K may be dramatically different for various materials, and even for such "soft stuff" as water this modulus is actually rather high. For example, even at the bottom of the deepest, $10-\mathrm{km}$ ocean well $(\mathcal{P} \approx 10^3\ \text{bar} \approx 0.1\mathrm{GPa})$, the water's density increases by just about 5%. As a result, in most human-scale experiments, water may be treated as incompressible - a condition that will be widely used in the next chapter. Many solids are even much less compressible see, for example, the first two rows of Table 1 .

Quite naturally, the most compressible media are gases. For a portion of gas, a certain background pressure $\mathcal{P}$ is necessary just for containing it within its volume V, so that Eq. (36) is only valid for small increments of pressure, $\Delta\mathcal{P}$:

$$\frac{\Delta V}{V} = -\frac{\Delta\mathcal{P}}{K}. \tag{7.3.7}$$

Moreover, the compression of gases also depends on thermodynamic conditions. (In contrast, for most condensed media, the temperature effects are very small.) For example, at ambient conditions most gases are reasonably well described by the equation of state for the model called the ideal classical gas:

$$\mathcal{P}V = Nk_{\mathrm{B}}T, \quad \text{i.e. } \mathcal{P} = \frac{Nk_{\mathrm{B}}T}{V}. \tag{7.3.8}$$

where N is the number of molecules in volume V, and $k_{\mathrm{B}} \approx 1.38 \times 10^{-23}\ \mathrm{J/K}$ is the Boltzmann constant. [11] For a small volume change ΔV at a constant temperature T, this equation gives

$$\Delta\mathcal{P}|_{T=\text{const}} = -\frac{Nk_{\mathrm{B}}T}{V^2}\Delta V = -\frac{\mathcal{P}}{V}\Delta V, \quad \text{i.e. } \left.\frac{\Delta V}{V}\right|_{T=\text{const}} = -\frac{\Delta\mathcal{P}}{P}. \tag{7.3.9}$$

Comparing this expression with Eq. (36), we get a remarkably simple result for the isothermal compression of gases,

$$K|_{T=\text{const}} = \mathcal{P}, \tag{7.3.10}$$

which means in particular that the bulk modulus listed in Table 1 is actually valid, at the ambient conditions, for almost any gas. Note, however, that the change of thermodynamic conditions (say, from isothermal to adiabatic [12]) may affect the compressibility of the gas. Now let us consider the second, rather different, fundamental experiment: a purely shear deformation shown in Figure 2. Since the traces of the matrices (15) and (20), which describe this situation, are equal to 0 , for their off-diagonal elements, Eq. (32) gives merely $\sigma_{jj}{}' = 2\mu s_{jj}$, so that the deformation angle α (see Figure 2) is just

$$\alpha = \frac{1}{\mu}\frac{F}{A}. \tag{7.3.11}$$

Note that the angle does not depend on the thickness h of the sample, though of course the maximal linear deformation $q_x = \alpha h$ is proportional to the thickness. Naturally, as Table 1 shows, $\mu = 0$ for all fluids, because they do not resist static shear stress.

However, not all situations, even apparently simple ones, involve just either K or μ. Let us consider stretching a long and thin elastic rod of a uniform cross-section of area A - the so-called tensile stress experiment shown in Figure 6.13

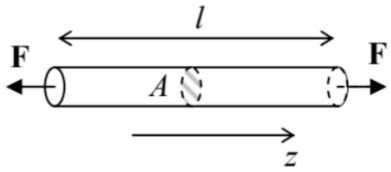

Figure 7.6. The tensile stress experiment.

Though the deformation of the rod near its clamped ends depends on the exact way forces $\mathbf{F}$ are applied (we will discuss this issue later on), we may expect that over most of its length the tension forces are directed virtually along the rod, $d\mathbf{F} = F_z \mathbf{n}_z$, and hence, with the coordinate choice shown in Figure 6, $\sigma_{xj} = \sigma_{yj} = 0$ for all j, including the diagonal elements σ_{xx} and σ_{yy}. Moreover, due to the open lateral surfaces, on which, evidently, $dF_x = dF_y = 0$, there cannot be an internal stress force of any direction, acting on any elementary internal boundary parallel to these surfaces. This means that $\sigma_{zx} = \sigma_{zy} = 0$. So, of all components of the stress tensor only one, σ_{zz}, is not equal to zero, and for a uniform sample, $\sigma_{zz} = \text{const} = F/A$. For this case, Eq. (34) shows that the strain tensor is also diagonal, but with different diagonal elements:

$$s_{zz} = \left(\frac{1}{9K} + \frac{1}{3\mu}\right)\sigma_{zz},$$
$$s_{xx} = s_{yy} = \left(\frac{1}{9K} - \frac{1}{6\mu}\right)\sigma_{zz}.$$

Since the tensile stress is most common in engineering practice (and in physical experiment design), both combinations of the elastic moduli participating in these two relations have deserved their own names. In particular, the constant in Eq. (42) is usually denoted as $1/E$ (but in many texts, as $1/Y$), where E is called Young's modulus: 14

$$\frac{1}{E} \equiv \frac{1}{9K} + \frac{1}{3\mu}, \quad \text{i.e. } E \equiv \frac{9K\mu}{3K+\mu} \tag{7.3.12}$$

As Figure 6 shows, in the tensile stress geometry $s_{zz} \equiv \partial q_z/\partial z = \Delta l/l$ so that Young's modulus scales the linear relation between the relative extension of the rod and the force applied per unit area: [15]

$$\frac{\Delta l}{l} = \frac{1}{E}\frac{F}{A}. \tag{7.3.13}$$

The third column of Table 1 above shows the values of this modulus for two well-known solids: diamond (with the highest known value of E of all bulk materials [16]) and the steels (solid solutions of $\sim 10\%$ of carbon in iron) used in construction. Again, for all fluids, Young's modulus equals zero - as it follows from Eq. (44) for $\mu = 0$.

I am confident that the reader of these notes has been familiar with Eq. (42), in the form of Eq. (45), from their undergraduate studies. However, most probably this cannot be said about its counterpart, Eq. (43), which shows that at the tensile stress, the rod's cross-section dimensions also change. This effect is usually characterized by the following dimensionless Poisson's ratio: [17]

$$-\frac{s_{xx}}{s_{zz}} = -\frac{s_{yy}}{s_{zz}} = -\left(\frac{1}{9K} - \frac{1}{6\mu}\right) \Big/ \left(\frac{1}{9K} + \frac{1}{3\mu}\right) = \frac{1}{2}\frac{3K-2\mu}{3K+\mu} \equiv v, \tag{7.3.14}$$

According to this formula, for realistic materials with $K>0, \mu \geq 0, v$ may vary from (-1) to $(+1/2)$, but for the vast majority of materials, [18] its values are between 0 and $1/2-$ see the corresponding column of Table 1. The lower limit of this range is reached in porous materials like cork, whose lateral dimensions almost do not change at the tensile stress. Some soft materials such as natural and synthetic rubbers present the opposite case: $v \approx 1/2$. [19] Since according to Eqs. (13) and (42), the volume change is

$$\frac{\Delta V}{V}=s_{xx}+s_{yy}+s_{zz}=\frac{1}{E}\frac{F}{A}(1-2v)\equiv(1-2v)\frac{\Delta l}{l}, \tag{7.3.15}$$

such materials virtually do not change their volume at the tensile stress. The ultimate limit of this trend, $\Delta V/V=0$, is provided by fluids and gases, because, as follows from Eq. (46) with $\mu=0$, their Poisson ratio v is exactly $1/2$. However, for most practicable construction materials such as various steels (see Table 1) the volume change (47) is as high as $\sim 40\%$ of that of the length.

Due to the clear physical sense of the coefficients E and v, they are frequently used as a pair of independent elastic moduli, instead of K and μ. Solving Eqs. (44) and (46) for them, we get

$$K=\frac{E}{3(1-2v)}, \quad \mu=\frac{E}{2(1+v)}. \tag{7.3.16}$$

Using these formulas, the two (equivalent) formulations of Hooke's law, expressed by Eqs. (32) and (34), may be rewritten as

$$\begin{aligned}\sigma_{ij'} &= \frac{E}{1+v}\left(s_{ij'}+\frac{v}{1-2v}\mathrm{Tr(s)}\delta_{jj'}\right)\\ s_{ij'} &= \frac{1+v}{E}\left(\sigma_{ij'}-\frac{v}{1+v}\mathrm{Tr}(\sigma)\delta_{ij'}\right)\end{aligned}$$

The linear relation between the strain and stress tensor in elastic continua enables one more step in our calculation of the potential energy U due to deformation, started at the end of Sec.2. Indeed, to each infinitesimal part of this strain increase, we may apply Eq. (30), with the elementary work $\delta \mathscr{W}$ of the surface forces increasing the potential energy of "our" part of the body by the equal amount δU. Let us slowly increase the deformation from a completely unstrained state (in which we may take $U=0$) to a certain strained state, in the absence of bulk forces $\mathbf{f}$, keeping the deformation type, i.e. the relation between the elements of the stress tensor, intact. In this case, all elements of the tensor σ_{ij} ' are proportional to the same single parameter characterizing the stress (say, the total applied force), and according to Hooke's law, all elements of the tensor s_{jj} are proportional to that parameter as well. In this case, integration of Eq. (30) through the variation yields the following final value: 20

$$U=\int_V u(\mathbf{r})d^3r, \quad u(\mathbf{r})=\frac{1}{2}\sum_{j,j'=1}^{3}\sigma_{ij'}S_{jj}. \tag{7.3.17}$$

Evidently, this $u(\mathbf{r})$ may be interpreted as the volumic density of the potential energy of the elastic deformation.

---

[8] Named after Robert Hooke (1635-1703), the polymath who was the first to describe the law in its simplest, 1D version.

[9] Since the strain tensor elements, defined by Eq. (9), are dimensionless, while the strain, defined by Eq. (18), has the dimensionality similar to pressure (of force per unit area), so do the elastic moduli K and μ.

[10] It may be proved that such a situation may be implemented not only in a fluid with pressure $\mathcal{P}$ but also in a solid sample of an arbitrary shape, for example by placing it into a compressed fluid.

[11] For the derivation and a detailed discussion of Eq. (37) see, e.g., SM Sec. 3.1.

[12] See, e.g., SM Sec. 1.3.

[13] Though the analysis of compression in this situation gives similar results, in practical experiments a strong compression of a long sample may lead to the loss of the horizontal stability - the so-called buckling - of the rod.

[14] Named after another polymath, Thomas Young (1773-1829) - somewhat unfairly, because his work on elasticity was predated by a theoretical analysis by L. Euler in 1727 and detailed experiments by Giordano Riccati in 1782.

[15] According to Eq. (47), E may be thought of as the force per unit area, which would double the initial sample's length, if only the Hooke's law was valid for deformations that large - as it typically isn't.

[16] It is probably somewhat higher (up to 2,000 GPa) in such nanostructures as carbon nanotubes and monatomic sheets (graphene), though there is still substantial uncertainty in experimentally measured elastic moduli of these structures - for a review see, e.g., G. Dimitrios et al., Prog. Mater. Sci. 90, 75 (2017).

[17] In some older texts, the Poisson's ratio is denoted σ, but its notation as v dominates modern literature.

[18] The only known exceptions are certain exotic solids with very specific internal microstructure - see, e.g., R. Lakes, Science 235, 1038 (1987) and references therein.

[19] For example, silicone rubbers (synthetic polymers broadly used in engineering and physics experiment design) have, depending on their particular composition, synthesis, and thermal curing, $v = 0.47 \div 0.49$, and as a result combine respectable bulk moduli $K = (1.5 \div 2)$ GPa with very low Young's moduli: $E = (0.0001 \div 0.05)$ GPa.

[20] For clarity, let me reproduce this integration for the extension of a simple 1D spring. In this case, $\delta U = \delta \mathscr{W} = F\delta x$, and if the spring's force is elastic, $F = \kappa x$, the integration yields $U = \kappa x^2/2 \equiv Fx/2$.

7.4: Equilibrium

Now we are fully equipped to discuss the elastic deformation dynamics, but let us start with statics. The static (equilibrium) state may be described by requiring the right-hand side of Eq. (25) to vanish. To find the elastic deformation, we need to plug σ_{ij} ' from Hooke's law (49a), and then express the elements s_{ij} ' via the displacement distribution - see Eq. (9). For a uniform material, the result is [21]

$$\frac{E}{2(1+v)}\sum_{j'=1}^{3}\frac{\partial^2 q_j}{\partial r_{j'}^2}+\frac{E}{2(1+v)(1-2v)}\sum_{j'=1}^{3}\frac{\partial^2 q_{j'}}{\partial r_j \partial r_{j'}}+f_j=0. \tag{7.4.1}$$

Taking into account that the first sum in Eq. (51) is just the j^{th} component of $\nabla^2\mathbf{q}$, while the second sum is the j^{th} component of $\nabla(\nabla\cdot\mathbf{q})$, we see that all three equations (51) for three Cartesian components ($j=$ 1,2 and 3) of the deformation vector $\mathbf{q}$, may be conveniently merged into one vector equation

$$\frac{E}{2(1+v)}\nabla^2\mathbf{q}+\frac{E}{2(1+v)(1-2v)}\nabla(\nabla\cdot\mathbf{q})+\mathbf{f}=0 \tag{7.4.2}$$

For some applications, it is more convenient to recast this equation into a different form, using the wellknown vector identity [22] $\nabla^2\mathbf{q}=\nabla(\nabla\cdot\mathbf{q})-\nabla\times(\nabla\times\mathbf{q})$. The result is

$$\frac{E(1-v)}{(1+v)(1-2v)}\nabla(\nabla\cdot\mathbf{q})-\frac{E}{2(1+v)}\nabla\times(\nabla\times\mathbf{q})+\mathbf{f}=0. \tag{7.4.3}$$

It is interesting that in problems without volume-distributed forces $(\mathbf{f}=0)$, Young's modulus E cancels out. Even more fascinating, in this case the equation may be re-written in a form not involving the Poisson ratio v either. Indeed, calculating the divergence of the remaining terms of Eq. (53), taking into account MA Eqs. (9.2) and (11.2), we get a surprisingly simple equation

$$\nabla^2(\nabla\cdot\mathbf{q})=0 \tag{7.4.4}$$

A natural question here is how do the elastic moduli affect the deformation distribution if they do not participate in the differential equation describing it. The answer is different is two cases. If what is fixed at the body's boundary are deformations, then the moduli are irrelevant, because the deformation distribution through the body does not depend on them. On the other hand, if the boundary conditions describe fixed stress (or a combination of stress and strain), then the elastic constants creep into the solution via the recalculation of these conditions into the strain.

As a simple but representative example, let us calculate the deformation distribution in a (generally, thick) spherical shell under the different pressures inside and outside it − see Figure 7 a.

(b)

Figure 7.7. The spherical shell problem: (a) the general case, and (b) the thin shell limit.

Due to the spherical symmetry of the problem, the deformation is obviously sphericallysymmetric and radial, $\mathbf{q}(\mathbf{r})=q(r)\mathbf{n}_r$, i.e. is completely described by one scalar function $q(r)$. Since the curl of such a radial vector field is zero, [23] Eq. (53) is reduced to

$$\nabla(\nabla\cdot\mathbf{q})=0, \tag{7.4.5}$$

This means that the divergence of the function $q(r)$ is constant within the shell. In the spherical coordinates: [24]

$$\frac{1}{r^2}\frac{d}{dr}\left(r^2 q\right)=\text{ const}. \tag{7.4.6}$$

Naming this constant $3a$ (with the numerical factor chosen just for the later notation's convenience), and integrating Eq. (56) over r, we get its solution,

$$q(r)=ar+\frac{b}{r^2}, \tag{7.4.7}$$

which also includes another integration constant, b. The constants a and b may be determined from the boundary conditions. Indeed, according to Eq. (19),

$$\sigma_{rr} = \begin{cases} -\mathcal{P}_1, & \text{at } r = R_1, \\ -\mathcal{P}_2, & \text{at } r = R_2. \end{cases} \tag{7.4.8}$$

In order to relate this stress to strain, let us use Hooke's law, but for that, we first need to calculate the strain tensor components for the deformation distribution (57). Using Eqs. (17), we get

$$s_{rr} = \frac{\partial q}{\partial r} = a - 2\frac{b}{r^3}, \quad s_{\theta\theta} = s_{\varphi\varphi} = \frac{q}{r} = a + \frac{b}{r^3}, \tag{7.4.9}$$

so that $\mathrm{Tr}(\mathrm{s}) = 3a$. Plugging these relations into Eq. (49a) for σ_{rr}, we get

$$\sigma_{rr} = \frac{E}{1+v}\left[\left(a - 2\frac{b}{r^3}\right) + \frac{v}{1-2v}3a\right]. \tag{7.4.10}$$

Now plugging this relation into Eqs. (58), we get a system of two linear equations for the coefficients a and b. Solving this system, we get:

$$a = \frac{1-2v}{E}\frac{\mathcal{P}_1 R_1^3 - \mathcal{P}_2 R_2^3}{R_2^3 - R_1^3}, \quad b = \frac{1+v}{2E}\frac{(\mathcal{P}_1 - \mathcal{P}_2) R_1^3 R_2^3}{R_2^3 - R_1^3}. \tag{7.4.11}$$

Formulas (57) and (61) give a complete solution to our problem. (Note that the elastic moduli are back, as was promised.) The solution is rich in physical content and deserves at least some analysis. First of all, note that according to Eq. (48), the coefficient $(1-2v)/E$ in the expression for a is just $1/3K$, so that the first term in Eq. (57) for the net deformation describes the hydrostatic compression. Now note that the second of Eqs. (61) yields $b = 0$ if $R_1 = 0$. Thus for a solid sphere, we have only the hydrostatic compression, which was discussed in the previous section. Perhaps less intuitively, making two pressures equal also gives $b = 0$, i.e. the purely hydrostatic compression, for arbitrary $R_2 > R_1$.

However, in the general case, $b \neq 0$, so that the second term in the deformation distribution (57), which describes the shear deformation, [25] is also substantial. In particular, let us consider the important thin-shell limit, when $R_2 - R_1 \equiv t < R_{1,2} \equiv R$ - see Figure 7 b. In this case, $q(R_1) \approx q(R_2)$ is just the change of the shell radius R, for which Eqs. (57) and (61) (with ${R_2}^3 - {R_1}^3 \approx 3R^2 t$) give

$$\Delta R \equiv q(R) \approx aR + \frac{b}{R^2} \approx \frac{(\mathcal{P}_1 - \mathcal{P}_2) R^2}{3t}\left(\frac{1-2v}{E} + \frac{1+v}{2E}\right) = (\mathcal{P}_1 - \mathcal{P}_2)\frac{R^2}{t}\frac{1-v}{2E}. \tag{7.4.12}$$

Naively, one could think that at least in this limit the problem could be analyzed by elementary means. For example, the total force exerted by the pressure difference $(\mathcal{P}_1 - \mathcal{P}_2)$ on the diametrical crosssection of the shell (see, e.g., the dashed line in Figure 7 b) is $F = \pi R^2 (\mathcal{P}_1 - \mathcal{P}_2)$, giving the stress,

$$\sigma = \frac{F}{A} = \frac{\pi R^2 (\mathcal{P}_1 - \mathcal{P}_2)}{2\pi R t} = (\mathcal{P}_1 - \mathcal{P}_2)\frac{R}{2t}, \tag{7.4.13}$$

directed along the shell's walls. One can check that this simple formula may be indeed obtained, in this limit, from the strict expressions for $\sigma_{\theta\theta}$ and $\sigma_{\varphi\varphi}$, following from the general treatment carried out above. However, if we now tried to continue this approach by using the simple relation (45) to find the small change Rs_{zz} of the sphere's radius, we would arrive at a result with the structure of Eq. (62), but without the factor $(1-v) < 1$ in the numerator. The reason for this error (which may be as significant as 330% for typical construction materials - see Table 1) is that Eq. (45), while being valid for thin rods of arbitrary cross-section, is invalid for thin but broad sheets, and in particular the thin shell in our problem. Indeed, while at the tensile stress both lateral dimensions of a thin rod may contract freely, in our problem all dimensions of the shell are under stress - actually, under much more tangential stress than the radial one [26]

---

[21] As follows from Eqs. (48), the coefficient before the first sum in Eq. (51) is just the shear modulus μ, while that before the second sum is equal to $(K + \mu/3)$.

[22] See, e.g., MA Eq. (11.3).

[23] If this is not immediately evident, please have a look at MA Eq. (10.11) with $\mathbf{f} = f_r(r)\mathbf{n}_r$.

[24] See, e.g., MA Eq. (10.10) with $\mathbf{f} = q(r)\mathbf{n}_r$

[25] Indeed, according to Eq. (48), the material-dependent factor in the second of Eqs. (61) is just $1/4\mu$.

[26] Strictly speaking, this is only true if the pressure difference is not too small, namely, if $|\mathcal{P}_1 - \mathcal{P}_2| >> \mathcal{P}_{1,2} t/R$.

7.5: Rod Bending

The general approach to the static deformation analysis, outlined in the beginning of the previous section, may be simplified not only for symmetric geometries, but also for the uniform thin structures such as thin plates (also called "membranes" or "thin sheets") and thin rods. Due to the shortage of time, in this course I will demonstrate typical approaches to such systems only on the example of thin rods. (The theory of thin plates and shells is conceptually similar, but mathematically more involved. [27])

Besides the tensile stress analyzed in Sec. 3, two other major types of rod deformation are bending and torsion. Let us start from a "local" analysis of bending caused by a pair of equal and opposite external torques $\tau = \pm \mathbf{n}_y \tau_y$ perpendicular to the rod axis z (Figure 8), assuming that the rod is "quasi-uniform", i.e. that on the longitudinal scale of this analysis (comparable with the linear scale a of the cross-section) its material parameters and the cross-section A do not change substantially.

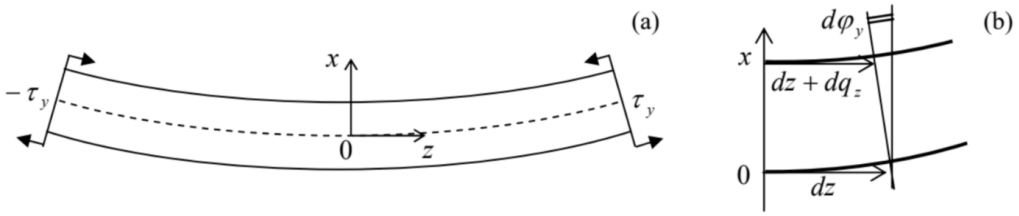

Figure 7.8. Rod bending, in a local reference frame (specific for each cross-section).

Just as in the tensile stress experiment (Figure 6), the components of the stress forces $d\mathbf{F}$, normal to the rod length, have to equal zero on the surface of the rod. Repeating the arguments made for the tensile stress discussion, we have to conclude that only one diagonal component of the tensor (in Figure 8 , σ_{zz}) may differ from zero:

$$\sigma_{ij'} = \delta_{jz}\sigma_{zz}. \tag{7.5.1}$$

However, in contrast to the tensile stress, at pure static bending, the net force directed along the rod has to vanish:

$$F_z = \int_S \sigma_{zz} d^2r = 0, \tag{7.5.2}$$

where S is the rod's cross-section, so that σ_{zz} has to change its sign at some point of the x-axis (in Figure 8, selected to lie in the plane of the bent rod). Thus, the bending deformation may be viewed as a combination of stretching some layers of the rod (bottom layers in Figure 8) with compression of other (top) layers.

Since it is hard to make more immediate conclusions about the stress distribution, let us turn over to strain, assuming that the rod's cross-section is virtually constant on the length of our local analysis. From the above representation of bending as a combination of stretching and compression, it evident that the longitudinal deformation q_z has to vanish along some neutral line on the rod's crosssection - in Figure 8, represented by the dashed line. [28] Selecting the origin of the x-coordinate on this line, and expanding the relative deformation in the Taylor series in x, due to the cross-section smallness we may keep just the first, linear term:

$$s_{zz} \equiv \frac{dq_z}{dz} = -\frac{x}{R}. \tag{7.5.3}$$

The constant R has the sense of the curvature radius of the bent rod. Indeed, on a small segment dz, the cross-section turns by a small angle $d\varphi_y = -dq_z/x$ (Figure 8b). Using Eq. (66), we get $d\varphi_y = dz/R$, which is the usual definition of the curvature radius R in the differential geometry, for our special choice of the coordinate axes. [29]Expressions for other components of the strain tensor are harder to guess (like at the tensile stress, not all of them are equal to zero!), but what we already know about σ_{zz} and S_{zz} is already sufficient to start formal calculations. Indeed, plugging Eq. (64) into Hooke's law in the form (49b), and comparing the result for s_{zz} with Eq. (66), we find

$$\sigma_{zz} = -E\frac{x}{R} \tag{7.5.4}$$

From the same Eq. (49b), we could also find the transverse components of the strain tensor, and conclude that they are related to s_{zz} exactly as at the tensile stress:

$$s_{xx} = s_{yy} = -\upsilon s_{zz}, \tag{7.5.5}$$

and then, integrating these relations along the cross-section of the rod, find the deformation of the crosssection's shape. More important for us, however, is the calculation of the relation between the rod's curvature and the net torque acting on a given cross-section S (taking $dA_z > 0$):

$$\tau_y \equiv \int_S (\mathbf{r} \times d\mathbf{F})_y = -\int_S x\sigma_{zz} d^2r = \frac{E}{R}\int_S x^2 d^2r = \frac{EI_y}{R}, \tag{7.5.6}$$

where I_y is a geometric constant defined as

$$I_y \equiv \int_S x^2 dxdy. \tag{7.5.7}$$

Note that this factor, defining the bending rigidity of the rod, grows as fast as a^4 with the linear scale a of the cross-section. [30]

In these expressions, x has to be counted from the neutral line. Let us see where exactly does this line pass through the rod's cross-section. Plugging the result (67) into Eq. (65), we get the condition defining the neutral line:

$$\int_S x dxdy = 0 \tag{7.5.8}$$

This condition allows a simple interpretation. Imagine a thin sheet of some material, with a constant mass density σ per unit area, cut in the form of the rod's cross-section. If we place a reference frame into its center of mass, then, by its definition,

$$\sigma \int_S \mathbf{r} dxdy = 0 \tag{7.5.9}$$

Comparing this condition with Eq. (71), we see that one of the neutral lines has to pass through the center of mass of the sheet, which may be called the "center of mass of the cross-section". Using the same analogy, we see that the integral I_y given by Eq. (72) may be interpreted as the moment of inertia of the same imaginary sheet of material, with σ formally equal to 1 , for its rotation about the neutral line - cf. Eq. (4.24). This analogy is so convenient that the integral is usually called the moment of inertia of the cross-section and denoted similarly - just as has been done above. So, our basic result (69) may be re-written as

$$\frac{1}{R} = \frac{\tau_y}{EI_y}. \tag{7.5.10}$$

This relation is only valid if the deformation is small in the sense $R \gg a$. Still, since the deviations of the rod from its unstrained shape may accumulate along its length, Eq. (73) may be used for calculations of large "global" deviations of the rod from equilibrium, on a length scale much larger than a. To describe such deformations, Eq. (73) has to be complemented by conditions of the balance of the bending forces and torques. Unfortunately, this requires a bit more differential geometry than I have time for, and I will only discuss this procedure for the simplest case of relatively small transverse deviations $q \equiv q_x$ of the rod from its initial straight shape, which will be used for the z-axis (Figure 9a), for example by some bulk-distributed force $\mathbf{f} = \mathbf{n}_x f_x(z)$. (The simplest example is a uniform gravity field, for which $f_x = -\rho g =$ const.) Note that in the forthcoming discussion the reference frame will be global, i.e. common for the whole rod, rather than local (pertaining to each cross-section) as it was in the previous analysis - cf. Figure 8 .

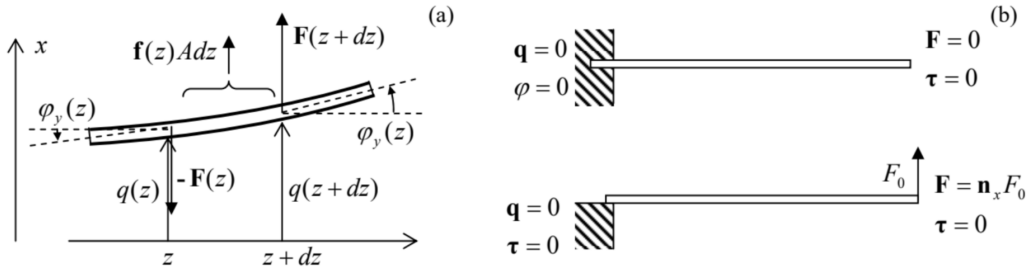

Figure 7.9. A global picture of rod bending: (a) the forces acting on a small fragment of a rod, and (b) two bending problem examples, each with two typical but different boundary conditions.

First of all, we may write a differential static relation for the average vertical force $\mathbf{F} = \mathbf{n}_x F_x(z)$ exerted on the part of the rod located to the left of its cross-section - located at point z. This relation expresses the balance of vertical forces acting on a small fragment dz of the rod (Figure 9a), necessary for the absence of its linear acceleration: $F_x(z+dz) - F_x(z) + f_x(z)Adz = 0$, giving

$$\frac{dF_x}{dz} = -f_x A, \tag{7.5.11}$$

where A is the cross-section area. Note that this vertical component of the internal forces has been neglected at our derivation of Eq. (73), and hence our final results will be valid only if the ratio F_x/A is much smaller than the magnitude of σ_{zz} described by Eq. (67). However, these forces create the very torque $\tau = \mathbf{n}_y \tau_y$ that causes the bending, and thus have to be taken into account at the analysis of the global picture. Such account may be made by writing the balance of torque components, acting on the same rod fragment of length dz, necessary for the absence of its angular acceleration: $d\tau_y + F_x dz = 0$, giving

$$\frac{d\tau_y}{dz} = -F_x. \tag{7.5.12}$$

These two equations should be complemented by two geometric relations. The first of them is $d\varphi_y/dz = 1/R$, which has already been discussed above. We may immediately combine it with the basic result (73) of the local analysis, getting:

$$\frac{d\varphi_y}{dz} = \frac{\tau_y}{EI_y}. \tag{7.5.13}$$

The final equation is the geometric relation evident from Figure 9a:

$$\frac{dq_x}{dz} = \varphi_y, \tag{7.5.14}$$

which is (as all expressions of our simple analysis) only valid for small bending angles, $|\varphi_y| << 1$. The four differential equations (74)-(77) are sufficient for the full solution of the weak bending problem, if complemented by appropriate boundary conditions. Figure 9 b shows the conditions most frequently met in practice. Let us solve, for example, the problem shown on the top panel of Figure 9 b : bending of a rod, "clamped" at one end (say, immersed into a rigid wall), under its own weight. Considering, for the sake of simplicity, a uniform rod, [31] we may integrate these equations one by one, each time using the appropriate boundary conditions. To start, Eq. (74) with $f_x = -\rho g$ yields

$$F_x = \rho g A z + \text{ const } = \rho g A (z - l), \tag{7.5.15}$$

where the integration constant has been selected to satisfy the right-end boundary condition: $F_x = 0$ at $z = l$. As a sanity check, at the left wall $(z = 0)$, $F_x = -\rho g A l = -mg$, meaning that the whole weight of the rod is exerted on the wall - fine.

Next, plugging Eq. (78) into Eq. (75) and integrating, we get

$$\tau_y = -\frac{\rho g A}{2}\left(z^2 - 2lz\right) + \text{ const } = -\frac{\rho g A}{2}\left(z^2 - 2lz + l^2\right) \equiv -\frac{\rho g A}{2}(z-l)^2, \tag{7.5.16}$$

where the integration constant's choice ensures the second right-boundary condition: $\tau_y = 0$ at $z = l-$ see Figure 9 b again. Now proceeding in the same fashion to Eq. (76), we get

$$\varphi_y = -\frac{\rho g A}{2EI_y}\frac{(z-l)^3}{3} + \text{ const } = -\frac{\rho g A}{6EI_y}\left[(z-l)^3 + l^3\right], \tag{7.5.17}$$

where the integration constant is selected to satisfy the clamping condition at the left end of the rod: $\varphi_y = 0$ at $z = 0$. (Note that this is different from the support condition illustrated on the lower panel of Figure 9 b, which allows the angle at $z = 0$ to be different from zero, but requires the torque to vanish.) Finally, integrating Eq. (77) with φ_y given by Eq. (80), we get the rod's global deformation law,

$$q_x(z) = -\frac{\rho g A}{6EI_y}\left[\frac{(z-l)^4}{4} + l^3 z + \text{const}\right] = -\frac{\rho g A}{6EI_y}\left[\frac{(z-l)^4}{4} + l^3 z - \frac{l^4}{4}\right], \tag{7.5.18}$$

where the integration constant is selected to satisfy the second left-boundary condition: $q = 0$ at $z = 0$. So, the bending law is sort of complicated even in this very simple problem. It is also remarkable how fast does the end's displacement grow with the increase of the rod's length:

$$q_x(l) = -\frac{\rho g A l^4}{8EI_y}. \tag{7.5.19}$$

To conclude the solution, let us discuss the validity of this result. First, the geometric relation (77) is only valid if $|\varphi_y(l)| << 1$, and hence if $|q_x(l)| << l$. Next, the local formula Eq. (76) is valid if $1/R = \tau(l)/EI_y << 1/a \sim A^{-1/2}$. Using the results (79) and (82), we see that the latter condition is equivalent to $|q_x(l)| << l^2/a$, i.e. is weaker than the former one, because all our analysis has been based on the assumption $l >> a$.

Another point of concern may be that the off-diagonal stress component $\sigma_{xz} \sim F_x/A$, which is created by the vertical gravity forces, has been ignored in our local analysis. For that approximation to be valid, this component must be much smaller than the diagonal component $\sigma_{zz} \sim aE/R = a\tau/I_y$ taken into account in that analysis. Using Eqs. (78) and (80), we are getting the following estimates: $\sigma_{xz} \sim \rho g l$, $\sigma_{zz} \sim a\rho g A l^2/I_y \sim a^3 \rho g l^2/I_y$. According to its definition (70), I_y may be crudely estimated as a^4, so that we finally get the simple condition $a << l$, which has been assumed from the very beginning of our solution.

---

[27] For its review see, e.g., Secs. 11-15 in L. Landau and E. Lifshitz, Theory of Elasticity, 3^{rd} ed., ButterworthHeinemann, 1986.

[28] Strictly speaking, that dashed line is the intersection of the neutral surface (the continuous set of such neutral lines for all cross-sections of the rod) with the plane of the drawing.

[29] Indeed, for $(dx/dz)^2 << 1$, the general formula MA Eq. (4.3) for the curvature (with the appropriate replacements $f \to x$ and $x \to z$) is reduced to $1/R = d^2x/dz^2 = d(dx/dz)/dz = d\left(\tan\varphi_y\right)/dz \approx d\varphi_y/dz$.

[30] In particular, this is the reason why the usual electric wires are made not of a solid copper core, but rather a twisted set of thinner sub-wires, which may slip relative to each other, increasing the wire flexibility.

[31] As should be clear from their derivation, Eqs. (74)-(77) are valid for any distribution of parameters A, E, I_y, and ρ over the rod's length, provided that the rod is quasi-uniform, i.e. its parameters' changes are so slow that the local relation (76) is still valid at any point.

7.6: Rod Torsion

One more class of analytically solvable elasticity problems is torsion of quasi-uniform, straight rods by a couple of axially-oriented torques $\tau = \pm \mathbf{n}_z \tau_z -$ see Figure 10 .

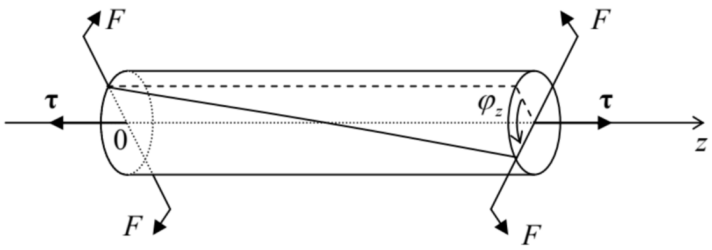

Figure 7.10. Rod torsion.

This problem is simpler than the bending in the sense that due to its longitudinal uniformity, $d\varphi_z/dz =$ const, it is sufficient to relate the torque τ_z to the so-called torsion parameter

$$\kappa \equiv \frac{d\varphi_z}{dz}. \tag{7.6.1}$$

If the deformation is elastic and small (in the sense $\kappa a << 1$, where a is again the characteristic size of the rod's cross-section), κ is proportional to τ_z. Hence our task is to calculate their ratio,

$$C \equiv \frac{\tau_z}{\kappa} \equiv \frac{\tau_z}{d\varphi_z/dz}, \tag{7.6.2}$$

called the torsional rigidity of the rod.

As the first guess (as we will see below, of a limited validity), one may assume that the torsion does not change either the shape or size of the rod's cross-sections, but leads just to their mutual rotation about a certain central line. Using a reference frame with the origin on that line, this assumption immediately enables the calculation of Cartesian components of the displacement vector $d\mathbf{q}$, by using Eq. (6) with $d\varphi = \mathbf{n}_z d\varphi_z$:

$$dq_x = -y d\varphi_z = -\kappa y dz, \quad dq_y = x d\varphi_z = \kappa x dz, \quad dq_z = 0. \tag{7.6.3}$$

From here, we can calculate all Cartesian components (9) of the symmetrized strain tensor:

$$s_{xx} = s_{yy} = s_{zz} = 0, \quad s_{xy} = s_{yx} = 0, \quad s_{xz} = s_{zx} = -\frac{\kappa}{2} y, \quad s_{yz} = s_{zy} = \frac{\kappa}{2} x. \tag{7.6.4}$$

The first of these equalities means that the elementary volume does not change, i.e. we are dealing with purely shear deformation. As a result, all nonzero components of the stress tensor, calculated from Eqs. (32), are proportional to the shear modulus alone:

$$\sigma_{xx} = \sigma_{yy} = \sigma_{zz} = 0, \quad \sigma_{xy} = \sigma_{yx} = 0, \quad \sigma_{xz} = \sigma_{zx} = -\mu\kappa y, \quad \sigma_{yz} = \sigma_{zy} = \mu\kappa x. \tag{7.6.5}$$

(Note that for this problem, with a purely shear deformation, using alternative elastic moduli E and v would be rather unnatural. If so desired, we may always use the second of Eqs. (48): $\mu = E/2(1+v)$.)

Now it is straightforward to use this result to calculate the full torque as an integral over the cross-section's area A :

$$\tau_z \equiv \int_A (\mathbf{r} \times d\mathbf{F})_z = \int_A (x dF_y - y dF_x) = \int_A (x\sigma_{yz} - y\sigma_{xz})\, dx dy \tag{7.6.6}$$

Using Eq. (87), we get $\tau_z = \mu\kappa I_z$, i.e.

$$C = \mu I_z, \text{ where } I_z \equiv \int_A \left(x^2 + y^2\right) dx dy \tag{7.6.7}$$

Again, just as in the case of thin rod bending, we have got an integral, in this case I_z, similar to a moment of inertia, this time for the rotation about the z-axis passing through a certain point of the crosssection. For any axially-symmetric cross-section, this evidently should be the central point. Then, for example, for the practically important case of a uniform round pipe with internal radius R_1 and external radius R_2, Eq. (89) yields

$$C = \mu 2\pi \int_{R_1}^{R_2} \rho^3 d\rho = \frac{\pi}{2}\mu\left(R_2^4 - R_1^4\right). \tag{7.6.8}$$

In particular, for the solid rod of radius R (which may be treated as a pipe with $R_1 = 0$ and $R_2 = R$), this result gives the following torsional rigidity

$$C = \frac{\pi}{2}\mu R^4, \tag{7.6.9}$$

while for a hollow pipe of small thickness $t << R$, Eq. (90) is reduced to

$$C = 2\pi\mu R^3 t. \tag{7.6.10}$$

Note that per unit cross-section area A (and hence per unit mass of the rod) this rigidity is twice higher than that of a solid rod:

$$\left.\frac{C}{A}\right|_{\text{thin round pipe}} = \mu R^2 > \left.\frac{C}{A}\right|_{\text{solid round rod}} = \frac{1}{2}\mu R^2 \tag{7.6.11}$$

This fact is one reason for the broad use of thin pipes in engineering and physical experiment design.

However, for rods with axially-asymmetric cross-sections, Eq. (89) gives wrong results. For example, for a narrow rectangle of area $A = w \times t$ with $t << w$, it yields $C = \mu t w^3/12$ [WRONG!], even functionally different from the correct result - cf. Eq. (104) below. The reason of the failure of the above analysis is that does not describe possible bending $q_z(x, y)$ of the rod's cross-section in the direction along the rod. (For axially-symmetric rods, such bending is evidently forbidden by the symmetry, so that Eq. (89) is valid, and the results (90)-(92) are absolutely correct.) Let us describe [32] this counter-intuitive effect by taking

$$q_z = \kappa\psi(x, y), \tag{7.6.12}$$

(where ψ is some function to be determined), but still keeping Eq. (87) for two other components of the displacement vector. The addition of ψ does not perturb the equality to zero of the diagonal components of the strain tensor, as well as of s_{xy} and s_{yx}, but contributes to other off-diagonal components:

$$s_{xz} = s_{zx} = \frac{\kappa}{2}\left(-y + \frac{\partial\psi}{\partial x}\right), \quad s_{yz} = s_{zy} = \frac{\kappa}{2}\left(x + \frac{\partial\psi}{\partial y}\right), \tag{7.6.13}$$

and hence to the corresponding elements of the stress tensor:

$$\sigma_{xz} = \sigma_{zx} = \mu\kappa\left(-y + \frac{\partial\psi}{\partial x}\right), \quad \sigma_{yz} = \sigma_{zy} = \mu\kappa\left(x + \frac{\partial\psi}{\partial y}\right). \tag{7.6.14}$$

Now let us find the requirement imposed on the function $\psi(x, y)$ by the fact that the stress force component parallel to the rod's axis,

$$dF_z = \sigma_{zx}dA_x + \sigma_{zy}dA_y = \mu\kappa dA\left[\left(-y + \frac{\partial\psi}{\partial x}\right)\frac{dA_x}{dA} + \left(x + \frac{\partial\psi}{\partial y}\right)\frac{dA_y}{dA}\right], \tag{7.6.15}$$

has to vanish at the rod's surface(s), i.e. at each border of its cross-section. The coordinates $\{x, y\}$ of any point at a border may be considered as unique functions, $x(l)$ and $y(l)$, of the arc l of that line - see Figure 11 .

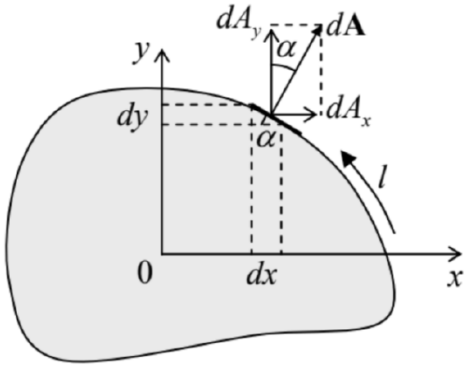

Figure 7.11. Deriving Eq. (99).

As this sketch shows, the elementary area ratios participating in Eq. (96) may be readily expressed via the derivatives of these functions: $dA_x/dA = \sin\alpha = dy/dl, dA_y/dA = \cos\alpha = -dx/dl$, so that we may write

$$\left[\left(-y+\frac{\partial\psi}{\partial x}\right)\left(\frac{dy}{dl}\right)+\left(x+\frac{\partial\psi}{\partial y}\right)\left(-\frac{dx}{dl}\right)\right]_{\text{border}}=0 \tag{7.6.16}$$

Introducing, instead of ψ, a new function $\chi(x,y)$, defined by its derivatives as

$$\frac{\partial\chi}{\partial x}\equiv\frac{1}{2}\left(-x-\frac{\partial\psi}{\partial y}\right),\quad \frac{\partial\chi}{\partial y}\equiv\frac{1}{2}\left(-y+\frac{\partial\psi}{\partial x}\right) \tag{7.6.17}$$

we may rewrite Eq. (97) as

$$2\left(\frac{\partial\chi}{\partial y}\frac{dy}{dl}+\frac{\partial\chi}{\partial x}\frac{dx}{dl}\right)_{\text{border}}\equiv 2\left.\frac{d\chi}{dl}\right|_{\text{border}}=0, \tag{7.6.18}$$

so that the function χ should be constant at each border of the cross-section.

In particular, for a singly-connected cross-section, limited by just one continuous border line (as in Figure 11), this constant is arbitrary, because according to Eqs. (98), its choice does not affect the longitudinal deformation function $\psi(x,y)$ and hence the deformation as the whole. Now let use the definition (98) of the function χ to calculate the 2D Laplace operator of this function:

$$\nabla^2_{x,y}\chi\equiv\frac{\partial^2\chi}{\partial^2 x}+\frac{\partial^2\chi}{\partial^2 y}=\frac{1}{2}\frac{\partial}{\partial x}\left(-x-\frac{\partial\psi}{\partial y}\right)+\frac{1}{2}\frac{\partial}{\partial y}\left(-y+\frac{\partial\psi}{\partial y}\right)\equiv -1. \tag{7.6.19}$$

This a 2D Poisson equation (frequently met, for example, in electrostatics), but with a very simple, constant right-hand side. Plugging Eqs. (98) into Eqs. (95), and those into Eq. (88), we may express the torque τ, and hence the torsional rigidity C, via the same function:

$$C\equiv\frac{\tau_z}{\kappa}=-2\mu\int_A\left(x\frac{\partial\chi}{\partial x}+y\frac{\partial\chi}{\partial y}\right)dxdy. \tag{7.6.20}$$

Sometimes, it is easier to use this result in either of its two different forms. The first of them may be readily obtained from Eq. (101a) using integration by parts:

$$\begin{aligned} C &= -2\mu\left(\int dy\int x d\chi+\int dx\int y d\chi\right)=-2\mu\left[\int dy\left(x\chi_{\text{border}}-\int\chi dx\right)+\int dx\left(y\chi_{\text{border}}-\int\chi dy\right)\right] \\ &= 4\mu\left[\int_A\chi dxdy-\chi_{\text{border}}\int dxdy\right], \end{aligned}$$

while the proof of one more form,

$$C=4\mu\int_A\left(\nabla_{x,y}\chi\right)^2 dxdy \tag{7.6.21}$$

is left for the reader's exercise.

Thus, if we need to know the rod's rigidity alone, it is sufficient to calculate the function $\chi(x,y)$ from Eq. (100) with the boundary condition $\chi|_{\text{border}} = \text{const}$, and then plug it into any of Eqs. (101). Only if we are also curious about the longitudinal deformation (93) of the cross-section, we may continue by using Eq. (98) to find the function $\psi(x,y)$ describing this deformation. Let us see how does this general result work for the two examples discussed above. For the round cross-section of radius R, both the Poisson equation (100) and the boundary condition, $\chi = \text{const}$ at $x^2+y^2=R^2$, are evidently satisfied by the axially-symmetric function

$$\chi = -\frac{1}{4}\left(x^2+y^2\right) + \text{const}. \tag{7.6.22}$$

For this case, either of Eqs. (101) yields

$$C = 4\mu\int_A \left[\left(-\frac{1}{2}x\right)^2 + \left(-\frac{1}{2}y\right)^2\right] dxdy = \mu\int_A \left(x^2+y^2\right) d^2r, \tag{7.6.23}$$

i.e. the same result (89) that we had for $\psi = 0$. Indeed, plugging Eq. (102) into Eqs. (98), we see that in this case $\partial\psi/\partial x = \partial\psi/\partial y = 0$, so that $\psi(x,y) = \text{const}$, i.e. the cross-section is not bent. (As was discussed in Sec. 1, a uniform translation $dq_z = \kappa\psi = $ const does not constitute a deformation.)

Now, turning to a rod with a narrow rectangular cross-section $A = w\times t$ with $t << w$, we may use this strong inequality to solve the Poisson equation (100) approximately, neglecting the second derivative of χ along the wider dimension (say, y). The remaining 1D differential equation $d^2\chi/d^2x = -1$, with boundary conditions $\chi|_{x=+t/2} = \chi|_{x=-t/2}$ has an evident solution: $\chi = -x^2/2 + $ const. Plugging this expression into any form of Eq. (101), we get the following (correct) result for the torsional rigidity:

$$C = \frac{1}{6}\mu w t^3. \tag{7.6.24}$$

Now let us have a look at the cross-section bending law (93) for this particular case. Using Eqs. (96), we get

$$\frac{\partial\psi}{\partial y} = -x - 2\frac{\partial\chi}{\partial x} = x, \quad \frac{\partial\psi}{\partial x} = y + 2\frac{\partial\chi}{\partial y} = y. \tag{7.6.25}$$

Integrating these differential equations over the cross-section, and taking the integration constant (again, not contributing to the deformation) for zero, we get a beautifully simple result:

$$\psi = xy, \quad \text{i.e. } q_z = \kappa xy. \tag{7.6.26}$$

It means that the longitudinal deformation of the rod has a "propeller bending" form: while the regions near the opposite corners (on the same diagonal) of the cross-section bend toward one direction of the z axis, the corners on the other diagonal bend in the opposite direction. (This qualitative conclusion remains valid for rectangular cross-sections with any "aspect ratio" t/w.)

For rods with several surfaces, i.e. with cross-sections limited by several boundaries (say, hollow pipes), finding the function $\chi(x,y)$ requires a bit more care, and Eq. (103b) has to be modified, because it may be equal to a different constant at each boundary. Let me leave the calculation of the torsional rigidity for this case for the reader's exercise.

---

[32] I would not be terribly shocked if the reader skipped the balance of this section at the first reading. Though the calculation described in it is very elegant, instructive, and typical for the advanced theory of elasticity, its results will not be used in other chapters of this course or other parts of this series.

7.7: 3D Acoustic Waves

Now moving from the statics to dynamics, we may start with Eq. (24), which may be transformed into the vector form exactly as this was done for the static case in the beginning of Sec. 4. Comparing Eqs. (24) and (52), we immediately see that the result may be represented as

$$\rho\frac{\partial^2\mathbf{q}}{\partial t^2}=\frac{E}{2(1+v)}\nabla^2\mathbf{q}+\frac{E}{2(1+v)(1-2v)}\nabla(\nabla\cdot\mathbf{q})+\mathbf{f}(\mathbf{r},t). \tag{7.7.1}$$

Let us use this general equation for the analysis of the perhaps most important type of timedependent deformations: acoustic waves. First, let us consider the simplest case of a virtually infinite, uniform elastic medium, with no external forces: $\mathbf{f}=0$. In this case, due to the linearity and homogeneity of the equation of motion, and taking clues from the analysis of the simple 1D model (see Figure 6.4a) in Secs. 6.3-6.5, [33] we may look for a particular time-dependent solution in the form of a sinusoidal, linearly-polarized, plane traveling wave

$$\mathbf{q}(\mathbf{r},t)=\mathrm{Re}\left[\mathbf{a}e^{i(\mathbf{k}\cdot\mathbf{r}-\omega t)}\right], \tag{7.7.2}$$

where $\mathbf{a}$ is the constant complex amplitude of a wave (now a vector!), and $\mathbf{k}$ is the wave vector, whose magnitude is equal to the wave number k. The direction of these two vectors should be clearly distinguished: while a determines the wave's polarization, i.e. the direction of particle displacements, the vector $\mathbf{k}$ is directed along the spatial gradient of the full phase of the wave

$$\Psi\equiv\mathbf{k}\cdot\mathbf{r}-\omega t+\arg a, \tag{7.7.3}$$

i.e. along the direction of the wave front propagation.

The importance of the angle between these two vectors may be readily seen from the following simple calculation. Let us point the z-axis of an (inertial) reference frame along the direction of vector $\mathbf{k}$, and the x-axis in such direction that the vector $\mathbf{q}$, and hence a, lie within the $\{x,z\}$ plane. In this case, all variables may change only along the z-axis, i.e. $\nabla=\mathbf{n}_z(\partial/\partial z)$, while the amplitude vector may be represented as the sum of just two Cartesian components:

$$\mathbf{a}=a_x\mathbf{n}_x+a_z\mathbf{n}_z. \tag{7.7.4}$$

Let us first consider a longitudinal wave, with the particle motion along the wave direction: $a_x=0, a_z=a$. Then the vector $\mathbf{q}$ in Eq. (107), describing this wave, has only one (z) component, so that $\nabla\cdot\mathbf{q}=dq_z/dz$ and $\nabla(\nabla\cdot\mathbf{q})=\mathbf{n}_z\left(\partial^2\mathbf{q}/\partial z^2\right)$, and the Laplace operator gives the same expression: $\nabla^2\mathbf{q}=\mathbf{n}_z\left(\partial^2\mathbf{q}/\partial z^2\right)$. As a result, Eq. (107), with $\mathbf{f}=0$, is reduced to a 1D wave equation

$$\rho\frac{\partial^2 q_z}{\partial t^2}=\left[\frac{E}{2(1+v)}+\frac{E}{2(1+v)(1-2v)}\right]\frac{\partial^2 q_z}{\partial z^2}\equiv\frac{E(1-v)}{(1+v)(1-2v)}\frac{\partial^2 q_z}{\partial z^2}, \tag{7.7.5}$$

similar to Eq. (6.40). As we already know from Sec. 6.4, this equation is indeed satisfied with the solution (108), provided that ω and k obey a linear dispersion relation, $\omega=v_1k$, with the following longitudinal wave velocity:

$$v_1^2=\frac{E(1-v)}{(1+v)(1-2v)\rho}\equiv\frac{K+(4/3)\mu}{\rho} \tag{7.7.6}$$

The last expression allows a simple interpretation. Let us consider a static experiment, similar to the tensile test experiment shown in Figure 6, but with a sample much wider than l in both directions perpendicular to the force. Then the lateral contraction is impossible $(s_{xx}=s_{yy}=0)$, and we can calculate the only finite stress component, σ_{zz}, directly from Eq. (34) with $\mathrm{Tr(s)}=s_{zz}$:

$$\sigma_{zz}=2\mu\left(s_{zz}-\frac{1}{3}s_{zz}\right)+3K\left(\frac{1}{3}s_{zz}\right)\equiv\left(K+\frac{4}{3}\mu\right)s_{zz}. \tag{7.7.7}$$

We see that the numerator in Eq. (112) is nothing more than the static elastic modulus for such a uniaxial deformation, and it is recalculated into the velocity exactly as the spring constant in the 1D waves considered in Secs. 6.3-6.4 - cf. Eq. (6.42).

Formula (114) becomes especially simple in fluids, where $\mu=0$, and the wave velocity is described by the well-known expression

$$v_1=\left(\frac{K}{\rho}\right)^{1/2} \tag{7.7.8}$$

Note, however, that for gases, with their high compressibility and temperature sensitivity, the value of K participating in this formula may differ, at high frequencies, from that given by Eq. (40), because fast compressions/extensions of gas are usually adiabatic rather than isothermal. This difference is noticeable in Table 1 , one of whose columns lists the values of v_l for representative materials.

Now let us consider an opposite case of transverse waves with $a_x = a, a_z = 0$. In such a wave, the displacement vector is perpendicular to $\mathbf{n}_z$, so that $\nabla \cdot \mathbf{q} = 0$, and the second term on the right-hand side of Eq. (107) vanishes. On the contrary, the Laplace operator acting on such vector still gives the same nonzero contribution, $\nabla^2 \mathbf{q} = n_z \left(\partial^2 \mathbf{q}/\partial z^2\right)$, to Eq. (107) so that the equation yields

$$\rho \frac{\partial^2 q_x}{\partial t^2} = \frac{E}{2(1+v)} \frac{\partial^2 q_x}{\partial z^2}, \tag{7.7.9}$$

and we again get the linear dispersion relation, $\omega = v_t k$, but with a different velocity:

$$\text{Transverse waves: velocity} \qquad \nu_{\mathrm{t}}^2 = \frac{E}{2(1+\nu)\rho} = \frac{\mu}{\rho}. \tag{7.7.10}$$

We see that the speed of the transverse waves depends exclusively on the shear modulus μ of the medium. [34] This is also very natural: in such waves, the particle displacements $\mathbf{q} = \mathbf{n}_x q$ are perpendicular to the elastic forces $d\mathbf{F} = \mathbf{n}_z dF$, so that the only one component σ_{xz} of the stress tensor is involved. Also, the strain tensor s_{ij} ' has no diagonal components, $\mathrm{Tr}(\mathrm{s}) = 0$, so that μ is the only elastic modulus actively participating in Hooke's law (32). In particular, fluids cannot carry transverse waves at all (formally, their velocity (116) vanishes), because they do not resist shear deformations. For all other materials, the longitudinal waves are faster than the transverse ones. [35] Indeed, for all known natural materials the Poisson ratio is positive so that the velocity ratio that follows from Eqs. (112) and (116),

$$\frac{v_{\mathrm{l}}}{v_{\mathrm{t}}} = \left(\frac{2-2v}{1-2v}\right)^{1/2} \tag{7.7.11}$$

is above $\sqrt{2} \approx 1.4$. For the most popular construction materials, with $v \approx 0.3$, the ratio is about $2-$ see Table 1.

Let me emphasize again that for both the longitudinal and the transverse waves, the dispersion relation between the wave number and frequency is linear: $\omega = vk$. As was already discussed in Chapter 6 , in this case of acoustic waves (or just "sound"), the phase and group velocities are equal, and waves of more complex form, consisting of several (or many) Fourier components of the type (108), preserve their form during propagation. This means that both Eqs. (111) and (115) are satisfied by solutions of the type (6.41):

$$q_{\pm}(z,t) = f_{\pm}\left(t \mp \frac{z}{v}\right), \tag{7.7.12}$$

where the functions $f_{\pm}$describe the propagating waveforms. (However, if the initial wave is a mixture, of the type (110), of the longitudinal and transverse components, then these components, propagating with different velocities, will "run from each other".) As one may infer from the analysis of a periodic system model in Chapter 6 , the wave dispersion becomes essential at very high (hypersound) frequencies where the wave number k becomes close to the reciprocal distance d between the particles of the medium (e.g., atoms or molecules), and hence the approximation of the medium as a continuum, used through this chapter, becomes invalid.

As we already know from Chapter 6, besides the velocity, the waves of each type are characterized by one more important parameter, the wave impedance Z of the continuum, for acoustic waves frequently called its acoustic impedance. Generalizing Eq. (6.46) to the 3D case, we may define the impedance as the magnitude of the ratio of the force per unit area (i.e. the corresponding component of the stress tensor) exerted by the wave, and the particles' velocity. For the longitudinal waves,

$$Z_1 \equiv \left|\frac{\sigma_{zz}}{\partial q_z/\partial t}\right| = \left|\frac{\sigma_{zz}}{s_{zz}} \frac{s_{zz}}{\partial q_z/\partial t}\right| = \left|\frac{\sigma_{zz}}{s_{zz}} \frac{\partial q_z/\partial z}{\partial q_z/\partial t}\right|. \tag{7.7.13}$$

Plugging in Eqs. (108), (112), and (113), we get

$$Z_1 = [(K + 4\mu/3)\rho]^{1/2}, \tag{7.7.14}$$

in a clear analogy with the first of Eqs. (6.48). Similarly, for the transverse waves, the appropriately modified definition, $Z_{\rm t} \equiv |\sigma_{xz}/(\partial q_x/\partial z)|$, yields

$$Z_{\rm t} = (\mu\rho)^{1/2} \tag{7.7.15}$$

Just like in the 1D model studied in Chapter 6, one role of the wave impedance is to scale the power carried by the wave. For plane 3D waves in infinite media, with their infinite wave front area, it is more appropriate to speak about the power density, i.e. power $/ = d\mathscr{P}/dA$ per unit area of the front, and characterize it by not only its magnitude,

$$\mu = \frac{d\mathbf{F}}{dA}\cdot\frac{\partial \mathbf{q}}{\partial t}, \tag{7.7.16}$$

but also the direction of the energy propagation, that (for a plane wave in an isotropic medium) coincides with the direction of the wave vector: $\boldsymbol{h} \equiv /\mathbf{n}_{\mathbf{k}}$. Using the definition (18) of the stress tensor, the Cartesian components of this Umov vector [36] may be expressed as

$$\mu_j = \sum_{j'} \sigma_{ij'}\frac{\partial q_{j'}}{\partial t}. \tag{7.7.17}$$

Returning to plane waves propagating along axis z, and acting exactly like in Sec. 6 ., for both the longitudinal and transverse waves we again arrive at Eq. (6.49), but for $/$ rather than $\mathscr{P}$ (due to a different definition of the wave impedance - per unit area rather than per particle chain). For the sinusoidal waves of the type (108), it yields

$$\mu_z = \frac{\omega^2 Z}{2} aa^*, \tag{7.7.18}$$

with Z being the corresponding impedance – either Z_1 or $Z_{\rm t}$.

Just as in the 1D case, one more important effect, in which the notion of impedance is crucial, is wave reflection from at an interface between two media. The two boundary conditions, necessary for the analysis of these processes, may be obtained from the continuity of the vectors $\mathbf{q}$ and $d\mathbf{F}$. (The former condition is evident, while the latter one may be obtained by applying the $2^{\rm nd}$ Newton law to the infinitesimal volume $dV = dAdz$, where segment dz straddles the interface.) Let us start from the simplest case of the normal incidence on a plane interface between two uniform media with different elastic moduli and mass densities. Due to the symmetry, it is evident that the longitudinal/transverse incident wave may only excite similarly polarized reflected and transferred waves. As a result, we may literally repeat the calculations of Sec. 6.4, again arriving at the fundamental relations (6.55) and (6.56), with the only replacement of Z and Z' with the corresponding values of either Z_1 (120) or $Z_{\rm t}$ (121). Thus, at the normal incidence, the wave reflection is determined solely by the acoustic impedances of the media, while the sound velocities are not involved.

The situation, however, becomes more complicated at a nonzero incidence angle $\theta^{\rm i)}$ (Figure 12), where the transmitted wave is generally also refracted, i.e. propagates under a different angle, $\theta \neq \theta^{(\rm i)}$, beyond the interface. Moreover, at $\theta^{(\rm i)} \neq 0$ the directions of particle motion (vector $\mathbf{q}$) and of the stress forces (vector $d\mathbf{F}$) in the incident wave are neither exactly parallel nor exactly perpendicular to the interface, and thus this wave serves as an actuator for the reflected and refracted waves of both polarizations - see Figure 12, drawn for the particular case when the incident wave is transverse. The corresponding four angles, $\theta_{\rm t}^{(\rm r)}, \theta_{\rm t}^{(\rm r)}, \theta_1', \theta_{\rm t}'$, may be readily related to $\theta^{(\rm i)}$ by the "kinematic" condition that the incident wave, as well as the reflected and refracted waves of both types, should have the same spatial distribution along the interface plane, i.e. for the interface particles participating in all five waves. According to Eq. (108), the necessary boundary condition is the equality of the tangential components (in Figure $12, k_x$), of all five wave vectors:

$$k_{\rm t}\sin\theta_{\rm t}^{(\rm r)} = k_1\sin\theta_1^{(\rm r)} = k_1'\sin\theta_1' = k_{\rm t}'\sin\theta_{\rm t}' = k_x \equiv k_{\rm t}\sin\theta_{\rm t}^{(\rm i)}. \tag{7.7.19}$$

Since the acoustic wave vector magnitudes k, at fixed frequency ω, are inversely proportional to the corresponding wave velocities, we immediately get the following relations:

$$\theta_{\rm t}^{(\rm r)} = \theta_{\rm t}^{(\rm i)}, \quad \frac{\sin\theta_1^{(\rm r)}}{v_1} = \frac{\sin\theta_1'}{v_1'} = \frac{\sin\theta_{\rm t}'}{v_{\rm t}'} = \frac{\sin\theta_{\rm t}^{(\rm i)}}{v_{\rm t}} \tag{7.7.20}$$

so that generally all four angles are different. (This is of course an analog of the well-known Snell law in optics - where, however, only transverse waves are possible.) These relations show that, just like in optics, the direction of a wave propagating into a

medium with lower velocity is closer to the normal (in Figure 12, the z-axis). In particular, this means that if $v' > v$, the acoustic waves, at larger angles of incidence, may exhibit the effect of total internal reflection, so well known from optics 37 , when the refracted wave vanishes. In addition, Eqs. (126) show that in acoustics, the reflected longitudinal wave, with velocity $v_1 > v_t$, may vanish at sufficiently large angles of the transverse wave incidence.

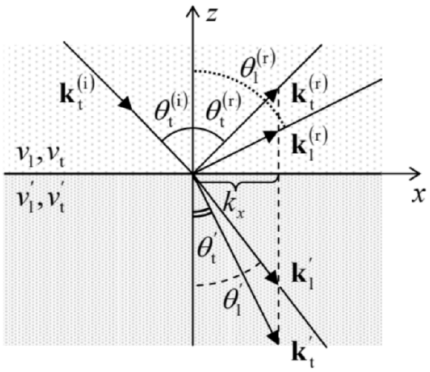

Figure 7.12. Deriving the "kinematic" conditions (126) of the acoustic wave reflection and refraction (for the case of a transverse incident wave).

All these facts automatically follow from general expressions for amplitudes of the reflected and refracted waves via the amplitude of the incident wave. These relations are straightforward to derive (again, from the continuity of the vectors $\mathbf{q}$ and $d\mathbf{F}$), but since they are much bulkier than those in the electromagnetic wave theory (where they are called the Fresnel formulas [38]), I would not have time/space to spell out and discuss them. Let me only note that, in contrast to the case of normal incidence, these relations involve eight media parameters: the impedances Z, Z', and the velocities v, v' on both sides of the interface, and for both the longitudinal and transverse waves.

There is another factor that makes boundary acoustic effects more complex. Within certain frequency ranges, interfaces (and in particular surfaces) of elastic solids may sustain so-called surface acoustic waves (SAW), in particular, the Rayleigh waves and the Love waves. [39] The main feature that distinguishes such waves from their bulk (longitudinal and transverse) counterparts, discussed above, is that the displacement amplitudes are largest at the interface and decay exponentially into the bulk of both adjacent media. The characteristic depth of this penetration is of the order of the wavelength, though not exactly equal to it.

In the Rayleigh waves, the particle displacement vector $\mathbf{q}$ has two components: one longitudinal (and hence parallel to the interface) and another transverse (perpendicular to the interface). In contrast to the bulk waves, these components are coupled (via their interaction with the interface) and hence propagate with a single velocity v_{R}. As a result, the trajectory of each particle in the Rayleigh wave is an ellipse in the plane perpendicular to the interface. A straightforward analysis [40] of the Rayleigh waves on the surface of an elastic solid (i.e. its interface with vacuum) yields the following equation for v_{R} :

$$\left(2-\frac{v_{\mathrm{R}}^2}{v_{\mathrm{t}}^2}\right)^4=16\left(1-\frac{v_{\mathrm{R}}^2}{v_{\mathrm{t}}^2}\right)^2\left(1-\frac{v_{\mathrm{R}}^2}{v_{\mathrm{l}}^2}\right)^2. \tag{7.7.21}$$

According to this formula, and Eqs. (112) and (116), for realistic materials with the Poisson index between 0 and $1/2$, the Rayleigh waves are slightly (by 4 to 13%) slower than the bulk transverse waves – and hence substantially slower than the bulk longitudinal waves.

In contrast, the Love waves are purely transverse, with $\mathbf{q}$ oriented parallel to the interface. However, the interaction of these waves with the interface reduces their velocity v_{L} in comparison with that (v_{t}) of the bulk transverse waves, keeping it within the narrow interval between v_{t} and v_{R} :

$$v_{\mathrm{R}}<v_{\mathrm{L}}<v_{\mathrm{t}}<v_{\mathrm{l}} \tag{7.7.22}$$

The practical importance of surface acoustic waves is that their amplitude decays very slowly with distance r from their point-like source: $a \propto 1/r^{1/2}$, while any bulk waves decay much faster, as $a \propto 1/r$. (Indeed, in the latter case the power $\mathscr{P} \propto a^2$, emitted by such source, is distributed over a spherical surface area proportional to r^2, while in the former case all the power goes into a thin surface circle whose length scales as r.) At least two areas of applications of the surface acoustic waves have to be mentioned: in geophysics (for the earthquake detection and the Earth crust seismology), and electronics (for signal processing, with a focus on frequency filtering). Unfortunately, I cannot dwell on these interesting topics and I have to refer the reader to special literature. [41]

[33] Note though that Eq. (107) is more complex than the simple wave equation (6.40).

[34] Because of that, one can frequently meet the term shear waves. Note also that in contrast to the transverse waves in the simple 1D model analyzed in Chapter 6 (see Figure 6.4a), those in a 3D continuum do not need a prestretch tension $\mathscr{T}$. We will return to the effect of tension in the next section.

[35] Because of this difference between v_1 and v_t, in geophysics, the longitudinal waves are known as P-waves (with the letter P standing for "primary") because they arrive at the detection site, say from an earthquake, first - before the transverse waves, called the S-waves, with S standing for "secondary".

[36] Named after Nikolai Alekseevich Umov, who introduced this concept in 1874 - ten years before a similar notion for electromagnetic waves (see, e.g., EM Sec. 6.4) was suggested by J. Poynting. In a dissipation-free, elastic medium, the Umov vector obeys the following continuity equation: $\partial\left(\rho v^2/2+u\right)/\partial t+\nabla\cdot\boldsymbol{h}=0$, with u given by Eq. (52), which expresses the conservation of the total (kinetic plus potential) energy of the elastic deformation.

[37] See, e.g., EM Sec. 7.5.

[38] Their discussion may be also found in EM Sec. 7.5.

[39] Named, respectively, after Lord Rayleigh (born J. Strutt, 1842-1919) who has theoretically predicted the very existence of surface acoustic waves, and A. Love (1863-1940).

[40] Unfortunately, I do not have time/space to reproduce this calculation either; see, e.g., Sec. 24 in L. Landau and E. Lifshitz, Theory of Elasticity, 3rd ed., Butterworth-Heinemann, 1986.

[41] See, for example, K. Aki and P. Richards, Quantitative Seismology, 2nd ed., University Science Books, 2002 and D. Morgan, Surface Acoustic Waves, 2nd ed., Academic Press, 2007.

7.8: Elastic Waves in Thin Rods

From what we have discussed at the end of the last section, it should be pretty clear that generally, the propagation of acoustic waves in elastic bodies of finite size may be very complicated. There is, however, one important limit in which several important results may be readily obtained. This is the limit of (relatively) low frequencies, where the corresponding wavelength is much larger than at least one dimension of a system. Let us consider, for example, various waves that may propagate along thin rods, in this case "thin" meaning that the characteristic size a of the rod's cross-section is much smaller than not only the length of the rod, but also the wavelength $\lambda = 2\pi/k$. In this case, there is a considerable range of distances z along the rod,

$$a << \Delta z << \lambda, \tag{7.8.1}$$

in that we can neglect the material's inertia, and apply the results of our earlier static analyses.

For example, for a longitudinal wave of stress, which is essentially a wave of periodic tensile extensions and compressions of the rod, within the range (129) we may use the static relation (42):

$$\sigma_{zz} = E s_{zz}. \tag{7.8.2}$$

For what follows, it is easier to use the general equation of elastic dynamics not in its vector form (107), but rather in the precursor, Cartesian-component form (25), with $f_j = 0$. For plane waves propagating along the z-axis, only one component (with $j' \to z$) of the sum on the right-hand side of this equation is not equal to zero, and it is reduced to

$$\rho \frac{\partial^2 q_j}{\partial^2 t^2} = \frac{\partial \sigma_{jz}}{\partial z}. \tag{7.8.3}$$

In our current case of longitudinal waves, all components of the stress tensor but σ_{zz} are equal to zero. With σ_{zz} from Eq. (130), and using the definition $s_{zz} = \partial q_z/\partial z$, Eq. (131) is reduced to a simple wave equation,

$$\rho \frac{\partial^2 q_z}{\partial^2 t^2} = E \frac{\partial^2 q_z}{\partial z^2}, \tag{7.8.4}$$

which shows that the velocity of such tensile waves is

$$v = \left(\frac{E}{\rho} \right)^{1/2} \tag{7.8.5}$$

Comparing this result with Eq. (112), we see that the tensile wave velocity, for any realistic material with a positive Poisson ratio, is lower than the velocity v_1 of longitudinal waves in the bulk of the same material. The reason for this difference is simple: in thin rods, the cross-section is free to oscillate (e.g., shrink in the longitudinal extension phase of the passing wave), [42] so that the effective force resisting the longitudinal deformation is smaller than in a border-free space. Since (as it is clearly visible from the wave equation), the scale of the force determines that of v^2, this difference translates into slower waves in rods. Of course, as the wave frequency is increased to $ka \sim 1$, there is a (rather complex and cross-section-depending) crossover from Eq. (133) to Eq. (112).

Proceeding to transverse waves in rods, let us first have a look at long bending waves, for which the condition (129) is satisfied, so that the vector $\mathbf{q} = \mathbf{n}_x q_x$ (with the x-axis being the bending direction see Figure 8) is virtually constant in the whole cross-section. In this case, the only component of the stress tensor contributing to the net transverse force F_x is σ_{xz}, so that the integral of Eq. (131) over the crosssection is

$$\rho A \frac{\partial^2 q_x}{\partial t^2} = \frac{\partial F_x}{\partial z}, \quad \text{with } F_x = \int_A \sigma_{xz} d^2 r. \tag{7.8.6}$$

Now, if Eq. (129) is satisfied, we again may use the static local relations (75)-(77), with all derivatives d/dz duly replaced with their partial form $\partial/\partial z$, to express the force F_x via the bending deformation q_x. Plugging these relations into each other one by one, we arrive at a rather unusual differential equation

$$\rho A \frac{\partial^2 q_x}{\partial t^2} = -E I_y \frac{\partial^4 q_x}{\partial z^4}. \tag{7.8.7}$$

Looking for its solution in the form of a sinusoidal wave (108), we get the following nonlinear dispersion relation: 43

$$\omega = \left(\frac{EI_y}{\rho A}\right)^{1/2} k^2. \tag{7.8.8}$$

Such relation means that the bending waves are not acoustic at any frequency, and cannot be characterized by a single velocity that would be valid for all wave numbers k, i.e. for all spatial Fourier components of a waveform. According to our discussion in Sec. 6.3, such strongly dispersive systems cannot pass non-sinusoidal waveforms too far without changing their waveform rather considerably.

This situation changes, however, if the rod is pre-stretched with a tension force $\mathscr{T}$ - just as in the discrete 1D model that was analyzed in Sec. 6.3. The calculation of the effect of this force is essentially similar; let us repeat it for the continuous case, for a minute neglecting the bending stress - see Figure 13.

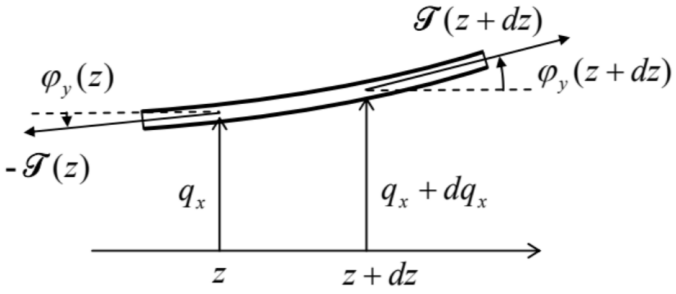

Fig. 7.13. Additional forces in a thin rod ("string"), due to the background tension $\mathscr{T}$.

Still sticking to the limit of small angles φ, the additional vertical component $d\mathscr{T}_x$ of the net force acting on a small rod fragment of length dz is $\mathscr{T}_x(z-dz) - \mathscr{T}_x(z) = \mathscr{T}\varphi_y(z+dz) - \mathscr{T}\varphi_y(z) \approx \mathscr{T}\left(\partial\varphi_y/\partial z\right)dz$, so that $\partial F_x/\partial z = \mathscr{T}\left(\partial\varphi_y/\partial z\right)$. With the geometric relation (77) in its partial-derivative form $\partial q_x/\partial z = \varphi_y$, this additional term becomes $\mathscr{T}\left(\partial^2 q_x/\partial z^2\right)$. Now adding it to the right-hand side of Eq. (135), we get the following dispersion relation

$$\omega^2 = \frac{1}{\rho A}\left(EI_y k^4 + \mathscr{T}^2\right) \tag{7.8.9}$$

Since the product ρA in the denominator of this expression is just the rod's mass per unit length (which was denoted μ in Chapter 6), at low k (and hence low frequencies), this expression is reduced to the linear dispersion law, with the velocity given by Eq. (6.43):

$$v = \left(\frac{\mathscr{T}}{\rho A}\right)^{1/2}. \tag{7.8.10}$$

So Eq. (137) describes a smooth crossover from the "guitar-string" acoustic waves to the highly dispersive bending waves (136).

Now let us consider another type of transverse waves in thin rods - the so-called torsional waves, which are essentially the dynamic propagation of the torsional deformation discussed in Sec. 6 . The easiest way to describe these waves, again within the limits (129), is to write the equation of rotation of a small segment dz of the rod about the z-axis, passing through the "center of mass" of its cross-section, under the difference of torques $\tau = \mathbf{n}_z\tau_z$ applied on its ends - see Figure 10:

$$\rho I_z dz \frac{\partial^2\varphi_z}{\partial t^2} = d\tau_z, \tag{7.8.11}$$

where I_z is the "moment of inertia" defined by Eq. (91), which now, after its multiplication by ρdz, i.e. by the mass per unit area, has turned into the genuine moment of inertia of a dz-thick slice of the rod. Dividing both sides of Eq. (139) by dz, and using the static local relation (84), $\tau_z = C\kappa = C\left(\partial\varphi_z/\partial z\right)$, we get the following differential equation

$$\rho I_z \frac{\partial^2\varphi_z}{\partial t^2} = C\frac{\partial^2\varphi_z}{\partial z^2}. \tag{7.8.12}$$

Just as Eqs. (111), (115), and (132), this equation describes an acoustic (dispersion-free) wave, which propagates with the following frequency-independent velocity

$$v = \left(\frac{C}{\rho I_z}\right)^{1/2}. \tag{7.8.13}$$

As we have seen in Sec. 6, for rods with axially-symmetric cross-sections, the torsional rigidity C is described by the simple relation (89), $C = \mu I_z$, so that Eq. (141) is reduced to Eq. (116) for the transverse waves in infinite media. The reason for this similarity is simple: in a torsional wave, particles oscillate along small arcs (Figure 14a), so that if the rod's cross-section is round, its surface is stress-free, and does not perturb or modify the motion in any way, and hence does not affect the transverse velocity.

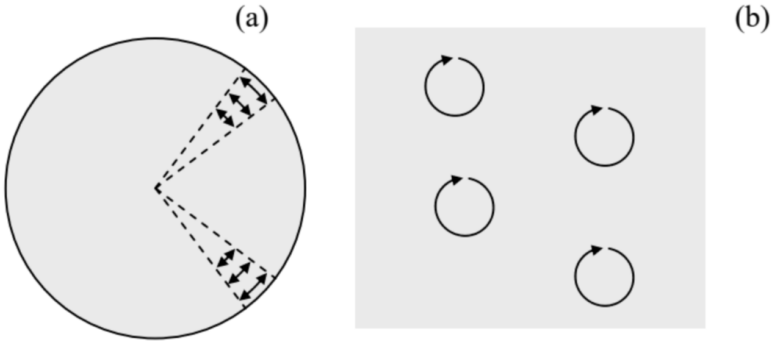

Figure 7.14. Particle trajectories in two different transverse waves with the same velocity: (a) torsional waves in a thin round rod and (b) circularly-polarized waves in an infinite (or very broad) sample.

This fact raises an interesting issue of the relation between the torsional and circularly-polarized waves. Indeed, in Sec. 7, I have not emphasized enough that Eq. (116) is valid for a transverse wave polarized in any direction perpendicular to vector $\mathbf{k}$ (in our notation, directed along the z-axis). In particular, this means that such waves are doubly-degenerate: any isotropic elastic continuum can carry simultaneously two non-interacting transverse waves propagating in the same direction with the same velocity (116), with two mutually perpendicular linear polarizations (directions of the vector a), for example, directed along the x - and y-axes. [44] If both waves are sinusoidal (108), with the same frequency, each point of the medium participates in two simultaneous sinusoidal motions within the $[x, y]$ plane:

$$q_x = \mathrm{Re}\left[a_x e^{i(kz-\omega t)}\right] = A_x \cos\Psi, \quad q_y = \mathrm{Re}\left[a_y e^{i(kz-\omega t)}\right] = A_y \cos(\Psi + \varphi), \tag{7.8.14}$$

where $\Psi \equiv kz - \omega t + \varphi_x$, and $\varphi \equiv \varphi_y - \varphi_x$. Basic geometry tells us that the trajectory of such a motion on the $[x, y]$ plane is an ellipse (Figure 15), so that such waves are called elliptically polarized. The most important particular cases of such polarization are:

(i) $\varphi = 0$ or π. a linearly-polarized wave, with vector a is directed at angle $\theta = \tan^{-1}(A_y/A_x)$ relatively the axis x; and

(ii) $\varphi = \pm\pi/2$ and $A_x = A_y$: two possible circularly-polarized waves, with the right or left polarization, respectively. [44]

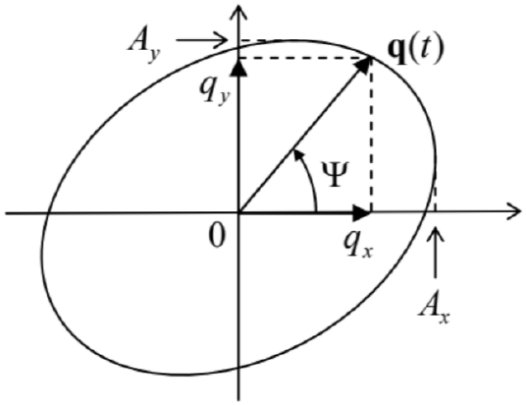

Figure 7.15. The trajectory of a particle in an elliptically polarized transverse wave, within the plane perpendicular to the direction of wave propagation.

Now comparing the trajectories of particles in the torsional wave in a thin round rod (or pipe) and the circularly-polarized wave in a broad sample (Figure 14), we see that, despite the same wave propagation velocity, these transverse waves are rather different. In the former case (Figure 14a) each particle moves back and forth along an arc, with the arc length different for different particles

(and vanishing at the rod's center), so that the waves are not plane. On the other hand, in a circularly polarized wave, all particles move along similar, circular trajectories, so that such wave is plane.

To conclude this chapter, let me briefly mention the opposite limit, when the size of the body, from whose boundary the waves are completely reflected, [46] is much larger than the wavelength. In this case, the waves propagate almost as in an infinite 3D continuum (which was analyzed in Sec. 7), and the most important new effect is the finite numbers of wave modes in the body. Repeating the 1D analysis at the end of Sec. 6.5, for each dimension of a 3D cuboid of volume $V = l_1 l_2 l_3$, and taking into account that the numbers k_n in each of 3 dimensions are independent, we get the following generalization of Eq. (6.75) for the number ΔN of different traveling waves with wave vectors within a relatively small volume d^3k of the wave vector space:

$$dN = g\frac{V}{(2\pi)^3}d^3k \gg 1, \quad \text{for } \frac{1}{V} << d^3k << k^3, \tag{7.8.15}$$

where $k \gg>> 1/l_{1,2,3}$ is the center of this volume, and g is the number of different possible wave modes with the same wave vector $\mathbf{k}$. For the mechanical waves analyzed above, with one longitudinal mode, and two transverse modes with different polarizations, $g = 3$.

Note that since the derivation of Eqs. (6.75) and (143) does not use other properties of the waves (in particular, their dispersion relations), the mode counting rule is ubiquitous in physics, being valid, in particular, for electromagnetic waves (where $g = 2$) and quantum "de Broglie waves" (i.e. wavefunctions), whose degeneracy factor g is usually determined by the particle's spin. [47]

---

[42] For this reason, the tensile waves can be called longitudinal only in a limited sense: while the stress wave is purely longitudinal: $\sigma_{xx} = \sigma_{yy} = 0$, the strain wave is not: $s_{xx} = s_{yy} = -\sigma_{zz} \neq 0$, i.e. $\mathbf{q}(\mathbf{r}, t) \neq \mathbf{n}_z q_z$.

[43] Note that since the "moment of inertia" I_y, defined by Eq. (70), may depend on the bending direction (unless the cross-section is sufficiently symmetric), the dispersion relation (136) may give different results for different directions of the bending wave polarization.

[44] As was shown in Sec. 6.3, this is true even in the simple 1D model shown in Figure 6.4a.

[45] The circularly polarized waves play an important role in quantum mechanics, where they may be most naturally quantized, with their elementary excitations (in the case of mechanical waves we are discussing, called phonons) having either positive or negative angular momentum $L_z = \pm\hbar$.

[46] For acoustic waves, such a condition is easy to implement. Indeed, from Sec. 7 we already know that the strong inequality of wave impedances Z is sufficient for such reflection. The numbers of Table 1 show that, for example, the impedance of a longitudinal wave in a typical metal (say, steel) is almost two orders of magnitude higher than that in air, ensuring their virtually full reflection from the surface.

[47] See, e.g., EM Secs. 7.8 and QM Sec. 1.7.

7.9: Exercise Problems

7.1. A uniform thin sheet of an isotropic, elastic material, of thickness t and area $A \gg t^2$, is compressed by two plane, parallel, broad, rigid surfaces - see the figure on the right. Assuming no slippage between the sheet and the surfaces, calculate the relative compression $(-\Delta t/t)$ as a function of the compressing force. Compare the result with that for the tensile stress, calculated in Sec. 7.

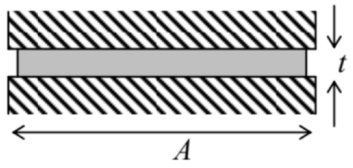

7.2. Two opposite edges of a thin, very wide sheet of an isotropic, elastic material have been clamped in two rigid, plane, parallel walls that are pulled apart with force F, along the sheet's length l. Find the relative extension $\Delta l/l$ of the sheet in the direction of the force, and its relative compression $\Delta t/t$ in the perpendicular direction, and compare the results with Eqs. (7.45)-(7.46) for the tensile stress and the solution of the previous problem.

7.3. Calculate the radial extension ΔR of a thin, long, round cylindrical pipe, due to its rotation with a constant angular velocity ω about its symmetry axis (see the figure on the right), in terms of the elastic moduli E and v. The external pressure both inside and outside the pipe is negligible.

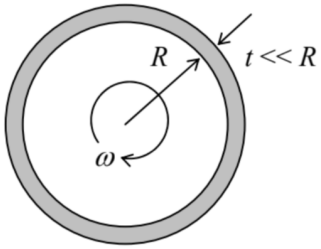

7.4. A long, uniform rail with the cross-section shown in the figure on the right, is being bent with the same (small) torque twice: first within the xz plane and then within the yz-plane. Assuming that $t << l$, find the ratio of the rail bending deformations in these two cases.

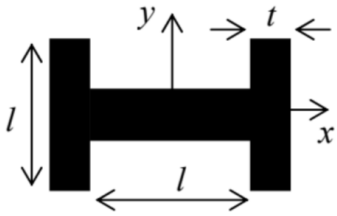

7.5. Two thin rods of the same length and mass are made of the same elastic, isotropic material. The cross-section of one of them is a circle, while the other one is an equilateral triangle - see the figure on the right. Which of the rods is stiffer for bending along its length? Quantify the relation. Does the result depend on the bending plane orientation?

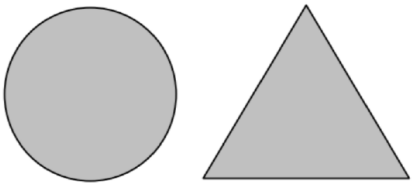

7.6. A thin, elastic, uniform, initially straight beam is placed on two point supports at the same height – see the figure on the right. What support placement minimizes the largest deviation of the beam from the horizontal baseline, under its own weight?

Hint: An approximate answer (with an accuracy better than 1%) is acceptable.

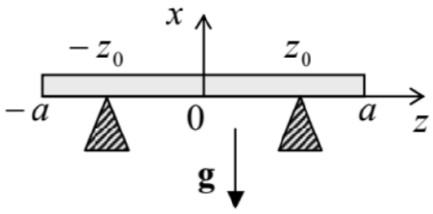

7.7. Calculate the largest longitudinal compression force $\mathscr{T}$ that may be withstood by a thin, straight, elastic rod without bucking (see the figure on the right) for two shown cases:

(i) the rod's ends are clamped, and

(ii) the rod it free to turn about the support points.

7.8. An elastic, light, thin poll with a square cross-section of area $A = a \times a$, had been firmly dug into the ground in the vertical position, sticking out by height $h >> a$. What largest compact mass M may be placed straight on the top of the poll without the stability loss?

7.9. Calculate the potential energy of a small and slowly changing, but otherwise arbitrary bending deformation of a uniform, elastic, initially straight rod. Can the result be used to derive the dispersion relation (136)?

7.10. Calculate the torsional rigidity of a thin, uniform rod whose cross-section is an ellipse with semi-axes a and b.

7.11. Calculate the potential energy of a small but otherwise arbitrary torsional deformation $\varphi_z(z)$ of a uniform, straight, elastic rod.

7.12. Calculate the spring constant $\kappa \equiv dF/dl$ of a coil spring made of a uniform, elastic wire, with circular cross-section of diameter d, wound as a dense round spiral of $N \ggg 1$ turns of radius $R \gg d-$ see the figure on the right.

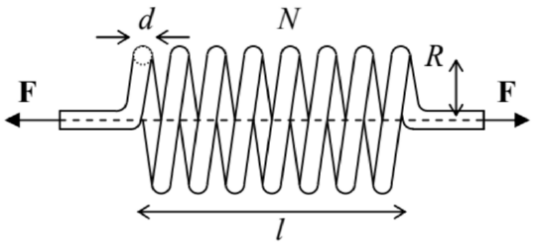

7.13. The coil spring, described in the previous problem, is now used as what is sometimes called the torsion spring - see the figure on the right. Find the corresponding spring constant $d\tau/d\varphi$, where τ is the torque of the external forces relative to the center of the coil (point 0).

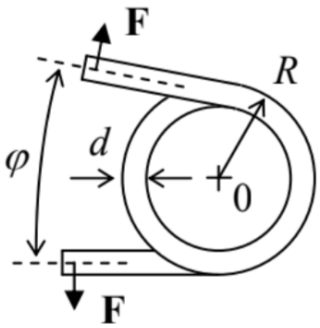

7.14. Use Eqs. (99) and (100) to recast Eq. (101b) for the torsional rigidity C of a thin rod into the form given by Eq. (101c).

7.15. * Generalize Eq. (101b) to the case of rods with more than one cross-section's boundary. Use the result to calculate the torsional rigidity of a thin round pipe, and compare it with Eq. (91).

7.16. A long steel wire has a circular cross-section with a 3-mm diameter, and is pre-stretched with a constant force of 10 N. Which of the longitudinal and transverse waves with frequency 1kHz has the largest group velocity in the wire? Accept the following parameters for the steel (see Table 1): $E = 170\text{GPa}, v = 0.30, \rho = 7.8\ \text{g}/\text{cm}^3$.

7.17. Define and calculate the wave impedances for (i) tensile and (ii) torsional waves in a thin rod, appropriate in the long-wave limit. Use the results to calculate the fraction of each wave's power $\mathscr{P}$ reflected from a firm connection of a long rod with a round cross-section to a similar rod, but with a twice smaller diameter – see the figure on the right.

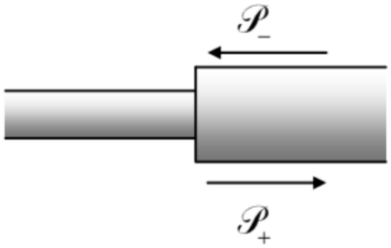

CHAPTER OVERVIEW

8: Fluid Mechanics

This chapter describes the basic notions of fluid mechanics, discusses a few core problems of statics and dynamics of ideal and viscous fluids, and gives a very brief, rather superficial review of such a complicated phenomenon as turbulence. In addition, the viscous fluid flow discussion is used as a platform for an elementary introduction to numerical methods of the partial differential equation solution - whose importance extends well beyond this particular field.

8.1: Hydrostatics

The mechanics of fluids (defined as the materials that cannot keep their geometric form on their own, and include both liquids and gases) is both more simple and more complex than that of the elastic solids, with the simplicity falling squarely to the domain of statics. [1] Indeed, fluids, by definition, cannot resist static shear deformations. There are two ways to express this fact. First, we can formally take the shear modulus μ, describing this resistance, to equal zero. Then the Hooke's law (7.32) shows that the stress tensor is diagonal:

$$\sigma_{ij'} = \sigma_{jj}\delta_{ij'} \tag{8.1.1}$$

Alternatively, the same conclusion may be reached just by looking at the stress tensor definition (7.19) and/or Figure 7.3, and saying that in the absence of shear stress, the elementary interface $d\mathbf{F}$ has to be perpendicular to the area element dA, i.e. parallel to the vector $d\mathbf{A}$.

Moreover, in fluids at equilibrium, all three diagonal components σ_{ij} of the stress tensor have to be equal. To prove that, it is sufficient to single out (mentally rather than physically), from a static fluid, a small volume in the shape of a right prism, with mutually perpendicular faces normal to the two directions we are interested in - in Figure 1, along the x - and y-axes.

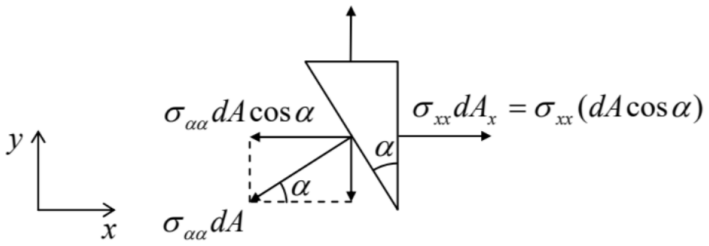

Fig. 8.1. Proving the pressure isotropy.

The prism is in equilibrium if each Cartesian component of the vector of the total force exerted on all its faces equals zero. For the x-component this balance may be expressed as $\sigma_{xx} dA_x - (\sigma_{\alpha\alpha} dA)\cos\alpha = 0$. However, from the geometry (Figure 1), $dA_x = dA\cos\alpha$, so that the above expression yields $\sigma_{\alpha\alpha} = \sigma_{xx}$. A similar argument for the y-component gives $\sigma_{\alpha\alpha} = \sigma_{yy}$ so that $\sigma_{xx} = \sigma_{yy}$. Changing the orientation of the prism, we can get such equalities for any pair of diagonal components of the stress tensor, σ_{jj}, so that all three of them have to be equal.

This common diagonal element of the stress matrix is usually denoted as $(-\mathcal{P})$, because in the vast majority of cases, the parameter $\mathcal{P}$, called pressure, is positive. Thus we arrive at the key relation (which has already been mentioned in Sec. 7.2):

$$\sigma_{ij'} = -\mathcal{P}\delta_{jj'} \tag{8.1.2}$$

In the absence of bulk forces, pressure should be constant through the volume of fluid, due to the translational symmetry. Let us see how this result is affected by bulk forces. With the simple stress tensor (2), the general condition of equilibrium of a continuous medium, expressed by Eq. (7.25) with the left-hand side equal to zero, becomes

$$-\frac{\partial \mathcal{P}}{\partial r_j} + f_j = 0, \tag{8.1.3}$$

and may be re-written in the following convenient vector form:

$$-\nabla P + \mathbf{f} = 0. \tag{8.1.4}$$

In the simplest case of a heavy fluid with mass density ρ, in a uniform gravity field $\mathbf{f} = \rho\mathbf{g}$, the equation of equilibrium becomes,

$$-\nabla\mathcal{P} + \rho\mathbf{g} = 0, \tag{8.1.5}$$

with only one nonzero component (vertical, near the Earth surface). If, in addition, the fluid may be considered incompressible, with its density ρ constant,[2] this equation may be readily integrated over the vertical coordinate (say, y) to give the so-called Pascal equation: [3]

$$P + \rho g y = \text{ const}, \tag{8.1.6}$$

where the direction of the y-axis is taken opposite to that of vector $\mathbf{g}$.

Two manifestations of this key equation are well known. The first one is the fact that in interconnected vessels filled with a fluid, its pressure is equal at all points at the same height (y), regardless of the vessel shape, provided that the fluid is in equilibrium. The second result is the buoyant force $\mathbf{F}_{\rm b}$ exerted by a liquid on a (possibly, partly) submerged body, i.e. the vector sum of the elementary pressure forces $d\mathbf{F} = \mathcal{P}d\mathbf{A}$ exerted on all elementary areas dA of the submerged part of the body's surface - see Figure 2. According to Eq. (6), with the constant equal to zero (corresponding to zero pressure at the liquid's surface taken for $y = 0$, see Figure 2a), the vertical component of this elementary force is

$$dF_y = dF\cos\varphi = \mathcal{P}dA\cos\varphi = -\rho g y\cos\varphi dA = -\rho g y dA_h. \tag{8.1.7}$$

where $dA_h = \cos\varphi dA$ is the horizontal footprint (say, $dxdz$) of the elementary area dA. Now integrating this relation over all the surface, we get the total vertical buoyant force: 4

$$F_{\rm b} = \rho g\int_S (-y)dA_h \equiv \rho g V, \tag{8.1.8}$$

where V is the volume of the submerged part of the body's volume, while ρ is the liquid's density, so that by magnitude, $F_{\rm b}$ equals the weight of the liquid which would fill the submerged volume.

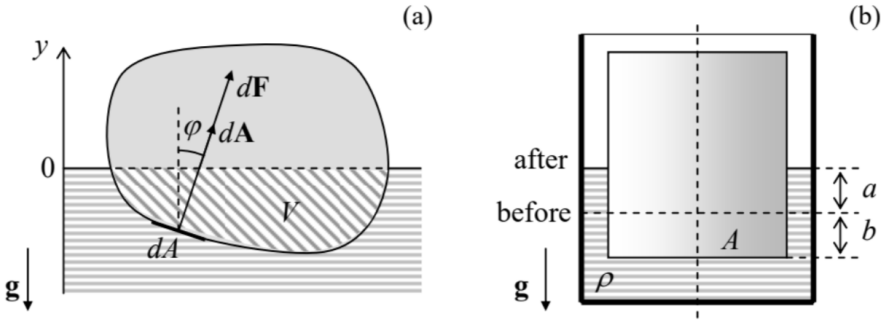

Figure 8.2. Calculating the buoyant force.

This well-known Archimedes principle may be proved even more simply using the following argument: the fluid's pressure forces, and hence the resulting buoyant force, cannot depend on what is inside the body's volume. Hence F_b would be the same if we filled the volume V in question with a fluid similar to the surrounding one. But in this case, the surface does not play any role, and the fluid should be still in equilibrium, so that both forces acting on it, the buoyant force $\mathbf{F}_{\rm b}$ and the internal liquid's weight $m\mathbf{g} = \rho V\mathbf{g}$, have to be equal and opposite, thus proving Eq. (8) again.

Despite the simplicity of the Archimedes principle, its different, erroneous formulations, such as "The buoyant force's magnitude is equal to the weight of the displaced liquid" [WRONG!] creep from one undergraduate textbook to another, leading to application errors. A typical example is shown in Figure 2 b, where a solid vertical cylinder with the base area A is pressed into a liquid inside a container of comparable size, pushing the liquid's level up. The correct answer for the buoyant force, following from Eq. (8), is

$$F_{\rm b} = \rho g V = \rho g A(a+b), \tag{8.1.9}$$

because the volume V of the submerged part of the cylinder is evidently $A(a+b)$. But the wrong formulation cited above, using the term displaced liquid, would give a different answer:

$$F_{\rm b} = \rho g V_{\rm displaced} = \rho g A b. \quad [\,\text{WRONG!}\,] \tag{8.1.10}$$

(The latter result is correct only asymptotically, in the limit of a very large container.)

Another frequent error in hydrostatics concerns the angular stability of a freely floating body the problem evidently of vital importance for the boat/ship design. It is sometimes claimed that the body is stable only if the so-called buoyancy center, the effective point of buoyant force application (in Fig, 3 , point B), is above the center of mass (0) of the whole floating body. [5] However, as Figure 3 shows, this is unnecessary; indeed in the shown case, point B (which is just the center of mass the liquid would have in the submerged part) is below point 0 , even at a small tilt. Still, in this case, the torque created by the pair of forces $\mathbf{F}_{\rm b}$ and $m\mathbf{g}$ tries to return the body to the equilibrium position, which is therefore stable. As Figure 3 shows, the actual condition of the angular stability may be expressed as the requirement for point M (in shipbuilding, called the metacenter of the ship's hull) to be above the ship's center of mass 0. [6]

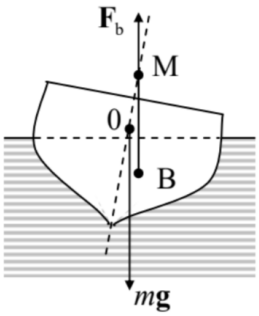

Figure 8.3. Angular stability of a floating body.

To conclude this section, let me note that the integration of Eq. (4) may be more complex in the case if the bulk forces $\mathbf{f}$ depend on position, [7] and/or if the fluid is substantially compressible. In the latter case, Eq. (4) has to be solved together with the medium-specific equation of state $\rho = \rho(\mathcal{P})$ describing its compressibility law - whose example is given by Eq. (7.38) for ideal gases: $\rho \equiv mN/V = m\mathcal{P}/k_{\mathrm{B}}T$, where m is the mass of one gas molecule.

---

[1] It is often called hydrostatics because water has always been the most important liquid for the human race and hence for science and engineering.

[2] As was discussed in Sec. 7.3 in the context of Table 7.1, this is an excellent approximation, for example, for human-scale experiments with water.

[3] The equation, and the SI unit of pressure $1\ \mathrm{Pa} \equiv 1\ \mathrm{N/m^2}$, are named after Blaise Pascal (1623-1662) who has not only pioneered hydrostatics, but also invented the first mechanical calculator, and made several other important contributions to mathematics - and to Christian philosophy!

[4] The force is strictly vertical, because the horizontal components of the elementary forces $d\mathbf{F}$ exerted on opposite elementary areas dA, at the same height y, cancel.

[5] Please note the crucial difference between the whole body and that of its submerged part.

[6] A small tilt of the body leads to a small lateral displacement of point B, but does not affect the position of the metacenter M.

[7] A simple example of such a problem is given by the fluid equilibrium in a container rotating with a constant angular velocity ω. If we solve such a problem in a reference frame rotating together with the container, the real bulk forces should be complemented by the centrifugal "force" (4.93), depending on $\mathbf{r}$.

8.2: Surface Tension Effects

Besides the bulk (volume-distributed) forces, one more possible source of pressure is surface tension. This effect results from the difference between the potential energy of atomic interactions on the interface between two different fluids and that in their bulks, and thus may be described by an additional potential energy

$$U_{\rm i} = \gamma A, \tag{8.2.1}$$

where A is the interface area, and γ is called the surface tension constant - or just the "surface tension". For a stable interface of any two fluids, γ is always positive. [8] For surfaces of typical liquids (or their interfaces with air), at room temperature, the surface tension equals a few 10^{-2} J/m^2, corresponding to the potential energy $U_{\rm i}$ of a few 10^{-2}eV per surface molecule - i.e. just a fraction of the full binding (or "cohesive") energy of the same liquid, which is typically of the order of 10^{-1}eV per molecule.

In the absence of other forces, the surface tension makes a liquid drop spherical to minimize its surface area A at a fixed volume. For the analysis of the surface tension effects for more complex geometries, and in the presence of other forces, it is convenient to reduce it to a certain additional effective pressure drop $\Delta\mathcal{P}_{\rm ef}$ at the interface. To calculate $\Delta\mathcal{P}_{\rm ef}$, let us consider the condition of equilibrium of a small part dA of a smooth interface between two fluids (Figure 2), in the absence of bulk forces.

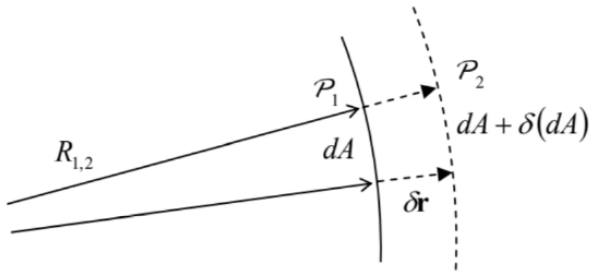

Figure 8.4. Deriving the Young-Laplace formula (13).

If the pressures $\mathcal{P}_{1,2}$ on the two sides of the interface are different, the work of stress forces on fluid 1 at a small virtual displacement $\delta\mathbf{r} = \mathbf{n}\delta r$ of the interface (where $\mathbf{n} = d\mathbf{A}/dA$ is the unit vector normal to the interface) equals

$$\delta\mathscr{W} = dA\delta r\,(\mathcal{P}_1 - \mathcal{P}_2)\,. \tag{8.2.2}$$

For equilibrium, this work has to be compensated by an equal change of the interface energy, $\delta U_{\rm i} = \gamma\delta(dA)$. Differential geometry tells us that in the linear approximation in δr, the relative change of the elementary surface area, corresponding to a fixed solid angle $d\Omega$, may be expressed as

$$\frac{\delta(dA)}{dA} = \frac{\delta r}{R_1} + \frac{\delta r}{R_2}, \tag{8.2.3}$$

where $R_{1,2}$ are the so-called principal radii of the interface curvature. [10] Combining Eqs. (10)-(12), we get the Young-Laplace formula 11

$$\mathcal{P}_1 - \mathcal{P}_2 = \Delta\mathcal{P}_{\rm ef} \equiv \gamma\left(\frac{1}{R_1} + \frac{1}{R_2}\right). \tag{8.2.4}$$

In particular, this formula shows that the additional pressure created by surface tension inside a spherical drop of a liquid, of radius R, equals $2\gamma/R$, i.e. decreases with R. In contrast, according to Eqs. (5)-(6), the effects of bulk forces, for example gravity, grow as $\rho g R$. The comparison of these two pressure components shows that if the drop radius (or more generally, the characteristic linear size of a fluid sample) is much larger than the so-called capillary length

$$a_{\rm c} \equiv \left(\frac{2\gamma}{\rho g}\right)^{1/2} \tag{8.2.5}$$

the surface tension may be safely ignored - as will be done in all following sections of this chapter, besides a brief discussion at the end of Sec. 4. For the water surface, or more exactly its interface with air at ambient conditions, $\gamma \approx 0.073$ J/m^2 (i.e. N/m), while $\rho \approx 1,000$ kg/m^3, so that $a_{\rm c} \approx 4$ mm.

On the other hand, in very narrow tubes, such as blood capillary vessels with radius $a \sim 1\mu\text{m}$, i.e. $a << a_c$, the surface tension effects are very important. The key notion for the analysis of these effects is the contact angle θ_c (also called the "wetting angle") at an equilibrium edge of a liquid wetting a solid - see Figure 5 .

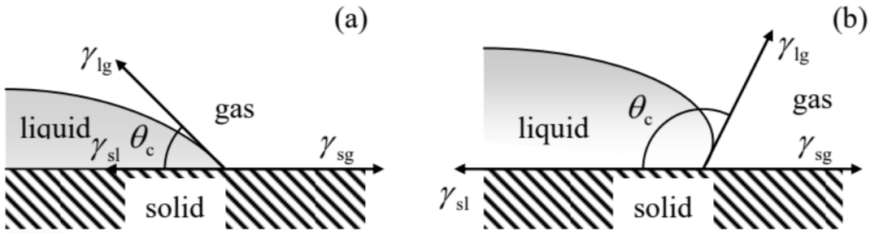

Figure 8.5. Contact angles for (a) hydrophilic and (b) hydrophobic surfaces.

According to its definition (10), the constant γ may be interpreted as a force (per unit length of the interface boundary) directed normally to the boundary, and "trying" to reduce the interface area. As a result, the balance of horizontal components of the three such forces, shown in Figure 5a, immediately yields the Young's equation

$$\gamma_{sl} + \gamma_{lg} \cos\theta_c = \gamma_{sg}, \tag{8.2.6}$$

where the indices of constants γ correspond to three possible interfaces between the liquid, solid, and gas. For the so-called hydrophilic surfaces that "like to be wet" by a particular liquid (not necessarily water), meaning that $\gamma_{sl} < \gamma_{sg}$, this relation yields $\cos\theta_c > 0$, i.e. $\theta_c < \pi/2-$ the situation shown in Figure 5a. On the other hand, for hydrophobic surfaces with $\gamma_{sl} > \gamma_{sg}$, Eq. (15) yields larger contact angles, $\theta_c > \pi/2$ - see Figure 5*b*.

Let us use this notion to solve the simplest and perhaps the most practically important problem of this field - find the height h of the fluid column lifted by the surface tension forces in a narrow vertical tube made of a hydrophilic material, assuming its internal surface to be a round cylinder of radius a - see Figure 6. Inside an incompressible fluid, pressure drops with height according to the Pascal equation (6), so that just below the surface, $\mathcal{P} \approx \mathcal{P}_0 - \rho g h$, where $\mathcal{P}_0$ is the background (e.g., atmospheric) pressure. This means that at $a << h$ the pressure variation along the concave surface (called the meniscus) of the liquid is negligible, so that according to the Young-Poisson equation (13), the sum $(1/R_1 + 1/R_2)$ has to be virtually constant along the surface. Due to the axial symmetry of the problem, this means that the surface has to be a part of a sphere. From the contact angle definition, the radius R of the sphere is equal to $a/\cos\theta_c-$ see Figure 6. Plugging this relation into Eq. (3) with $\mathcal{P}_1 - \mathcal{P}_2 = \rho g h$, we get the following result for h :

$$\rho g h = \frac{2\gamma \cos\theta_c}{a}. \tag{8.2.7}$$

In hindsight, this result might be obtained more directly - by requiring the total weight $\rho g V = \rho g \left(\pi a^2 h\right)$ of the lifted liquid's column to be equal to the vertical component $F\cos\theta_c$ of the full surface tension force $F = pp$, acting on the perimeter $p = 2\pi a$ of the meniscus. Using the definition (11) of the capillary length a_c, Eq. (16a) may be represented as the so-called Jurin rule:

$$h = \frac{a_c^2}{a}\cos\theta_c \le \frac{a_c^2}{a} \tag{8.2.8}$$

according to our initial assumption $h >> a$, Eq. (16) is only valid for narrow tubes, with radius $a << a_c$.

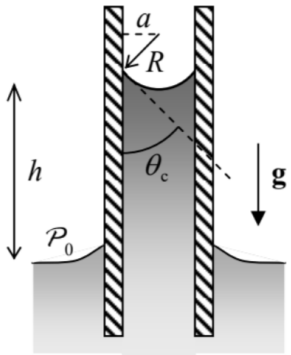

Figure 8.6. Liquid's rise in a vertical capillary tube.

This capillary rise is the basic mechanism of lifting water with nutrients from roots to the branches and leaves of plants, so that the tallest tree heights correspond to the Jurin rule (16), with $\cos\theta_c \approx 1$, and the pore radius a limited from below by a few microns, because of the viscosity effects restricting the fluid discharge - see Sec. 5 below.

---

[8] Indeed, if the γ of the interface of certain two fluids is negative, it self-reconfigures to decrease $U_{\rm i}$, i.e. increase $|U_{\rm i}|$, by increasing the interface area, i.e. fragments the system into a macroscopically-uniform solution.

[9] This equality follows from the general relation (7.30), with the stress tensor elements expressed by Eq. (2), but in this simple case of the net stress force $d\mathbf{F} = (\mathcal{P}_1 - \mathcal{P}_2)\, d\mathbf{A}$ parallel to the interface element vector $d\mathbf{A}$, it may be even more simply obtained just from the definition of work: $\delta\mathcal{W} = d\mathbf{F}\cdot\delta\mathbf{r}$ at the virtual displacement $\delta\mathbf{r} = \mathbf{n}\delta r$.

[10] This general formula may be verified by elementary means for a sphere of radius r (for which $R_1 = R_2 = r$ and $dA = r^2 d\Omega$, so that $\delta(dA)/dA = \delta\left(r^2\right)/r^2 = 2\delta r/r$), and for a round cylindrical interface of radius R (for which $R_1 = r$, $R_2 = \infty$, and $dA = r d\varphi dz$, so that $\delta(dA)/dA = \delta r/r$). For more on curvature, see, for example, M. do Camo, Differential Geometry of Curves and Surfaces, 2nd ed., Dover, 2016.

[11] This result (not to be confused with Eq. (15), called Young's equation) was derived in 1806 by Pierre-Simon Laplace (of the Laplace operator/equation fame) on the basis of the first analysis of the surface tension effects by Thomas Young (yes, the same Young who performed the famous two-slit experiment with light!) a year earlier.

8.3: Kinematics

In contrast to the stress tensor, which is useful and simple - see Eq. (2), the strain tensor is not a very useful notion in fluid mechanics. Indeed, besides a very few situations, [12] typical problems of this field involve fluid flow, i.e. a state when the velocity of fluid particles has some nonzero time average. This means that the trajectory of each particle is a long line, and the notion of its displacement $\mathbf{q}$ becomes impracticable. However, particle's velocity $\mathbf{v} \equiv d\mathbf{q}/dt$ remains a very useful notion, especially if it is considered as a function of the observation point $\mathbf{r}$ and (generally) time t. In an important class of fluid dynamics problem, the so-called stationary (or "steady", or "static") flow, the velocity defined in this way does not depend on time, $\mathbf{v} = \mathbf{v}(\mathbf{r})$.

There is, however, a price to pay for the convenience of this notion: namely, due to the difference between the vectors $\mathbf{q}$ and $\mathbf{r}$, particle's acceleration $\mathbf{a} = d^2\mathbf{q}/dt^2$ (that participates, in particular, in the 2^{nd} Newton law) cannot be calculated just as the time derivative of the velocity $\mathbf{v}(\mathbf{r}, t)$. This fact is evident, for example, for the static flow case, in which the acceleration of individual fluid particles may be very significant even if $\mathbf{v}(\mathbf{r})$ does not depend on time - just think about the acceleration of a drop of water flowing over the Niagara Falls' rim, first accelerating fast and then virtually stopping below, while the water velocity $\mathbf{v}$ at every particular point, as measured from a bank-based reference frame, is nearly constant. Thus the main task of fluid kinematics is to express a via $\mathbf{v}(\mathbf{r}, t)$; let us do this.

Since each Cartesian component v_j of the velocity $\mathbf{v}$ has to be considered as a function of four independent scalar variables: three Cartesian components r_j of the vector $\mathbf{r}$ and time t, its full time derivative may be represented as

$$\frac{dv_j}{dt} = \frac{\partial v_j}{\partial t} + \sum_{j'=1}^{3} \frac{\partial v_j}{\partial r_{j'}} \frac{dr_{j'}}{dt}. \tag{8.3.1}$$

Let us apply this general relation to a specific set of infinitesimal changes $\{dr_1, dr_2, dr_3\}$ that follows a small displacement $d\mathbf{q}$ of a certain particular particle of the fluid, $d\mathbf{r} = d\mathbf{q} = \mathbf{v}dt$, i.e.

$$dr_j = v_j dt. \tag{8.3.2}$$

In this case, dv_j/dt is the j^{th} component a_j of the particle's acceleration a, so that Eq. (17) yields the following key relation of fluid kinematics:

$$a_j = \frac{\partial v_j}{\partial t} + \sum_{j'=1}^{3} v_{j'} \frac{\partial v_j}{\partial r_{j'}}. \tag{8.3.3}$$

Using the del operator ∇, this result may be rewritten in the following compact vector form: [13]

$$\mathbf{a} = \frac{\partial \mathbf{v}}{\partial t} + (\mathbf{v} \cdot \nabla)\mathbf{v}. \tag{8.3.4}$$

This relation already signals the main technical problem of the fluid dynamics: many equations involving particle's acceleration are nonlinear in velocity, excluding such a powerful tool as the linear superposition principle (which was used so frequently in the previous chapters of this course) from the applicable mathematical arsenal.

One more basic relation of the fluid kinematics is the so-called continuity equation, which is essentially just the differential version of the mass conservation law. Let us mark, inside a fluid flow, an arbitrary volume V limited by a stationary (time-independent) surface S. The total mass of the fluid inside the volume may change only due to its flow through the boundary:

$$\frac{dM}{dt} \equiv \frac{d}{dt}\int_V \rho d^3r = -\int_S \rho v_n d^2r \equiv -\int_S \rho \mathbf{v} \cdot d\mathbf{A}, \tag{8.3.5}$$

where the elementary area vector $d\mathbf{A}$ is defined just as in Sec. 7.2 – see Figure 7. Now using the same divergence theorem that has been used several times in this course [14] the surface integral in Eq. (20a) may be transformed into the integral of $\nabla(\rho\mathbf{v})$ over the volume V, so that this relation may be rewritten as

$$\int_V \left(\frac{\partial \rho}{\partial t} + \nabla \cdot \mathbf{j} \right) d^3r = 0 \tag{8.3.6}$$

where the vector $\mathbf{j} \equiv \rho\mathbf{v}$ is called either the mass flux density (or the "mass current"). Since Eq. (20b) is valid for an arbitrary stationary volume V, the function under the integral has to vanish at any point:

$$\text{Continuity equation} \qquad \frac{\partial \rho}{\partial t} + \nabla \cdot \mathbf{j} = 0. \tag{8.3.7}$$

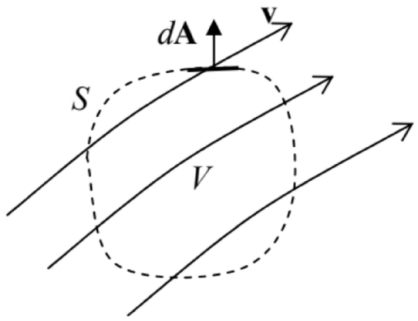

Fig. 8.7. Deriving the continuity equation.

Note that this continuity equation is valid not only for mass, but also for other conserved physics quantities (e.g., the electric charge, probability, etc.), with the proper re-definition of ρ and $\mathbf{j}$. [15]

---

[12] One of them is sound propagation, where the particle displacements $\mathbf{q}$ are typically small, so that results of Sec. 7.7 are applicable. As a reminder, they show that in fluids, with $\mu = 0$, the transverse sound cannot propagate, while the longitudinal sound can - see Eq. (7.114).

[13] Note that the operator relation $d/dt = \partial/\partial t + (\mathbf{v} \cdot \nabla)$ is applicable to an arbitrary (scalar or vector) function; it is frequently called the convective derivative. (Alternative adjectives, such as "Lagrangian", "substantial", or "Stokes", are sometimes used for this derivative as well.) The relation has numerous applications well beyond the fluid dynamics - see, e.g., EM Chapter 9 and QM Chapter 1 .

[14] If the reader still needs a reminder, see MA Eq. (12.1).

[15] See, e.g., EM Sec. 4.1, QM Sec. 1.4, and SM Sec. 5.6.

8.4: Dynamics - Ideal Fluids

Let us start our discussion of fluid dynamics from the simplest case when the stress tensor obeys Eq. (2) even in motion. Physically, this means that the fluid viscosity effects, leading to mechanical energy loss, are negligible. (The conditions of this assumption will be discussed in the next section.) Then the equation of motion of such an ideal fluid (essentially the 2^{nd} Newton law for its unit volume) may be obtained from Eq. (7.25) using the simplifications of its right-hand side, discussed in Sec. 1:

$$\rho \mathbf{a} = -\nabla \mathcal{P} + \mathbf{f}. \tag{8.4.1}$$

Now using the basic kinematic relation (19), we arrive at the following Euler equation: [16]

$$\rho \frac{\partial \mathbf{v}}{\partial t} + \rho (\mathbf{v} \cdot \nabla) \mathbf{v} = -\nabla \mathcal{P} + \mathbf{f}. \tag{8.4.2}$$

Generally, this equation has to be solved together with the continuity equation (21) and the equation of state of the particular fluid, $\rho = \rho(\mathcal{P})$. However, as we have already discussed, in many situations the compressibility of water and other important liquids is very low and may be ignored, so that ρ may be treated as a given constant. Moreover, in many cases the bulk forces $\mathbf{f}$ are conservative and may be represented as a gradient of a certain potential function $u(\mathbf{r})$– the potential energy per unit volume:

$$\mathbf{f} = -\nabla u \tag{8.4.3}$$

for example, for a uniform, vertical gravity field, $u(\mathbf{r}) = \rho g y$, where y is referred to some (arbitrary) horizontal level. In this case, the right-hand side of Eq. (23) becomes $-\nabla(\mathcal{P} + u)$. For these cases, it is beneficial to recast the left-hand of that equation as well, using the following well-known identity of vector algebra [17]

$$(\mathbf{v} \cdot \nabla) \mathbf{v} = \nabla \left(\frac{v^2}{2} \right) - \mathbf{v} \times (\nabla \times \mathbf{v}) \tag{8.4.4}$$

As a result, the Euler equation takes the following form:

$$\rho \frac{\partial \mathbf{v}}{\partial t} - \rho \mathbf{v} \times (\nabla \times \mathbf{v}) + \nabla \left(\mathcal{P} + u + \rho \frac{v^2}{2} \right) = 0 \tag{8.4.5}$$

In a stationary flow, the first term of this equation vanishes. If the second term, describing fluid's vorticity, is zero as well, then equation (26) has the first integral of motion,

$$\mathcal{P} + u + \frac{\rho}{2} v^2 = \text{ const} \tag{8.4.6}$$

called the Bernoulli equation. [18] Numerous examples of the application of Eq. (27) to simple problems of stationary flow in pipes, in the Earth gravity field, should be well known to the readers from their undergraduate courses, so I hope I can skip their discussion without much harm.

In the general case, an ideal fluid may have vorticity, so that Eq. (27) is not always valid. Moreover, due to the absence of viscosity in an ideal fluid, the vorticity, once created, does not decrease along the so-called streamline - the fluid particle's trajectory, to which the velocity is tangential at every point. [19] Mathematically, this fact [20] is expressed by the following Kelvin theorem: $(\nabla \times \mathbf{v}) \cdot d\mathbf{A} =$ const along any small contiguous group of streamlines crossing an elementary area dA. [21]

However, in many important cases, the vorticity of fluid is negligible. For example, if the vorticity exists in some part of the fluid volume (say, induced by local turbulence, see Sec. 6 below), but decays due to the fluid's viscosity, to be discussed in Sec. 5, well before it reaches the region of our interest. (If this viscosity is sufficiently small, its effects on the fluid's flow in the region of interest are negligible, i.e. the ideal-fluid approximation is still acceptable.) Another important case is when a solid body of an arbitrary shape is embedded into an ideal fluid whose flow is uniform (meaning, by definition, that $\mathbf{v}(\mathbf{r}, t) = \mathbf{v}_0 =$ const) at large distances, [22] its vorticity is zero everywhere. Indeed, since $\nabla \times \mathbf{v} = 0$ at the uniform flow, the vorticity is zero at distant points of any streamline, and according to the Kelvin theorem, should equal zero everywhere.In such cases, the velocity distribution, as any curl-free vector field, may be represented as a gradient of some effective potential function,

$$\mathbf{v} = -\nabla \phi. \tag{8.4.7}$$

Such potential flow may be described by a simple differential equation. Indeed, the continuity equation (21) for a steady flow of an incompressible fluid is reduced to $\nabla \cdot \mathbf{v} = 0$. Plugging Eq. (28) into this relation, we get the scalar Laplace equation,

$$\nabla^2\phi = 0, \tag{8.4.8}$$

which should be solved with appropriate boundary conditions. For example, the fluid flow may be limited by solid bodies, inside which the fluid cannot penetrate. Then the fluid velocity $\mathbf{v}$ at the solid body boundaries should not have a normal component; according to Eq. (28), this means

$$\left.\frac{\partial\phi}{\partial n}\right|_{\text{surfaces}} = 0. \tag{8.4.9}$$

On the other hand, if at large distances the fluid flow is known, e.g., uniform, then:

$$\nabla\phi = -\mathbf{v}_0 = \text{ const}, \text{ at } r \to \infty. \tag{8.4.10}$$

As the reader may already know (for example, from a course of electrodynamics [23]), the Laplace equation (29) is readily solvable analytically in several simple (symmetric) but important situations. Let us consider, for example, the case of a round cylinder, with radius R, immersed into a flow with the initial velocity $\mathbf{v}_0$ perpendicular to the cylinder's axis (Figure 8). For this problem, it is natural to use the cylindrical coordinates, with the z-axis coinciding with the cylinder's axis. In this case, the velocity distribution is obviously independent of z, so that we may simplify the general expression of the Laplace operator in cylindrical coordinates [24] by taking $\partial/\partial z = 0$. As a result, Eq. (29) is reduced to [25]

$$\frac{1}{\rho}\frac{\partial}{\partial\rho}\left(\rho\frac{\partial\phi}{\partial r}\right) + \frac{1}{\rho^2}\frac{\partial^2\phi}{\partial\theta^2} = 0, \text{ at } \rho \geq R. \tag{8.4.11}$$

The general solution of this equation may be obtained using the variable separation method, similar to that used in Sec. 6.5 – see Eq. (6.67). The result is [26]

$$\phi = a_0 + b_0\ln\rho + \sum_{n=1}^{\infty}\left(c_n\cos n\varphi + s_n\sin n\varphi\right)\left(a_n\rho^n + b_n\rho^{-n}\right), \tag{8.4.12}$$

where the coefficients a_n and b_n have to be found from the boundary conditions (30) and (31). Choosing the x-axis to be parallel to the vector $\mathbf{v}_0$ (Figure 8a), so that $x = r\cos\varphi$, we may spell out these conditions in the following form:

$$\frac{\partial\phi}{\partial\rho} = 0, \text{ at } \rho = R,$$
$$\phi \to -v_0\rho\cos\varphi + \phi_0, \text{ at } \rho >> R,$$

where ϕ_0 is an arbitrary constant, which does not affect the velocity distribution and may be taken for zero. The condition (35) is incompatible with any term of the sum (33) except the term with $n = 1$ (with $s_1 = 0$ and $c_1 a_1 = -v_0$), so that Eq. (33) is reduced to

$$\phi = \left(-v_0\rho + \frac{c_1 b_1}{\rho}\right)\cos\varphi. \tag{8.4.13}$$

Now, plugging this solution into Eq. (34), we get $c_1 b_1 = -v_0 R^2$, so that, finally,

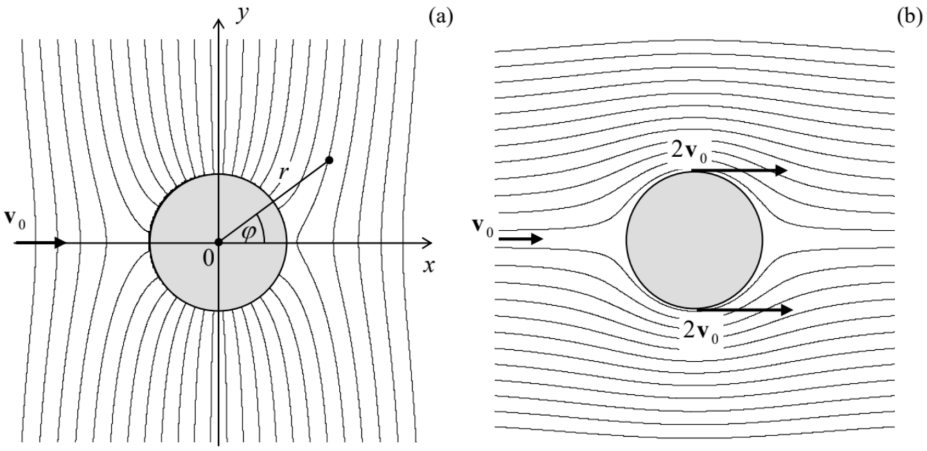

Figure 8.8. The flow of an ideal, incompressible fluid around a cylinder: (a) equipotential surfaces and (b) streamlines.

Figure 8 a shows the surfaces of constant velocity potential ϕ given by Eq. (37a). To find the fluid velocity, it is easier to rewrite that equality in the Cartesian coordinates $x = \rho\cos\varphi, y = \rho\sin\varphi$:

$$\phi = -v_0 x\left(1+\frac{R^2}{\rho^2}\right) = -v_0 x\left(1+\frac{R^2}{x^2+y^2}\right). \tag{8.4.14}$$

From here, we may readily calculate the Cartesian components $v_x = -\partial\phi/\partial x$ and $v_y = -\partial\phi/\partial y$ of fluid's velocity. Figure 8 b shows the flow streamlines. (They may be found by integration of the evident equation $dy/dx = v_y(x,y)/v_x(x,y)$. For our simple problem, this integration may be done analytically, giving $y\left[1-R^2/\left(x^2+y^2\right)\right] =$ const, where the constant is specific for each streamline.) One can see that the largest potential gradient, and hence the maximum fluid's speed, is achieved at the vertical diameter's ends $(\rho = R, \varphi = \pm\pi/2)$, where

$$v = v_x = -\left.\frac{\partial\phi}{\partial x}\right|_{\substack{r=R\\x=0}} = 2v_0. \tag{8.4.15}$$

Now the pressure distribution may be calculated by plugging Eq. (37) into the Bernoulli equation (27) with $u(\mathbf{r}) = 0$. The result shows that the pressure reaches its maximum at the ends of the longitudinal diameter $y = 0$, while at the ends of the transverse diameter $x = 0$, where the velocity is largest, it is lower by $2\rho{v_0}^2$. (Here ρ is the fluid density again - sorry for the notation jitters!) Note that the distributions of both the velocity and the pressure are symmetric with respect to the transverse axis $x = 0$, so that the fluid flow does not create any net drag force in its direction. It may be shown that this result, which stems from the conservation of the mechanical energy of an ideal fluid, remains valid for a solid body of arbitrary shape moving inside an infinite volume of an ideal fluid - the so-called D'Alambert paradox. However, if a body moves near an ideal fluid's surface, its energy may be transformed into that of the surface waves, and the drag becomes possible.

Speaking about the surface waves: the description of such waves in a gravity field [27] is one more classical problem of the ideal fluid dynamics. [28] Let us consider an open surface of an ideal fluid of density ρ in a uniform gravity field $\mathbf{f} = \rho\mathbf{g} = -\rho g\mathbf{n}_y$ - see Figure 9. If the wave amplitude A is sufficiently small, we can neglect the nonlinear term $(\mathbf{v}\cdot\nabla)\mathbf{v} \propto A^2$ in the Euler equation (23) in comparison with the first term, $\partial\mathbf{v}/\partial t$, which is linear in A. For a wave with frequency ω and wave number k, the particle's velocity $\mathbf{v} = d\mathbf{q}/dt$ is of the order of ωA, so that this approximation is legitimate if $\omega^2 A \gg k(\omega A)^2$, i.e. when

$$kA << 1, \tag{8.4.16}$$

i.e. when the wave's amplitude A is much smaller than its wavelength $\lambda = 2\pi/k$. Due to this assumption, we may neglect the fluid vorticity effects, and (for an incompressible fluid) again use the Laplace equation (29) for the wave's analysis.

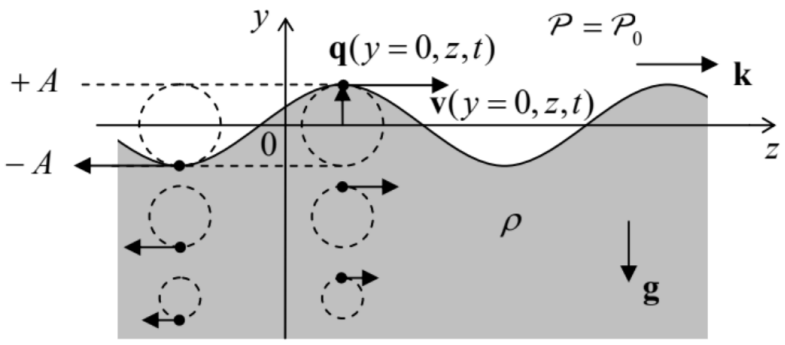

Figure 8.9. Small surface wave on a deep heavy fluid. Dashed lines show fluid particle trajectories. (For clarity, the displacement amplitude A is strongly exaggerated.)

Looking for its solution in the natural form of a sinusoidal wave, uniform in one of the horizontal directions (x),

$$\phi = \mathrm{Re}\left[\Phi(y)e^{i(kz-\omega t)}\right], \tag{8.4.17}$$

we get a very simple equation

$$\frac{d^2\Phi}{dy^2} - k^2\Phi = 0, \tag{8.4.18}$$

with an exponential solution (properly decaying at $y \to -\infty$), $\Phi = \Phi_A \exp\{ky\}$, so that Eq. (40) becomes

$$\phi = \mathrm{Re}\left[\Phi_A e^{ky} e^{i(kz-\omega t)}\right] = \Phi_A e^{ky} \cos(kz - \omega t), \tag{8.4.19}$$

where the last form is valid if Φ_A is real - which may be always arranged by a proper selection of the origins of z and/or t. Note that the rate k of the wave's decay in the vertical direction is exactly equal to the wave number of its propagation in the horizontal direction - along the fluid's surface. Because of that, the trajectories of fluid particles are exactly circular - see Figure 9. Indeed, using Eqs. (28) and (42) to calculate velocity components,

$$v_x = 0, \quad v_y = -\frac{\partial \phi}{\partial y} = -k\Phi_A e^{ky} \cos(kz - \omega t), \quad v_z = -\frac{\partial \phi}{\partial z} = k\Phi_A e^{ky} \sin(kz - \omega t), \tag{8.4.20}$$

we see that v_y and v_z, at the same height y, have equal real amplitudes, and are phase-shifted by $\pi/2$. This result becomes even more clear if we use the velocity definition $\mathbf{v} = d\mathbf{q}/dt$ to integrate Eqs. (43) over time to recover the particle displacement law $\mathbf{q}(t)$. Due to the strong inequality (39), the integration may be done at fixed y and z :

$$q_y = q_A e^{ky} \sin(kz - \omega t), \quad q_z = q_A e^{ky} \cos(kz - \omega t), \quad \text{with } q_A \equiv \frac{k}{\omega}\Phi_A. \tag{8.4.21}$$

Note that the phase of oscillations of v_z coincides with that of q_y. This means, in particular, that at the wave's "crest", particles are moving in the direction of the wave's propagation - see arrows in Figure 9.

It is remarkable that all this picture follows from the Laplace equation alone! The "only" remaining feature to calculate is the dispersion law $\omega(k)$, and for that, we need to combine Eq. (42) with what remains, in our linear approximation, of the Euler equation (23). In this approximation, and with the bulk force potential $u = \rho g y$, the equation is reduced to

$$\nabla\left(-\rho\frac{\partial \phi}{\partial t} + \mathcal{P} + \rho g y\right) = 0. \tag{8.4.22}$$

This equality means that the function in the parentheses is constant in space; at the surface, and at negligible surface tension, it should be equal to the pressure $\mathcal{P}_0$ above the surface (say, the atmospheric pressure), which we assume to be constant. This means that on the surface, the contributions to $\mathcal{P}$ that come from the first and the third term in Eq. (45), should compensate each other. Let us take the average surface position for $y = 0$; then the surface with waves is described by the relation $y(z,t) = q_y(y,z,t)-$ see Figure 9. Due to the strong relation (39), we can use Eqs. (42) and (44) with $y = 0$, so that the above compensation condition yields

$$-\rho\omega\Phi_A \sin(kz - \omega t) + \rho g \frac{k}{\omega}\Phi_A \sin(kz - \omega t) = 0. \tag{8.4.23}$$

This condition is identically satisfied on the whole surface (and for any Φ_A) as soon as

$$\omega^2 = gk, \tag{8.4.24}$$

This equality is the dispersion relation we were looking for. Looking at this simple result (which includes just one constant, g), note, first of all, that it does not involve the fluid's density. This is not too surprising, because due to the weak equivalence principle, particle masses always drop out from the solutions of problems involving gravitational forces alone. Second, the dispersion law (47) is strongly nonlinear, and in particular does not have an acoustic wave limit at all. This means that the surface wave propagation is strongly dispersive, with both the phase velocity $v_{\mathrm{ph}} \equiv \omega/k = g/\omega$ and the group velocity $v_{\mathrm{gr}} \equiv d\omega/dk = g/2\omega \equiv v_{\mathrm{ph}}/2$ diverging at $\omega \to 0$.

This divergence is an artifact of our assumption of the infinitely thick fluid's layer. A rather straightforward generalization of the above calculations to a layer of a finite thickness h, using the additional boundary condition $v_y|_{y=h} = 0$ (left for the reader's exercise), yields a more general dispersion relation:

$$\omega^2 = gk \tanh kh. \tag{8.4.25}$$

It shows that relatively long waves, with $\lambda \gg h$, i.e. with $kh \ll 1$, propagate without dispersion (i.e. have $\omega/k = $ const $\equiv v$), with the following velocity:

$$v = (gh)^{1/2}. \tag{8.4.26}$$

For the Earth's oceans, this velocity is rather high, approaching $300\ \mathrm{m/s}(!)$ for $h = 10\ \mathrm{km}$. This result explains, in particular, the very fast propagation of tsunami waves.

In the opposite limit of very short waves (large k), Eq. (47) also does not give a good description of experimental data, due to surface tension effects - see Sec. 2 above. Using Eq. (13), it is easy (and hence also left for the reader's exercise) to show that their account leads (at $kh >> 1$) to the following modification of Eq. (47):

$$\omega^2 = gk + \frac{\kappa k^3}{\rho}. \tag{8.4.27}$$

According to this formula, the surface tension is important at wavelengths smaller than the capillary constant a_c given by Eq. (14). Much shorter waves, for that Eq. (50) yields $\omega \propto k^{3/2}$, are called the capillary waves - or just "ripples".

---

[16] It was derived in 1755 by the same Leonhard Euler whose name has already been (reverently) mentioned several times in this course.

[17] It readily follows, for example, from MA Eq. (11.6) with $\mathbf{g} = \mathbf{f} = \mathbf{v}$.

[18] Named after Daniel Bernoulli (1700-1782), not to be confused with Jacob Bernoulli or one of several Johanns of the same famous Bernoulli family, which gave the world so many famous mathematicians and scientists.

[19] Perhaps the most spectacular manifestation of the vorticity conservation is the famous toroidal vortex rings (see, e.g., a nice photo and a movie at https://en.Wikipedia.org/wiki/Vortex_ring), predicted in 1858 by H. von Helmholtz, and then demonstrated by P. Tait in a series of spectacular experiments with smoke in the air. The persistence of such a ring, once created, is only limited by the fluid's viscosity - see the next section.

[20] This theorem was first formulated (verbally) by Hermann von Helmholtz.

[21] Its proof may be found, e.g., in Sec. 8 of L. Landau and E. Lifshitz, Fluid Mechanics, 2nd ed., ButterworthHeinemann, 1987.

[22] This case is very important, because the motion of a solid body, with a constant velocity $\mathbf{u}$, in the otherwise stationary fluid, gives exactly the same problem (with $\mathbf{v}_0 = -\mathbf{u}$), in a reference frame bound to the body.

[23] See, e.g., EM Secs. 2.3-2.8.

[24] See, e.g., MA Eq. (10.3).

[25] Let me hope that the letter ρ, used here to denote the magnitude of the 2D radius-vector $\boldsymbol{\rho} = \{x, y\}$, will not be confused with the fluid's density - which does not participate in this boundary problem.

[26] See, e.g., EM Eq. (2.112). Note that the most general solution of Eq. (32) also includes a term proportional to φ, but this term should be zero for such a single-valued function as the velocity potential.

[27] The alternative, historic term "gravity waves" for this phenomenon may nowadays lead to confusion with the relativistic effect of gravity waves - which may propagate in free space.

[28] It was solved by Sir George Biddell Airy (1801-19892), of the Airy functions fame. (He was also a prominent astronomer and, in particular, established Greenwich as the prime meridian.)

8.5: Dynamics- Viscous Fluids

The viscosity of many fluids, at not overly high velocities, may be described surprisingly well by adding, to the static stress tensor (2), additional components proportional to the velocity $\mathbf{v} \equiv d\mathbf{q}/dt$:

$$\sigma_{ij'} = -\mathcal{P}\delta_{ij'} + \tilde{\sigma}_{jj'}(\mathbf{v}). \tag{8.5.1}$$

In the view of our experience with the Hooke's law (7.32) expressing a stress tensor proportional to particle displacements $\mathbf{q}$, we may expect a similar expression with the replacement $\mathbf{q} \to \mathbf{v} = d\mathbf{q}/dt$:

$$\tilde{\sigma}_{jj'} = 2\eta\left(e_{jj} - \frac{1}{3}\delta_{jj'}\,\mathrm{Tr}(\mathrm{e})\right) + 3\zeta\left(\frac{1}{3}\delta_{ij'}\,\mathrm{Tr}(\mathrm{e})\right) \tag{8.5.2}$$

where $e_{ij'}$ are the elements of the **symmetrized strain derivative tensor**:

$$e_{ij'} \equiv \frac{ds_{jj'}}{dt} = \frac{1}{2}\left(\frac{\partial v_j}{\partial r_{j'}} + \frac{\partial v_{j'}}{\partial r_j}\right). \tag{8.5.3}$$

Experiment confirms that Eq. (52) gives a good description of the viscosity effects in a broad range of isotropic fluids. The coefficient η is called either the **shear viscosity**, or the dynamic viscosity, or just viscosity, while ζ is called the **second (or bulk) viscosity**.

In the most frequent case of virtually incompressible fluids, $\mathrm{Tr}(\mathrm{e}) = d[\mathrm{Tr}(\mathrm{s})]/dt = (dV/dt)/V = 0$, so that the term proportional to ζ vanishes, and η is the only important viscosity parameter. [29] Table 1 shows the approximate values of the viscosity, together with the mass density ρ, for several representative fluids.

Table 8.1. Important parameters of several representative fluids (approximate values)

Fluid (all at 300 K, until indicated otherwise)	$\eta(\mathrm{mPa\cdot s})$	$\rho\ (\mathrm{kg/m^3})$
Glasses	$10^{21} - 10^{24}$	$2,200 - 2,500$
Earth magmas (at 800 to 1,400 K)	$10^{4} - 10^{14}$	$2,200 - 2,800$
Machine oils (SAE 10W-40 W)	$65 - 320$	900
Water	0.89	1,000
Mercury	1.53	13,530
Liquid helium 4 (at 4.2K, 10 Pa)	0.019	130
Air (at 10 Pa)	0.018	1.3

One can see that η may vary in very broad limits; the extreme cases of liquids are glasses (which, somewhat counter-intuitively, are not stable solids even at room temperature, but rather may "flow", though extremely slowly, until they eventually crystallize) and liquid helium (whose viscosity is of the order of that of gases, [30] despite its much higher density).

Incorporating the additional components of σ_{jj}, to the equation (23) of fluid motion, absolutely similarly to how it was done at the derivation of Eq. (7.107) of the elasticity theory, and with the account of Eq. (19), we arrive at the famous **Navier-Stokes equation**: [31]

$$\rho\frac{\partial \mathbf{v}}{\partial t} + \rho(\mathbf{v}\cdot\nabla)\mathbf{v} = -\nabla\mathcal{P} + \mathbf{f} + \eta\nabla^2\mathbf{v} + \left(\zeta + \frac{\eta}{3}\right)\nabla(\nabla\cdot\mathbf{v}) \tag{8.5.4}$$

The apparent simplicity of this equation should not mask an enormous range of phenomena, notably including turbulence (see the next section), that are described by it, and the complexity of its solutions even for some simple geometries. In most problems interesting for practice, the only option is to use numerical methods, but due to a large number of parameters $(\rho, \eta, \zeta,$ plus geometrical parameters of the involved bodies, plus the distribution of bulk forces $\mathbf{f}$, plus boundary conditions), this way is strongly plagued by the curse of dimensionality that was discussed in the end of Sec. 5.8.

Let us see how does the Navier-Stokes equation work, on several simple examples. As the simplest case, let us consider the so-called Couette flow of an incompressible fluid layer between two wide, horizontal plates (Figure 10), caused by their mutual sliding with a constant relative velocity $\mathbf{v}_0$.

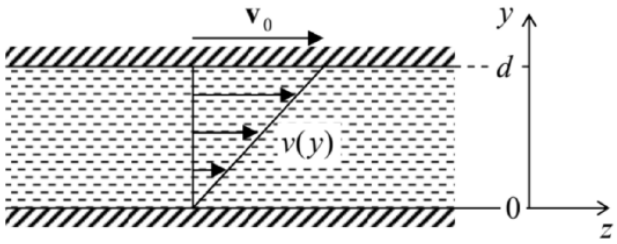

Figure 8.10. The simplest problem of the viscous fluid flow.

Let us assume a laminar (vorticity-free) fluid flow. (As will be discussed in the next section, this assumption is only valid within certain limits.) Then we may use the evident symmetry of the problem, to take, in the reference frame shown in Figure 10, $\mathbf{v} = \mathbf{n}_2 v(y)$. Let the bulk forces be vertical, $\mathbf{f} = \mathbf{n}_y f$, so they do not give an additional drive to the fluid flow. Then for the stationary flow $(\partial \mathbf{v}/\partial t = 0)$, the vertical, y-component of the Navier-Stokes equation is reduced to the static Pascal equation (6), showing that the pressure distribution is not affected by the plate (and fluid) motion. In the horizontal, z component of the equation, only one term, $\nabla^2 v$, survives, so that for the only Cartesian component of the fluid's velocity we get the 1D Laplace equation

$$\frac{d^2 v}{dy^2} = 0. \tag{8.5.5}$$

In contrast to the ideal fluid (see, e.g., Figure 8b), the relative velocity of a viscous fluid and a solid wall it flows by should approach zero at the wall, [32] so that Eq. (54) should be solved with boundary conditions

$$v = \begin{cases} 0, & \text{at } y = 0, \\ v_0, & \text{at } y = d. \end{cases} \tag{8.5.6}$$

Using the evident solution of this boundary problem, $v(y) = (y/d)v_0$, illustrated by arrows in Figure 10, we can now calculate the horizontal drag force acting on a unit area of each plate. For the bottom plate,

$$\frac{F_z}{A_y} = \sigma_{zy}|_{y=0} = \eta \left. \frac{\partial v}{\partial y} \right|_{y=0} = \eta \frac{v_0}{d}. \tag{8.5.7}$$

(For the top plate, the derivative $\partial v/\partial y$ has the same value, but the sign of dA_y has to be changed to reflect the direction of the outer normal to the solid surface so that we get a similar force but with the negative sign.) The well-known result (56) is often used, in undergraduate physics courses, for a definition of the dynamic viscosity η, and indeed shows its meaning very well. [33]

As the next, slightly less trivial example let us consider the so-called Poiseuille problem: 34 finding the relation between the constant external pressure gradient $\chi \equiv -\partial \mathcal{P}/\partial z$ applied along a round pipe with internal radius R (Figure 11), and the so-called discharge Q - defined as the mass of fluid flowing through the pipe's cross-section in unit time.

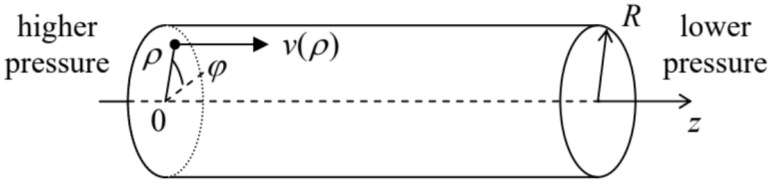

Figure 8.11. The Poiseuille problem.

Again assuming a laminar flow, we can involve the problem's uniformity along the z-axis and its axial symmetry to infer that $\mathbf{v} = \mathbf{n}_z v(\rho)$, and $\mathcal{P} = -\chi z + f(\rho, \varphi) + \text{const}$ (where $\rho = \{\rho, \varphi\}$ is again the 2D radius-vector rather than the fluid density), so that the Navier-Stokes equation (53) for an incompressible fluid (with $\nabla \cdot \mathbf{v} = 0$) is reduced to the following 2D Poisson equation:

$$\eta \nabla_2^2 v = -\chi \tag{8.5.8}$$

After spelling out the 2D Laplace operator in polar coordinates for our axially-symmetric case $\partial/\partial\varphi = 0$, Eq. (57) becomes a simple ordinary differential equation,

$$\eta \frac{1}{\rho}\frac{d}{d\rho}\left(\rho \frac{dv}{d\rho}\right) = -\chi, \tag{8.5.9}$$

which has to be solved on the segment $0 \le \rho \le R$, with the following boundary conditions:

$$v = 0, \quad \text{at } \rho = R,$$
$$\frac{dv}{d\rho} = 0, \quad \text{at } \rho = 0.$$

(The latter condition is required by the axial symmetry.) A straightforward double integration yields:

$$v = \frac{\chi}{4\eta}\left(R^2 - \rho^2\right), \tag{8.5.10}$$

so that the (easy) integration of the mass flow density over the cross-section of the pipe,

$$Q \equiv \int_A \rho v d^2 r = 2\pi\rho \frac{\chi}{4\eta}\int_0^R \left(R^2 - \rho'^2\right)\rho' d\rho', \tag{8.5.11}$$

immediately gives us the so-called Poiseuille (or "Hagen-Poiseuille") law for the fluid discharge:

$$Q = \frac{\pi}{8}\rho\frac{\chi}{\eta}R^4 \tag{8.5.12}$$

where (sorry!) ρ is the mass density again. The most prominent (and practically important) feature of this result is the very strong dependence of the discharge on the pipe's radius.

Of course, not for each cross-section shape the 2D Poisson equation (57) is so readily solvable. For example, consider a very simple, square-shape cross-section with side a (Figure 12). In this case, it is natural to use the Cartesian coordinates, so that Eq. (57) becomes

$$\frac{\partial^2 v}{\partial x^2} + \frac{\partial^2 v}{\partial y^2} = -\frac{\chi}{\eta} = \text{const}, \quad \text{for } 0 \le x, y \le a, \tag{8.5.13}$$

and (for the coordinate choice shown in Figure 12) has to be solved with boundary conditions

$$v = 0, \quad \text{at } x, y = 0, a. \tag{8.5.14}$$

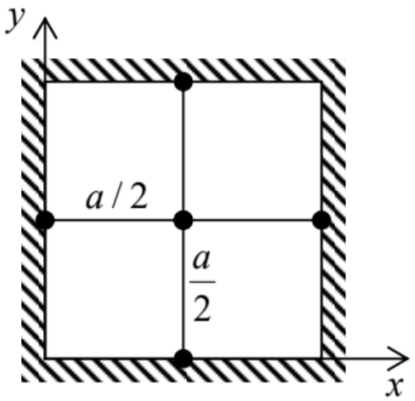

Figure 8.12. Application of the finitedifference method with a very coarse mesh (with step $h = a/2$) to the problem of viscous fluid flow in a pipe with a square cross-section.

For this boundary problem, analytical methods such as the variable separation give answers in the form of infinite sums (series), [35] which ultimately require computers anyway - for their plotting and comprehension. Let me use this pretext to discuss how

explicitly numerical methods may be used for such problems - or for any partial differential equations involving the Laplace operator. The simplest of them is the finite-difference method [36] in which the function to be calculated, $f(\mathbf{r})$, is represented by its values $f(\mathbf{r}_1), f(\mathbf{r}_2), \ldots$ in discrete points of a rectangular grid (frequently called the mesh) of the corresponding dimensionality (Figure 13).

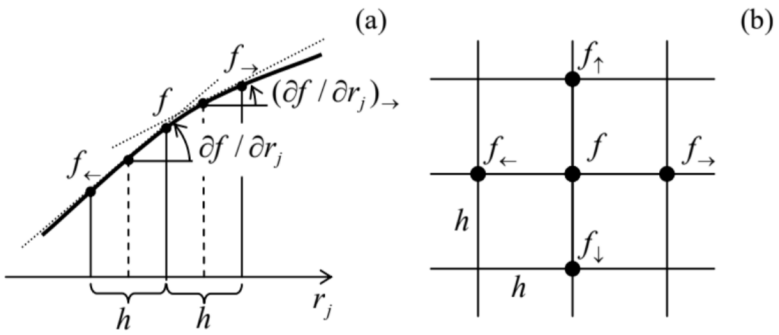

Figure 8.13. The idea of the finitedifference method in (a) one and (b) two dimensions.

In Sec. 5.7, we have already discussed how to use such a grid to approximate the first derivative of the function - see Eq. (5.97). Its extension to the second derivative is straightforward - see Figure 13a:37

$$\frac{\partial^2 f}{\partial r_j^2} \equiv \frac{\partial}{\partial r_j}\left(\frac{\partial f}{\partial r_j}\right) \approx \frac{1}{h}\left(\left.\frac{\partial f}{\partial r_j}\right|_{\rightarrow} - \left.\frac{\partial f}{\partial r_j}\right|_{\leftarrow}\right) \approx \frac{1}{h}\left[\frac{f_\rightarrow - f}{h} - \frac{f - f_\leftarrow}{h}\right] \equiv \frac{f_\rightarrow + f_\leftarrow - 2f}{h^2}. \tag{8.5.15}$$

The relative error of this approximation is of the order of $h^2 \partial^4 f/\partial r_j^4$, quite acceptable in many cases. As a result, the left-hand side of Eq. (63), treated on a square mesh with step h (Figure 13b), may be approximated with the so-called five-point scheme:

$$\frac{\partial^2 v}{\partial x^2} + \frac{\partial^2 v}{\partial y^2} \approx \frac{v_\rightarrow + v_\leftarrow - 2v}{h^2} + \frac{v_\uparrow + v_\downarrow - 2v}{h^2} = \frac{v_\rightarrow + v_\leftarrow + v_\uparrow + v_\downarrow - 4v}{h^2}. \tag{8.5.16}$$

(The generalization to the seven-point scheme, appropriate for 3D problems, is straightforward.) Let us apply this scheme to the pipe with the square cross-section, using an extremely coarse mesh with step $h = a/2$ (Figure 12). In this case, the fluid velocity v should equal zero at the walls, i.e. in all points of the five-point scheme except for the central point (in which the velocity is evidently the largest), so that Eqs. (63) and (66) yield 38

$$\frac{0+0+0+0-4v_{\max}}{(a/2)^2} \approx -\frac{\chi}{\eta}, \quad \text{i.e. } v_{\max} \approx \frac{1}{16}\frac{\chi a^2}{\eta} \tag{8.5.17}$$

This result for the maximal velocity is only $\sim 20\%$ different from the exact value. Using a slightly finer mesh with $h = a/4$, which gives a readily solvable system of three linear equations for three different velocity values (the exercise left for the reader), brings us within just a couple of percent from the exact result. So such numerical methods may be practically more efficient than the "analytical" ones, even if the only available tool is a calculator app on your smartphone rather than an advanced computer.

Of course, many practical problems of fluid dynamics do require high-performance computing, especially in conditions of turbulence (see the next section) with its complex, irregular spatial-temporal structure. In these conditions, the finite-difference approach discussed above may become unsatisfactory, because it implies the same accuracy of the derivative approximation through the whole area of interest. A more powerful (but also much more complex for implementation) approach is the finite-element method in which the discrete-point mesh is based on triangles with uneven sides, and is (in most cases, automatically) generated in accordance with the system geometry, giving many more mesh points at the location(s) of the highest gradients of the calculated function (Figure 14), and hence a better calculation accuracy for the same total number of points. Unfortunately, I do not have time for going into the details of that method, so the interested reader is referred to the special literature on this subject. [39]

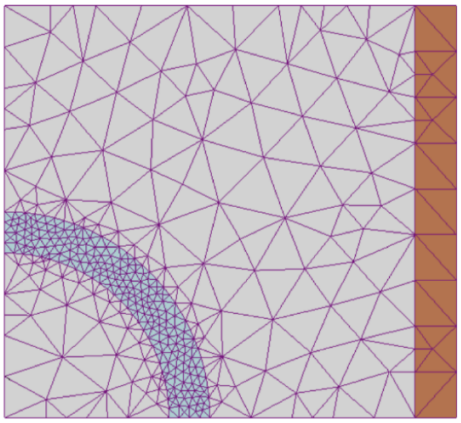

Figure 8.14. A typical finite-element mesh generated automatically for a system with relatively complex geometry - a round cylindrical shell inside another one, with mutually perpendicular axes. (Adapted from the original by I. Zureks, https://commons.wikimedia.org/w/in dex.php?curid = 2358783, under the CC license BY-SA 3.0.)

Before proceeding to our next topic, let me mention one more important problem that is analytically solvable using the Navier-Stokes equation: a slow motion of a solid sphere of radius R, with a constant velocity $\mathbf{v}_0$, through an incompressible viscous fluid - or equivalently, a slow flow of the fluid (uniform at large distances) around an immobile sphere. Indeed, in the limit $v \to 0$, the second term on the left-hand side of Eq. (53) is negligible (just as at the surface wave analysis in Sec. 3), and the equation takes the form

$$-\nabla \mathcal{P} + \eta \nabla^2 \mathbf{v} = 0, \tag{8.5.18}$$

which should be complemented with the incompressibility condition $\nabla \cdot \mathbf{v} = 0$ and boundary conditions

$$\begin{aligned} \mathbf{v} &= 0, \quad \text{at } r = R, \\ \mathbf{v} &\to \mathbf{v}_0, \text{ at } r \to \infty. \end{aligned}$$

In spherical coordinates, with the polar axis directed along the vector $\mathbf{v}_0$, this boundary problem has the axial symmetry (so that $\partial \mathbf{v}/\partial \varphi = 0$ and $v_\varphi = 0$), and allows the following analytical solution:

$$v_r = v_0 \cos\theta \left(1 - \frac{3R}{2r} + \frac{R^3}{2r^2}\right), \quad v_\theta = -v_0 \sin\theta \left(1 - \frac{3R}{4r} - \frac{R^3}{4r^2}\right). \tag{8.5.19}$$

Calculating the pressure distribution from Eq. (68), and integrating it over the surface of the sphere, it is now straightforward to obtain the famous Stokes formula for the drag force acting on the sphere:

$$F = 6\pi \eta R v_0. \tag{8.5.20}$$

Historically, this formula has played an important role in the first precise (better than 1%) calculation of the fundamental electric charge e by R. Millikan and H. Fletcher from their famous oil drop experiments in 1909-1913.

For what follows in the next section, it is convenient to recast this result into the following form:

$$C_{\mathrm{d}} = \frac{24}{Re}, \tag{8.5.21}$$

where C_{d} is the drag coefficient defined as

$$C_{\mathrm{d}} \equiv \frac{F}{\rho v_0^2 A/2}, \tag{8.5.22}$$

with $A \equiv \pi R^2$ being the sphere's cross-section "as seen by the incident fluid flow", and Re is the socalled Reynolds number. [40] In the general case, the number is defined as

$$\mathrm{Re} \equiv \frac{\rho v l}{\eta}, \tag{8.5.23}$$

where l is the linear-size scale of the problem, and v is its velocity scale. (In the particular case of Eq. (72) for the sphere, l is identified with the sphere's diameter $D = 2R$, and v with v_0). The physical sense of these two definitions will be discussed in the next section.

---

[29] Probably the most important effect we miss by neglecting ζ is the attenuation of the (longitudinal) acoustic waves, into which the second viscosity makes a major (and in some cases, the main) contribution - whose (rather straightforward) analysis is left for the reader's exercise.

[30] Actually, at even lower temperatures (for $\mathrm{He4}$, at $T < T_\lambda \approx 2.17\ \mathrm{K}$), helium becomes a superfluid, i.e. loses its viscosity completely, as a result of the Bose-Einstein condensation - see, e.g., SM Sec. 3.4.

[31] Named after Claude-Louis Navier (1785-1836) who had suggested the equation, and Sir George Gabriel Stokes (1819-1903) who has demonstrated its relevance by solving the equation for several key situations.

[32] This is essentially an additional experimental fact, but may be understood as follows. The tangential component of the velocity should be continuous at the interface between two viscous fluids, in order to avoid infinite stress see Eq. (52), and solid may be considered as an ultimate case of fluid, with infinite viscosity.

[33] The very notion of viscosity η was introduced (by nobody other than the same Sir Isaac Newton) via a formula similar to Eq. (56), so that any effect resulting in a drag force proportional to velocity is frequently called the Newtonian viscosity.

[34] It was solved by G. Stokes in 1845 to explain the experimental results obtained by Gotthilf Hagen in 1839 and (independently) by Jean Poiseuille in 1840-41.

[35] See, e.g., EM Sec. 2.5.

[36] For more details see, e.g., R. Leveque, Finite Difference Methods for Ordinary and Partial Differential Equations, SIAM, 2007.

[37] As a reminder, at the beginning of Sec. 6.4 we have already discussed the reciprocal transition - from a similar sum to the second derivative in the continuous limit $(h \to 0)$.

[38] Note that value (67) of $v_{\max}$ is exactly the same as given by the analytical formula (60) for the round crosssection with the radius $R = a/2$. This is not an occasional coincidence. The velocity distribution given by (60) is a quadratic function of both x and y. For such functions, with all derivatives higher than $\partial^2 f / \partial r_j^2$ equal to zero, equation (66) is exact rather than approximate.

[39] I can recommend, e.g., C. Johnson, Numerical Solution of Partial Differential Equations by the Finite Element Method, Dover, 2009, or T. Hughes, The Finite Element Method, Dover, 2000.

[40] This notion was introduced in 1851 by the same G. Stokes but eventually named after O. Reynolds who popularized it three decades later.

8.6: Turbulence

As Figure 15 shows, the Stokes' result $(71)-(72)$ is only valid at $\mathrm{Re} << 1$, while for larger values of the Reynolds number, i.e. at higher velocities v_0, the drag force is larger. This very fact is not quite surprising, because at the derivation of the Stokes' result, the nonlinear term $(\mathbf{v}\cdot\nabla)\mathbf{v}$ in the Navier-Stokes equation (53), which scales as v^2, was neglected in comparison with the linear terms, scaling as v. What is more surprising is that the function $C_{\mathrm{d}}(Re)$ exhibits such a complicated behavior over many orders of velocity's magnitude, giving a hint that the fluid flow at large Reynolds numbers should be also very complicated. Indeed, the reason for this complexity is a gradual development of very intricate, timedependent fluid patterns, called turbulence, rich with vortices - for example, see Figure 16. These vortices are especially pronounced in the region behind the moving body (the so-called wake), while the region before the body remains almost unperturbed. As Figure 15 indicates, the turbulence exhibits rather different behaviors at various velocities (i.e. values of Re), and sometimes changes rather abruptly - see, for example, the significant drag drop at $\mathrm{Re}\approx 5\times 10^5$.

In order to understand the conditions of this phenomenon, let us estimate the scale of various terms of the Navier-Stokes equation (53) for the generic case of a body with characteristic size l, moving in an otherwise static, incompressible fluid, with velocity v. In this case, the characteristic time scale of possible non-stationary phenomena is given by the ratio l/v, [41] so that we arrive at the following estimates:

$$\begin{array}{lcccc} \text{Equation term:} & \rho\frac{\partial \mathbf{v}}{\partial t} & \rho(\mathbf{v}\cdot\nabla)\mathbf{v} & \mathbf{f} & \eta\nabla^2\mathbf{v} \\ \text{Order of magnitude:} & \rho\frac{v^2}{l} & \rho\frac{v^2}{l} & \rho g & \eta\frac{v}{l^2} \end{array} \tag{8.6.1}$$

(I have skipped the term $\nabla\mathcal{P}$ because as we saw in the previous section, in typical fluid flow problems it balances the viscosity term, and hence is of the same order of magnitude.) Eq. (75) shows that the relative importance of the terms may be characterized by two dimensionless ratios. [42]

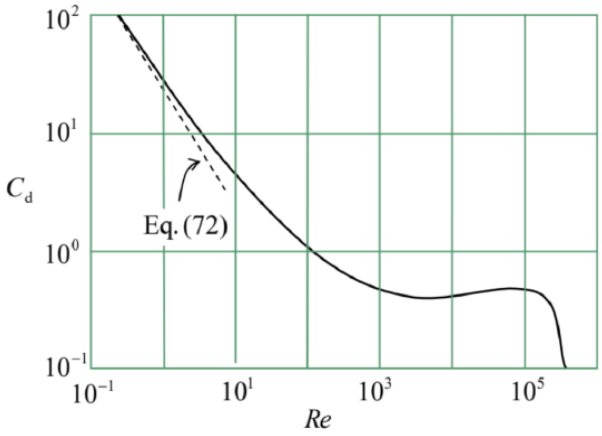

Figure 8.15. The drag coefficient C_{d} for a sphere in an incompressible fluid, as a function of the Reynolds number (Note the $\log-\log$ plot). The experimental data are from F. Eisner, Das Widerstandsproblem, in: Proc. 3^{rd} Int. Congress on Appl. Mech., Stockholm, 1931.

The first of them is the so-called Froude number [43]

$$F\equiv\frac{\rho v^2/l}{\rho g}\equiv\frac{v^2}{lg}, \tag{8.6.2}$$

which characterizes the relative importance of the gravity - or, upon appropriate modification, of other bulk forces. In most practical problems (with the important exception of surface waves, see Sec. 4 above) $F\ggg 1$, so that the gravity effects may be neglected.

Fig. 8.16. A snapshot of the turbulent tail (wake) behind a sphere moving in a fluid with a high Reynolds number, showing the so-called von Kármán vortex street. Adapted from the original (actually, a very nice animation, http://www.mcef.ep.usp.br/staff/jmen...areo/vort2.gif) by Cesareo de La Rosa Siqueira, as a copyright-free material, available at https://commons.wikimedia.org/w/index.php?curid=87351.

Much more important is another ratio, the Reynolds number (74), which may be rewritten as

$$Re \equiv \frac{\rho v l}{\eta} \equiv \frac{\rho v^2 / l}{\eta v / l^2}, \tag{8.6.3}$$

and hence is a measure of the relative importance of the fluid particle's inertia in comparison with the viscosity effects. [44] So again, it is natural that for a sphere, the role of the vorticity-creating term $(\mathbf{v}\cdot\nabla)\mathbf{v}$ becomes noticeable already at $\mathrm{Re} \sim 1-$ see Figure 15. What is very counter-intuitive is the onset of turbulence in systems where the laminar (turbulence-free) flow is formally an exact solution to the Navier-Stokes equation for any Re. For example, at $\mathrm{Re} > \mathrm{Re}_t \approx 2,100$ (with $l \equiv 2R$ and $v \equiv v_{\max}$) the laminar flow in a round pipe, described by Eq. (60), becomes unstable, and the resulting turbulence decreases the fluid discharge Q in comparison with the Poiseuille law (62). Even more strikingly, the critical value of Re is rather insensitive to the pipe wall roughness and does not diverge even in the limit of perfectly smooth walls.

Since $\mathrm{Re} \gg 1$ in many real-life situations, [45] turbulence is very important for practice. However, despite nearly a century of intensive research, there is no general, quantitative analytical theory of this phenomenon, [46] and most results are still obtained either by rather approximate analytical treatments, or by the numerical solution of the Navier-Stokes equations using the approaches discussed in the previous section, or in experiments (e.g.., on scaled models [47] in wind tunnels). Only certain general, semiquantitative features may be readily understood from simple arguments.

For example, Figure 15 shows that within a very broad range of Reynolds numbers, from $\sim 10^2$ to $\sim 3\times 10^5$, C_{d} of a sphere is of the order of 1 . Moreover, for a flat, thin, round disk, perpendicular to the incident flow, C_{d} is very close to 1.1 for any $\mathrm{Re} > 10^3$. The approximate equality $C_{\mathrm{d}} \approx 1$, meaning the drag force $F \approx \rho v_0^2 A/2$, may be understood (in the picture where the object is moved by an external force F with the velocity v_0 through a fluid which was initially at rest) as the equality of the forcedelivered power Fv_0 and the fluid's kinetic energy $\left(\rho v_0^2/2\right) V$ created in volume $V = v_0 A$ in unit time. This relation would be exact if the object gave its velocity v_0 to each and every fluid particle its crosssection runs into, for example by dragging all such particles behind itself. In reality, much of this kinetic energy goes into vortices, where the particle velocity may differ from v_0, so that the equality $C_{\mathrm{d}} \approx 1$ is only approximate.

Unfortunately, due to the time/space restrictions, for a more detailed discussion of these results I have to refer the reader to more specialized literature, [48] and will conclude this chapter with a brief discussion of just one issue: can the turbulence be "explained by a single mechanism"? (In other words, can it be reduced, at least on a semi-quantitative level, to a set of simpler phenomena that are commonly considered "well understood"?) Apparently the answer is no, 49 though nonlinear dynamics of simpler systems may provide some useful insights.

At the middle of the last century, the most popular qualitative explanation of turbulence had been the formation of an "energy cascade" that would transfer the energy from the regular fluid flow to a hierarchy of vortices of various sizes. [50] With our background, it is easier to retell that story in the timedomain language (with the velocity v serving as the conversion factor), using the fact that in a rotating vortex each Cartesian component of a particle's radius-vector oscillates in time, so that to some extent the vortex plays the role of an oscillatory motion mode.

Let us consider the passage of a solid body between two, initially close, small parts of the fluid. The body pushes them apart, but after its passage, these partial volumes are free to return to their initial positions. However, the dominance of inertia effects at motion with $\mathrm{Re} >> 1$ means that the volumes continue to "oscillate" for a while about those equilibrium positions. (Since

elementary volumes of an incompressible fluid cannot merge, these oscillations take the form of rotating vortices - see Figure 16 again.)

Now, from Sec. 5.8 we know that intensive oscillations in a system with the quadratic nonlinearity, in this case provided by the convective term $(\mathbf{v}\cdot\boldsymbol{\nabla})\mathbf{v}$, are equivalent, for small perturbations, to the oscillation of the system's parameters at the corresponding frequency. On the other hand, as was briefly discussed in Sec. 6.7, in a system with two oscillatory degrees of freedom, a periodic parameter change with frequency $\omega_{\rm p}$ may lead to the non-degenerate parametric excitation ("down-conversion") of oscillations with frequencies $\omega_{1,2}$ satisfying the relation $\omega_1+\omega_2=\omega_{\rm p}$. Moreover, the spectrum of oscillations in such a system also has higher combinational frequencies such as $(\omega_{\rm p}+\omega_1)$, thus pushing the oscillation energy up the frequency scale ("up-conversion"). In the presence of other oscillatory modes, these oscillations may in turn produce, via the same nonlinearity, even higher frequencies, etc. In a fluid, the spectrum of these "oscillatory modes" (actually, vortex structures) is essentially continuous, so that the above arguments make very plausible a sequential transfer of the energy from the moving body to a broad range of oscillatory modes - whose frequency spectrum is limited from above by the energy dissipation due to the fluid's viscosity. When excited, these modes interact (in particular, mutually phase-lock) via the system's nonlinearity, creating the complex motion we call turbulence.

Though not having much quantitative predictive power, such handwaving explanations, which are essentially based on the excitation of a large number of effective degrees of freedom, had been dominating the turbulence reviews until the mid-1960s. At that point, the discovery (or rather rediscovery) of quasi-random motions in classical dynamic systems with just a few degrees of freedom altered the discussion substantially. Since this phenomenon, called the deterministic chaos, extends well beyond the fluid dynamics, and I will devote to it a separate (albeit short) next chapter, and in its end will briefly return to the discussion of turbulence.

---

[41] The time scale of phenomena in non-autonomous systems may be different from l/v; for example, for forced oscillations of fluid flow with frequency ω, it is given by the oscillation period $\tau\equiv 2\pi/\omega$. For such problems, the ratio $S\equiv(l/v)/T$ serves as another, independent dimensionless constant, commonly called either the Strouhal number or the reduced frequency.

[42] For substantially compressible fluids (e.g., gases), the most important additional dimensionless parameter is the Mach number $M\equiv v/v_1$, where $v_1=(K/\rho)^{1/2}$ is the velocity of the longitudinal sound - which is, as we already know from Chapter 7, the only wave mode possible in an infinite fluid. Especially significant for practice are supersonic effects (including the shock wave in the form of the famous Mach cone with half-angle $\theta_{\rm M}=\sin^{-1}M^1$) that arise at $M>1$. For a more thorough discussion of these issues, I have to refer the reader to more specialized texts - either Chapter IX of the Landau-Lifshitz volume cited above or Chapter 15 in I. Cohen and P. Kundu, Fluid Mechanics, 4th ed., Academic Press, 2007 - which is generally a good book on the subject. Another popular, rather basic textbook is R. Granger, Fluid Mechanics, Dover, 1995.

[43] Named after William Froude (1810-1879) who has made several important contributions to applied hydrodynamics.

[44] Note that the "dynamic" viscosity η participates in this number (and many other problems of fluid dynamics) only in the combination η/ρ, which thereby has deserved a special name of kinematic viscosity.

[45] Indeed, the values of η and ρ for water listed in Table 1 imply that even for a few-meter-sized object (such as a human body or a small boat), $Re>1,000$ at any speed above just ~ 1 mm/s.

[46] A rare exception is the relatively recent theoretical result by S. Orszag (1971) for the turbulence threshold in a flow of an incompressible fluid through a gap of thickness t between two parallel plane walls (see Figure 10): $Re_{\rm t}\approx$ 5,772 (for $l=t/2, v=v_{\max}$). However, this result does not predict the turbulence patterns at $\mathrm{Re}>\mathrm{Re}_{\rm t}$.

[47] The crucial condition of correct modeling is the equality of the Reynolds numbers (74) (and if relevant, also of the Froude numbers and/or the Mach numbers) of the object of interest and its model.

[48] See, e.g., P. Davidson, Turbulence, Oxford U. Press, 2004.

[49] The following famous quote is attributed to Werner Heisenberg on his deathbed: "When I meet God, I will ask him two questions: Why relativity? And why turbulence? I think he will have an answer for the first question." Though probably inaccurate, this story reflects rather well the understandable frustration of the fundamental physics community, renown for their reductionist mentality, with the enormous complexity of phenomena which obey simple (e.g., the Navier-Stokes) equations, i.e. from their point of view, do not describe any new physics.

[50] This picture was suggested in 1922 by Lewis F. Richardson.

8.7: Exercise Problems

8.1. Find the first-order correction to the Pascal equation (6) for a liquid, due to its low but nonzero compressibility, and evaluate this correction for the water at the bottom of the Earth's oceans.

8.2. Find the stationary shape of the open surface of an incompressible, heavy fluid in a container rotated about its vertical axis with a constant angular velocity ω - see the figure on the right.

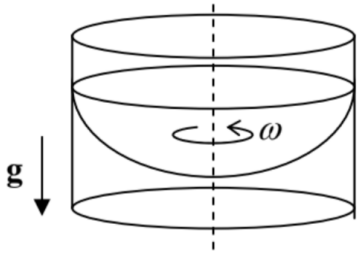

8.3.* Use two different approaches to calculate the stationary shape of the surface of an incompressible fluid of density ρ near a vertical plane wall, in a uniform gravity field - see the figure on the right. In particular, find the height h of liquid's rise at the wall surface as a function of the contact angle θ_c.

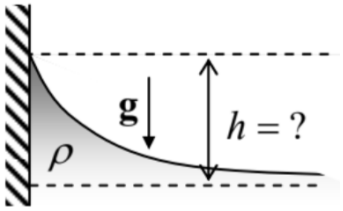

8.4. * A soap film with surface tension γ is stretched between two similar, coaxial, thin, round rings of radius R, separated by distance d - see the figure on the right. Neglecting gravity, calculate the equilibrium shape of the film, and the force needed for keeping the rings at the fixed distance.

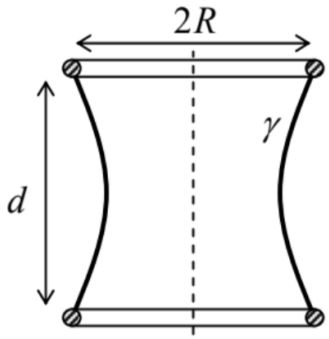

8.5. A solid sphere of radius R is kept in a steady, vorticity-free flow of an ideal incompressible fluid, with velocity v_0. Find the spatial distribution of velocity and pressure, and in particular their extreme values. Compare the results with those obtained in Sec. 4 for a round cylinder.

8.6. A small source, located at distance d from a plane wall of a container filled with an ideal, incompressible fluid of density ρ, injects additional fluid isotropically, at a constant mass current ("discharge") $Q \equiv dM/dt-$ see the figure on the right. Calculate the fluid's velocity distribution, and its pressure on the

Hint: Recall the charge image method in electrostatics, [51] and contemplate its possible analog.

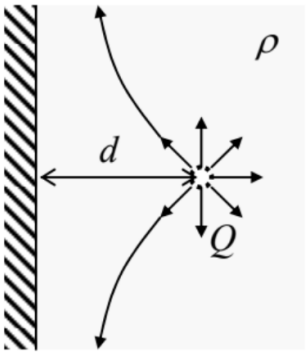

8.7. Calculate the average kinetic, potential, and full energies (per unit area) of a traveling sinusoidal wave, of a small amplitude q_A, on the horizontal surface on an ideal, incompressible, deep fluid of density ρ, in a uniform gravity field $\mathbf{g}$.

8.8. Calculate the average power (per unit width of wave's front) carried by the surface wave discussed in the previous problem, and relate the result to the wave's energy.

8.9. Derive Eq. (48) for the surface waves on a finite-thickness layer of a heavy liquid.

8.10. Derive Eq. (50) for the capillary waves ("ripples").

8.11 .* Derive a 2D differential equation describing the propagation of relatively long $(\lambda >> h)$ waves on the surface of a broad, plane layer of thickness h, of an ideal, incompressible fluid, and use it to calculate the longest standing wave modes and frequencies in a layer covering a spherical planet of radius $R \gg >$ h.

Hint: The second task requires some familiarity with the basic properties of spherical harmonics. [52]

8.12. Calculate the velocity distribution and the dispersion relation of the waves propagating along the horizontal interface of two ideal, incompressible fluids of different densities.

8.13. Use the finite-difference approximation for the Laplace operator, with the mesh step $h = a/4$, to find the maximum velocity and total mass flow Q of a viscous, incompressible fluid through a long pipe with a square-shaped cross-section of side a. Compare the results with those described in Sec. 5 for the same problem with the mesh step $h = a/2$, and for a pipe with the circular cross-section of the same area.

8.14. A layer, of thickness h, of a heavy, viscous, incompressible fluid flows down a long and wide inclined plane, under its own weight - see the figure on the right. Find the stationary velocity distribution profile, and the total fluid discharge (per unit width.)

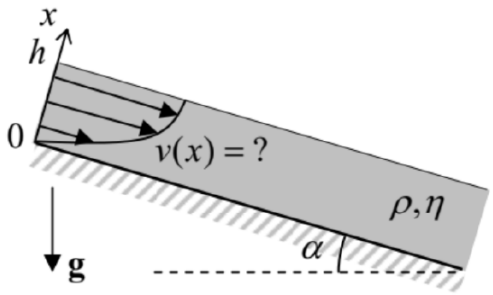

8.15. Calculate the drag torque exerted on a unit length of a solid round cylinder of radius R that rotates about its axis, with angular velocity ω, inside an incompressible fluid with viscosity η, kept static far from the cylinder.

8.16. Calculate the tangential force (per unit area) exerted by an incompressible fluid, with density ρ and viscosity η, on a broad solid plane placed over its surface and forced to oscillate, along the surface, with amplitude a and frequency ω.

8.17. A massive barge, with a flat bottom of area A, floats in shallow water, with clearance $h \ll A^{1/2}-$ see the figure on the right. Analyze the time dependence of the barge's velocity $V(t)$, and the water velocity profile, after the barge's engine has been turned off. Discuss the limits of large and small values of the dimensionless parameter $M/\rho A h$.

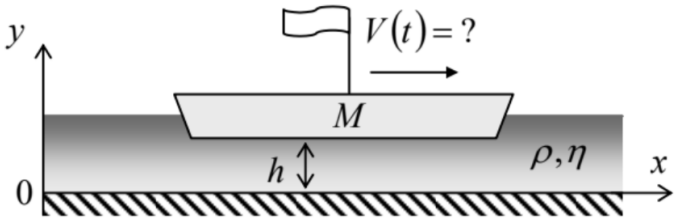

8.18. * Derive a general expression for mechanical energy loss rate in a viscous incompressible fluid that obeys the Navier-Stokes equation, and use this expression to calculate the attenuation coefficient of the surface waves, assuming that the viscosity is small. (Quantify this condition).

8.19. Use the Navier-Stokes equation to calculate the coefficient of attenuation of a plane, sinusoidal acoustic wave.

---

[51] See, e.g., EM Secs. 2.9, 3.3, and 4.3.

[52] See, e.g., EM Sec. 2.8 and/or QM Sec. 3.6.

CHAPTER OVERVIEW

9: Deterministic Chaos

This chapter gives a very brief review of chaotic phenomena in deterministic maps and dynamic systems with and without dissipation, and an even shorter discussion of the possible role of chaos in fluid turbulence.

9.1: Chaos in Maps

The possibility of quasi-random dynamics of deterministic systems with a few degrees of freedom (nowadays called the deterministic chaos - or just "chaos") had been noticed before the 20^{th} century, [1] but has become broadly recognized only after the publication of a 1963 paper by theoretical meteorologist Edward Lorenz. In that work, he examined numerical solutions of the following system of three nonlinear, ordinary differential equations,

$$\begin{aligned}\dot{q}_1 &= a_1 (q_2 - q_1) \\ \dot{q}_2 &= a_2 q_1 - q_2 - q_1 q_3, \\ \dot{q}_3 &= q_1 q_2 - a_3 q_3,\end{aligned}$$

as a rudimentary model of heat transfer through a horizontal layer of fluid separating two solid plates. (Experiment shows that if the bottom plate is kept hotter than the top one, the liquid may exhibit turbulent convection.) He has found that within a certain range of the constants $a_{1,2,3}$, the solution to Eq. (1) follows complex, unpredictable, non-repeating trajectories in the 3D q-space. Moreover, the functions $q_j(t)$ (where $j = 1, 2, 3$) are so sensitive to initial conditions $q_j(0)$ that at sufficiently large times t, solutions corresponding to slightly different initial conditions become completely different.

Very soon it was realized that such behavior is typical for even simpler mathematical objects called maps so that I will start my discussion of chaos from these objects. A 1D map is essentially a rule for finding the next number q_{n+1} of a discrete sequence numbered by the integer index n, in the simplest cases using only its last known value q_n. The most famous example is the so-called logistic map: [2]

$$q_{n+1} = f(q_n) \equiv r q_n (1 - q_n). \tag{9.1.1}$$

The basic properties of this map may be understood using the (hopefully, self-explanatory) graphical representation shown in Figure 1. [3] One can readily see that at $r < 1$ (Figure 1a) the logistic map sequence rapidly converges to the trivial fixed point $q^{(0)} = 0$, because each next value of q is less than the previous one. However, if r is increased above 1 (as in the example shown in Figure 1b), the fixed point $q^{(0)}$ becomes unstable. Indeed, at $q_n << 1$, the map yields $q_{n+1} \approx r q_n$, so that at $r > 1$, the values q_n grow with each iteration. Instead of the unstable point $q^{(0)} = 0$, in the range $1 < r < r_1$, where $r_1 \equiv 3$, the map has a stable fixed point $q^{(1)}$ that may be found by plugging this value into both parts of Eq. (2):

$$q^{(1)} = f\left(q^{(1)}\right) \equiv r q^{(1)} \left(1 - q^{(1)}\right), \tag{9.1.2}$$

giving $q^{(1)} = 1 - 1/r -$ see the left branch of the plot shown in Figure 2.

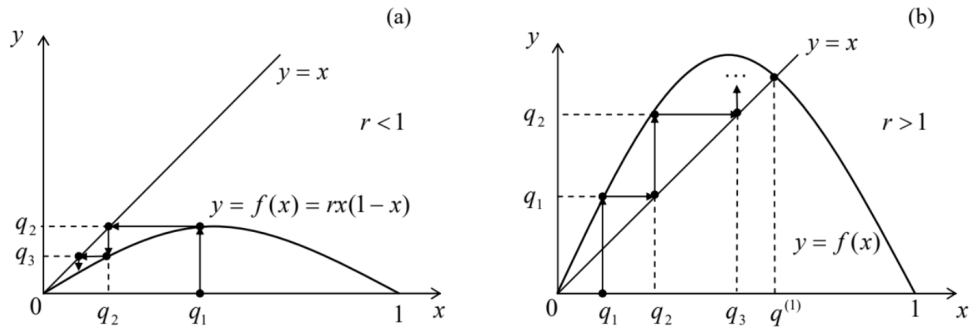

Figure 9.1. Graphical analysis of the logistic map for: (a) $r < 1$ and (b) $r > 1$.

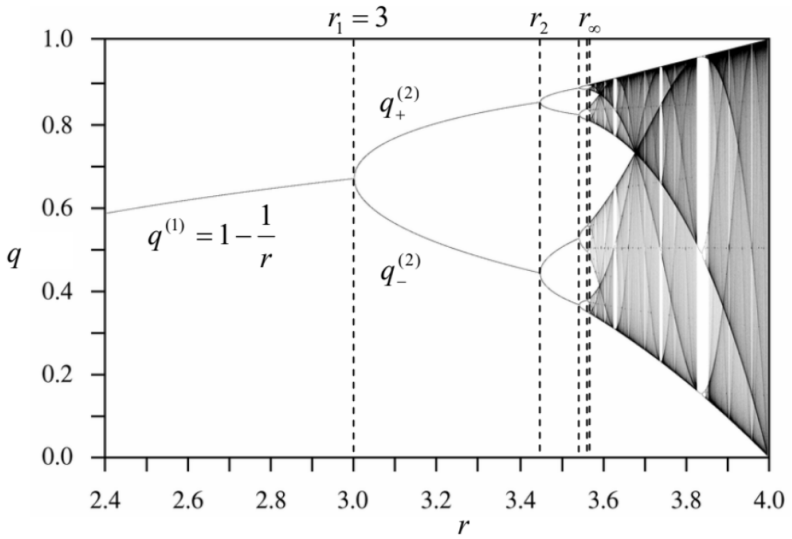

Figure 9.2. The fixed points and chaotic regions of the logistic map. Adapted, under the CCO 1.0 Universal Public Domain Dedication, from the original by Jordan Pierce, available at

http://en.wikipedia.org/wiki/Logistic_map.

(A very nice live simulation of the map is also available on this website.)

However, at $r > r_1 = 3$, the fixed point $q^{(1)}$ also becomes unstable. To prove that, let us take $q_n \equiv q^{(1)} + \tilde{q}_n$, assume that the deviation $\tilde{q}_n$ from the fixed point $q^{(1)}$ is small, and linearize the map (2) in $\tilde{q}_n$ – just as we repeatedly did for differential equations earlier in this course. The result is

$$\tilde{q}_{n+1} = \left.\frac{df}{dq}\right|_{q=q^{(1)}} \tilde{q}_n = r\left(1 - 2q^{(1)}\right)\tilde{q}_n = (2-r)\tilde{q}_n. \tag{9.1.3}$$

To prove that, let us take

$$\tilde{q}_{n+1} = \left.\frac{df}{dq}\right|_{q=q^{(1)}} \tilde{q}_n = r\left(1 - 2q^{(1)}\right)\tilde{q}_n = (2-r)\tilde{q}_n. \tag{9.1.4}$$

It shows that at $0 < 2 - r < 1$, i.e. at $1 < r < 2$, the deviations $\tilde{q}_n$ decrease monotonically. At $-1 < 2 - r < 0$, i.e. in the range $2 < r < 3$, the deviations' sign alternates, but their magnitude still decreases – as in a stable focus, see Sec. 5.6. However, at $-1 < 2 - r$, i.e. $r > r_1 \equiv 3$, the deviations grow by magnitude, while still changing their sign, at each step. Since Eq. (2) has no other fixed points, this means that at $n \to \infty$, the values q_n do not converge to one point; rather, within the range $r_1 < r < r_2$, they approach a limit cycle of alternation of two points, $q_+^{(2)}$ and $q_-^{(2)}$, which satisfy the following system of algebraic equations:

$$q_+^{(2)} = f\left(q_-^{(2)}\right), \quad q_-^{(2)} = f\left(q_+^{(2)}\right). \tag{9.1.5}$$

These points are also plotted in Figure 2, as functions of the parameter r. What has happened at the point $r_1 = 3$ is called the period-doubling bifurcation.

The story repeats at $r = r_2 \equiv 1 + \sqrt{6} \approx 3.45$, where the system goes from the 2-point limit cycle to a 4-point cycle, then at $r = r_3 \approx 3.54$, where the limit cycle becomes consisting of 8 alternating points, etc. Most remarkably, the period-doubling bifurcation points r_n, at that the number of points in the limit cycle doubles from 2^{n-1} points to 2^n points, become closer and closer. Numerical calculations show that at $n \to \infty$, these points obey the following asymptotic behavior:

$$r_n \to r_\infty - \frac{C}{\delta^n}, \text{ where } r_\infty = 3.5699\ldots, \quad \delta = 4.6692\ldots \tag{9.1.6}$$

The parameter δ is called the Feigenbaum constant; for other maps, and some dynamic systems (see the next section), period-doubling sequences follow a similar law, but with different values of δ.

More important for us, however, is what happens at $r > r_\infty$. Numerous numerical experiments, repeated with increasing precision, [4] have confirmed that here the system is fully disordered, with no reproducible limit cycle, though (as Figure 2 shows) at $r \approx r_\infty$,

all sequential values q_n are still confined to a few narrow regions. [5] However, as parameter r is increased well beyond r_∞, these regions broaden and merge. This is the so-called deep chaos, with no apparent order at all. [6]

The most important feature of the chaos (in this and any other system) is the exponential divergence of trajectories. For a 1D map, this means that even if the initial conditions q_1 in two map implementations differ by a very small amount Δq_1, the difference Δq_n between the corresponding sequences q_n is growing, on average, exponentially with n. Such exponents may be used to characterize chaos. Indeed, an evident generalization of Eq. (4) to an arbitrary point q_n is

$$\Delta q_{n+1} = e_n \Delta q_n, \quad e_n \equiv \left.\frac{df}{dq}\right|_{q=q_n}. \tag{9.1.7}$$

Let us assume that Δq_1 is so small that N first values q_n are relatively close to each other. Then using Eq. (7) iteratively for these steps, we get

$$\Delta q_N = \Delta q_1 \prod_{n=1}^{N} e_n, \quad \text{so that } \ln\left|\frac{\Delta q_N}{\Delta q_1}\right| = \sum_{n=1}^{N} \ln|e_n|. \tag{9.1.8}$$

Numerical experiments show that in most chaotic regimes, at $N \to \infty$ such a sum fluctuates about an average, which grows as λN, with the parameter

$$\lambda \equiv \lim_{\Delta q_1 \to 0} \lim_{N \to \infty} \frac{1}{N} \sum_{n=1}^{N} \ln|e_n|, \tag{9.1.9}$$

called the Lyapunov exponent [7] being independent of the initial conditions. The bottom panel in Figure 3 shows λ as a function of the parameter r for the logistic map (2). (Its top panel shows the same data as Figure 2, and it reproduced here just for the sake of comparison.)

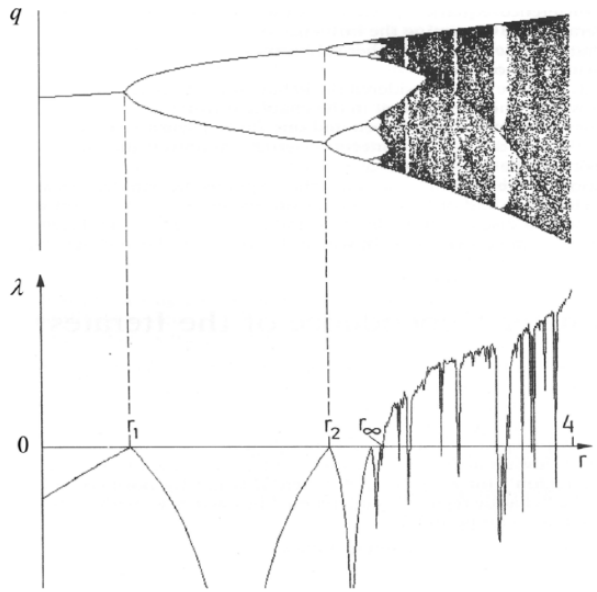

Figure 9.3. The Lyapunov exponent for the logistic map. Adapted, with permission, from the monograph by Schuster and Just (cited below). C Wiley-VCH Verlag GmbH & Co. KGaA.

Note that at $r < r_\infty$, λ is negative, indicating the sequence's stability, besides the points $r_1, r_2, \ldots$ where λ would become positive if the limit cycle changes (bifurcations) had not brought it back into the negative territory. However, at $r > r_\infty$, λ becomes positive, returning to negative values only in limited intervals of stable limit cycles. It is evident that in numerical experiments (which dominate the studies of deterministic chaos) the Lyapunov exponent may be used as a good measure of the chaos' depth. [8]

Despite all the abundance of results published for particular maps, [9] and several interesting general observations (like the existence of the Feigenbaum bifurcation sequences), to the best of my knowledge, nobody can yet predict the patterns like those shown in

Figure 2 and 3 from just looking at the mapping rule itself, i.e. without carrying out actual numerical experiments. Unfortunately, the understanding of deterministic chaos in other systems is not much better.

---

[1] It may be traced back at least to an 1892 paper by the same Jules Henri Poincaré who was already reverently mentioned in Chapter 5. Citing it: "...it may happen that small differences in the initial conditions produce very great ones in the final phenomena. [...] Prediction becomes impossible."

[2] Its chaotic properties were first discussed in 1976 by Robert May, though the map itself is one of the simple ecological models repeatedly discussed much earlier, and may be traced back at least to the 1838 work by Pierre François Verhulst.

[3] Since the maximum value of the function $f(q)$, achieved at $q = 1/2$, equals $r/4$, the mapping may be limited to segment $x = [0, 1]$, if the parameter r is between 0 and 4. Since all interesting properties of the map, including chaos, may be found within these limits, I will discuss only this range of r.

[4] The reader should remember that just as the usual ("nature") experiments, numerical experiments also have limited accuracy, due to unavoidable rounding errors.

[5] The geometry of these regions is essentially fractal, i.e. has a dimensionality intermediate between 0 (which any final set of geometric points would have) and 1 (pertinent to a 1D continuum). An extensive discussion of fractal geometries and their relation to the deterministic chaos may be found, e.g., in the book by B. Mandelbrot, The Fractal Geometry of Nature, W. H. Freeman, 1983.

[6] This does not mean that chaos' development is always a monotonic function of r. As Figure 2 shows, within certain intervals of this parameter, the chaotic behavior suddenly disappears, being replaced, typically, with a fewpoint limit cycle, just to resume on the other side of the interval. Sometimes (but not always!) the "route to chaos" on the borders of these intervals follows the same Feigenbaum sequence of period-doubling bifurcations.

[7] After Alexandr Mikhailovich Lyapunov (1857-1918), famous for his studies of the stability of dynamic systems.

[8] N-dimensional maps that relate N-dimensional vectors rather than scalars, may be characterized by N Lyapunov exponents rather than one. For chaotic behavior, it is sufficient for just one of them to become positive. For such systems, another measure of chaos, the Kolmogorov entropy, may be more relevant. This measure, and its relation with the Lyapunov exponents, are discussed, for example, in SM Sec. 2.2.

[9] See, e.g., Chapters 2-4 in H. Schuster and W. Just, Deterministic Chaos, 4^{th} ed., Wiley-VCH, 2005, or Chapters 8-9 in J. Thompson and H. Stewart, Nonlinear Dynamics and Chaos, 2^{nd} ed., Wiley, 2002 .

9.2: Chaos in Dynamic Systems

Proceeding to the discussion of chaos in dynamic systems, it is more natural, with our background, to illustrate this discussion not with the Lorenz Eqs. (1), but with the system of equations describing a dissipative pendulum driven by a sinusoidal external force, which was repeatedly discussed in Chapter 5. Introducing two new variables, the normalized momentum $p \equiv (dq/dt)/\omega_0$, and the external force's full phase $\psi \equiv \omega t$, we may rewrite Eq. (5.42) describing the pendulum, in a form similar to Eq. (1), i.e. as a system of three first-order ordinary differential equations:

$$\begin{aligned} \dot{q} &= \omega_0 p, \\ \dot{p} &= -\omega_0 \sin q - 2\delta p + (f_0/\omega_0)\cos\psi, \\ \dot{\psi} &= \omega. \end{aligned}$$

Figure 4 several results of a numerical solution of Eq. (10). [10] In all cases, parameters δ, ω_0, and f_0 are fixed, while the external frequency ω is gradually changed. For the case shown on the top panel, the system still tends to a stable periodic solution, with very low contents of higher harmonics. If the external force frequency is reduced by a just few percent, the 3^{rd} subharmonic may be excited. (This effect has already been discussed in Sec. 5.8 - see, e.g., Figure 5.15.) The next panel shows that just a small further reduction of the frequency ω leads to a new tripling of the period, i.e. the generation of a complex waveform with the 9^{th} subharmonic. Finally (see the bottom panel of Figure 4), even a minor further change of ω leads to oscillations without any visible period, e.g., to the chaos.

In order to trace this transition, a direct inspection of the oscillation waveforms $q(t)$ is not very convenient, and trajectories on the phase plane $[q, p]$ also become messy if plotted for many periods of the external frequency. In situations like this, the Poincaré (or "stroboscopic") plane, already discussed in Sec. 5.6, is much more useful. As a reminder, this is essentially just the phase plane $[q, p]$, but with the points highlighted only once a period, e.g., at $\psi = 2\pi n$, with $n = 1, 2, \ldots$ On this plane, periodic oscillations of frequency ω are represented just as one fixed point - see, e.g. the top panel in the right column of Figure 4. The 3^{rd} subharmonic generation, shown on the next panel, means the oscillation period's tripling and is reflected on the Poincaré plane as splitting of the fixed point into three. It is evident that this transition is similar to the period-doubling bifurcation in the logistic map, besides the fact (already discussed in Sec. 5.8) that in systems with an antisymmetric nonlinearity, such as the pendulum (10), the 3^{rd} subharmonic is easier to excite. From this point, the 9^{th} harmonic generation (shown on the 3^{rd} panel of Figure 4), i.e. one more splitting of the points on the Poincare plane, may be understood as one more step on the Feigenbaum-like route to chaos - see the bottom panel of that figure.

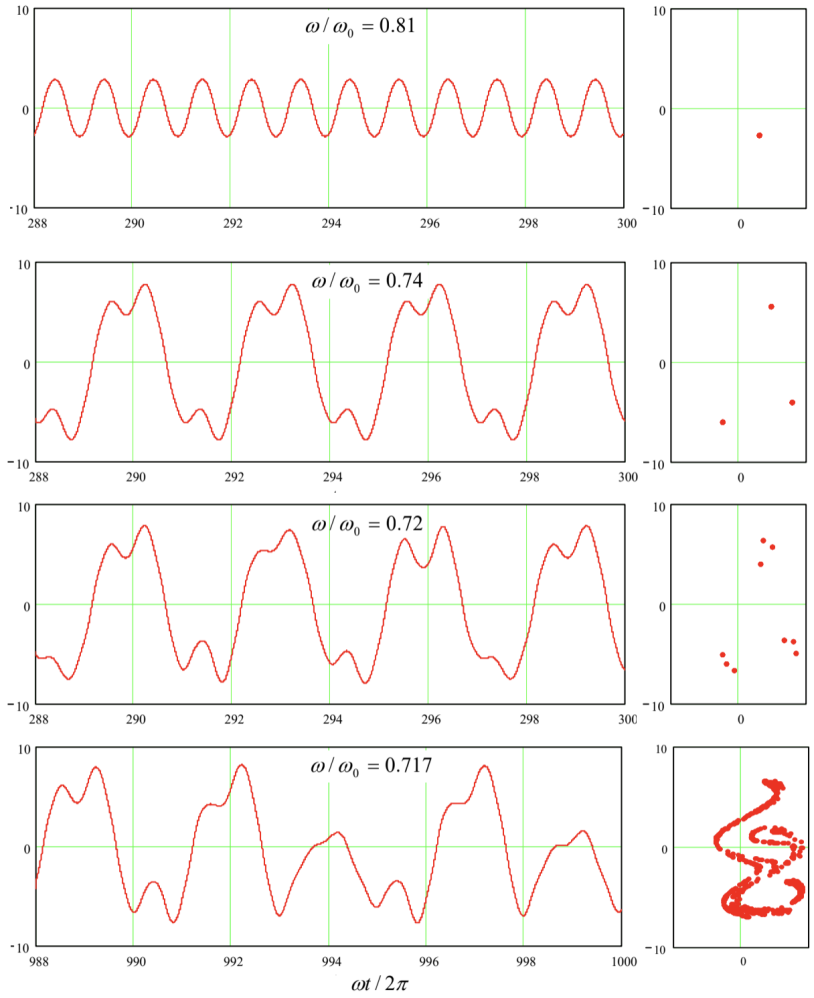

Figure 9.4. Oscillations in a pendulum with weak damping, $\delta/\omega_0 = 0.1$, driven by a sinusoidal external force with a fixed effective amplitude $f_0/{\omega_0}^2 = 1$, and several close values of the frequency ω (listed on the panels). Left panel column: the oscillation waveforms $q(t)$ recorded after certain initial transient intervals. Right column: representations of the same processes on the Poincaré plane of the variables $[q, p]$, with the q-axis turned vertically, for the convenience of comparison with the left panels. So, the transition to chaos in dynamic systems may be at least qualitatively similar to than in 1D maps, with a law similar to Eq. (6) for the critical values of some parameter of the system (in Figure 4, frequency ω), though with a system-specific value of the coefficient δ. Moreover, we may consider the first two differential equations of the system (10) as a 2D map that relates the vector $\{q_{n+1}, p_{n+1}\}$ of the coordinate and momentum, measured at $\psi = 2\pi(n+1)$, with the previous value $\{q_n, p_n\}$ of that vector, reached at $\psi = 2\pi n$.

Unfortunately, this similarity also implies that the deterministic chaos in dynamic systems is at least as complex, and is as little understood, as in maps. For example, Figure 5 shows (a part of) the phase diagram of the externally-driven pendulum, with the red bar marking the route to chaos traced in Figure 4 , and shading/hatching styles marking different oscillation regimes. One can see that the pattern is at least as complex as that shown in Figs. 2 and 3, and, besides a few features, [11] is equally unpredictable from the form of the equation.

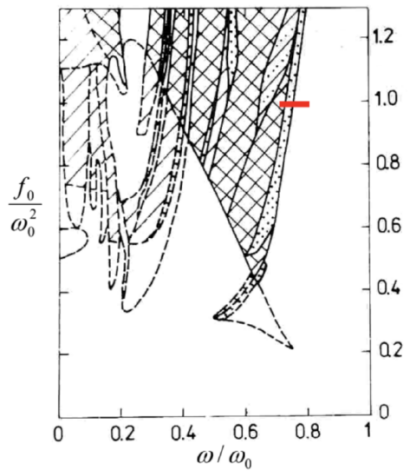

Figure 9.5. The phase diagram of an externally-driven pendulum with weak damping $(\delta/\omega_0 = 0.1)$. The regions of oscillations with the basic period are not shaded; the notation for other regions is as follows. Doted: subharmonic generation; cross-hatched: chaos; hatched: either chaos or the basic period (depending on the initial conditions); hatch-dotted: either the basic period or subharmonics. Solid lines show the boundaries of single-regime regions, while dashed lines are the boundaries of the regions where several types of motion are possible. (Figure courtesy V. Kornev.)

Are there any valuable general results concerning the deterministic chaos in dynamic systems? The most important (though an almost evident) result is that this phenomenon is impossible in any system described by one or two first-order differential equations with time-independent right-hand sides. Indeed, let us start with a single equation

$$\dot{q} = f(q), \tag{9.2.1}$$

where $f(q)$ is any single-valued function. This equation may be directly integrated to give

$$t = \int^{q} \frac{dq'}{f(q')} + \text{const}\,, \tag{9.2.2}$$

showing that the relation between q and t is unique and hence does not leave any place for chaos.

Next, let us explore a system of two such equations:

$$\dot{q}_1 = f_1(q_1, q_2)\,,$$
$$\dot{q}_2 = f_2(q_1, q_2)\,.$$

Consider its phase plane shown schematically in Figure 6. In a "usual" system, the trajectories approach either some fixed point (Figure 6a) describing static equilibrium, or a limit cycle (Figure 6b) describing periodic oscillations. (Both notions are united by the term attractor because they "attract" trajectories launched from various initial conditions.) On the other hand, phase plane trajectories of a chaotic system of equations that describe physical variables (which cannot be infinite), should be confined to a limited phase plane area, and simultaneously cannot start repeating each other. (This topology is frequently called the strange attractor.) For that, the 2D trajectories need to cross - see, e.g., point A in Figure 6c.

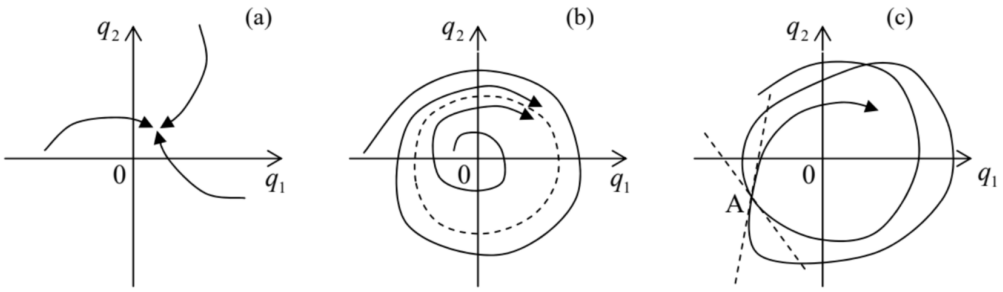

Figure 9.6. Attractors in dynamical systems: (a) a fixed point, (b) a limit cycle, and (c) a strange attractor.

However, in the case described by Eqs. (13), such a crossing is clearly impossible, because according to these equations, the tangent of a phase plane trajectory is a unique function of the coordinates $\{q_1, q_2\}$:

$$\frac{dq_1}{dq_2} = \frac{f_1(q_1, q_2)}{f_2(q_1, q_2)}. \tag{9.2.3}$$

Thus, in this case the deterministic chaos is impossible. [12] It becomes, however, readily possible if the right-hand sides of a system similar to Eq. (13) depend either on other variables of the system or time. For example, if we consider the first two differential equations of the system (10), in the case $f_0 = 0$ they have the structure of the system (13) and hence the chaos is impossible, even at $\delta < 0$ when (as we know from Sec. 5.4) the system allows self-excitation of oscillations - leading to a limit-cycle attractor. However, if $f_0 \neq 0$, this argument does not work any longer, and (as we have already seen) the system may have a strange attractor - which is, for dynamic systems, a synonym for the deterministic chaos.

Thus, chaos is only possible in autonomous dynamic systems described by three or more differential equations of the first order. [13]

---

[10] In the actual simulation, a small term εq, with $\varepsilon < 1$, has been added to the left-hand side of this equation. This term slightly tames the trend of the solution to spread along the q-axis, and makes the presentation of results easier, without affecting the system's dynamics too much.

[11] In some cases, it is possible to predict a parameter region where chaos cannot happen, due to the lack of any instability-amplification mechanism. Unfortunately, typically the analytically predicted boundaries of such a region form a rather loose envelope of the actual (numerically simulated) chaotic regions.

[12] A mathematically strict formulation of this statement is called the Poincare-Bendixon theorem, which was proved by Ivar Bendixon as early as in 1901.

[13] Since a typical dynamic system with one degree of freedom is described by two such equations, the number of first-order equations describing a dynamic system is sometimes called the number of its half-degrees of freedom. This notion is very useful and popular in statistical mechanics - see, e.g., SM Sec. 2.2 and on.

9.3: Chaos in Hamiltonian Systems

The last conclusion is of course valid for Hamiltonian systems, which are just a particular type of dynamic systems. However, one may wonder whether these systems, that feature at least one first integral of motion, $H = \text{const}$, and hence are more "ordered" than the systems discussed above, can exhibit chaos at all. The answer is yes because such systems still can have mechanisms for exponential growth of a small initial perturbation.

As the simplest way to show it, let us consider the so-called mathematical billiard, i.e. system with a ballistic particle (a "ball") moving freely by inertia on a horizontal plane surface ("table") limited by rigid impenetrable walls. In this idealized model of the usual game of billiards, the ball's velocity $\mathbf{v}$ is conserved when it moves on the table, and when it runs into a wall, the ball is elastically reflected from it as from a mirror, [14] with the reversal of the sign of the normal velocity v_n, and the conservation of the tangential velocity v_τ, and hence without any loss of its kinetic (and hence the full) energy

$$E = H = T = \frac{m}{2}v^2 = \frac{m}{2}\left(v_n^2 + v_\tau^2\right). \tag{9.3.1}$$

This model, while being a legitimate 2D dynamic system, [15] allows geometric analyses for several simple table shapes. The simplest case is a rectangular billiard of area $a \times b$ (Figure 7), whose analysis may be readily carried out just by the replacement of each ball reflection event with the mirror reflection of the table in that wall - see the dashed lines on panel (a).

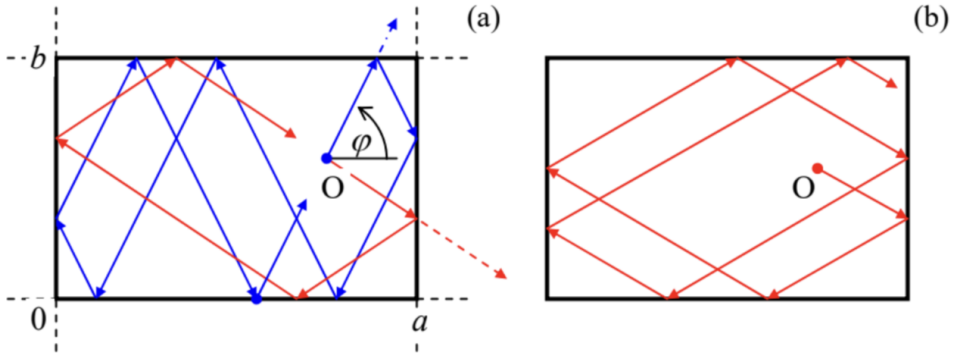

Figure 9.7. Ball motion on a rectangular billiard at (a) a commensurate, and (b) an incommensurate launch angle.

Such analysis (left for the reader' pleasure :-) shows that if the tangent of the ball launching angle φ is commensurate with the side length ratio:

$$\tan\varphi = \pm\frac{m}{n}\frac{b}{a}, \tag{9.3.2}$$

where n and m are non-negative integers without common integer multipliers, the ball returns exactly to the launch point O, after bouncing m times from each wall of length a, and n times from each wall of length b. (Red lines in Figure 7a show an example of such a trajectory for $n = m = 1$, while blue lines, for $m = 3, n = 1$.) The larger is the sum $(m+n)$, the more complex is such closed trajectory - "orbit". Finally, if $(n+m) \to \infty$, i.e. $\tan\varphi$ and b/a are incommensurate (meaning that their ratio is an irrational number), the trajectory covers all the table area, and the ball never returns exactly into the launch point. Still, this is not genuine chaos. Indeed, a small shift of the launch point O shifts all the trajectory fragments by the same displacement. Moreover, at any time t, each of Cartesian components $v_j(t)$ of the ball's velocity (with coordinate axes parallel to the table sides) may take only two values, $\pm v_j(0)$, and hence may vary only as much as the initial velocity is being changed.

In 1963, i.e. well before E. Lorenz's work, Yakov Sinai showed that the situation changes completely if an additional wall, in the shape of a circle, is inserted into the rectangular billiard (Figure 8). For most initial conditions, the ball's trajectory eventually runs into the circle (see the red line on panel (a) as an example), and the further trajectory becomes essentially chaotic. Indeed, let us consider the ball's reflection from the circle-shaped wall - Figure 8b. Due to the conservation of the tangential velocity, and the sign change of the normal velocity component, the reflection obeys a simple law: $\theta_r = \theta_1$. Figure 8 b shows that as the result, the magnitude of a small difference $\delta\varphi$ between the angles of two close trajectories (as measured in the lab system), doubles at each reflection from the curved wall. This means that the small deviation grows along the ball trajectory as

$$|\delta\varphi(N)| \sim |\delta\varphi(0)| \times 2^N \equiv |\delta\varphi(0)|e^{N\ln 2}, \tag{9.3.3}$$

where N is the number of reflections from the convex wall. [16] As we already know, such exponential divergence of trajectories, with a positive Lyapunov exponent, is the main feature of deterministic chaos. [17]

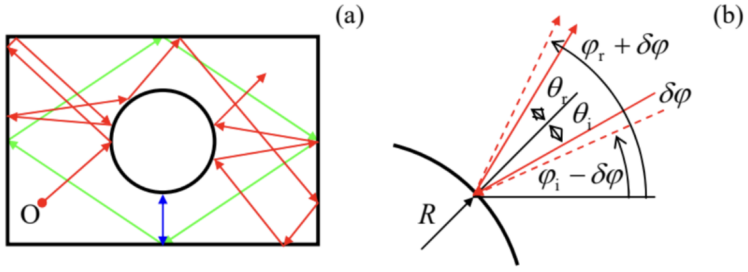

Figure 9.8. (a) Motion on a Sinai billiard table, and (b) the mechanism of the exponential divergence of close trajectories.

The most important new feature of the dynamic chaos in Hamiltonian systems is its dependence on initial conditions. (In the systems discussed in the previous two previous sections, that lack the integrals of motion, the initial conditions are rapidly "forgotten", and the chaos is usually characterized after an initial transient period - see, e.g., Figure 4.) Indeed, even a Sinai billiard allows periodic motion, along closed orbits, at certain initial conditions - see the blue and green lines in Figure 8a as examples. Thus the chaos "depth" in such systems may be characterized by the "fraction"18 of the phase space of initial parameters (for a 2D billiard, of the 3D space of initial values of x, y, and φ) resulting in chaotic trajectories.

This conclusion is also valid for Hamiltonian systems that are met in experiment more frequently than the billiards, for example, coupled nonlinear oscillators without damping. Perhaps the earliest and the most popular example is the so-called Hénon-Heiles system, [19] which may be described by the following Lagrangian function:

$$L = \frac{m_1}{2}\left(\dot{q}_1^2 - \omega_1^2 q_1^2\right) + \frac{m_2}{2}\left(\dot{q}_2^2 - \omega_2^2 q_2^2\right) - \varepsilon\left(q_1^2 - \frac{1}{3}q_2^2\right) q_2. \tag{9.3.4}$$

$$\begin{aligned} m_1\left(\ddot{q}_1 + \omega_1^2 q_1\right) &= -2\varepsilon q_1 q_2, \\ m_2\left(\ddot{q}_2 + \omega_2^2 q_2\right) &= -\varepsilon\left(q_1^2 - q_2^2\right), \end{aligned}$$

and find their first integral of motion (physically, the energy conservation law):

$$H = E = \frac{m_1}{2}\left(\dot{q}_1^2 + \omega_1^2 q_1^2\right) + \frac{m_2}{2}\left(\dot{q}_2^2 + \omega_2^2 q_2^2\right) + \varepsilon\left(q_1^2 - \frac{1}{3}q_2^2\right) q_2 = \text{const}. \tag{9.3.5}$$

In the context of our discussions in Chapters 5 and 6 , Eqs. (19) may be readily interpreted as those describing two oscillators, with small-oscillation frequencies ω_1 and ω_2, coupled only as described by the quadratic terms on the right-hand sides of the equations. This means that as the oscillation amplitudes $A_{1,2}$, and hence the total energy E of the system, are close to zero, the oscillator subsystems are virtually independent, each performing sinusoidal oscillations at its own frequency. This observation suggests a convenient way to depict the system's motion. [20] Let us consider a Poincaré plane for one of the oscillators (say, with the coordinate q_2), similar to that discussed in Sec. 2 above, with the only difference is that (because of the absence of an explicit function of time in the system's equations), the trajectory on the phase plane $[q_2, \dot{q}_2]$ is highlighted at the moments when $q_1 = 0$.

Let us start from the limit $A_{1,2} \to 0$, when the oscillations of q_2 are virtually sinusoidal. As we already know (see Figure 5.9 and its discussion), if the representation point highlighting was perfectly synchronous with frequency ω_2 of the oscillations, there would be only one point on the Poincaré plane - see, e.g. the right top panel of Figure 4. However, at the q_1 - initiated highlighting, there is not such synchronism, so that each period, a different point of the elliptical (at the proper scaling of the velocity, circular) trajectory is highlighted, so that the resulting points, for certain initial conditions, reside on a circle of radius A_2. If we now vary the initial conditions, i.e. redistribute the initial energy between the oscillators, but keep the total energy E constant, on the Poincaré plane we get a set of ellipses.

Now, if the initial energy is increased, the nonlinear interaction of the oscillations starts to deform these ellipses, causing also their crossings - see, e.g., the top left panel of Figure 9. Still, below a certain threshold value of E, all Poincaré points belonging to a certain initial condition sit on a single closed contour. Moreover, these contours may be calculated approximately, but with pretty good accuracy, using straighforward generalization of the method discussed in Sec. 5.2.21

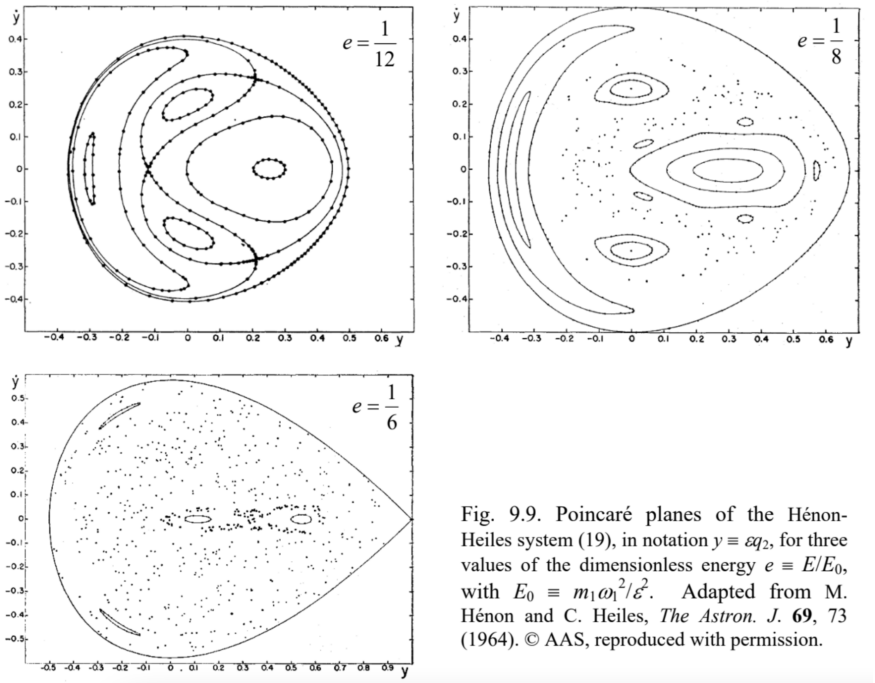

Fig. 9.9. Poincaré planes of the Hénon-Heiles system (19), in notation $y \equiv \varepsilon q_2$, for three values of the dimensionless energy $e \equiv E/E_0$, with $E_0 \equiv m_1\omega_1^2/\varepsilon^2$. Adapted from M. Hénon and C. Heiles, *The Astron. J.* **69**, 73 (1964). © AAS, reproduced with permission.

Figure 9.9. Poincaré planes of the HénonHeiles system (19), in notation $y \equiv \varepsilon q_2$, for three values of the dimensionless energy $e \equiv E/E_0$, with $E_0 \equiv m_1{\omega_1}^2/\varepsilon^2$. Adapted from M. Hénon and C. Heiles, The Astron. J. $\mathbf{69}, 73$ (1964). \odot AAS, reproduced with permission.

However, starting from some value of energy, certain initial conditions lead to sequences of points scattered over parts of the Poincaré plane, with a nonzero area - see the top right panel of Figure 9. This means that the corresponding oscillations $q_2(t)$ do not repeat from one (quasi-) period to the next one – cf. Figure 4 for the dissipative, forced pendulum. This is chaos. [22] However, some other initial conditions still lead to closed contours. This feature is similar to that in Sinai billiards, and is typical for Hamiltonian systems. As the energy is increased, larger and larger parts of the Poincaré plane correspond to the chaotic motion, signifying deeper and deeper chaos - see the bottom panel of Figure 9.

---

[14] A more scientific-sounding name for such a reflection is specular-from the Latin word "speculum" meaning a metallic mirror.

[15] Indeed, it is fully described by the following Lagrangian function: $L = mv^2/2 - U(\rho)$, with $U(\rho) = 0$ for the 2D radius vectors ρ belonging to the table area, and $U(\rho) = +\infty$ outside the area.

[16] Superficially, Eq. (17) is also valid for a plane wall, but as was discussed above, a billiard with such walls features a full correlation between sequential reflections, so that angle φ always returns to its initial value. In a Sinai billiard, such correlation disappears. Concave walls may also make a billiard chaotic; a famous example is the stadium billiard, suggested by Leonid Bunimovich in 1974, with two straight, parallel walls connecting two semi-circular, concave walls. Another example, which allows a straightforward analysis (first carried out by Martin Gutzwiller in the 1980s), is the so-called Hadamard billiard: an infinite (or rectangular) table with a nonhorizontal surface of negative curvature.

[17] Curved-wall billiards are also a convenient platform for studies of quantum properties of classically chaotic systems (for their conceptual discussion, see QM Sec. 3.5), in particular, the features called "quantum scars" see, e.g., the spectacular numerical simulation results by E. Heller, Phys. Rev. Lett. $\mathbf{53}, 1515$ (1984).

[18] Actually, quantitative characterization of the fraction is not trivial, because it may have fractal dimensionality. Unfortunately, due to lack of time I have to refer the reader interested in this issue to special literature, e.g., the monograph by B. Mandelbrot (cited above) and references therein.

[19] It was first studied in 1964 by Michel Hénon and Carl Heiles as a simple model of star rotation about a galactic center. Most studies of this equation have been carried out for the following particular case: $m_2 = 2m_1, m_1{\omega_1}^2 = m_2{\omega_2}^2$. In this case, introducing new variables $x \equiv \varepsilon q_1, y \equiv \varepsilon q_2$, and $\tau \equiv \omega_1 t$, it is possible to rewrite Eqs. (18)-(20) in parameter-free forms. All the results shown in Figure 9 below are for this case.

[20] Generally, the system has a trajectory in 4D space, e.g., that of coordinates $q_{1,2}$ and their time derivatives, although the first integral of motion (20) means that for each fixed energy E, the motion is limited to a 3D subspace. Still, this is one dimension too many for a convenient representation of the motion.

[21] See, e.g., M. Berry, in: S. Jorna (ed.), Topics in Nonlinear Dynamics, AIP Conf. Proc. No. 46, AIP, 1978, pp. 16-120.

[22] This fact complies with the necessary condition of chaos, discussed at the end of Sec. 2 because Eqs. (19) may be rewritten as a system of four differential equations of the first order.

9.4: Chaos and Turbulence

This extremely short section consists of essentially just one statement, extending the discussion in Sec. 8.5. The (re-) discovery of the deterministic chaos in systems with just a few degrees of freedom in the 1960s has changed the tone of the debates concerning turbulence origins, very considerably. At first, an extreme point of view that equated the notions of chaos and turbulence, became the debate's favorite. [23] However, after initial excitement, significant role of the Richardson-style energy-cascade mechanisms, involving many degrees of freedom, has been rediscovered and could not be ignored any longer. To the best knowledge of this author, who is a very distant albeit interested observer of that field, most experimental and numerical-simulation data carry features of both mechanisms, so that the debate continues. [24] Due to the age difference, most readers of these notes have much better chances than their author to see where will this discussion end. [25]

---

[23] An important milestone on that way was the work by S. Newhouse et al., Comm. Math. Phys. **64**, 35 (1978), who proved the existence of a strange attractor in a rather abstract model of fluid flow.

[24] See, e.g., U. Frisch, Turbulence: The Legacy of A. N. Kolmogorov, Cambridge U. Press, 1996.

[25] The reader interested in the deterministic chaos as such may also like to have a look at a very popular book by S. Strogatz, Nonlinear Dynamics and Chaos, Westview, 2001.

9.5: Exercise Problems

9.1. Generalize the reasoning of Sec. 1 to an arbitrary 1D map $q_{n+1} = f(q_n)$, with a function $f(q)$ differentiable at all points of interest. In particular, derive the condition of stability of an N-point limit cycle $q^{(1)} \to q^{(2)} \to \ldots \to q^{(N)} \to q^{(1)} \ldots$

9.2. Use the stability condition, derived in the previous problem, to analyze the possibility of the deterministic chaos in the so-called tent map, with

$$f(q) = \begin{cases} rq, & \text{for } 0 \le q \le 1/2, \\ r(1-q), & \text{for } 1/2 \le q \le 1, \end{cases} \quad \text{with } 0 \le r \le 2 \tag{9.5.1}$$

9.3. A dynamic system is described by the following system of differential equations:

$$\begin{aligned} \dot{q}_1 &= -q_1 + a_1 q_2^3, \\ \dot{q}_2 &= a_2 q_2 - a_3 q_2^3 + a_4 q_2 \left(1 - q_1^2\right). \end{aligned}$$

Can it exhibit chaos at some set of constant parameters $a_1 - a_4$?

9.4. A periodic function of time has been added to the right-hand side of the first equation of the system considered in the previous problem. Is deterministic chaos possible now?

CHAPTER OVERVIEW

10: A Bit More of Analytical Mechanics

This concluding chapter reviews two alternative approaches to analytical mechanics, whose major value is a closer parallel to quantum mechanics in general and its quasiclassical (WKB) approximation in particular. One of them, the Hamiltonian formalism, is also convenient for the derivation of an important asymptotic result, the adiabatic invariance, for classical systems with slowly changing parameters.

10.1: Hamilton Equations

Throughout this course, we have seen how analytical mechanics, in its Lagrangian form, is invaluable for solving various particular problems of classical mechanics. Now let us discuss several alternative formulations [1] that may not be much more useful for this purpose, but shed additional light on possible extensions of classical mechanics, most importantly to quantum mechanics.

As was already discussed in Sec. 2.3, the partial derivative $p_j \equiv \partial L/\partial \dot{q}_j$ participating in the Lagrange equation (2.19),

$$\frac{d}{dt}\frac{\partial L}{\partial \dot{q}_j} - \frac{\partial L}{\partial q_j} = 0 \tag{10.1.1}$$

may be considered as the generalized momentum corresponding to the generalized coordinate q_i, and the full set of these momenta may be used to define the Hamiltonian function (2.32):

$$H \equiv \sum_j p_j \dot{q}_j - L. \tag{10.1.2}$$

Now let us rewrite the full differential of this function [2] in the following form:

$$\begin{aligned} dH &= d\left(\sum_j p_j \dot{q}_j - L\right) = \sum_j \left[d(p_j)\,\dot{q}_j + p_j d\left(\dot{q}_j\right)\right] - dL \\ &= \sum_j \left[d(p_j)\,\dot{q}_j + p_j d\left(\dot{q}_j\right)\right] - \left[\frac{\partial L}{\partial t}dt + \sum_j \left(\frac{\partial L}{\partial q_j}d(q_j) + \frac{\partial L}{\partial \dot{q}_j}d\left(\dot{q}_j\right)\right)\right]. \end{aligned}$$

According to the definition of the generalized momentum, the second terms of each sum over j in the last expression cancel each other, while according to the Lagrange equation (1), the derivative $\partial L/\partial q_j$ is equal to $\dot{p}_j$, so that

$$dH = -\frac{\partial L}{\partial t}dt + \sum_j \left(\dot{q}_j dp_j - \dot{p}_j dq_j\right) \tag{10.1.3}$$

So far, this is just a universal identity. Now comes the main trick of Hamilton's approach: let us consider H as a function of the following independent arguments: time t, the generalized coordinates q_j, and the generalized momenta p_j - rather than generalized velocities $\dot{q}_j$. With this commitment, the general "chain rule" of differentiation of a function of several arguments gives

$$dH = \frac{\partial H}{\partial t}dt + \sum_j \left(\frac{\partial H}{\partial q_j}dq_j + \frac{\partial H}{\partial p_j}dp_j\right) \tag{10.1.4}$$

where dt, dq_j, and dp_j are independent differentials. Since Eq. (5) should be valid for any choice of these argument differentials, it should hold in particular if they correspond to the real law of motion, for which Eq. (4) is valid as well. The comparison of Eqs. (4) and (5) gives us three relations:

$$\frac{\partial H}{\partial t} = -\frac{\partial L}{\partial t}.$$
$$\dot{q}_j = \frac{\partial H}{\partial p_j}, \quad p_j = -\frac{\partial H}{\partial q_j}.$$

Comparing the first of them with Eq. (2.35), we see that

$$\frac{dH}{dt} = \frac{\partial H}{\partial t}, \tag{10.1.5}$$

meaning that the function $H(t, q_j, p_j)$ can change in time only via its explicit dependence on t. Two Eqs. (7) are even more substantial: provided that such function $H(t, q_j, p_j)$ has been calculated, they give us two first-order differential equations (called the Hamilton equations) for the time evolution of the generalized coordinate and generalized momentum of each degree of freedom of the system. [3]

Let us have a look at these equations for the simplest case of a system with one degree of freedom, with the Lagrangian function (3.3):

$$L = \frac{m_{\text{ef}}}{2}\dot{q}^2 - U_{\text{ef}}(q,t) \tag{10.1.6}$$

In this case, $p \equiv \partial L/\partial \dot{q} = m_{\text{ef}}\,\dot{q}$, and $H \equiv p\dot{q} - L = m_{\text{ef}}\,\dot{q}^2/2 + U_{\text{ef}}\,(q,t)$. To honor our new commitment, we need to express the Hamiltonian function explicitly via $t, q,$ and p (rather than $\dot{q}$). From the above expression for p, we immediately have $\dot{q} = p/m_{\text{ef}}$; plugging this expression back to Eq. (9), we get

$$H = \frac{p^2}{2m_{\text{ef}}} + U_{\text{ef}}(q,t). \tag{10.1.7}$$

Now we can spell out Eqs. (7) for this particular case:

$$\dot{q} \equiv \frac{\partial H}{\partial p} = \frac{p}{m_{\text{ef}}},$$
$$\dot{p} \equiv -\frac{\partial H}{\partial q} = -\frac{\partial U_{\text{ef}}}{\partial q}.$$

While the first of these equations just repeats the definition of the generalized momentum corresponding to the coordinate q, the second one gives the equation of momentum's change. Differentiating Eq. (11) over time, and plugging Eq. (12) into the result, we get:

$$\ddot{q} = \frac{\dot{p}}{m_{\text{ef}}} = -\frac{1}{m_{\text{ef}}}\frac{\partial U_{\text{ef}}}{\partial q}. \tag{10.1.8}$$

So, we have returned to the same equation (3.4) that had been derived from the Lagrangian approach. [4]

Thus, the Hamiltonian formalism does not give much new for the solution of this problem - and indeed most problems of classical mechanics. (This is why its discussion had been postponed until the very end of this course.) Moreover, since the Hamiltonian function $H\,(t, q_j, p_j)$ does not include generalized velocities explicitly, the phenomenological introduction of dissipation in this approach is less straightforward than that in the Lagrangian equations, whose precursor form (2.17) is valid for dissipative forces as well. However, the Hamilton equations (7), which treat the generalized coordinates and momenta in a manifestly symmetric way, are heuristically fruitful - besides being very appealing aesthetically. This is especially true in the cases where these arguments participate in H in a similar way. For example, in the very important case of a dissipation-free linear ("harmonic") oscillator, for which $U_{\text{ef}} = \kappa_{\text{ef}}\,q^2/2$, Eq. (10) gives the famous symmetric form

$$H = \frac{p^2}{2m_{\text{ef}}} + \frac{\kappa_{\text{ef}}x^2}{2} \equiv \frac{p^2}{2m_{\text{ef}}} + \frac{m_{\text{ef}}\omega_0^2 x^2}{2}, \qquad \text{where } \omega_0^2 \equiv \frac{\kappa_{\text{ef}}}{m_{\text{ef}}}. \tag{10.1.9}$$

The Hamilton equations (7) for this system preserve that symmetry, especially evident if we introduce the normalized momentum $p \equiv p/m_{\text{ef}}\,\omega_0$ (already used in Secs. 5.6 and 9.2):

$$\frac{dq}{dt} = \omega_0 p, \qquad \frac{dp}{dt} = -\omega_0 q. \tag{10.1.10}$$

More practically, the Hamilton approach gives additional tools for the search for the integrals of motion. To see that, let us consider the full time derivative of an arbitrary function $f\,(t, q_j, p_j)$:

$$\frac{df}{dt} = \frac{\partial f}{\partial t} + \sum_j \left(\frac{\partial f}{\partial q_j}\dot{q}_j + \frac{\partial f}{\partial p_j}\dot{p}_j \right). \tag{10.1.11}$$

Plugging in $\dot{q}_j$ and $\dot{p}_j$ from the Hamilton equations (7), we get

$$\frac{df}{dt} = \frac{\partial f}{\partial t} + \sum_j \left(\frac{\partial H}{\partial p_j}\frac{\partial f}{\partial q_j} - \frac{\partial H}{\partial q_j}\frac{\partial f}{\partial p_j} \right) \equiv \frac{\partial f}{\partial t} + \{H, f\}. \tag{10.1.12}$$

The last term on the right-hand side of this expression is the so-called Poisson bracket, [5] and is defined, for two arbitrary functions $f\,(t, q_j, p_j)$ and $g\,(t, q_j, p_j)$, as

$$\{g, f\} \equiv \sum_j \left(\frac{\partial g}{\partial p_j}\frac{\partial f}{\partial q_j} - \frac{\partial f}{\partial p_j}\frac{\partial g}{\partial q_j} \right) \tag{10.1.13}$$

From this definition, one can readily verify that besides evident relations $\{f, f\} = 0$ and $\{f, g\} = -\{g, f\}$, the Poisson brackets obey the following important Jacobi identity:

$$\{f, \{g, h\}\} + \{g, \{h, f\}\} + \{h, \{f, g\}\} = 0. \tag{10.1.14}$$

Now let us use these relations for a search for integrals of motion. First, Eq. (17) shows that if a function f does not depend on time explicitly, and

$$\{H, f\} = 0, \tag{10.1.15}$$

then $df f dt = 0$, i.e. that function is an integral of motion. Moreover, it turns out that if we already know two integrals of motion, say f and g, then the following function,

$$F \equiv \{f, g\} \tag{10.1.16}$$

is also an integral of motion - the so-called Poisson theorem. In order to prove it, we may use the Jacobi identity (19) with $h = H$. Next, using Eq. (17) to express the Poisson brackets $\{g, H\}, \{H, g\}$, and $\{H, \{f, g\}\} = \{H, F\}$ via the full and partial time derivatives of the functions f, g, and F, we get

$$\left\{f, \frac{\partial g}{\partial t} - \frac{dg}{dt}\right\} + \left\{g, \frac{df}{dt} - \frac{\partial f}{\partial t}\right\} + \frac{dF}{dt} - \frac{\partial F}{\partial t} = 0 \tag{10.1.17}$$

so that if f and g are indeed integrals of motion, i.e., $df/dt = dg/dt = 0$, then

$$\frac{dF}{dt} = \frac{\partial F}{\partial t} + \left\{g, \frac{\partial f}{\partial t}\right\} - \left\{f, \frac{\partial g}{\partial t}\right\} = \frac{\partial F}{\partial t} - \left[\left\{\frac{\partial f}{\partial t}, g\right\} + \left\{f, \frac{\partial g}{\partial t}\right\}\right]. \tag{10.1.18}$$

Plugging Eq. (21) into the first term of the right-hand side of this equation, and differentiating it by parts, we get $dF/dt = 0$, i.e. F is indeed an integral of motion as well.

Finally, one more important role of the Hamilton formalism is that it allows one to trace the close formal connection between classical and quantum mechanics. Indeed, using Eq. (18) to calculate the Poisson brackets of the generalized coordinates and momenta, we readily get

$$\{q_j, q_{j'}\} = 0, \quad \{p_j, p_{j'}\} = 0, \quad \{q_j, p_{j'}\} = -\delta_{jj'}. \tag{10.1.19}$$

In quantum mechanics, the operators of these variables ("observables") obey commutation relations [6]

$$[\hat{q}_j, \hat{q}_{j'}] = 0, \quad [\hat{p}_j, \hat{p}_{j'}] = 0, \quad [\hat{q}_j, \hat{p}_{j'}] = i\hbar\delta_{jj'}, \tag{10.1.20}$$

where the definition of the commutator, $[\hat{g}, \hat{f}] \equiv \hat{g}\hat{f} - \hat{f}\hat{g}$, is to a certain extent [7] similar to that (18) of the Poisson bracket. We see that the classical relations (24) are similar to the quantum-mechanical relations (25) if the following parallel has been made:

$$\{g, f\} \leftrightarrow \frac{i}{\hbar}[\hat{g}, \hat{f}]. \tag{10.1.21}$$

This analogy extends well beyond Eqs. (24)-(25). For example, making the replacement (26) in Eq. (17), we get

$$\frac{d\hat{f}}{dt} = \frac{\partial \hat{f}}{\partial t} + \frac{i}{\hbar}[\hat{H}, \hat{f}], \quad \text{i.e. } i\hbar\frac{d\hat{f}}{dt} = i\hbar\frac{\partial \hat{f}}{\partial t} + [\hat{f}, \hat{H}] \tag{10.1.22}$$

which is the correct equation of operator evolution in the Heisenberg picture of quantum mechanics. [8] The parallel (26) may give important clues in the search for the proper quantum-mechanical operator of a given observable - which is not always elementary.

---

[1] Due to not only William Rowan Hamilton (1805-1865), but also Carl Gustav Jacob Jacobi (1804-1851).

[2] Actually, this differential was already spelled out (but partly and implicitly) in Sec. 2.3 - see Eqs. (2.33)-(2.35).

[3] Of course, the right-hand side of each equation (7) may include coordinates and momenta of other degrees of freedom as well, so that the equations of motion for different j are generally coupled.

[4] The reader is highly encouraged to perform a similar check for a few more problems, for example those listed at the end of the chapter, to get a better feeling of how the Hamiltonian formalism works.

[5] Named after Siméon Denis Poisson (1781-1840), of the Poisson equation and the Poisson statistical distribution fame.

[6] See, e.g., QM Sec. 2.1

[7] There is, of course, a conceptual difference between the "usual" products of the function derivatives participating in the Poisson brackets, and the operator "products" (meaning their sequential action on a state vector) forming the commutator.

[8] See, e.g., QM Sec. 4.6.

10.2: Adiabatic Invariance

One more application of the Hamiltonian formalism in classical mechanics is the solution of the following problem. [9] Earlier in the course, we already studied some effects of time variation of parameters of a single oscillator (Sec. 5.5) and coupled oscillators (Sec. 6.5). However, those discussions were focused on the case when the parameter variation speed is comparable with the own oscillation frequency (or frequencies) of the system. Another practically important case is when some system's parameter (let us call it λ) is changed much more slowly (adiabatically [10]),

$$\left|\frac{\dot{\lambda}}{\lambda}\right| << \frac{1}{T}, \tag{10.2.1}$$

where τ is a typical period of oscillations in the system. Let us consider a 1D system whose Hamiltonian $H(q,p,\lambda)$ depends on time only via such a slow evolution of such parameter $\lambda = \lambda(t)$, and whose initial energy restricts the system's motion to a finite coordinate interval - see, e.g., Figure 3.2c.

Then, as we know from Sec. 3.3, if the parameter λ is constant, the system performs a periodic (though not necessarily sinusoidal) motion back and forth the q-axis, or, in a different language, along a closed trajectory on the phase plane $[q,p]$ - see Figure 1. [11] According to Eq. (8), in this case H is constant along the trajectory. (To distinguish this particular value from the Hamiltonian function as such, I will call it E, implying that this constant coincides with the full mechanical energy $E-$ as does for the Hamiltonian (10), though this assumption is not necessary for the calculation made below.)

The oscillation period T may be calculated as a contour integral along this closed trajectory:

$$\tau \equiv \int_0^\tau dt = \oint \frac{dt}{dq}dq \equiv \oint \frac{1}{\dot{q}}dq. \tag{10.2.2}$$

Using the first of the Hamilton equations (7), we may represent this integral as

$$\tau = \oint \frac{1}{\partial H/\partial p}dq. \tag{10.2.3}$$

At each given point q, $H = E$ is a function of p alone, so that we may flip the partial derivative in the denominator just as the full derivative, and rewrite Eq. (30) as

$$\tau = \oint \frac{\partial p}{\partial E}dq. \tag{10.2.4}$$

For the particular Hamiltonian (10), this relation is immediately reduced to Eq. (3.27), now in the form of a contour integral:

$$\tau = \left(\frac{m_{\text{ef}}}{2}\right)^{1/2} \oint \frac{1}{[E - U_{\text{ef}}(q)]^{1/2}}dq \tag{10.2.5}$$

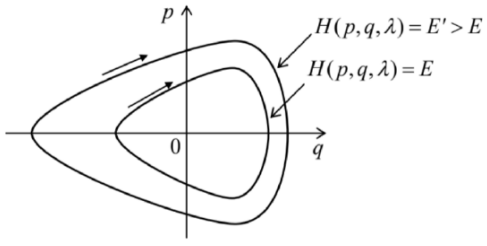

Fig. 10.1. Phase-plane representation of periodic oscillations of a 1D Hamiltonian system, for two values of energy (schematically).

Naively, it may look that these formulas may be also used to find the motion period's change when the parameter λ is being changed adiabatically, for example, by plugging the given functions $m_{\text{ef}}(\lambda)$ and $U_{\text{ef}}(q,\lambda)$ into Eq. (32). However, there is no guarantee that the energy E in that integral would stay constant as the parameter changes, and indeed we will see below that this is not necessarily the case. Even more interestingly, in the most important case of the harmonic oscillator $\left(U_{\text{ef}} = \kappa_{\text{ef}}q^2/2\right)$, whose oscillation period τ does not depend on E (see Eq. (3.29) and its discussion), its variation in the adiabatic limit (28) may be readily

predicted: $\tau(\lambda) = 2\pi/\omega_0(\lambda) = 2\pi[m_{\rm ef}(\lambda)/\kappa_{\rm ef}(\lambda)]^{1/2}$, but the dependence of the oscillation energy E (and hence the oscillation amplitude) on λ is not immediately obvious.

In order to address this issue, let us use Eq. (8) (with $E = H$) to represent the rate of the energy change with $\lambda(t)$, i.e. in time, as

$$\frac{dE}{dt} = \frac{\partial H}{\partial t} = \frac{\partial H}{\partial \lambda}\frac{d\lambda}{dt}. \tag{10.2.6}$$

Since we are interested in a very slow (adiabatic) time evolution of energy, we can average Eq. (33) over fast oscillations in the system, for example over one oscillation period T, treating $d\lambda/dt$ as a constant during this averaging. (This is the most critical point of this argumentation, because at any non- vanishing rate of parameter change the oscillations are, strictly speaking, non-periodic. [12]) The averaging yields

$$\overline{\frac{dE}{dt}} = \frac{d\lambda}{dt}\overline{\frac{\partial H}{\partial \lambda}} \equiv \frac{d\lambda}{dt}\frac{1}{\tau}\int_0^\tau \frac{\partial H}{\partial \lambda}dt. \tag{10.2.7}$$

Transforming this time integral to the contour one, just as we did at the transition from Eq. (29) to Eq. (30), and then using Eq. (31) for τ, we get

$$\overline{\frac{dE}{dt}} = \frac{d\lambda}{dt}\frac{\oint \frac{\partial H/\partial \lambda}{\partial H/\partial p}dq}{\oint \frac{\partial p}{\partial E}dq} \tag{10.2.8}$$

At each point q of the contour, H is a function of not only λ, but also of p, which may be also λ dependent, so that if E is fixed, the partial differentiation of the relation $E = H$ over λ yields

$$\frac{\partial H}{\partial \lambda} + \frac{\partial H}{\partial p}\frac{\partial p}{\partial \lambda} = 0, \text{ i.e. } \frac{\partial H/\partial \lambda}{\partial H/\partial p} = -\frac{\partial p}{\partial \lambda}. \tag{10.2.9}$$

Plugging the last relation to Eq.(35), we get

$$\overline{\frac{dE}{dt}} = -\frac{d\lambda}{dt}\frac{\oint \frac{\partial p}{\partial \lambda}dq}{\oint \frac{\partial p}{\partial E}dq} \tag{10.2.10}$$

Since the left-hand side of Eq. (37) and the derivative $d\lambda/dt$ do not depend on q, we may move them into the integrals over q as constants, and rewrite Eq. (37) as

$$\oint \left(\frac{\partial p}{\partial E}\overline{\frac{dE}{dt}} + \frac{\partial p}{\partial \lambda}\frac{d\lambda}{dt}\right)dq = 0. \tag{10.2.11}$$

Now let us consider the following integral over the same phase-plane contour,

$$J \equiv \frac{1}{2\pi}\oint p dq, \tag{10.2.12}$$

called the action variable. Just to understand its physical sense, let us calculate J for a harmonic oscillator (14). As we know very well from Chapter 5, for such an oscillator, $q = A\cos\Psi, p = -\ m_{\rm ef}\,\omega_0 A\sin\Psi$ (with $\Psi = \omega_0 t +$ const), so that J may be easily expressed either via the oscillations' amplitude A, or via their energy $E = H = m_{\rm ef}\omega_0^2 A^2/2$:

$$J = \frac{1}{2\pi}\oint p dq = \frac{1}{2\pi}\int_{\Psi=0}^{\Psi=2\pi}(-m_{\rm ef}\omega_0 A\sin\Psi)\,d(A\cos\Psi) = \frac{m_{\rm ef}\omega_0}{2}A^2 = \frac{E}{\omega_0}. \tag{10.2.13}$$

Returning to a general system with adiabatically changed parameter λ, let us use the definition of J, Eq. (39), to calculate its time derivative, again taking into account that at each point q of the trajectory, p is a function of E and λ :

$$\frac{dJ}{dt} = \frac{1}{2\pi}\oint \frac{dp}{dt}dq = \frac{1}{2\pi}\oint\left(\frac{\partial p}{\partial E}\frac{dE}{dt} + \frac{\partial p}{\partial \lambda}\frac{d\lambda}{dt}\right)dq. \tag{10.2.14}$$

Within the accuracy of our approximation, in which the contour integrals (38) and (41) are calculated along a closed trajectory, the factor dE/dt is indistinguishable from its time average, and these integrals coincide so that the result (38) is applicable to Eq. (41)

as well. Hence, we have finally arrived at a very important result: at a slow parameter variation, $dJ/dt = 0$, i.e. the action variable remains constant:

$$J = \text{ const} \tag{10.2.15}$$

This is the famous adiabatic invariance. [13] In particular, according to Eq. (40), in a harmonic oscillator, the energy of oscillations changes proportionately to its own (slowly changed) frequency.Before moving on, let me briefly note that the adiabatic invariance is not the only application of the action variable J. Since the initial choice of generalized coordinates and velocities (and hence the generalized momenta) in analytical mechanics is arbitrary (see Sec. 2.1), it is almost evident that J may be taken for a new generalized momentum corresponding to a certain new generalized coordinate Θ, [14] and that the pair $\{J, \Theta\}$ should satisfy the Hamilton equations (7), in particular,

$$\frac{d\Theta}{dt} = \frac{\partial H}{\partial J}. \tag{10.2.16}$$

Following the commitment of Sec. 1 (made there for the "old" arguments q_j, p_j), before the differentiation on the right-hand side of Eq. (43), H should be expressed as a function (besides t) of the "new" arguments J and Θ. For time-independent Hamiltonian systems, H is uniquely defined by $J-$ see, e.g., Eq. (40). Hence in this case the right-hand side of Eq. (43) does not depend on either t or Θ, so that according to that equation, Θ (called the angle variable) is a linear function of time:

$$\Theta = \frac{\partial H}{\partial J} t + \text{ const} . \tag{10.2.17}$$

For a harmonic oscillator, according to Eq. (40), the derivative $\partial H/\partial J = \partial E/\partial J$ is just $\omega_0 \equiv 2\pi/T$, so that $\Theta = \omega_0 t +$ const, i.e. it is just the full phase Ψ that was repeatedly used in this course $-$ especially in Chapter 5 . It may be shown that a more general form of this relation,

$$\frac{\partial H}{\partial J} = \frac{2\pi}{\tau}, \tag{10.2.18}$$

is valid for an arbitrary system described by Eq. (10). Thus, Eq. (44) becomes

$$\Theta = 2\pi \frac{t}{\tau} + \text{ const} . \tag{10.2.19}$$

This means that for an arbitrary (nonlinear) 1D oscillator, the angle variable Θ is a convenient generalization of the full phase Ψ. Due to this reason, the variables J and Θ present a convenient tool for discussion of certain fine points of the dynamics of strongly nonlinear oscillators - for whose discussion I, unfortunately, do not have time/space. [15]

---

[9] Various aspects of this problem and its quantum-mechanical extensions were first discussed by L. Le Cornu (1895), Lord Rayleigh (1902), H. Lorentz (1911), P. Ehrenfest (1916), and M. Born and V. Fock (1928).

[10] This term is also used in thermodynamics and statistical mechanics, where it implies not only a slow parameter variation (if any) but also thermal insulation of the system - see, e.g., SM Sec. 1.3. Evidently, the latter condition is irrelevant in our current context.

[11] In Sec. 5.6, we discussed this plane for the particular case of sinusoidal oscillations - see Figure 5.9

[12] Because of the implied nature of this conjecture (which is very close to the assumptions made at the derivation of the reduced equations in Sec. 5.3), new, more strict (but also much more cumbersome) proofs of the final Eq. (42) are still being offered in literature - see, e.g., C. Wells and S. Siklos, Eur. J. Phys. 28, 105 (2007) and/or A. Lobo et al., Eur. J. Phys. 33, 1063 (2012).

[13] For certain particular oscillators, e.g., a point pendulum, Eq. (42) may be also proved directly - an exercise highly recommended to the reader.

[14] This, again, is a plausible argument but not a strict proof. Indeed: though, according to its definition (39), J is nothing more than a sum of several (formally, the infinite number of) values of the momentum p, they are not independent, but have to be selected on the same closed trajectory on the phase plane. For more mathematical vigor, the reader is referred to Sec. 45 of Mechanics by Landau and Lifshitz (which was repeatedly cited above), which discusses the general rules of the so-called canonical transformations from one set of Hamiltonian arguments to another one - say from $\{p, q\}$ to $\{J, \Theta\}$.

[15] An interested reader may be referred, for example, to Chapter 6 in J. Jose and E. Saletan, Classical Dynamics, Cambridge U. Press, 1998.

10.3: The Hamilton Principle

Now let me show that the Lagrange equations of motion, that were derived in Sec. 2.1 from the Newton laws, may be also obtained from the so-called Hamilton principle, [16] namely the condition of a minimum (or rather an extremum) of the following integral called action:

$$S \equiv \int_{t_{\rm ini}}^{t_{\rm fin}} L dt, \tag{10.3.1}$$

where $t_{\rm ini}$ and $t_{\rm fin}$ are, respectively, the initial and final moments of time, at which all generalized coordinates and velocities are considered fixed (not varied) - see Figure 2.

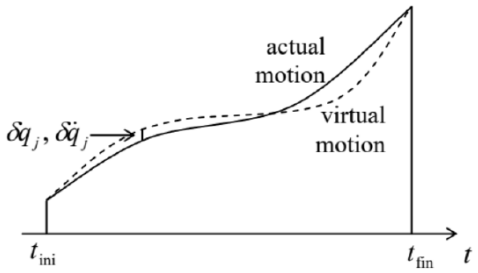

Figure 10.2. Deriving the Hamilton principle.

The proof of that statement (in the realm of classical mechanics) is rather simple. Considering, similarly to Sec. 2.1, a possible virtual variation of the motion, described by infinitesimal deviations $\{\delta q_j(t), \delta \dot{q}_j(t)\}$ from the real motion, the necessary condition for S to be minimal is

$$\delta S \equiv \int_{t_{\rm ini}}^{t_{\rm fin}} \delta L dt = 0, \tag{10.3.2}$$

where δS and δL are the variations of the action and the Lagrange function, corresponding to the set $\{\delta q_j(t), \delta \dot{q}_j(t)\}$. As has been already discussed in Sec. 2.1, we can use the operation of variation just as the usual differentiation (but at a fixed time, see Figure 2), swapping these two operations if needed see Figure 2.3 and its discussion. Thus, we may write

$$\delta L = \sum_j \left(\frac{\partial L}{\partial q_j} \delta q_j + \frac{\partial L}{\partial \dot{q}_j} \delta \dot{q}_j \right) = \sum_j \frac{\partial L}{\partial q_j} \delta q_j + \sum_j \frac{\partial L}{\partial \dot{q}_j} \frac{d}{dt} \delta q_j. \tag{10.3.3}$$

After plugging the last expression into Eq. (48), we can integrate the second term by parts:

$$\begin{aligned} \delta S &= \int_{t_{\rm ini}}^{t_{\rm fin}} \sum_j \frac{\partial L}{\partial q_j} \delta q_j dt + \sum_j \int_{t_{\rm ini}}^{t_{\rm fin}} \frac{\partial L}{\partial \dot{q}_j} \frac{d}{dt} \delta q_j dt \\ &= \int_{t_{\rm ini}}^{t_{\rm fin}} \sum_j \frac{\partial L}{\partial q_j} \delta q_j dt + \sum_j \left[\frac{\partial L}{\partial \dot{q}_j} \delta q_j \right]_{t_{\rm ini}}^{t_{\rm fin}} - \sum_j \int_{t_{\rm ini}}^{t_{\rm fin}} \delta q_j d \left(\frac{\partial L}{\partial \dot{q}_j} \right) = 0 \end{aligned}$$

Since the generalized coordinates in the initial and final points are considered fixed (not affected by the variation), all $\delta q_j\,(t_{\rm ini})$ and $\delta q_j\,(t_{\rm fin})$ vanish, so that the second term in the last form of Eq. (50) vanishes as well. Now multiplying and dividing the last term of that expression by dt, we finally get

$$\delta S = \int_{t_{\rm ini}}^{t_{\rm fin}} \sum_j \frac{\partial L}{\partial q_j} \delta q_j dt - \sum_j \int_{t_{\rm ini}}^{t_{\rm fin}} \delta q_j \frac{d}{dt} \left(\frac{\partial L}{\partial \dot{q}_j} \right) dt = - \int_{t_{\rm ini}}^{t_{\rm fin}} \sum_j \left[\frac{d}{dt} \left(\frac{\partial L}{\partial \dot{q}_j} \right) - \frac{\partial L}{\partial q_j} \right] \delta q_j dt = 0 \tag{10.3.4}$$

This relation should hold for an arbitrary set of functions $\delta q_j(t)$, and for any time interval, and this is only possible if the expressions in the square brackets equal zero for all j, giving us the set of the Lagrange equations (2.19). So, the Hamilton principle indeed gives the Lagrange equations of motion.

It is fascinating to see how does the Hamilton principle work for particular cases. As a very simple example, let us consider the usual 1D linear oscillator, with the Lagrangian function used so many times before in this course:

$$L = \frac{m}{2}\dot{q}^2 - \frac{m\omega_0^2}{2}q^2. \tag{10.3.5}$$

As we know very well, the Lagrange equations of motion for this L are exactly satisfied by any sinusoidal function with the frequency ω_0, in particular by a symmetric function of time

$$q_{\rm e}(t) = A\cos\omega_0 t, \quad \text{so that } \dot{q}_{\rm e}(t) = -A\omega_0 \sin\omega_0 t. \tag{10.3.6}$$

On a limited time interval, say $0 \le \omega_0 t \le +\pi/2$, this function is rather smooth and may be well approximated by another simple, reasonably selected functions of time, for example

$$q_{\rm a}(t) = A\left(1 - \lambda t^2\right), \quad \text{so that } \dot{q}_{\rm a}(t) = -2A\lambda t, \tag{10.3.7}$$

provided that the parameter λ is also selected in a reasonable way. Let us take $\lambda = (\pi/2\omega_0)^2$, so that the approximate function $q_{\rm a}(t)$ coincides with the exact function $q_{\rm e}(t)$ at both ends of our time interval (Figure 3):

$$q_{\rm a}\left(t_{\rm ini}\right) = q_{\rm e}\left(t_{\rm ini}\right) = A, \quad q_{\rm a}\left(t_{\rm fin}\right) = q_{\rm e}\left(t_{\rm fin}\right) = 0, \quad \text{where } t_{\rm ini} \equiv 0, \quad t_{\rm fin} \equiv \frac{\pi}{2\omega_0}, \tag{10.3.8}$$

and check which of them the Hamilton principle "prefers", i.e. which function gives the least action.

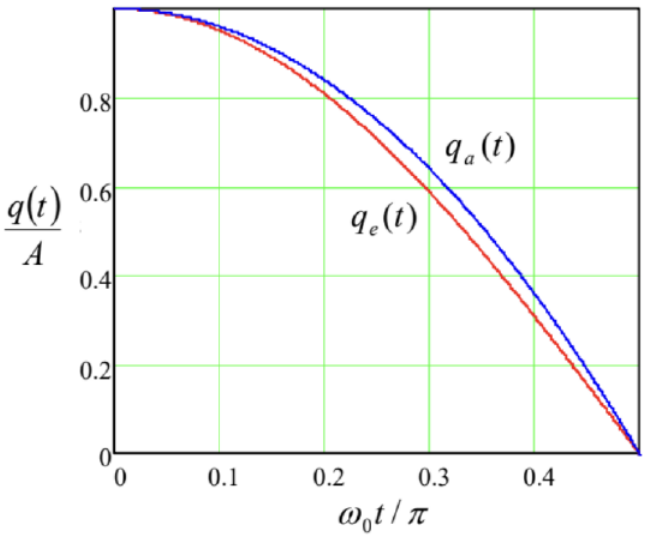

Figure 10.3. Plots of the functions $q(t)$ given by Eqs. (53) and (54).

An elementary calculation of the action (47), corresponding to these two functions, yields

$$S_{\rm e} = \left(\frac{\pi}{8} - \frac{\pi}{8}\right) m\omega_0 A^2 = 0, \quad S_{\rm a} = \left(\frac{4}{3\pi} - \frac{2\pi}{15}\right) m\omega_0 A^2 \approx (0.4244 - 0.4189) m\omega_0 A^2 > 0, \tag{10.3.9}$$

with the first terms in all the parentheses coming from the time integrals of the kinetic energy, and the second terms, from those of the potential energy.

This result shows, first, that the exact function of time, for which these two contributions exactly cancel, [17] is indeed "preferable" for minimizing the action. Second, for the approximate function, the two contributions to the action are rather close to the exact ones, and hence almost cancel each other, signaling that this approximation is very reasonable. It is evident that in some cases when the exact analytical solution of the equations of motion cannot be found, the minimization of S by adjusting one or more free parameters, incorporated into a guessed "trial" function, may be used to find a reasonable approximation for the actual law of motion. 18It is also very useful to make the notion of action S, defined by Eq. (47), more transparent by calculating it for the simple case of a single particle moving in a potential field that conserves its energy $E = T + U$. In this case, the Lagrangian function $L = T - U$ may be represented as

$$L = T - U = 2T - (T + U) = 2T - E = mv^2 - E, \tag{10.3.10}$$

with a time-independent E, so that

$$S = \int L dt = \int mv^2 dt - Et + \text{ const.} \tag{10.3.11}$$

Representing the expression under the remaining integral as $m\mathbf{v}\cdot\mathbf{v}dt = \mathbf{p}\cdot(d\mathbf{r}/dt)dt = \mathbf{p}\cdot d\mathbf{r}$, we finally get

$$S = \int \mathbf{p}\cdot d\mathbf{r} - Et + \text{ const } = S_0 - Et + \text{ const }, \tag{10.3.12}$$

where the time-independent integral

$$S_0 \equiv \int \mathbf{p}\cdot d\mathbf{r} \tag{10.3.13}$$

is frequently called the abbreviated action.

This expression may be used to establish one more important connection between classical and quantum mechanics - now in its Schrödinger picture. Indeed, in the quasiclassical (WKB) approximation of that picture [19] a particle of fixed energy is described by a de Broglie wave

$$\Psi(\mathbf{r},t) \propto \exp\left\{i\left(\int \mathbf{k}\cdot d\mathbf{r} - \omega t + \text{ const}\right)\right\}, \tag{10.3.14}$$

where the wave vector $\mathbf{k}$ is proportional to the particle's momentum, and the frequency ω, to its energy:

$$\mathbf{k} = \frac{\mathbf{p}}{\hbar}, \quad \omega = \frac{E}{\hbar}. \tag{10.3.15}$$

Plugging these expressions into Eq. (61) and comparing the result with Eq. (59), we see that the WKB wavefunction may be represented as

$$\Psi \propto \exp\{iS/\hbar\}. \tag{10.3.16}$$

Hence Hamilton's principle (48) means that the total phase of the quasiclassical wavefunction should be minimal along the particle's real trajectory. But this is exactly the so-called eikonal minimum principle well known from the optics (though valid for any other waves as well), where it serves to define the ray paths in the geometric optics limit - similar to the WKB approximation condition. Thus, the ratio $S/\hbar$ may be considered just as the eikonal, i.e. the total phase accumulation, of the de Broglie waves. [20]

Now, comparing Eq. (60) with Eq. (39), we see that the action variable J is just the change of the abbreviated action S_0 along a single phase-plane contour (divided by 2π). This means, in particular, that in the WKB approximation, J is the number of de Broglie waves along the classical trajectory of a particle, i.e. an integer value of the corresponding quantum number. If the system's parameters are changed slowly, the quantum number has to stay integer, and hence J cannot change, giving a quantummechanical interpretation of the adiabatic invariance. This is really fascinating: a fact of classical mechanics may be "derived" (or at least understood) more easily from the quantum mechanics' standpoint. [21]

---

[16] It is also called the "principle of least action", or the "principle of stationary action". (These names may be fairer in the context of a long history of the development of the principle, starting from its simpler particular forms, which includes the names of P. de Fermat, P. Maupertuis, L. Euler, and J.-L. Lagrange.)

[17] Such cancellation, i.e. the equality $S = 0$, is of course not the general requirement; it is specific only for this particular example.

[18] This is essentially a classical analog of the variational method of quantum mechanics - see, e.g., QM Sec. 2.9.

[19] See, e.g., QM Sec. 3.1.

[20] Indeed, Eq. (63) was the starting point for R. Feynman's development of his path-integral formulation of quantum mechanics - see, e.g., QM Sec. 5.3.

[21] As a reminder, we have run into a similarly pleasant surprise at our discussion of the non-degenerate parametric excitation in Sec. 6.7.

[22] See, e.g., Chapters 6-9 in I. C. Percival and D. Richards, Introduction to Dynamics, Cambridge U. Press, 1983.

10.4: The Hamilton-Jacobi Equation

The action S, defined by Eq. (47), may be used for one more analytical formulation of classical mechanics. For that, we need to make one more, different commitment: S has to be considered a function of the following independent arguments: the final time point $t_{\rm fin}$ (which I will, for brevity, denote as t in this section), and the set of generalized coordinates (but not of the generalized velocities!) at that point:

$$S \equiv \int_{t_{\rm ini}}^{t} L dt = S\left[t, q_j(t)\right] \tag{10.4.1}$$

Let us calculate the variation of this (from the variational point of view, new!) function, resulting from an arbitrary combination of variations of the final values $q_j(t)$ of the coordinates while keeping t fixed. Formally this may be done by repeating the variational calculations described by Eqs. (49)-(51), besides that now the variations δq_j at the finite point (t) do not necessarily equal zero. As a result, we get

$$\delta S = \sum_j \frac{\partial L}{\partial \dot{q}_j} \delta q_j \Bigg|_t - \int_{t_{\rm ini}}^{t} dt \sum_j \left[\frac{d}{dt}\left(\frac{\partial L}{\partial \dot{q}_j} \right) - \frac{\partial L}{\partial q_j} \right] \delta q_j. \tag{10.4.2}$$

For the motion along the real trajectory, i.e. satisfying the Lagrange equations, the second term of this expression equals zero. Hence Eq. (65) shows that, for (any) fixed time t,

$$\frac{\partial S}{\partial q_j} = \frac{\partial L}{\partial \dot{q}_j}. \tag{10.4.3}$$

But the last derivative is nothing else than the generalized momentum p_j – see Eq. (2.31), so that

$$\frac{\partial S}{\partial q_j} = p_j. \tag{10.4.4}$$

(As a reminder, both parts of this relation refer to the final moment t of the trajectory.) As a result, the full derivative of the action $S\left[t, q_j(t)\right]$ over time takes the form

$$\frac{dS}{dt} = \frac{\partial S}{\partial t} + \sum_j \frac{\partial S}{\partial q_j} \dot{q}_j = \frac{\partial S}{\partial t} + \sum_j p_j \dot{q}_j. \tag{10.4.5}$$

Now, by the very definition (64), the full derivative dS/dt is nothing more than the function L, so that Eq. (67) yields

$$\frac{\partial S}{\partial t} = L - \sum_j p_j \dot{q}_j. \tag{10.4.6}$$

However, according to the definition (2) of the Hamiltonian function H, the right-hand side of Eq. (69) is just $(-H)$, so that we get an extremely simply-looking Hamilton-Jacobi equation

$$\frac{\partial S}{\partial t} = -H. \tag{10.4.7}$$

This simplicity is, however, rather deceiving, because in order to use this equation for the calculation of the function $S(t, q_i)$ for any particular problem, the Hamiltonian function has to be first expressed as a function of time t, generalized coordinates q_j, and the generalized momenta p_j (which may be, according to Eq. (67), represented just as derivatives $\partial S/\partial q_j$). Let us see how does this procedure work for the simplest case of a 1D system with the Hamiltonian function given by Eq. (10). In this case, the only generalized momentum is $p = \partial S/\partial q$, so that

$$H = \frac{p^2}{2m_{\rm ef}} + U_{\rm ef}(q,t) = \frac{1}{2m_{\rm ef}} \left(\frac{\partial S}{\partial q} \right)^2 + U_{\rm ef}(q,t), \tag{10.4.8}$$

and Eq. (70) is reduced to a partial differential equation,

$$\frac{\partial S}{\partial t} + \frac{1}{2m_{\rm ef}} \left(\frac{\partial S}{\partial q} \right)^2 + U_{\rm ef}(q,t) = 0. \tag{10.4.9}$$

Its solution may be readily found in the easiest case of time-independent potential energy $U_{\text{ef}} = U_{\text{ef}}(q)$. In this case, Eq. (72) is evidently satisfied by the following variable-separated solution:

$$S(t,q) = S_0(q) + \text{ const } \times t. \tag{10.4.10}$$

Plugging this solution into Eq. (72), we see that since the sum of the two last terms on the left-hand side of that equation represents the full mechanical energy E, the constant in Eq. (73) is nothing but (-E). Thus for the function $S_0(q)$ we get an ordinary differential equation

$$-E + \frac{1}{2m_{\text{ef}}}\left(\frac{dS_0}{dq}\right)^2 + U_{\text{ef}}(q) = 0. \tag{10.4.11}$$

Integrating it, we get

$$S_0 = \int \left\{2m_{\text{ef}}\left[E - U_{\text{ef}}(q)\right]\right\}^{1/2} dq + \text{ const} \tag{10.4.12}$$

so that, finally, the action is equal to

$$S = \int \left\{2m_{\text{ef}}\left[E - U_{\text{ef}}(q)\right]\right\}^{1/2} dq - Et + \text{ const}. \tag{10.4.13}$$

For the case of 1D motion of a single 1D particle, i.e. for $q = x, m_{\text{ef}} = m, U_{\text{ef}}(q) = U(x)$, this solution is just the 1D case of the more general Eqs. (59)-(60), which were obtained above by a much more simple way. (In particular, S_0 is just the abbreviated action.)

This particular case illustrates that the Hamilton-Jacobi equation is not the most efficient way for the solution of most practical problems of classical mechanics. However, it may be rather useful for studies of certain mathematical aspects of dynamics. [22] Moreover, in the early 1950s this approach was extended to a completely different field - the optimal control theory, in which the role of action S is played by the so-called cost function - a certain functional of a system (understood in a very general sense of this term), that should be minimized by an optimal choice of a control signal - a function of time that affects the system's evolution in time. From the point of view of this mathematical theory, Eq. (70) is a particular case of a more general Hamilton-Jacobi-Bellman equation. [23]

---

[23] See, e.g., Chapters 6-9 in I. C. Percival and D. Richards, Introduction to Dynamics, Cambridge U. Press, 1983.

[24] See, e.g., T. Bertsekas, Dynamic Programming and Optimal Control, vols. 1 and 2, Aetna Scientific, 2005 and 2007. The reader should not be intimidated by the very unnatural term "dynamic programming", which was invented by the founding father of this field, Richard Ernest Bellman, to lure government bureaucrats into funding his research, deemed too theoretical at that time. (Presently, it has a broad range of important applications.)

10.5: Exercise Problems

In each of Problems 10.1-10.3, for the given system:

(i) derive the Hamilton equations of motion, and

(ii) check whether the equations are equivalent to those derived from the Lagrangian formalism.

10.1. Our "testbed" system: a bead on a ring, being rotated with a fixed angular velocity ω about its vertical diameter – see Figure 2.1, reproduced on the right.

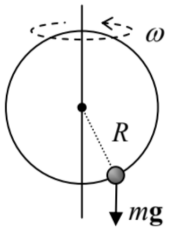

10.2. The system considered in Problem 2.3: a pendulum hanging from a horizontal support whose motion law $x_0(t)$ is fixed - see the figure on the right. (No vertical plane constraint.)

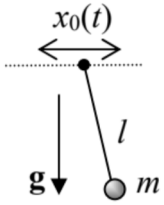

10.3. The system considered in Problem 2.8: a block of mass m that can slide, without friction, along the inclined surface of a heavy wedge of mass m '. The wedge is free to move, also without friction, along a horizontal surface - see the figure on the right. (Both motions are within the vertical plane containing the steepest slope line.)

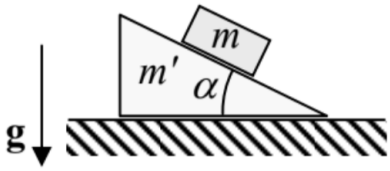

10.4. Find and solve the equations of motion of a particle with the following Hamiltonian function:

$$H = \frac{1}{2m}(\mathbf{p} + a\mathbf{r})^2, \tag{10.5.1}$$

where a is a constant scalar.

10.5. Let L be the Lagrangian function, and H the Hamiltonian function, of the same system. What three of the following four statements,

(i) $\frac{dL}{dt} = 0$,

(ii) $\frac{\partial L}{\partial t} = 0$,

(iii) $\frac{dH}{dt} = 0$,

(iv) $\frac{\partial H}{\partial t} = 0$,

are equivalent? Give an example when those three equalities hold, but the fourth one does not.

10.6. Calculate the Poisson brackets of a Cartesian component of the angular momentum $\mathbf{L}$ of a particle moving in a central force field and its Hamiltonian function H, and discuss the most evident implication of the result.

10.7. After small oscillations had been initiated in the point pendulum shown in Figure on the right, the string is being pulled up slowly, so that the pendulum's length l is being reduced. Neglecting dissipation,

(i) prove by a direct calculation that the oscillation energy is indeed changing proportionately to the oscillation frequency, as it follows from the constancy of the corresponding adiabatic invariant (40); and

(ii) find the l-dependence of the amplitudes of the angular and linear deviations from the equilibrium.

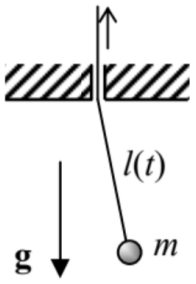

10.8. The mass m of a small body that performs 1D oscillations in the potential well $U(x) = ax^{2n}$, with $n > 0$, is being changed slowly. Calculate the oscillation energy E as a function of m.

10.9. A stiff ball is bouncing vertically from the floor of an elevator whose upward acceleration changes very slowly. Neglecting the energy dissipation, calculate how much does the bounce height h change during the acceleration's increase from 0 to g. Is your result valid for an equal but abrupt increase of the elevator's acceleration?

Index

Glossary

Sample Word 1 | Sample Definition 1

Detailed Licensing

Overview

Title: Essential Graduate Physics - Classical Mechanics (Likharev)

Webpages: 88

Applicable Restrictions: Noncommercial

All licenses found:

- CC BY-NC-SA 4.0: 85.2% (75 pages)
- Undeclared: 14.8% (13 pages)

By Page